

THE PROVENANCE, COMPOSITION AND FATE OF ORGANIC CARBON ON AN ARCTIC GLACIER



The
University
Of
Sheffield.



A thesis submitted for the degree of Doctor of Philosophy
in the Faculty of Social Sciences at the University of Sheffield

by

Krystyna Anna Koziol

(MSc, BSc)

Department of Geography
University of Sheffield
& Department of Arctic Geophysics,
University Centre in Svalbard (UNIS)

September 2014

Abstract

Arctic glaciers are predicted to lose mass rapidly in the next century, leading to the release of organic matter to downstream ecosystems, crucially including nutrients and pollutants. The aim of this study was to collect a comprehensive record of organic carbon (OC) fluxes on a glacier of well-known glaciological characteristics, providing a benchmark example of the biogeochemical impact of glacial melt. Foxfonna, a small Svalbard glacier with net mass losses of -0.74 ± 0.10 m w.e. a^{-1} in the period 1990–2012, represents a rapid melt scenario. The supraglacial OC fluxes associated with atmospheric deposition, glacier ice melt, runoff and biological activity, were quantified in a supraglacial catchment (1.3 km^2) during two balance years (2011–2012) on Foxfonna. The three fluxes related to physical processes ranged from $0.4\text{--}0.7 \text{ Mg OC a}^{-1}$ and majorly exceeded the biological growth flux. Collectively, these fluxes contributed to a net annual OC storage change of $+0.65 \pm 0.12 \text{ Mg OC a}^{-1}$ ($0.37 \pm 0.11 \text{ Mg a}^{-1}$ particulate OC), implying retention. This flux would account for the entire $1.14 \pm 0.23 \text{ Mg OC}$ store found in supraglacial debris (cryoconite) in *c.* 3 years. On the glacier surface, hydrological processes were found to arrange the timing of the release of different organic matter types, liberating the dissolved OC (DOC) from snowpack during meltwater percolation, followed by cells at the time of snowpack saturation with meltwater. Both these organic matter types enriched the OC content of superimposed ice, delaying their ultimate release from the glacier. The particulate OC remaining on the glacier surface in the end of the ablation season can contribute to surface darkening and further melt. This work has shown that physical processes will govern the timing and intensity of the release of various OC types from future shrinking glaciers in multiple ways.

Acknowledgements

I am indebted for the research grants, which made it possible to complete the project despite it being initially self-funded. My fieldwork was supported by the bursary from the University of Sheffield (UoS) Centenary Fund and a grant from Gilchrist Educational Trust (2011), as well as the Arctic Field Grant from the Research Council of Norway and the Henrietta Hutton Research Grant from the Royal Geographical Society (with IBG; both in 2012). The Faculty of Social Sciences, UoS, waived my tuition fees, while the Richard Stapley Educational Trust provided a small maintenance grant in 2011/2012 academic year.

A big 'thank you' goes to my team of supervisors: Prof. Andy Hodson, Dr. Helen Moggridge and Prof. Carl Bøggild, for inspiring discussions, the time invested in this project, but mostly for their continuous positive attitude and faith in me.

My work benefited greatly from the help of institutions and individuals lending data: the orthophotomap and DEM of Foxfonna for 2006 from Store Norske Spitsbergen Kulkompani AS and the aerial photographs of the glacier (in 1961, 1990 and 2009) from the Norwegian Polar Institute (NPI). Justyna Dudek (Jagiellonian University, Poland) taught me how to process these datasets, while Dr. Nick Rutter (University of Northumbria) collected and partly processed the thermistor data used in this project, with further contributions from Emma Brown, a UoS student. The mass balance of Foxfonna in the years 2007-2013 was monitored by Prof. Andy Hodson, Dr. Tris Irvine-Fynn, and numerous other surveyors. Dr. Karoline Bælum and Thomas Gölles helped me obtain and interpret radar profiles of Foxfonna, and the survey data from 2007 are credited to Karoline, Dr. Adam Booth, Prof. Tavi Murray and Prof. Doug Benn. The data processing would have been much more difficult also without the help of Dr. Mariusz Grabiec, Dr. Dariusz Ignatiuk and Dr. Leszek Kolondra.

My own fieldwork would not have been possible without the logistical support of UNIS and my numerous field assistants, many of whom were also UNIS students. The greatest credit for field assistance I owe to Marek Pencarski, Tris Irvine-Fynn, Jenny Bussell, Andy Gray and Emma Brown. In the last stage of preparing my manuscript, I was helped by a squad of proofreaders, foremost amongst whom was Sonia Coates.

Privately, I would like to thank my friends, who kept believing in this happy ending, particularly Ania, Justyna, Angelika, Sonia, Lenka, Kate, Andy and Sharon. I cannot mention you all, but I appreciate those not mentioned just as much! Emma, my mentor, helped me re-learn to think positively. Last on the page and closest to the heart, I thank my parents Bożena and Krzysztof, grandparents: Helena and the late Józef, my sister Asia and my ex-partner Marek for the support in times of doubt, and for being there to share the joys.

Dziękuję!

CHAPTER 1. INTRODUCTION	17
1.1. WHY ORGANIC CARBON ON GLACIERS?	17
1.2. RESEARCH PROBLEM AND STUDY AIMS	18
1.3. STRUCTURE OF THE THESIS	19
CHAPTER 2. ORGANIC CARBON IN GLACIERS – RESEARCH RATIONALE AND AIMS OF THE PRESENT THESIS	21
2.1. GLACIERS AS ORGANIC CARBON RESERVOIRS	21
2.2. GLACIAL SYSTEM CHANGE AND ITS ENVIRONMENTAL IMPACTS	22
2.2.1. GLACIAL MASS BALANCE: METHODS OF ESTIMATION	22
2.2.2. GLACIAL MASS BALANCE: CURRENT GLOBAL PATTERNS	24
2.2.3. GLACIAL SURFACE AND SUBSURFACE ENERGY BALANCE	26
2.2.3.1. The surface albedo of glaciers and its connection to organic matter	28
2.2.4. HYDROLOGICAL ZONES ON THE GLACIER SURFACE	30
2.2.5. GLACIER DYNAMICS IN BRIEF AND ITS CONNECTION TO THE THERMAL STATE OF THE GLACIER	31
2.2.6. AN OUTLOOK OF THE GLACIAL BIOGEOCHEMISTRY	32
2.3. GLACIAL ORGANIC MATTER (OM): ITS ORIGIN, CHARACTERISATION AND IMPACTS	34
2.3.1. SOURCES OF GLACIAL ORGANIC MATTER	35
2.3.2. THE COMPOSITION AND PROPERTIES OF GLACIAL ORGANIC MATTER	36
2.3.3. IMPACTS OF GLACIAL ORGANIC MATTER ON THE WIDER ENVIRONMENT	42
2.4. GLACIAL ORGANIC CARBON STUDIES: PARTIAL FLUX ESTIMATES AND SUPRAGLACIAL PROCESSES	44
2.4.1. THE ATMOSPHERIC SUPPLY OF ORGANIC CARBON	45
2.4.2. ORGANIC MATTER REMOVAL WITH RUNOFF	48
2.4.3. THE IMPACT OF BIOLOGICAL ACTIVITY ON GLACIERS ON THE ORGANIC CARBON FLUXES	50
2.4.4. GLACIAL STORAGE OF ORGANIC MATTER	51
2.5. RESEARCH AIMS	52
CHAPTER 3. THE GLACIOLOGICAL CHARACTERISTICS OF FOXFONNA	55
SUMMARY	55
3.1. INTRODUCTION	55
3.2. METHODS	57
3.2.1. GLACIER MASS BALANCE	57

3.2.1.1. Direct measurements of glacier mass balance on Foxfonna	58
3.2.1.1.1. Errors in mass balance estimation using direct method	62
3.2.1.2. Mass balance (geodetic method) and landscape change observations	64
3.2.1.3. Water balance in 2011 and 2012	66
3.2.1.4. Radar surveys of Foxfonna	68
3.2.1.5. Albedo as a possible driver for mass balance changes	70
3.2.2. GLACIER MOVEMENT	71
3.3. RESULTS	71
3.3.1. GLACIER MASS BALANCE (DIRECT MEASUREMENTS)	71
3.3.2. GLACIER MASS BALANCE (GEODETIC METHOD)	76
3.3.3. METEOROLOGICAL CONDITIONS OF THE MASS BALANCE MEASUREMENT PERIODS	77
3.3.3. WATER BALANCE OF THE SUPRAGLACIAL CATCHMENT IN 2011 AND 2012	80
3.3.4. LONG-TERM GLACIER MORPHOLOGY CHANGE DEDUCED FROM PHOTOGRAMMETRIC RECORD	81
3.3.5. SURFACE ALBEDO SURVEY	85
3.3.6. GLACIER THICKNESS CHANGE AND INTERNAL STRUCTURE	85
3.3.7. GLACIER MOVEMENT	90
3.4. DISCUSSION	90
3.4.1. MASS BALANCE: MULTI-METHOD COMPARISON AND SPATIAL PATTERNS	90
3.4.2. ICE THICKNESS AND INTERNAL STRUCTURE EVOLUTION	97
3.4.3. GLACIER MOVEMENT	99
3.5. CONCLUSION AND IMPLICATIONS FOR THE ORGANIC CARBON BUDGET OF THE GLACIER	99

CHAPTER 4. ORGANIC CARBON FLUXES ON FOXFONNA, A PREDOMINANTLY COLD

POLYTHERMAL ARCTIC GLACIER **101**

SUMMARY	101
4.1. INTRODUCTION	101
4.2. MATERIALS AND METHODS	103
4.2.1. FIELD SAMPLING	103
4.2.1.1. Fluvial export (Q_c) and melt release of OC (M_c) estimation	105
4.2.1.2. Atmospheric deposition (A), supplied with snow or in other forms	106
4.2.1.3. Net glacier mass balance contribution (I_c) and the role of superimposed ice (S_I) in the OC budget	107
4.2.1.4. Biological production (Δ_{bio})	107
4.2.1.5. Storage in supraglacial debris (SOC)	108
4.2.2. LABORATORY ANALYSIS	108

4.2.3. BUDGET CALCULATIONS	110
4.2.3.1. Error estimation for the OC fluxes	112
4.3. RESULTS	113
4.3.1. PARTIAL OC BUDGETS BASED ON THE WATER BALANCE OF THE CATCHMENT	113
4.3.2. ATMOSPHERIC DEPOSITION (<i>A</i>)	115
4.3.3. ORGANIC CARBON TRANSPORT BY MELTWATER RUNOFF (<i>Q_C</i>)	115
4.3.4. GLACIAL ICE MELT (<i>IC</i>) AND THE TRANSIENT STORE OF OC IN THE SUPERIMPOSED ICE (<i>SI</i>)	118
4.3.5. BIOLOGICAL ACTIVITY (ΔBIO)	119
4.3.5. LONG-TERM STORAGE ON THE GLACIER SURFACE (<i>SOC</i>) AND THE ORGANIC CARBON BUDGET	119
4.4. DISCUSSION	121
4.4.1. ATMOSPHERIC INPUTS	122
4.4.2. FLUVIAL EXPORT	123
4.4.3. LIBERATION OF OC FROM MELTING ICE AND THE SUPRAGLACIAL BIOLOGICAL ACTIVITY	124
4.4.4. THE RELATION BETWEEN OC FLUXES AND ITS LONG-TERM STORAGE	126
4.5. CONCLUSIONS	128
<u>CHAPTER 5. THERMAL AND HYDROLOGICAL CONTROLS OVER ORGANIC MATTER</u>	
<u>DISTRIBUTION IN THE SUPRAGLACIAL ENVIRONMENT</u>	<u>131</u>
SUMMARY	131
5.1. INTRODUCTION	131
5.2. METHODS	134
5.2.1. FIELDWORK	134
5.2.2. CHEMICAL AND BIOLOGICAL ANALYSIS	138
5.2.3. COMPUTATION OF WATER BALANCE	138
5.2.4. ESTIMATION OF ORGANIC CARBON AND CELL FLUXES	140
5.3. RESULTS	142
5.3.1. PHYSICAL PROCESSES IN THE SNOWPACK	142
5.3.2. HYDROLOGICAL BUDGET OF THE SUBCATCHMENT	142
5.3.3. ORGANIC CARBON AND CELL TRANSFER	144
5.4. DISCUSSION	148
5.4.1. HYDROLOGICAL EVOLUTION OF THE NEAR-SURFACE PART OF THE GLACIER	148
5.4.2. BIOGEOCHEMICAL CHANGES IN THE SUPRAGLACIAL ENVIRONMENT	148
5.4.3. ORGANIC CARBON AND CELL FLUXES	152
5.4.4. CONCEPTUAL MODEL	154
5.5. CONCLUSIONS	155

CHAPTER 6. DISCUSSION	157
6.1. RESEARCH AIMS REVISITED	157
6.2. THE SUMMARY AND INTERPRETATION OF MAIN FINDINGS	158
6.3. CONCEPTUAL UNDERSTANDING OF ORGANIC CARBON FLUXES AND STORAGE IN THE CONTEXT OF A GLACIER'S DEVELOPMENT	164
6.4. UNEXPECTED FINDINGS	169
6.5. LIMITATIONS OF THE CURRENT WORK	170
6.6. IMPLICATIONS FOR THE FATE OF SUPRAGLACIAL ECOSYSTEMS ON ARCTIC GLACIERS	171
6.7. RECOMMENDATIONS FOR FUTURE RESEARCH	173
6.8. MAJOR CONCLUSIONS	174
CHAPTER 7. CONCLUSIONS	177
7.1. ORGANIC MATTER ON GLACIERS IN THE CONTEXT OF GLOBAL CHANGE	177
7.2. CONTRIBUTION OF THE CURRENT WORK: THE FATE OF ORGANIC CARBON ON GLACIER SURFACE UPON MELT	179
7.3. IMPLICATIONS OF THE CURRENT STUDY: FROM SEA LEVEL RISE TO BIOGEOCHEMICAL CHANGE	181
7.4. FUTURE RESEARCH SUGGESTIONS: GEOMORPHOLOGICAL PROCESSES AND CHEMICAL FLUXES	182
APPENDIX 1. THERMISTOR DATA CORRECTION	209

List of tables

Table 3.1. Characteristics of ablation stakes on Foxfonna glacier (elevations in 2009).	58
Table 3.2. The description of zones used for spatial mass balance calculations.	59
Table 3.3. Accumulation surveys on Foxfonna glacier.	61
Table 3.5. Spatially averaged annual mass balance values for parts of Foxfonna glacier included in the monitoring at the time.	75
Table 3.6. Geodetic mass balance of Foxfonna glacier in the years 1990–2009. Errors reported as the standard deviation of differences to stable terrain, divided by the number of balance years constituting a given time period.	76
Table 3.7. Meteorological conditions in Svalbard Lufthavn station, for the three periods of geodetic mass balance measurements reported in Table 3.6, and for the period of direct mass balance measurements on the whole surface of Foxfonna (2010-2012). For comparison, data from the AWS located next to Foxfonna (on Breinosa plateau, 520 m a.s.l.) are given if available.	79
Table 3.8. Surface velocities on Foxfonna, measured in the period 14th August 2012 – 16/18th June 2014). Stake locations are shown in Figures 3.1 and 3.2.	90
Table 4.1. Procedural blanks for OC sampling and analysis (± 1 SD) ^a	109
Table 4.2. Blank corrected average sample concentrations (± 1 SD) of TOC and DOC.	109
Table 4.3. Organic carbon (OC) budget components [Mg a^{-1}] of Foxfonna glacier in 2011 and 2012. Ic and ΔSOC for 2011 highlighted in grey as these values are based on assumption that the OC concentration in glacial ice remained constant between sampled years.	116
Table 4.4. Components of biological growth (equation 4.4.) in $\mu\text{g C g}^{-1}$ sediment day^{-1} (± 1 SD).	119
Table.5.1. Summary of field measurements to describe the physical state of the glacier surface at Site T2.	137

List of figures

Fig. 2.1. A schematic of glacier hydrological zones above the ELA (equilibrium line altitude). ...	31
Fig. 2.2. Velocity distribution along the longitudinal profile of South Cascade glacier.....	32
Fig. 2.3. A schematic for interpretation of fluorescence excitation-emission matrices (with regions occupied by particular organic matter types).	38
Fig. 2.4. A schematic of a Van Krevelen diagram, with regions highlighted that are occupied by different OM types.	40
Fig. 2.5. Cryoconite debris accumulated on the surface of Foxfonna glacier, including reindeer bones that have melted out of the ice.	41
Fig. 2.6. A schematic of recognised and hypothetical organic carbon fluxes in a glacial setting.	45
Fig. 2.7. Elution sequences for different chemicals according to Meyer and Wania (2011). ...	450
Fig. 3.1. The location of Foxfonna glacier in the Longyearbyen area and within the Svalbard archipelago.	56
Fig. 3.2. Upper part of Foxfonna glacier, its aspect and ablation stakes.....	60
Fig. 3.3. Elevation zones of the lower part of Foxfonna glacier, for the period with all stakes A1-A6 existing.	61
Fig. 3.4. Sampling for snow water equivalent using a density cutter.....	62
Fig. 3.5a. Location map of the discharge monitoring sites in the forefield of Foxfonna glacier.	67
Fig. 3.5b. The discharge monitoring sites in the melt seasons of 2011 and 2012 (Fox Gauge and B1 on Fig. 3.5a., respectively).....	67
Fig. 3.6. Supraglacial catchment boundary in 2012 on Foxfonna. Supraglacial streams are shown as marked with a handheld GPS on 8 th August 2012.	69
Fig. 3.7. Net annual mass balance as recorded on upper Foxfonna stakes in the period 2007–2013.	72
Fig. 3.8. Winter mass balance (accumulation) measured on the stakes of upper Foxfonna glacier in the period 2007–2013.....	72
Fig. 3.9. Spatially averaged mass balance on the ice cap (upper part) of Foxfonna glacier.....	73
Fig. 3.10. Distribution of net mass balance on lower Foxfonna stakes (2010–2012).	73
Fig. 3.11. Winter mass balance as measured on stakes of the lower Foxfonna glacier in the years 2010–2012.	74
Fig. 3.12. Summer mass balance on lower Foxfonna stakes.	74
Fig. 3.13. Mass balance gradient across all stakes on Foxfonna in 2012.	75
Fig. 3.14. Lower Foxfonna spatially averaged winter (Bw) and net (Bn) mass balance in the years 2010–2012 [in m w.e.].	75

Fig. 3.15a. Map of the glacier extent and elevation change in the years 1990–2009.....	77
Fig. 3.15b. Map of Foxfonna glacier extent and elevation change in the years 1990–2006.	78
Fig. 3.15c. Map of the glacier extent and elevation change in the period 2006–2009	79
Fig. 3.16. Elevation class distribution across DEMs of Foxfonna for the years 1990, 2006 and 2009, each with a 5 m resolution.	82
Fig. 3.17. A fragment of the 1961 aerial image of Foxfonna glacier.....	84
Fig. 3.18. Partial water balance for the supraglacial catchment delineated on Foxfonna glacier in 2011 (a) and 2012 (b).....	81
Fig. 3.19. Albedo map on 23 rd July 2010.	85
Fig. 3.20. Surface (A) and bed topography (B) of the upper part of Foxfonna glacier, ice thickness map (C) and radar sounding lines (D).	86
Fig. 3.21. Ice thickness and bed topography map of the lower part of Foxfonna glacier in 2012, radar-surveyed by Thomas Gölles and the author (a). Along the majority of survey lines, relative amplitude of bed reflections were also analysed (b).	88
Fig. 3.22. An example radar picture taken in the vicinity of stakes A4 and A5 in March 2012. .	89
Fig. 3.23. A comparison between geodetic and direct net mass balance, as measured in the ablation stake locations for the period 2006–2009.....	92
Fig. 3.24. Topographical exposure to sunlight deduced from Foxfonna DEM for 2006.....	94
Fig. 3.25. Snow cover thickness distribution on Foxfonna in late April 2012.....	96
Fig. 4.1. Sampling points on Foxfonna glacier included in 2011 or 2012 field programme.	104
Fig. 4.2. Variability of atmospheric deposition of OC in the accumulation (A^{acc}) and ablation season (A^{abl}) and the amount stored in superimposed ice (SI) in 50 m elevation zones on Foxfonna glacier.....	115
Fig. 4.3. Discharge curve for 2011 (a) and 2012 (b) with DOC concentrations in B1 site marked.	117
Fig. 4.4. Qc flux connected to suspended sediment (TOC_{SSC}) in the glacier forefield in 2012..	118
Fig. 4.6. Cryoconite surface coverage in 50 m elevation bands of Foxfonna glacier, as surveyed on 25 th August 2011.....	121
Fig. 4.7. Supraglacial storage of OC and its distribution across elevation zones of Foxfonna (on 25 th August 2011).....	121
Fig. 5.1. Location of the subcatchment, which is the upper part of the catchment presented on Fig. 4.1.....	136
Fig. 5.2. The comparison of cumulative melt estimates given by applying density assumptions to surface lowering registered by a sonic ranger (M-SR) and the Brock & Arnold energy balance melt modelling (M-BA, Brock and Arnold 2000), corrected for subsurface heat flux.	140
Fig. 5.3. Temperature-related changes at the snow-ice interface in the melt season.....	143

Fig. 5.4. Hydrological balance of the studied subcatchment (see Fig. 5.1).	144
Fig. 5.5. Organic carbon (OC) and cells in 10 cm snowpit layers.....	146
Fig. 5.6. OC and cell flux in the supraglacial stream at the basin outlet (M point on the location map).....	147
Fig. 5.7. Subcatchment budgets of OC and cells, calculated for 28 th July 2012 (superimposed ice sampling day).....	147
Fig. 5.8. A hysteresis behaviour observed in the cell runoff (M site).....	150
Fig. 5.9. Photo taken after sampling the snowpack profile on 3 rd July 2012.....	151
Fig. 5.10. Conceptual model for organic matter behaviour in snow, slush and superimposed ice zones on the glacier surface.	155
Fig. 6.1. The summary of OC fluxes on Foxfonna glacier, averaged across the balance years 2011 and 2012.	161
Fig. 6.2. Conceptual diagram of glacial biogeochemical zones, in respect to the nature of organic matter contained within them.	166

Acronyms

AAR – accumulation area ratio	MSA – methanesulfonic acid
AIS – Antarctic Ice Sheet	NMHC – non-methane hydrocarbons
AWS – automatic weather station	NMR – nuclear magnetic resonance
BC – black carbon	OC – organic carbon
BrC – brown carbon	OM – organic matter
DDT – dichlorodiphehyl trichloroethan	PAH – polycyclic aromatic hydrocarbon
ΣDDTs – sum of DDT and its metabolites	PARAFAC – parallel factor analysis
DEM – digital elevation model	PC – particulate carbon
DGPS – differential global positioning system	PCB – polychlorinated biphenyl
DMS – dimethyl sulphide	ΣPCBs – a sum of different PCB congeners (compounds from the PCB family)
DOC – dissolved organic carbon	PCDD/F – polychlorinated dibenzo-p-dioxin/dibenzofuran
dw – dry weight	PFAS – perfluoroalkyl substance
EEM – excitation-emission matrix	PFBA – perfluorobutanoic acid
ELA – equilibrium line altitude	PFOA – perfluorooctanoate
ESI-FTICR-MS (abbreviated also to FTICR-MS)– electrospray ionisation coupled to Fourier transform ion cyclotron resonance mass spectrometry	PFOS – perfluorooctane-sulfonate
GPR – ground-penetrating radar	POC – particulate organic carbon
GPS – Global Positioning System	POP – persistent organic pollutant
GRACE – Gravity Recovery and Climate Experiment	ppb – parts per billion
GrIS – Greenland Ice Sheet	ppm – parts per million
HCB – hexachlorobenzene	RCP – Representative Concentration Pathway
HCH – hexachlorocyclohexane: α-HCH – alpha-HCH (a decomposition by-product of the insecticide lindane) γ-HCH – gamma-HCH (lindane)	RMSE – root mean square error
HCHO – formaldehyde (condensed formula)	RSE – root square error
HR-ToF-AMS – high resolution time-of-flight aerosol mass spectrometer	SCA – short chain acids
HULIS – humic-like substances	SD – standard deviation
	SLR – sea level rise
	SNSK – Store Norske Spitsbergen Kulkompani
	TOC – total organic carbon
	UAV – unmanned aerial vehicle
	UNIS – The University Centre in Svalbard

UV – ultraviolet

VOC – volatile organic compound

VPOC – vapour phase OC

WMO – World Meteorological Organisation

Chapter 1. Introduction

1.1. Why organic carbon on glaciers?

Glaciers and ice sheets, only recently recognised as a biome, are still awaiting full recognition of their role in the global carbon cycle in times of its rapid changes. They contain c. 15.4 Gt organic carbon (Prisco et al., 2008), in a multitude of chemical forms, whose fate depends on the sign of glacier mass change. This organic matter, although proportionally less abundant than soil or oceanic resources, plays an important role in stimulating heterotrophic microbial metabolism due to its increased bioavailability (Hood et al., 2015). Furthermore, they host a range of live and dormant organisms, that can survive in one of the most extreme environments on Earth. Yet there is only a limited understanding of the role of organic matter on glaciers, especially with respect to whether it is an actively exchanged component within an ecosystem, or merely subject to passive storage. With glaciers melting worldwide at an increasing rate and discharging both precious nutrients and harmful pollutants into downstream environments (Bogdal et al., 2009; Fellman et al., 2010; Hood et al., 2009), developing our understanding of glacial organic matter has never been so urgent.

According to recent predictions, glaciers and ice sheets worldwide will contribute between 0.54 m and 1.2 m of sea level rise by 2100 (Horton et al., 2014; Slangen et al., 2014). However, the organic carbon flux connected to this ice melt is difficult to establish, due to a relative paucity of data on the organic carbon content of glacial ice (Jenk et al., 2009; Kawamura et al., 1992, 2012a; Legrand et al., 2007), and a lack of process understanding to support spatial extrapolation of those existing results.

The linkage between the organic carbon cycle and physical processes on glaciers has been appreciated and described in a fragmentary fashion, but many questions remain unanswered in this field. Probably the best studied component of glacial organic carbon flux is that connected to riverine water runoff (Bhatia et al., 2013; Downes et al., 1986; Hood et al., 2009; Lawson et al., 2014), however studies in close proximity to glacier margins are absent. Also, biological activity on glaciers has been documented in many environments, including subglacial (Kaštovská et al., 2007; Skidmore et al., 2000) and supraglacial (Anesio et al., 2010; Cameron et al., 2012a; Edwards et al., 2011; Hodson et al., 2010a; Stibal et al., 2012b).

The links between glacial biological activity and physical processes were explored in the context of microbial cell fluxes in a small supraglacial catchment by Irvine-Fynn et al. (2012) and in a melting snowpack by Björkman et al. (2014), while Stibal et al. (2008, 2010, 2012) give the best characterisation to date of the relationship between organic carbon storage on glaciers and its likely sources and sinks. In particular, Stibal et al. (2008) showed how microbial

activity produced negligible carbon fluxes in comparison to supraglacial storage on the Werenskiöld glacier in the High Arctic. Furthermore, Stibal et al. (2010) described a pattern in the organic carbon content of debris along a supraglacial transect on the Greenland Ice Sheet, and interpreted it in respect to the relative importance of biological activity, wash-away with runoff, and aeolian inputs of organic carbon. This process study has, however, omitted the role played by ice melt in supplying organic carbon to the supraglacial environment. Finally, both Stibal et al. (2012) and Lutz et al. (2014) distinguished ecological zones that indirectly correspond to the hydrological zones *sensu* Müller (1962) on the glacial surface. This detailed zonal division of the glacier accumulation area remains an influential concept in modern glaciology, despite its history exceeding half a century.

Current research suggests that glaciers can be a source of organic nutrients, which are removed with runoff into the sea (Fellman et al., 2010; Hood et al., 2009). This glacial runoff may also contain organic pollutants with long residence times in the environment (Bogdal et al., 2009, 2010a). Supraglacial ecosystems are also estimated to sequester a globally significant amount of carbon dioxide via photosynthesis and fix it as organic matter (Anesio et al., 2009). Microbial activity on glacier surfaces may change the surface albedo of supraglacial ice (Lutz et al., 2014; Takeuchi, 2002b; Takeuchi et al., 2001a, 2001b) and thus feedback to glacier surface melt intensity and runoff fluxes.

Impacts of the organic carbon cycle on glaciers remain very difficult to predict in a global context, especially as the links between carbon fluxes and the physical state of glaciers remain under-explored. Therefore, this thesis aims to establish a more direct connection between the physical state of a glacier and its organic carbon cycle. This will facilitate an important new dimension in interpreting the wider impacts of melting glaciers.

1.2. Research problem and study aims

In order to address the knowledge gap in establishing the link between glacial organic carbon fluxes and physical changes in its environment, research will be conducted to develop a thorough glaciological understanding of a single field site and relate this to its biogeochemical characteristics. The main focus will be to establish the organic carbon budget of a single supraglacial catchment over a sequence of two balance years. No such studies of this duration have been conducted before. This dataset will be placed in the context of physical glacier change and small-scale hydrological development of the glacier surface, all of which may shape the organic carbon cycle. Hence, the organic carbon will be viewed as being partitioned between different supraglacial environments, corresponding to the hydrological zones *sensu* Müller (1962).

Research will be conducted on the small High Arctic glacier Foxfonna (78°08'N, 16°09'E). Both ice mass balance and organic carbon fluxes will be quantified for Foxfonna, placing it within context of changing glacial systems. This study will focus on developing an understanding of this particular glacial system, which can then be extrapolated to other comparable glaciers, while the organic carbon cycle on the ice sheet scale will remain outside the scope of this research. This is because, although the issue of carbon fluxes connected to ice sheets is indeed pressing, it is far beyond a single person's effort to examine it with a diligent monitoring programme. On the contrary, a small glacier such as Foxfonna offers the possibility to intimately link glaciological and biogeochemical observations, and enables spatially and temporally intensive monitoring.

Furthermore the organic matter types will be explored here mainly by apportioning dissolved organic carbon from the total organic carbon pool. The exciting variety of organic compounds found on and in glaciers is vast indeed, and thus cannot be included in its entirety in a single study of the PhD thesis format. Therefore, this thesis will concentrate on the crucial characteristics and processes linking organic carbon sources and sinks, depending on its properties, based on observations from a small Arctic glacier.

The specific aim of this study will be, therefore, to provide a conceptual understanding of the processes reigning the organic carbon cycle on a single glacier surface. This can be achieved by fulfilling the three following objectives:

- to characterise the glacial system studied to the extent which will enable the understanding of biogeochemical processes occurring on its surface (focusing on its mass balance, glacier dynamics and surface hydrology);
- to give best estimations of the organic carbon fluxes on the same glacier, and link them to its current physical state (quantifying the atmospheric inputs as linked to the accumulation of snow and the riverine export of organic carbon as connected to melt, in order to ascertain whether these factors are sufficient to characterise the organic carbon budget on this glacier);
- to characterise processes of organic carbon storage and removal in small scale, within the framework of supraglacial hydrological zones.

1.3. Structure of the thesis

Whilst more detailed research aims will be given in further sections, following a more thorough introduction to the research literature, here the general content of the thesis will be outlined. Research will be presented in an order that enables the connection between physical processes occurring on glaciers and the organic carbon cycle to be explored at a spectrum of scales. The literature review in Chapter 2 will provide a framework in which glaciers and their

organic carbon cycle will be placed in the context of global carbon cycle and global change. Furthermore, various aspects of glacial biogeochemistry will be described, with a particular focus on organic matter fluxes and their wider impacts. Since this thesis focuses on organic carbon fluxes and their role in the glacial environment, the necessary context will be given in Chapter 2 to connect the study subject to the wider understanding of glacial biogeochemistry, the role of microbial communities and externally supplied organic matter, as well as global trends in glacier change. Detailed research aims will follow at the end of Chapter 2.

The first part of the study's new research is a glaciological description of the site, based on monitoring data collected over two study years (2011–2012), as well as information obtained from archived resources. Therefore, in Chapter 3 a record of mass balance, geometry and surface morphology will be described for Foxfonna glacier, providing an overview of the recent changes in this glacial environment. This will be complimented by information on its thermal regime and ice dynamics. Combining these datasets will provide not only a background for further monitoring of Foxfonna's biogeochemical fluxes, but also show how representative the study site is as a particular glacier type.

Following this background research, an organic carbon budget for Foxfonna will be presented in Chapter 4. The first ever simultaneous estimations will be given for the glacier atmospheric inputs of OC, its removal with runoff, the flux connected to legacy ice melting, and biological activity on the glacier. As a result of budgeting these, an estimate of annual change in storage will be calculated for a supraglacial catchment, and compared to the long term storage of OC on the glacier surface in cryoconite debris.

A more detailed focus on the supraglacial processes governing OC transport and storage will be given in Chapter 5, by investigating the short term dynamics of the glacier at a point location. The temporal focus of this chapter will be the melting season when the snowpack is still present. Data will also be related to a flux study in a small supraglacial catchment, which represents the upper part of the catchment described in Chapter 4. The finer temporal scale of this chapter, combined with a study of the thermal evolution of the snow profile using thermistor strings, will provide a process-oriented understanding of storage mechanisms specific to particular types of organic matter on glaciers, in particular the total organic carbon, its dissolved fraction, and cells.

While the results in Chapters 3–5 will include separate discussions on their findings, Chapter 6 will present the integrated outcomes. In this chapter the new findings from this project will be summarised in a conceptual diagram, and implications for the wider impacts of glacial organic carbon cycle will be inferred. Finally, concluding remarks and a summary of the major findings will be presented in Chapter 7.

Chapter 2. Organic carbon in glaciers – research rationale and aims of the present thesis

2.1. Glaciers as organic carbon reservoirs

Glaciers worldwide store organic matter (Hood et al., 2015), crucially including pollutants (Stubbins et al., 2012), nutrients (Singer et al., 2012) and living cells (Price, 2007), both on their surfaces and in the ice itself. To date, this matter has only been quantified opportunistically as part of ice core studies, runoff or atmospheric pollution monitoring, and its cycle is largely unknown. The common denominator for a variety of substances of interest in the glacial environment is the *organic carbon* contained in them, i.e. the carbon associated with biota or biological production. This term encompasses all carbonaceous chemical species, with the exception of few simple ones, i.e. carbon dioxide, carbonates, carbonyls, cyanides, and carbides (Considine, 2005).

The ice that hosts those carbon species is predicted to undergo a rapid change within the 21st century. Global temperature change has been rapid over the years 1980–2010 (Hansen et al., 2010), and this temperature is predicted to increase by more than 2°C compared to preindustrial times within the second half of the current century (Joshi et al., 2011). A particularly intensive change has been observed in the high northern latitudes (Flato and Boer, 2001), but the West Antarctic has also been experiencing a rapid warming in the last five decades (Bromwich et al., 2013).

As global warming proceeds, feedbacks between the carbon compounds and melting cryosphere become increasingly important. This is not only due to the subsequent sea level rise (Cazenave and Llovel 2010; Nicholls and Cazenave 2010; Rignot et al. 2011, see Section 2.2.2. for wider description), but also due to the possible biogeochemical impacts which concern organic matter in particular (Bogdal et al., 2009; Fellman et al., 2010; Grannas et al., 2013; Hood et al., 2009). Therefore, the carbon stored in the frozen part of our planet needs investigating urgently. The detailed impacts of the released carbon species may be multifaceted, and are still widely unknown. The possibilities include influencing all, or selected living organisms, by acting as poisons, carcinogens or hormone disruptors (Guzzella et al., 2011; Maire et al., 2010; Mnif et al., 2011). A wide suite of organic chemicals fall within those categories, from a simple compound formaldehyde (HCHO) to complex aromatic molecules, e.g. 2,2',3,3',4,5,5',6,6'-Nonachlorobiphenyl (known also as PCB-208). Therefore, the fate of organic chemicals in the warming climate should be subjected to diligent study, so that humankind can be prepared for the possible impact on people and the surrounding biosphere.

2.2. Glacial system change and its environmental impacts

The rapid change of the global cryosphere (e.g. Moholdt et al. 2010; Gardner et al. 2011), is usually simplified to its impact on the global sea level (sea level rise, hereafter referred to as SLR). Glaciers are, however, contributing to environmental changes in multiple ways, including their geochemical storage release (e.g., Bogdal et al., 2010a). The glacial system will be described briefly here, along with its recent and predicted changes and their impacts. This will provide a background for the deeper insight into the biogeochemical fate of changing glaciers offered in the further sections of this chapter.

Glaciers are defined as constantly moving ice masses formed on land, that survive at least one year (Jania, 1997). They may be viewed as systems with mass inputs and outputs, interacting with other components of the environment (Benn and Evans, 2010). Key aspects of research in the field of glaciology are therefore glacier mass balance and glacier dynamics, with both aspects playing a role in the impacts of glacial change.

2.2.1. Glacial mass balance: methods of estimation

Glacier mass balance is the net effect of the mass input with precipitation and other forms of water deposition (whether already frozen or freezing upon the ice surface), and the output of melted or sublimated snow, firn and ice. Dynamical inputs and outputs also contribute to glacier mass balance, e.g. avalanching of snow onto the glacier or breaking off ice blocks on tidewater glacier fronts (calving). All the ice inputs and outputs contain impurities, so chemicals within ice may be considered within the mass balance context.

The estimations of the glacier mass balance come from different evaluation methods: hydrological balance calculation, direct measurements, geodetic datasets comparison and gravimetric satellite data. Upon these estimations, expanded with the knowledge of chemical compound concentrations, any other chemical than water may also have its budget constructed.

The *hydrological* method (Sicart et al., 2007) of the ice mass balance calculation is based on equation 2.1 (Benn and Evans, 2010):

$$(2.1.) \quad \Delta Sg = Pa + Ra + Ea + \Delta So,$$

where ΔSg is the change in glacial storage (net ice mass balance), Pa is the annual input of water from precipitation, Ra stands for runoff total, Ea means evaporation losses in a given year and ΔSo corresponds to other storage changes in the catchment, e.g. in subglacial aquifers. While this method provides the direct link to the hydrological cycle of a given catchment, its major disadvantage is the difficulty in component estimation. The storage

changes are usually unquantifiable and in best case scenario can be assumed negligible. The measurement of precipitation in the frequently inaccessible sites, with strong winds causing gauge undercatch problems (Førland and Hanssen-Bauer, 2000), also pose challenges for this mass balance estimation technique.

The *glaciological* or *direct* method is based on extrapolation of point measurements of accumulation (ice mass input) and ablation (ice mass loss). The accumulation of snow is expressed as water equivalent (w.e.) and measured in a series of snowpits or snow cores and by depth probing (Paterson, 1994). The snow densities obtained from snowpit investigations are averaged (for the whole glacier or polygons, into which its surface is divided) or extrapolated using a depth-density relationship. The latter method of snow density estimation is prone to error if the deepest sites have not been sampled for density, as the extrapolated densities might become unrealistic. Therefore, it is more applicable for small snow depths, while the averaging approach yields better results in firm areas of thick snow cover (Jansson, 1999). The ablation of ice is gauged on stakes piercing the glacier surface, which should be distributed representatively (Jansson, 1999). A majority of the glaciers currently monitored have their mass balance estimated using the direct method, and this method is providing the most accurate results about the short term variability (Cogley, 2009). These short term changes in the measured mass balance may be viewed in two different sampling setups: a fixed date or a stratigraphic system (Fischer, 2011; Huss et al., 2009). The fixed dates repeat every year, usually in connection to hydrological year, while the stratigraphic system requires tracking the events of maximum accumulation level and the minimum level occurring during the ablation season. In the longer term, the differences between the two systems cancel out.

A complimentary source of knowledge on the glacial mass balance are *geodetic* measurements of the glacier volume change (Cogley, 2009; Fischer, 2011), which is the method providing the mass balance series spanning the longest periods (Cogley, 2009). Also, it has advantages over the direct measurements of accounting for the tidewater glacier calving rates, dynamic glacier surface lowering and, to an extent, even basal melt rates and internal accumulation or ablation (Moholdt et al. 2010; Fischer 2011). The principle of the geodetic method is a comparison of at least two glacier elevation models obtained at different points in time, providing the summary of glacier volume change over the period between the geodetic surveys, which can then be used for mass change estimations using measured or assumed densities. A typical data source for the terrain models are photogrammetric surveys (aerial or land-based) and airborne LiDAR samplings (Fischer, 2011; Pope et al., 2007). The change is usually assumed to be equivalent to mass loss at the density of glacial ice, since the Sorge's law states that firn undergoes densification at a constant rate, and hence a uniform density distribution in any depth profile is held over time (Bader, 1954). For example, this law was

successfully applied for Svalbard-wide geodetic mass balance estimation by Nuth et al. (2010). The situations when geodetic ice mass balance measurements are prone to error include significant ELA shifts, which causes average density change (i.e. breaching of Sorge's law), and the measurements over short time periods (<3 years), when corrections for interseasonal variability are necessary (Cogley, 2009; Fischer, 2011). Also, during shorter time periods, the errors of the digital elevation models influence the final mass balance estimate to a higher extent (Zemp et al., 2010).

Finally, the changes in large-scale ice mass balance are best estimated by the *gravimetric* measurements from space using the Gravity Recovery and Climate Experiment (GRACE) satellite system (Jacob et al., 2012; Luthcke et al., 2008). This method relies on the mass distribution measurements tracked by fine gravity changes experienced by two travelling satellites, which thus are positioned at increasing or decreasing distance. The mass changes are defined for arbitrarily chosen regions of the planet ('mascons', a term initially coined for 'surface mass concentration', but then expanded to describe also the region for which it was defined). It is a very effective method for tracking large scale cryospheric changes, despite some ambiguity connected to the post-glacial isostatic rebound, or to meltwater turning into groundwater and therefore not producing a clear gravity signal straight away. The presence of permafrost limits the aforementioned effect, but then again, the melt of ground ice cannot be distinguished from glacier melt in this dataset (Jacob et al., 2012). Also, GRACE data is difficult to apply in smaller spatial resolution than 2 by 2 arc degrees (Luthcke et al., 2008).

2.2.2. Glacial mass balance: current global patterns

The GRACE satellite system data provides valuable large scale estimations of the glacial mass balance, including the largest ice masses near both poles. Jacob et al. (2012) report the Antarctic Ice Sheet (AIS) to be losing mass at a rate of $-165 \pm 72 \text{ Gt a}^{-1}$ in the years 2003–2010, while the Greenland Ice Sheet (GrIS) was experiencing a net loss of $222 \pm 9 \text{ Gt ice per year}$ (Jacob et al., 2012). On the other hand, Gardner et al. (2013) claim that ICESat is the best data source for mass loss estimates from these regions, and for the years 2003–2009 report both ice sheets combined to have been losing $290 \pm 50 \text{ Gt a}^{-1}$. The correspondent SLR equivalent was estimated for $1.06 \pm 0.19 \text{ mm a}^{-1}$ during 2003–2010 from both ice sheets combined by Jacob et al. (2012), while the ICESat estimates equalled to a moderate SLR contribution of $0.80 \pm 0.08 \text{ mm a}^{-1}$ during 2003–2009 (Gardner et al., 2013). Finally, Gardner et al. (2013) estimate the overall glacial SLR contribution in the period 2003–2009 for $1.51 \pm 0.16 \text{ mm a}^{-1}$, which agrees closely with Jacob et al's (2012) assessment of $1.48 \pm 0.26 \text{ mm a}^{-1}$ during 2003–2010. Rignot et al. (2011) also claim that the glacial mass loss estimates obtained from GRACE data and from the surface mass balance combined with the ice discharge tend to be in general

agreement. However, they also report these values to be subject to method-related errors of the magnitude $\pm 33 \text{ Gt a}^{-1}$ and $\pm 51 \text{ Gt a}^{-1}$ for GRACE and surface measurement, respectively, in the case of Greenland Ice Sheet. The two methods produced also errors of $\pm 75 \text{ Gt a}^{-1}$ and $\pm 150 \text{ Gt a}^{-1}$, respectively, in the estimations for the Antarctic Ice Sheet mass losses.

The differences between GRACE estimates for different time periods were also high. For example, the 2004–2009 annual mass loss from the Russian High Arctic has been estimated by Moholdt et al. (2012) as $7.1 \pm 5.5 \text{ Gt}$, while the estimates for the years 2003–2010 have been closer to zero (-4.6 ± 5.4). In Jacob et al.'s (2012) study, the following estimates are given for the years 2003–2010: $0 \pm 2 \text{ Gt a}^{-1}$ in Franz Josef Land, $-4 \pm 2 \text{ Gt a}^{-1}$ in Novaya Zemlya and $-1 \pm 2 \text{ Gt a}^{-1}$ in Severnaya Zemlya. Moholdt et al. (2012) report similar values for the archipelagos mentioned here, but with 0.1 Gt precision and higher error margins. The same regions, but over a shorter time period (2004–2009), showed respective changes of 0.7 ± 3.5 , -5.8 ± 3.0 and $-2.0 \pm 3.0 \text{ Gt a}^{-1}$. All the values mentioned above come from GRACE-derived datasets. In Moholdt et al.'s (2012) study, ICESat laser altimetry was also used, providing estimates of higher precision for the period 2004–2009: -0.9 ± 0.7 , -7.6 ± 1.2 and $-1.3 \pm 0.8 \text{ Gt a}^{-1}$ for the three archipelagos in the respective order. The overall Russian High Arctic annual mass loss was estimated from this more precise source as $-9.8 \pm 1.9 \text{ Gt ice}$ in the same period.

Other glaciers supplied an SLR equivalent of $0.41 \pm 0.08 \text{ mm a}^{-1}$ in total, according to Jacob et al. (2012), between 2003 and 2010, while Gardner et al. (2013) assessed their contribution in the period 2003–2009 for $0.71 \pm 0.08 \text{ mm a}^{-1}$. These glaciers showed a variety of responses to the warming signal. On the one hand, the Alaskan glaciers have demonstrated a strong decline in ice mass ($-46 \pm 7 \text{ Gt a}^{-1}$, 2003–2010; Jacob et al. 2012), as did those in northern Canada (Baffin Island having lost $33 \pm 5 \text{ Gt a}^{-1}$, while Ellesmere, Axel Heiberg and Devon Islands collectively were discharging $34 \pm 6 \text{ Gt water}$ to the ocean, annually). On the other hand, some Asian mountainous regions have shown small positive (or near nil) mass balances (in Tibet and Qilian Shan amounting to $7 \pm 7 \text{ Gt a}^{-1}$, in Siberia and Kamchatka: $2 \pm 10 \text{ Gt a}^{-1}$, in Altai: $3 \pm 6 \text{ Gt a}^{-1}$, in Caucasus: $1 \pm 3 \text{ Gt a}^{-1}$, and in High Mountain Asia: $-4 \pm 20 \text{ Gt a}^{-1}$). Despite a number of regions experiencing slightly positive mass balances (including Franz Josef Land, Scandinavia, European Alps, New Zealand and Northwest America excluding Alaska), the overall mass balance of glaciers and ice sheets worldwide has been strongly negative, amounting to $-536 \pm 93 \text{ Gt a}^{-1}$ (Jacob et al., 2012) or $-549 \pm 57 \text{ Gt a}^{-1}$ (Gardner et al., 2013).

On this background, the Svalbard archipelago has shown only a slightly negative mass balance of $-3 \pm 2 \text{ Gt a}^{-1}$ or $-5 \pm 2 \text{ Gt a}^{-1}$ in the years 2003–2010 or 2003–2009, respectively (according to Jacob et al. (2012) or Gardner et al. (2013), respectively), and its interannual variability was of similar magnitude to that in the neighbouring regions of Franz Josef Land, Novaya Zemlya and Iceland, as well as the Alps and Caucasus. Its response to the warming

signal has been far more restrained than that in the Alaska and Canadian Arctic, and so were the interannual changes of mass balance values (Jacob et al., 2012).

The future projections for the glacier mass balance indicate a worldwide mass loss, but with diverse magnitude across regions. For example, Hanna et al. (2013) reviewed the future mass changes of ice sheets in light of various climate predictions, and arrived at estimates of 6-45 mm SLR contribution from the negative mass balance of GrIS by 2100 (plus up to 85 mm of dynamic contribution from calving and another 27 mm from ice shelf melting, giving a total of up to 157 mm). At the same time, the prediction for the AIS as a whole is a near zero sea level contribution for the next 100–200 years. Smaller glaciers and ice caps are presumed to dominate the SLR contribution within the next century, losing an ice mass equivalent to between 46-51 mm (Raper and Braithwaite, 2006) and 240 ± 128 mm SLR (Meier et al., 2007); newer estimates arriving at a moderate value of 155 ± 41 mm SLR between 2006 and 2011, according to RCP 4.5 (Representative Concentration Pathway by IPCC (2014)) or 216 ± 44 mm SLR for RCP 8.5 (Radić et al., 2014). The projected SLR input of the Svalbard archipelago by 2100 is at the level of 14 ± 4 mm (Radić and Hock, 2011), or 12.4–15.8 mm depending on the RCP (4.5 or 8.5; Radić et al., 2014), although for the period 2012-2100 it was also estimated for a much lower value of 3.5 mm (Giesen and Oerlemans, 2013). Svalbard is predicted to rank between fourth and ninth largest region contributing to the global SLR contribution value (Giesen and Oerlemans, 2013; Radić and Hock, 2011; Radić et al., 2014; Slangen et al., 2014).

2.2.3. Glacial surface and subsurface energy balance

A glacier's mass balance is directly linked to its energy balance, which is captured by equation 2.2. (Hock, 2005):

$$(2.2.) Q_N + Q_H + Q_L + Q_S + Q_R + Q_M = 0$$

where Q_N denotes net radiation, Q_H and Q_L are turbulent heat fluxes, the former standing for the sensible heat flux, while the latter is latent heat flux, Q_S is the subsurface heat flux, Q_R is sensible heat flux supplied by rainfall, and Q_M is the energy used by melt. Since Q_R is usually the least significant term of the equation, successful melt estimations can be carried out using simple energy balance models of the type proposed by Brock and Arnold (2000), especially if expanded by an estimation of Q_S , as will be performed further in this work.

Equation 2.2. is the briefest summary of processes occurring on the glacier surface: the energy supplied from direct and scattered radiation combines with the turbulent heat supply, to provide energy for melt (Andreassen et al., 2008; Sicart et al., 2008). The processes changing this simple picture are rainfall, refreezing events and heat transfer into the subsurface, e.g. the removal of the 'cold content' of snow, which can be defined as the capacity of snow cover in negative temperatures to be a heat sink before it melts (Pellicciotti et al., 2009). However

usually less important than radiative and turbulent heat fluxes, the subsurface heat flux (Q_s) may account for as much as 10-13% change in the energy available for melt (these figures were estimated for the accumulation area of central Chilean glacier by Pellicciotti et al. (2009)). On a Norwegian glacier Storbreen, this flux was estimated as -2 W m^{-2} , which provided a small, but still significant change in melt energy of -1.8% (Andreassen et al., 2008). Wherever the ice becomes exposed, this heat flux becomes much smaller, and likely negligible.

The full capacity of the subsurface heat sink in the non-melting snow cover is called ‘the cold content of snowpack’ and may be calculated from equation 2.4. (Hock, 2005):

$$(2.4.) C = - \int_0^Z \rho_s(z) c_p T(z) dz ,$$

where C is the cold content of snow, Z denotes the maximum depth of subfreezing temperatures, T is temperature at a given depth z , and c_p is specific heat capacity of snow ($2.09 \times 10^3 \text{ J kg}^{-1} \text{ K}^{-1}$, Pellicciotti et al., 2009). At any point in time, the heat flux into subsurface can be estimated from equation 2.5. (Paterson, 1994):

$$(2.5.) Q_s = -k \frac{dT}{dz} ,$$

where k , the thermal conductivity of snow or ice, and T and z are defined as above. The thermal conductivity of snow may be calculated from empirical equations (e.g. Sturm et al., 1997) which are based on a wide scope of published measurements (equation 2.6.):

$$(2.6.) \quad k = 0.138 - 1.01\rho_s + 3.233 \rho_s^2 \quad \{0.156 \leq \rho \leq 0.6\}$$

$$k = 0.023 + 0.234\rho_s \quad \{\rho < 0.156\}$$

The flux into ice is usually negligible compared to the flux through the snowpack (Paterson, 1994), and the snow is warmed mainly by the release of latent heat from meltwater refreezing. Hence, in the calculation of energy available for melt Q_M from Brock and Arnold's (2000) model, there can be a correction for subsurface processes applied by accounting for Q_s as an energy sink and refreezing as an energy source.

The refreezing processes in the snowpack produce new ice of multiple types, depending on their setting and structure. For example, the term *ice glands* represents unstructured refreezing along flow paths, mostly vertical, within the snow. When meltwater starts to accumulate and freeze along a levelled surface, it forms *ice lenses* or *ice layers* (Sharp, 1951). *Ice layers* of thickness between 1 and 3 mm are known to change the snowpack properties, since they are virtually impervious to meltwater. Finally, the solid layer of ice formed at the bottom of a glacial snowpack is called the *superimposed ice* (Wadham and Nuttall, 2002). The superimposed ice is likely to dominate among the refrozen meltwater types on a High-Arctic glacier with a relatively small accumulation zone, like Foxfonna (Wadham and Nuttall, 2002).

Therefore, and due to the difficulty establishing the proportion between the ice types formed in the firn area, the bulk of ice originated from meltwater refreezing will be referred to in this thesis as *superimposed ice*.

In Brock and Arnold's (2000) energy balance model, which will be used for melt modelling in this work due to its limited complexity and sufficient accuracy for the type of estimations performed, there is a term for latent heat flux. However, since the model is applied to the snowpack surface, this term does not account for subsurface refreezing. Instead, the latent heat flux in this model represents the water vapour condensation in snowpack, which can cause a significant energy gain at the glacier surface (Sicart et al., 2008). Paterson (1994) shows the condensation to account for between 0 and 30% of the glacial surface energy balance in his review of heat flux proportions in energy balance of more than 30 glaciers. Unfortunately, the scaling of Q_s or refreezing heat flux has been omitted in this comparison. For the sake of their potential importance, both will be included in the analysis of snow and ice profiles presented in Chapter 5 of this work.

2.2.3.1. The surface albedo of glaciers and its connection to organic matter

A crucial parameter for glacier energy balance is the albedo of its surface. The albedo is defined as hemispherically averaged surface reflectivity in the waveband 0.35 to 2.8 μm (Brock et al., 2000; Hock, 2005). The albedo is therefore a parameter that scales the radiative heat flux. Since its value on glaciers can vary between 0.06 for debris-heavy ice and 0.91 for fresh snow, it is a strong control on melt processes and their spatial variability (Hock, 2005; Jonsell et al., 2003; Pellicciotti et al., 2005). The albedo variability can be approximated by other parameters which vary depending on the location and study purpose. For example the following five were identified by Gardner and Sharp (2010) in their review of physically based albedo modelling: specific surface area of snow/ice, concentration of light-absorbing carbon (frequently described in bulk as soot or *black carbon*, or BC, despite some of it being better characterised as organic *brown carbon*, BrC), solar zenith angle, cloud optical thickness and snow depth. Brock et al. (2000) researched the possibilities to parameterise albedo with a single variable on a European Alpine glacier, and found the snow albedo to be best approximated by accumulated maximum daily temperatures since last snowfall. This is because this parameter approximates both the snow grain size change and the concentration of impurities on the snow surface. The ice albedo was, on the other hand, inversely proportional to debris cover ($r^2 = -0.64$), but this variable is frequently unavailable for modelling. Hence the positive correlation with altitude ($r^2 = 0.43$, both r^2 values significant at $p < 0.05$ level) was found the best input for parameterisation instead (Brock et al., 2000).

The role of impurities in shaping both snow and ice albedo is pronounced. Hansen and Nazarenko (2004) claim that the climatic forcing due to soot emissions, which exert their influence by depressing snow and ice albedo, is twice as effective as the CO₂ atmospheric forcing for melting ice or snow. Flanner et al. (2007) describe its efficacy to be even higher, more than three times that of the carbon dioxide. The darkening impact of BC particles is also claimed to be six times stronger than the solar radiation blocking effect of those particles in the atmosphere (Flanner et al., 2009), which clearly shows their net impact on the cryosphere extent as negative. Painter et al. (2013) have shown the BC in snow forcing to be capable of triggering a major glacier extent change, such as the glacier retreat in the end of the Little Ice Age in the European Alps. BC was also modelled to cause a significant specific runoff increase due to snow melt in Nepalese Himalaya (from 70 to 204 mm), equivalent to 12-34% of the annual discharge of an average Tibetan glacier.

A particularly strong driver of climate warming in the Arctic, is the forcing due to snow surface darkening in April-May (Flanner, 2013), which is due to the carbonaceous impurities being frequently hydrophobic and likely to remain on the snow surface during melt (Doherty et al., 2010, 2013; Meyer et al., 2009a). This can make the snow albedo more sensitive to changes in solar zenith angle, and decrease it, especially at shorter wavelengths (Gardner and Sharp, 2010). The overall impact of BC on Arctic snow albedo is expected to be within 1–2%, which is a climatologically relevant change (Doherty et al., 2010).

Despite the usual description of the light-absorbing carbon as BC or soot, its chemical composition is usually complex, with approximately 40% of the visible UV light absorption happening due to the presence of dark organic compounds (BrC; Doherty et al., 2010). The composition of BC particles has a significant impact on their absorbing properties, for example clear coatings enhance their light absorption by 50-100% (Bond et al., 2006). BrC coatings cause 25% less absorption than clear coatings (Lack and Cappa, 2010), but still enhance the BC absorption, for example in 404 nm band by approximately 19% (Lack et al., 2012). In a snow sample from Boulder, Colorado, the combination of BrC with BC enhanced the light absorption of both by as much as 70%, as compared to the sum of their separate impacts (Lack et al., 2012). Compared to BC understood as soot-like elemental carbon (Bahadur et al., 2012), BrC has a modest but still important mass absorption efficiency (9.5 as opposed to 0.5 m² g⁻¹ at 550 nm), as Yang et al. (2009) show. At 404 nm, a higher mass absorption efficiency of 0.82 ± 0.43 m² g⁻¹ has been found for BrC (Lack et al., 2012).

The importance of albedo in generating melt on glaciers depends on the relative role of the net radiation flux opposed to turbulent heat fluxes variability (Hock and Holmgren, 2005), and hence, this factor is especially important in tropical glacier melt estimation (Sicart et al., 2008). Throughout latitudes, the shortwave radiative heat flux is an important element in melt

production on glaciers though, and it forms between 8 and 100% of the surface energy balance of Arctic glaciers (as reviewed by Paterson, 1994). Therefore, the role of the organic matter on glacier surfaces, where it can significantly change the albedo, deserves further attention in glaciological research.

2.2.4. Hydrological zones on the glacier surface

The energy balance of the glacier surface is spatially variable, which induces the differentiation of the glacier surface into hydrological zones (Benson, 1962; Müller, 1962; Paterson, 1994). The sequence of these, from the glacier top to bottom, is as follows (Figure 2.1):

1. Dry snow zone, where no melt or water percolation occurs.
2. Percolation zone (Müller's percolation zone A), where some surface melting happens, and the refreezing leads to the formation of ice layers, lenses and ice glands. As a result, the snow warms from the latent heat of melting, but never becomes isothermal.
3. Wet snow zone (Müller's: percolation zone B and slush zone), where by the end of summer, all snow deposited within the balance year reaches 0°C. Some of the meltwater might percolate into deeper firn layers, and refreeze there.
4. Superimposed ice zone, where the refrozen layer is continuous, and it extends at the bottom of snowpack deposited in a balance year. In the end of the accumulation season, the superimposed ice becomes exposed. This zone extends down-glacier to the ELA (equilibrium line altitude).
5. Ablation area, where melt during a balance year exceeds the thickness of snowpack and any refrozen layers occurring.

The zones mentioned above are defined in respect to the state of the glacier surface at the end of the melt season. However, zones of correspondent characteristics migrate up-glacier during the melt season, following the transient snow line instead of the annual snow line (Fig. 2.1.). The zones differ in their supraglacial hydrological processes, and they may also be relevant for the biogeochemical processes that are related to changes in temperature, melt intensity and water movement. The framework of melt zones is therefore useful to track processes, which develop during the melt season, either in temporal or spatial setup. In particular, time during melt season may be substituted for spatial differences in the melt processes in a cross-section along the glacier's centre line.

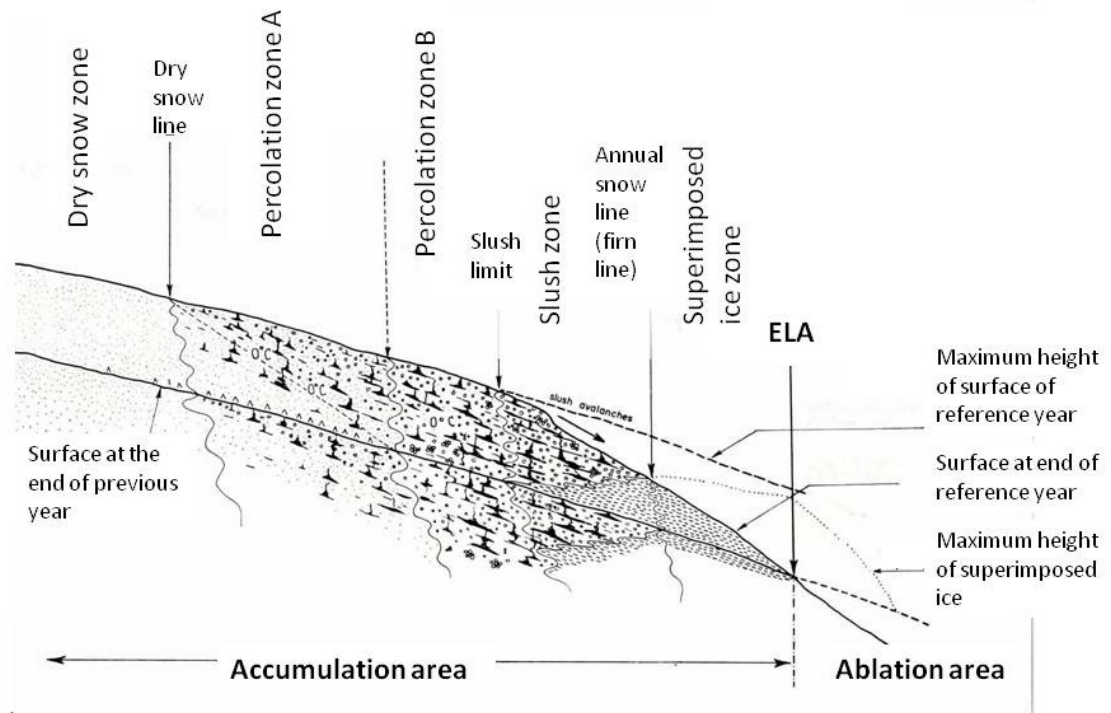


Fig. 2.1. A schematic of glacier hydrological zones above the ELA (equilibrium line altitude).

Adapted from Müller (1962)

2.2.5. Glacier dynamics in brief and its connection to the thermal state of the glacier

The simplest understanding of glacier motion is the concept of balance velocity, when the pulse obtained from the excess of mass in the upper part of the glacier is transferred downwards and towards the snout. The velocities along the glacier in such a case would be increasing towards the ELA, and decreasing in the downward direction in the ablation zone. This picture may be further complicated on tidewater glaciers, where velocities may increase towards the snout. An example of velocity distribution on South Cascade glacier is given on Fig. 2.2. The sketch shows also the characteristic emergence velocities in the ablation zone, and submerging velocity vectors in the accumulation zone.

There are, however, other mechanisms, that modify the motion: *sliding on the glacier bed*, *deformation of the ice* and *deformation of the bed*. *Sliding* takes place on the hard bed, and its surface roughness, as well as the subglacial water pressure, influence the velocities (e.g. Iken, 1981); soft beds contribute to ice displacement by their deformation. Finally, the deformation of ice under stress (i.e., the effect of existing forces, mainly gravity and friction), can be simplified by the use of Glen's flow law (equation 2.6.):

$$(2.6.) \quad \varepsilon_{xy} = A\tau_{xy}^n,$$

where ϵ_{xy} is the strain rate (rate of deformation), and τ_{xy} stands for the shear stress across the basal plane. A and n are parameters; A depends on temperature, and n does not. The value of n was determined in the range 1.5-3.9 (Paterson, 1994).

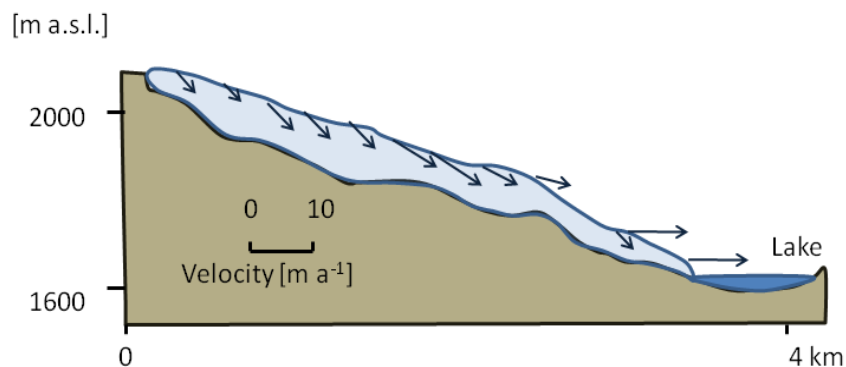


Fig. 2.2. Velocity distribution along the longitudinal profile of South Cascade glacier.

After Meier and Tangborn (1965)

The efficiency of ice deformation is enhanced with higher temperatures, while the sliding at bed is a lot more intensive if liquid water is present at the glacier bed. Hence, the presence of temperate ice (i.e., at the pressure melting point) and liquid water changes the ice movement regime substantially, enabling rapid movement (Blankenship et al., 2001). Glaciers frozen to their beds are known to be moving very slowly (Waller, 2001), with the surface velocity of few m a^{-1} (Benn and Evans, 2010). In the Arctic, both the pressure of overlying ice and the frictional heat contribute to the production of temperate ice at glacier beds, hence it is more likely for the ice at pressure melting point to occur at sloping beds and under thick ice. As glaciers shrink and retreat, they decrease in thickness, and may also favourably occupy areas where the ice was originally accumulated or dynamically thickened before, i.e. the less sloping parts of the glacier profile. As a result, smaller glaciers, that are products of prolonged periods of negative mass balance, are more likely to be frozen to beds and move slowly (Dowdeswell et al., 1995). It is likely that their slow movement will simplify the organic carbon fluxes in them, too.

2.2.6. An outlook of the glacial biogeochemistry

The biogeochemical role of glaciers spans across the global chemical cycles of all elements present in atmospheric precipitation, surface rocks and living organisms. It is exerted in particular by glacial erosion and fresh sediment production, as well as by the existence of vast areas with subfreezing temperatures, which exclude water and constituent impurities from the global hydrological cycle. Proglacial rivers and the changes in freshly exposed sediment from the glacier bed can also be recognised as glacial agents, facilitating specific biogeochemical

processes. Finally, glaciers are sources of sediment deposited further away from them, including the oceans, where they supply additional carbon to coastal waters and sea beds, as well as the proglacial plains, where the loess is formed (Anderson, 2007).

The characteristics of proglacial waters are, in general, the following (Anderson, 2007; Tranter, 2003):

- High suspended sediment load
- High in carbonates, even if underlying geology supplies only a few percent of carbonate rock
- Often high in sulphate originating from sulphide oxidation
- Similar cation fluxes to non-glacierised catchments, but depressed silicate fluxes
- Enriched in radiogenic strontium
- Their solute fluxes are increasing by 30-47% in the short stretch of recently deglaciated, proglacial zone

Under ice sheets, however, these characteristics change due to prolonged contact between meltwater and subglacial sediment, as well as to widespread anoxia. For example, the proportion between carbonate and silicate dissolution changes towards higher rates of silicate removal than from under small glaciers (Wadham et al., 2010).

Glaciers and ice sheets play an important role in the global distribution of nutrients, especially nitrogen and phosphorus (Hodson et al., 2004, 2005; Wynn et al., 2007). They enhance the nitrate load in comparison to snowfall, and this is largely due to their active microbial ecosystem (Hodson et al., 2005; Williams et al., 2006; Wynn et al., 2007). The efficiency of glaciers at eroding bedrock boosts the total phosphorus load in proglacial waters (Hodson et al., 2004). Also, even in Antarctic streams (Downes et al., 1986), the organic matter load in proglacial waters is high, and the organic matter derived from glaciers is found to be more bioavailable than typical riverine organic matter (Fellman et al., 2010; Hood et al., 2009, 2015; Singer et al., 2012), and primes the decomposition thereof (Bianchi, 2011).

The surface of a glacier, their interior, and bed are inhabited by a variety of living and dormant organisms, which take part in the cycling of chemical compounds contained in solid and liquid water in this environment. Based on the part of the glacier inhabited by an ecosystem, they can be divided into three types: supraglacial, englacial and subglacial (Hodson et al., 2008). While the englacial conditions for life are particularly harsh and hinder the ecosystem functioning beyond cell damage repair (i.e. cells remain in the dormant state, Price and Sowers, 2004), the subglacial and supraglacial ecosystems are, on the opposite, hotspots for life on glaciers and ice sheets. All these ecosystems undergo changes as a result of climatic forcing, with enhanced melt and glacier thinning likely to release englacial organisms into the

supraglacial settings, but also to reduce the extent of subglacial habitats by forcing beds of thinner glaciers into temperatures below pressure melting point (Hodson et al., 2008).

Additionally, the presence of a supraglacial ecosystem contributes to a significant albedo decrease on many glaciers (Hodson et al., 2008; Lutz et al., 2014; Takeuchi, 2002a, 2002b; Takeuchi et al., 2001b). The lowest albedo values noted on glaciers (Hock, 2005) are in fact due to the presence of organic-rich debris, which is also referred to as *cryoconite* (Hodson et al., 2008). Therefore it drives further melt of the glacier surface, unless the insulation threshold of debris thickness is achieved. This debris layer thickness has been shown to be best approximated by 0.02-0.04 m in the Canadian Rocky Mountains and the Himalaya (Mattson, 2000; Nakawo and Rana, 1999), but since this effect depends partly on the nocturnal energy dissipation into the atmosphere, it could be thicker in the High Arctic (Reznichenko et al., 2010).

The glacial surface is also host to spatially different hydrological processes (see Section 2.2.3), which influence the biogeochemistry of snowpack and surface ice. In particular, the elution of chemical compounds (Hodgkins and Tranter, 1998; Li et al., 2006; Zhao et al., 2006) and organisms (Björkman et al., 2014) occurs in the snow profile, at a pace and pattern that is unique for each of the chemical and biological components (e.g., Meyer et al., 2009a, 2009b, see Section 2.4.2 for further information).

Since glaciers and ice-caps are complex biogeochemical systems, our understanding of the changes they undergo is hindered by interferences between different cycles. Therefore, this thesis was set up to study what is possibly the least complicated glacier in terms of hydrology and biogeochemical processes. Hence the choice of a most likely cold-based, land-terminating, slow-moving glacier was ideal (see Chapter 3), since it limited the influence of ice dynamics, subglacial hydrology and the subglacial ecosystem on the biogeochemical processes influencing its organic carbon cycle. Thus, it was possible to capture the universal processes relating to most glacial sites, connected to precipitation and melt, in more detail than was feasible before.

2.3. Glacial organic matter (OM): its origin, characterisation and impacts

Glacial OC has received attention for a variety of reasons, including its impact on the surface albedo (Takeuchi, 2002a), the potential release of nutrients (Hood et al., 2009; Lawson et al., 2014) and pollutants (Bogdal et al., 2009, 2010a; Nizetto et al., 2010), as well as its importance for the ecosystem in this extreme environment (e.g., Stibal et al., 2012b). OM has been studied in terms of its abundance in cryoconite (Stibal et al., 2008a), glacial ice (Jenk et al., 2009; Xu et al., 2013) and the snow falling onto glaciers (e.g. Xu et al. 2009; Stubbins et al. 2012, or a review by Legrand et al. 2013), as well as in meltwater (Lafrenière and Sharp, 2011;

Singer et al., 2012). This section will synthesise existing research on the characteristics of this OM, as well as its origin and proglacial fate, in order to draw a broader picture of potential impacts of the glacial OC cycle, while the following Section 2.4. will offer a detailed insight into the cycle itself.

2.3.1. Sources of glacial organic matter

The OM on glaciers comes from three sources: atmospheric deposition, *in situ* production, and the incorporation of organic-rich debris by overriding soils or interaction with the surrounding rock (Bhatia et al., 2006; Downes et al., 1986; Telling et al., 2012; Xu et al., 2010). The origin may be also defined more broadly as locally produced, mainly from primary productivity *in situ* (autochthonous) or externally supplied (allochthonous). Both the dominance of the locally produced and externally supplied OM have been described on different glaciers. The field evidence supports the argument for its autochthonous origin in the interior of the Greenland Ice Sheet, Antarctic and in the Canadian Arctic Archipelago (Pautler et al., 2011, 2012; Stibal et al., 2010). On the other hand, the allochthonous OC was reported to dominate on smaller glaciers, located near sources of wind-blown OM and possibly incorporating soil-derived humics (Singer et al., 2012; Stibal et al., 2008a; Xu et al., 2013). However, the interaction of glaciers with rock and soil carbon resources is still poorly understood due to the inaccessibility of glacial beds where these processes mainly occur. Nevertheless, the estimates for subglacial OM stores show this to be an important element of the overall glacial carbon storage (Priscu et al., 2008; Wadham et al., 2013) and instances of inclusion of subglacial sediment into the structure of the glacier are well known (Murray et al., 1997; Woodward et al., 2003). There is also a described instance of elevated DOM concentration in basal ice interpreted as a result of overriding organic-rich lake sediments (Barker et al., 2006). Furthermore, the humic-like OM content in the runoff from the Greenland Ice Sheet is most likely due to the presence of overridden vegetation and soil (Bhatia et al., 2010).

Overall, the atmospheric supply frequently becomes omitted in the interpretation of OM characteristics in glacial ice, perhaps because it can be of mixed origin itself, ranging from wind-blown plant fragments and soil debris particles, to live microbes acting as condensation nuclei (Sattler et al., 2001). However, Xu et al. (2013) has shown an abundant source of organics in the snow accumulating on glaciers. Snow is known to be not only an effective scavenger of the atmospheric contaminants, but also a particulate deposition and gaseous constituent trap, once already fallen on the ground (Grannas et al., 2013; McNeill et al., 2012). Also, Stibal et al. (2008a) showed the disproportion between the microbial activity on glaciers and the organic content of the supraglacial debris, which reinforces the notion that the role of

atmospheric supply to glaciers is currently underestimated. Recently, the anthropogenic aerosol has been claimed to be a dominant source of OM on two Alaskan glaciers (Stubbins et al., 2012). Since some of the organic pollution is aromatic in nature, and therefore would show fluorescent properties, it is surprising it has not been recognised in the excitation-emission matrices (EEMs), which plot OM types based on those (and are typically used to distinguish microbial from plant- or soil-derived OM, see Fig. 2.3.).

Linked to the issue of OM origin on glaciers is the subject of OM age. Microbially produced carbon is considered a young resource, whereas plant and soil carbon is relatively recalcitrant, and represents a pool of longer history. The highest radiocarbon ages are, however, ascribed to the anthropogenic pollution, since the carbonaceous constituents come from fossil fuel burning (Stubbins et al., 2012). This age does not necessarily correspond to the time spent by the OM within the glacial system, which can be less than one season or exceed 400 ka (Petit et al., 1999). Hence, the attempts to radiocarbon-date glacial ice cores are faced with difficulties (Sigl et al., 2009), both in the ice accumulated post-1850s, as well as in the ice cores derived from the Greenland Ice Sheet. The latter class, represented by the GRIP ice core in Sigl et al.'s study, mainly showed layers to be much older than expected, which would corroborate with the OM included in the ice having a former history, e.g. in overridden forefield soil. Hence, only the relatively young OM in glaciers was successfully used for dating, including the most recent sections of ice cores that contain algae or pollens (Uetake et al., 2006).

2.3.2. The composition and properties of glacial organic matter

The organic matter composition and its physicochemical properties interlink closely. For example, the oldest OM on glaciers is usually thought to be recalcitrant (Bardgett et al., 2007; Barker et al., 2010), but not when it is the radiocarbon-depleted anthropogenic matter (Stubbins et al., 2012). The importance of the anthropogenic component in the OM composition in glaciers worldwide has yet to be fully explored. Still, the anthropogenic fingerprint in the OM makeup in glaciers has been shown in multiple locations across the globe: in Alaska (ibid.), European Alps (Bogdal et al., 2009, 2010a, 2010b), Himalaya (Kang et al., 2009; Wang et al., 2008a; Xu et al., 2009), Svalbard (Garmash et al., 2013; Kwok et al., 2013), and even the Greenland Ice Sheet (Jaffrezo et al., 1994; Masclat et al., 2000) and in the Antarctic (Fuoco et al., 2012). The labile component of glacial OM contains autochthonous carbon as well, with a higher proportion of carbohydrates than typical Arctic riverine OM (Lawson et al., 2014). The overall proportion of labile, bioavailable OM in glacial runoff was estimated to be 22-44% by Fellman et al. (2010), as a result of a 28-day incubation of the water collected in proglacial Alaskan rivers, which were carrying between 0.9 and 4 ppm DOC. Hood et al. (2009) estimate that even 76.9% of the discharged OM might be labile (0.10 of the 0.13

Tg DOC flux, DOC concentrations ranging there from 0.6 to 2.2 ppm). These labile organic constituents are impacting marine ecosystems, particularly as they are more readily decomposed by marine ecosystems than riverine ones (Fellman et al., 2010). The Arctic Ocean, therefore, is not only receiving a disproportionately large flux of terrestrial OM (Opsahl et al., 1999), but also a high fraction of this matter is easily consumed by marine microbial communities; glacier melting contributes vastly to this effect.

Further defining the characteristics of glacial OM greatly depends on the available analytical techniques. The basic division of OM is into DOM (dissolved OM) and POM (particulate OM); DOC and POC are their parallels if only the carbon contained within those organic matter types is concerned. The sum of both carbon types is described as TOC (total OC). However, defining the DOM or DOC is equivocal. Namely, the chemical definition of dissolved matter implies that it is composed of suspended particles of the size below 10^{-9} m (1 nm; Considine 2005), which is impossible to separate with the widely used membrane filters (smallest pore size for commercially distributed filter papers being 0.1 μm , i.e. 10^{-7} m). This means the laboratory practice merges the dissolved and the smaller colloiddally dispersed particles (10^{-9} - 10^{-6} m particle size) under the name of 'dissolved matter'. Moreover, the biggest particle size included in the dissolved fraction varies between 0.2 and 0.7 μm ($2\text{-}7 \times 10^{-7}$ m). Filters with pore size 0.22 or 0.7 μm are more popularly used, and occasionally also 0.2 or 0.3 μm (Dubnick et al., 2010; Gašparović et al., 2007; Kawamura et al., 2012b; Pautler et al., 2011; Stubbins et al., 2012; Voisin et al., 2012).

The next step in the division of the organic compounds contained in glacial ice or snow is offered by the combination of fluorescence EEMs and parallel factor analysis (PARAFAC) modelling (e.g., Pautler et al. (2012), Fig. 2.3.). This technique distinguishes peaks of proteinaceous (tryptophan, tyrosine peaks) and humic character (e.g. marine humic-like matter) by scanning the fluorescent properties of water samples. Further characterisation may be obtained in light of other 'scanning' techniques – ^1H NMR spectroscopy (Pautler et al. 2011, 2012) and electrospray ionization coupled to Fourier transform ion cyclotron resonance mass spectrometry (ESI-FTICR-MS; Grannas et al. 2006). Because of these, Pautler et al. (2011, 2012) were able to distinguish the following compounds in glacial ice:

1. amino acids: alanine, valine, leucine, isoleucine, aspartic acid, lysine, serine, glycine, histidine, phenylalanine and tyrosine;
2. amino acid derivatives: pyroglutamic acid, 3-aminoisobutyric acid, isobutyglycine, isovarylglycine and norvaline; also kynurenic acid and hydroxyisobutyric acid;
3. carboxylic acids: formic, acetic, lactic, pyruvic and fumaric acids, ectoine and a mixture of short chain acids (SCA), most likely C_4 to C_{10} acids;

4. methanol;
5. acetone;
6. some or all of the sugars: glucose, mannose, galactose, and amino sugars: glucosamine, mannosamine and galactosamine; also sucrose;
7. sugar-derivatives: muramic acid (ether of lactic acid and glucosamine) and levoglucosan (1,6-anhydro- β -D-glucopyranose);
8. choline.

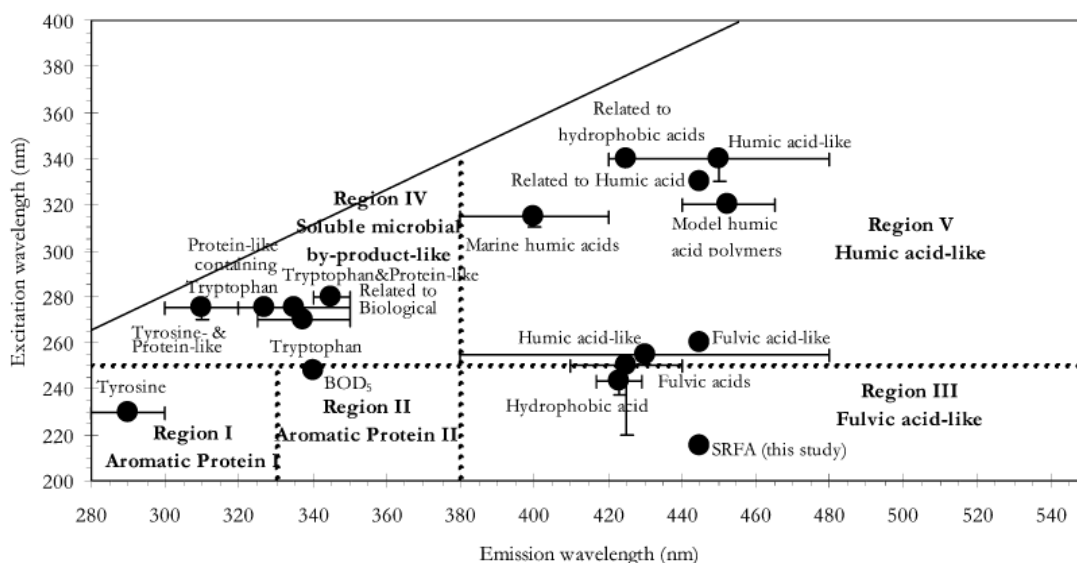


Fig. 2.3. A schematic for interpretation of fluorescence excitation-emission matrices (with regions occupied by particular organic matter types).

Source: Chen et al. (2003), reprinted with permission.

Grannas et al. (2006) have identified the following groups of compounds in the Franz Josef Land ice core: saturated lipids, protein, lignin, tannin, black carbon and a small amount of carbohydrate and amino sugar. A number of compounds with sulphur heteroatoms was also identified, including some not formerly described in the natural environment, large (C_{17} – C_{45}) organic sulphur species, which were interpreted as either direct anthropogenic emissions or the product of reactions of atmospheric sulphur dioxide with the HULIS (humic-like substances) aerosol. The proteins and humic-like substances were also reported frequently as a result of fluorescence EEMs analysis coupled to PARAFAC modelling, with a usual dominance of proteinaceous fluorescence (Barker et al., 2009, 2010; Dubnick et al., 2010; Fellman et al., 2010) at a proportion exceeding 80% of total fluorescence (Pautler et al., 2012; Stubbins et al., 2012). However, Stubbins et al. (2012) have also shown (using FTICR-MS technique for samples from an Alaskan glacier), that the majority of organic compounds in the ice were aliphatic, thus not fluorescent and not showing on the diagrams of the type presented in Figure 2.3. This

result has been reproduced in a different location and with a different technique. Namely, Xu et al. (2013) applied HR-ToF-AMS (Aerodyne high resolution time-of-flight aerosol mass spectrometer) to obtain snow characteristics on the Jima Yangzong glacier in the central Himalayas, and identified the mass contributions of particular elements and ion categories to the bulk of OM studied. This revealed the carbon content of the OM in snow on a Himalayan glacier to be between 55% and 67% (in winter/spring and summer, respectively), with the dominance of ion categories $C_xH_y^+$ (32 or 57%, depending on the season) and $C_xH_yO_1^+$ (36 or 17 %, respectively). The latter finding corroborates with the dominance of aliphatic compounds (Stubbins et al., 2012) in the OM input to glaciers, particularly if located relatively close to anthropogenic pollution sources. Only a small contribution of the ion categories found on the Jima Yangzong glacier (about 5% in both seasons) contained nitrogen heteroatoms, so could possibly be proteinaceous or originate from burned biomass. In contrast to those findings, Bhatia et al. (2010) described the supraglacial snow and meltwater samples from Greenland to contain mainly compounds with heteroatoms: predominantly nitrogen, sometimes accompanied by sulphur or phosphorus. The relative contribution of nitrogen in those samples can be also expressed as N:C ratios, which were between 0.27-0.33 for the samples collected by Bhatia et al. (2010) (C:N ratios of 3.0-3.7). In the study by Grannas et al. (2006) the nitrogen contribution was three to six times smaller than Bhatia et al's (occasionally even below that level). Again, this tallies with the evidence for *in situ* sources dominating the glacial OM composition in the Greenlandic interior, in contrast to the glaciated areas located a shorter distance from vegetated and populated land.

One way to comprehensively describe the character of OM contained in ice is to use the Van Krevelen diagram (a 2D diagram with O/C ratio on the x-axis and H/C ratio on the y-axis, see Fig. 2.4.). This was used by Grannas et al. (2006), Bhatia et al. (2010) and Singer et al. (2012) to describe glacial samples from Franz Josef Land, Greenland and the European Alps, respectively. These three areas show a broadly similar composition of OM, with the large contributions of lipids, proteins, lignin and tannin/terrestrial DOM in subglacial samples from Greenland, Alpine ice and the older layers of the Franz Josef Land ice core (AD 1300). The newer sample (AD 1950) in this location had an addition of black carbon/soot derived OM, similarly to supraglacial meltwater from the GrIS. Carbohydrates/amino sugars were present in the samples from all three regions, but in smaller amounts. The subglacial samples in Bhatia et al's (2010) study have shown a higher proportion of the 'terrestrial' DOM component (39.2-55.8%), while the highest lipid (4.7%) and protein contents (27.0%) were found in the supraglacial sample collected from a water pond within 1 km from the ice sheet margin.

Aside from the OM entrained into ice and supplied with snow, glaciers are covered with a discontinuous layer of organic-rich debris, hosting the cryoconite ecosystem (Fig. 2.5.). The

composition of the OM in this media is characteristic for a biologically active environment, containing extracellular polymeric substances (EPS), rich in polysaccharides (Hodson et al., 2010b; Langford et al., 2010), besides live and dead cells.

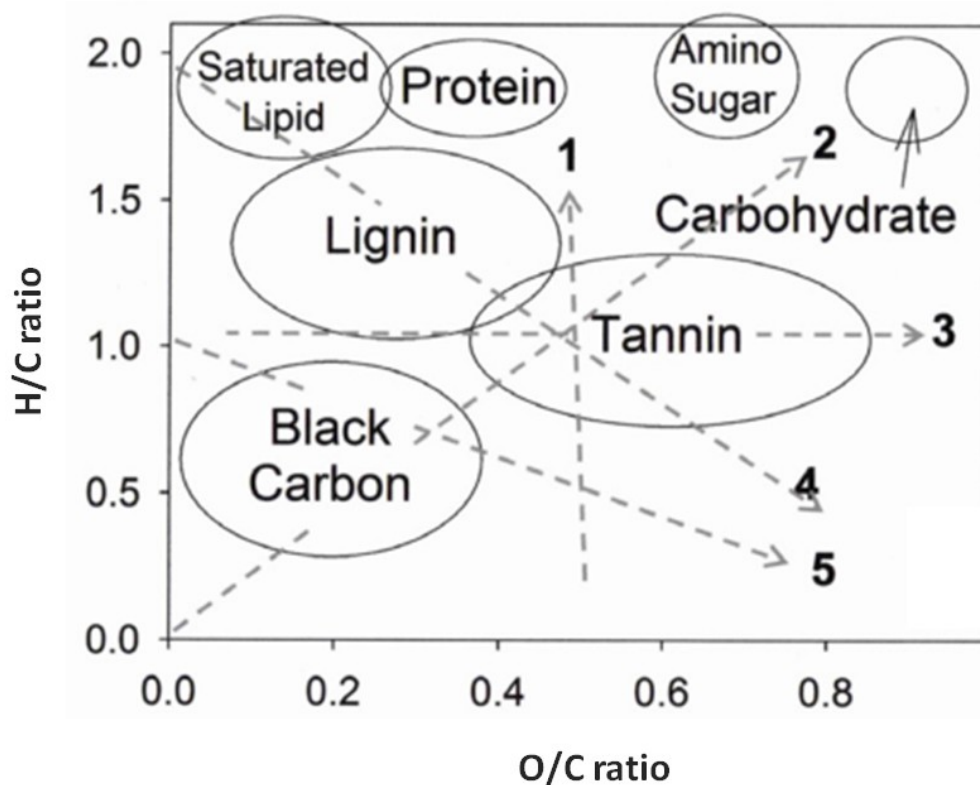


Fig. 2.4. A schematic of a Van Krevelen diagram, with regions highlighted that are occupied by different OM types.

Source: Grannas et al. (2006). The numbered arrows correspond to chemical reactions: 1 - hydrogenation or dehydrogenation; 2 - hydration or condensation; 3 - oxidation or reduction; 4 - methylation, demethylation or alkyl chain elongation; 5 - carboxylation or decarboxylation. Reprinted with permission.

A further characterisation of the cryoconite OM can be achieved by providing its elemental ratios. The C:N mass ratio of 12.98 (SD \pm 1.12) was reported for the Longyearbreen supraglacial sediment (Svalbard; Hodson, Cameron, et al. 2010), while Margesin et al. (2002) obtained ratios ranging from 20 to 40 in only three cryoconite samples, collected in the same area of the Stubaier Glacier (Tyrolean Alps). Šabacká et al. (2012) report the molar C:N ratio close to 7 for Antarctic cryoconite samples taken on Commonwealth, Canada and Taylor Glaciers in the McMurdo Dry Valleys area, which indicates the OM descent from an actively growing ecosystem, in contrast to the higher ratios found in allochthonous material. However, the supraglacial debris may show molar ratios exceeding that up to several times, yielding 8-9 in Greenland samples (Stibal et al., 2010), 11-13 on Werenskiöldbreen, Svalbard (Stibal et al.,

2006, 2008b), 8.9-14.2 on a sample of Tibetan and Himalayan glaciers (Takeuchi, 2002a), and reaching a single-cryoconite-hole value of 105.5 (reported from Foxfonna, Svalbard by Cameron et al. 2012).



Fig. 2.5. Cryoconite debris accumulated on the surface of Foxfonna glacier, including reindeer bones that have melted out of the ice.

Photo by the author

The most comprehensive characterisation of cryoconite OM to date has been performed by Xu et al. (2010), who used OM biomarkers and NMR techniques for this purpose. The main biomarkers found in the cryoconite matter were fatty acids, alkanols, alkanes, sterols and wax esters; other compound groups were also found, including *n*-alkenes, *n*-alkan-2-ones, and sugar derivatives. The fatty acid group was dominated by normal, branched, mono- and polyunsaturated fatty acids. Both the *n*-fatty acids (C_{12} – C_{30}) and *n*-alkanols (C_{14} – C_{30}) displayed an even/odd carbon number predominance, while *n*-alkanes (C_{17} – C_{31}) showed an odd/even carbon number predominance. The long chain fatty acids ($n > 20$) can be interpreted as originating from higher plants or moss, but the lack of detection of plant-derived lignin phenols contradicted the vascular plant origin hypothesis. The *n*-alkanes composition, with the carbon chains of 23–27 atoms dominating, supported the notion that the allochthonous OM in cryoconite mainly originates from mosses and lichens. There were also biomarkers identified (in smaller concentrations), which are connected to biomass burning (levoglucosan) and bacterial/fungal presence (trehalose). The NMR results highlighted the dominance of alkyl

carbon and the importance of carbohydrates and peptides in the cryoconite chemical composition, while the phenolic compounds connected to plant lignin were less abundant. In brief, the chemical composition of the cryoconite OM was broadly similar to the composition of the OM contained in glacial ice, with signatures of autochthonous microbial activity and aliphatic hydrocarbons which might be anthropogenic. Allochthonous plant material was also present, mostly derived from non-vascular plants, so possibly from short windborne transport.

Despite a recent growth in recognition of OM characteristics in the glacial domain, some issues remain underexplored, probably due to analytical capacity and financial constraints. In particular, the most promising techniques that 'scan' the spectrum of OM contained in the sample (FTICR-MS, NMR) are still costly to use, and therefore only a small number of samples can be analysed. This hinders the recognition of local and regional variability, which would better explain the issues of OM origin and fate in the glacial system. The same restriction applies to constraining OM age using radiocarbon dating, which is also limited by the interference of multiple OM types of different age and origin in one sample. This latter problem has received relatively little attention, yet is potentially important due to the possibility of change in the OM age arising from its reworking in the englacial and subglacial environment by microorganisms. It remains a puzzle to what extent the methane and other organic compounds found in the ice cores reflect their exact atmospheric composition at the time when the contact between the air pockets in snow and the ambient atmosphere ceased. This is partly due to it having been shown that the gaseous composition of ice cores may be changed by the presence of an ecosystem (Rohde et al., 2008; Tung et al., 2005).

2.3.3. Impacts of glacial organic matter on the wider environment

The OM released from glaciers may influence the ecosystems downstream, particularly as they continue to lose ice mass at a rapid pace. This impact can be expressed as seeding the forefield with cells, providing nutrients for terrestrial and marine ecosystems, and pollutant release. The evidence for those processes has only been gathered in the past decade.

The cell supply from a glacier to its the forefield has not yet been explicitly shown, however there are many facts to support this phenomenon indirectly. For example, there was a strong flux of cells found in a supraglacial catchment runoff (1.08×10^7 cells $m^{-2} h^{-1}$) in a budget study of a small supraglacial catchment by Irvine-Fynn et al. (2012). Also, the microbial diversity in a recently deglaciated terrain has been shown to be very high: in only 5-year-old part of a proglacial chronosequence, Schütte et al. (2010) found 4000 bacterial phylotypes in 0.5 g of soil; after 150 years of succession, this number increased to 7050. Also the abundance of cells increased along a chronosequence, by about 2 orders of magnitude in 100 years, starting at a level of 3.69×10^7 ($\pm 7.95 \times 10^6$) in 0-years-old soil (Sigler et al., 2002). Bacteria were found to

colonise the glacial forefield before plants and fungi (Bernasconi et al., 2011), and then subsequently their community changes as plants advance. The recently exposed areas show higher culturability of bacterial phyla found in them at 4°C, while the older soils are characterised by better culturability in 25°C (Liu et al., 2012). There is also a shift from the predominance of methanogenesis to methane oxidation as the deglaciated terrain becomes older (Barcena et al., 2010). Another link between the glacial and neighbouring proglacial microbial community is the adaptability of glacial viruses to infect proglacial lake bacteria (Anesio et al., 2007). The supraglacial microbial community is a likely source of the proglacial one, particularly as the organisms found on the glacier surface are of opportunistic type, with strong colonising potential, rather than niche-specific phyla. It is also a better developed ecosystem than the one found on glacial moraines (Stibal et al., 2006), with greater similarity in terms of physico-chemical properties (texture, pH, water and OM content) to the vegetated soil than to barren moraine or subglacial sediment (Kaštovská et al., 2007). The similarities found and the surprisingly high level of microbial community development on a recently deglaciated terrain suggests that glaciers play an important part in seeding life to their forefields, particularly when losing ice mass.

The carbonaceous nutrient release from glaciers has been most extensively shown by Fellman et al. (2010), who incubated the proglacial riverine water with the *in situ* and marine microbial community, proving that the latter uses more of these nutrients than the former community. The documented presence of labile DOC in proglacial rivers (Hood et al., 2009) and their relative abundance in nitrogen-rich OM (Hood and Berner, 2009) show the potential impact of glacial runoff on the riverine and marine ecosystems. Still, the direct link to the supraglacial, subglacial or englacial source of this organic material has yet to be investigated. This closer link has been tentatively established in the studies concentrating on OM characteristics of meltwater and ice (Singer et al., 2012; Stubbins et al., 2012), but the processes transferring the labile OM from the input to the output of the glacial system remain underexplored. There is also a relative paucity of information on the impact of glacial OC on the terrestrial ecosystem in their forefield, as opposed to the better studied aquatic ecosystem reaction. The magnitude and timescale on which these impacts work is still a widely unknown field.

The recently discovered impact of glacier-derived OM on their forefields is also their potential to become secondary pollutant sources. A comprehensive case study of this effect has been undertaken in the Swiss Alps. Bogdal et al. (2009) have observed the pattern of persistent organic pollutants (POPs) deposition in a proglacial lake Oberaar, finding their dynamics to be consistent with the atmospheric emissions' variability in the 1950s-1990s time period, in contrast to a sharp increase afterwards with no parallel in the atmospheric record.

This was hypothesised to result from the rapid melting of the Oberaargletscher upstream from the lake, which acted as a secondary pollutant source and supplied concentrations of organochlorines exceeding those noted in 1960s and 1970s sediment. The recent peak in POPs concentrations has not been found in low-altitude Swiss lakes (Bogdal et al., 2008, 2010b), diminishing the probability for these compounds to come from an unaccounted for atmospheric source. The thesis about glacial origin of PCBs or DDT was expanded into a conceptual model, using glacier flow modelling (Bogdal et al., 2010a). It was also confirmed by a study on two lakes located in nearby (8 km distance) catchments, only one of which was glaciated (Schmid et al., 2011). Elsewhere, the glacial release of pollutants is also considered a plausible explanation for high levels of DDT in Adelie penguin tissue in circum-Antarctic waters (Geisz et al., 2008). Also, in Svalbard fjord waters, the compounds: *trans*- and *cis*-chlordane, *trans*-nonachlor and oxychlordane were linked to the potential source in melting glaciers (Carlsson et al., 2012). However, the extent of the influence of the glacial POPs source has yet to be established elsewhere, particularly on polar glaciers with much longer residence time of pollutants (Hodson, 2014). It is a potentially important global store, especially as the primary emissions are diminished. Hopefully, improved analytical techniques will enhance the interpretation of secondary POPs emissions, e.g. by investigation of the chirality of non-racemic compound mixtures, which would indicate the extent of the biodegradation since the moment of primary emission (Bidleman et al., 2013).

2.4. Glacial organic carbon studies: partial flux estimates and supraglacial processes

In the context of the still underexplored, but potentially important influence of glacial OM on the proglacial areas and the wider biosphere, it is essential to expand the existing knowledge on the processes which may change the OM release dynamics in glacial settings. Currently, little is still known about the glacial part of the OC cycle. Its components have been only opportunistically quantified, without attempting to budget them on any single glacier. These partial fluxes and the processes connected to those are revised below.

The existing literature provides some information on the atmospheric input of organic matter to glaciers, its biological re-working and the output with meltwater. It is also recognised that some of the OM is stored on glaciers (Fig. 2.6). These processes will be the main focus here. Besides those, the organic matter entrained in the ice would undergo englacial transport, and some of the atmospheric input from snow or dust deposition is likely to be removed by the wind. The englacial mode of transportation may be important when viewed in the long term, however in a budget year it is unlikely to change the OC content of the glacier significantly, particularly on a slow moving, cold-based glacier. The wind redistribution process

is very difficult to measure and is usually already accounted for if aged snow layers are sampled. Finally, chemical reactions might lead to OM decomposition on the glacier surface, but their impact on the budget can also be minimised by considering the ‘net’ atmospheric contribution from the snow cover prior to melting. This impact will be reviewed here alongside atmospheric deposition studies.

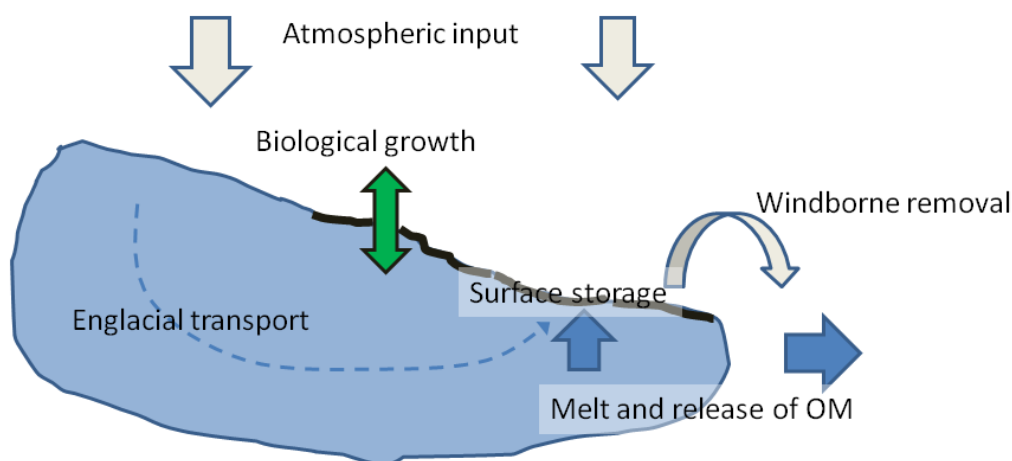


Fig. 2.6. A schematic of recognised and hypothetical organic carbon fluxes in a glacial setting.

2.4.1. The atmospheric supply of organic carbon

The atmospheric deposition of carbonaceous matter on glaciers has mainly been studied by tracking records of past atmospheric pollution through ice core analysis (e.g. Fuoco et al., 2012; Villa et al., 2003), and occasionally by snow sample collection (e.g. Kwok et al., 2013). Of particular interest recently is the deposition of dark OM in snow, including HULIS (humic-like substances) and soot-derived compounds. Sometimes these organic compounds are hidden in the general term of *black carbon*, because of their impact on the glacier albedo and melt dynamics. Since this causes ambiguity on the chemical composition of the light-absorbing species, the term *brown carbon* was coined for dark organic compounds. However, some published estimates of black carbon concentration in snow describe the two components together. The bulk BC in Nepalese Himalaya was estimated to deposit from the atmosphere at a rate of $2.89 \mu\text{g m}^{-2} \text{day}^{-1}$ (Yasunari et al., 2010). Its concentrations in Arctic snow were gathered by Doherty et al. (2010), with the medians for various regions ranging from 3 ng g^{-1} in Greenland to 26 ng g^{-1} in Western Arctic Russia. Svalbard snow was shown in the same study to exhibit a concentration in the midst of this spectrum, at the median level of 13 ng g^{-1} .

Another chemical species quantified in glaciers is organic acid ions, usually analysed in ice cores to provide past depositional records. For instance, Legrand et al. (2003) described

formate and acetate deposition recorded in a French Alpine ice core. In the summer layers, a uniform level of concentration of formate was found (80 ± 20 ppb), alongside changing levels of acetate (15 ppb before 1950, a threefold increase, and a subsequent drop in the 1980s). A higher concentration of formate was found in the Belukha ice core from Altai (Olivier et al., 2003) in a record corresponding to the period 1940–2000 ($4.6 \mu\text{eq L}^{-1}$, equal to approximately 207 ppb), and oxalate was also found in the same core ($0.4 \mu\text{eq L}^{-1}$). An ice core from Úrúmqi glacier no. 1, Tianshan (Li et al., 2001), has contained the three above mentioned ions and pyruvate as well, at the following concentrations: 102.8 ± 147.3 ppb (formate), 392.3 ± 390.8 ppb (acetate), 6.9 ± 14.8 ppb (oxalate) and 4.2 ± 8.3 ppb (pyruvate). The concentrations of formate and acetate measured there exceeded the Greenlandic ice core concentrations by 10 and 54 times, respectively (Greenlandic mean concentrations equalling 9.4 ± 15.5 ppb for formate and 7.3 ± 2.7 ppb for acetate; Legrand and Angelis 1996). In the Antarctic, formate concentrations measured approximately 100 times lower than in Tianshan (0.1–1.22 ppb), and acetate – 3000 times lower (<0.15 ppb; Legrand and Saigne 1988). On the other hand, the ice cores retrieved from both ice sheets contained MSA (at levels of 0.5–5.0 ppb for Greenland and 2.53–5.33 ppb for Antarctic Ice Sheet; Legrand and Saigne 1988; Legrand et al. 1993) in contrast to the Asian ice core, but they did not contain the pyruvate detected in Glacier No. 1 (Li et al., 2001). On the Tibetan Plateau, another ice core was obtained (Mt. Muztagata Glacier) that showed levels of formate of 186.6 ± 160.1 ppb and acetate of 136.4 ± 133.9 ppb (Wang et al., 2004).

A further group of organic chemicals traced quantitatively in glacial ice, are persistent organic pollutants (POPs), the presence of which raises high concern in cold regions due to their long-lasting impact on the environment, including biomagnification in the food chain (see review by Kozak et al., 2013). Interestingly, the deposition of these dates back to before the Industrial Revolution, as PAHs (polycyclic aromatic hydrocarbons) and PCBs (polychlorinated biphenyls) concentration peaks were found in an Antarctic ice core corresponding to volcanic eruptions in the period 1600–1930, including the Tambora 1815 event (Fuoco et al., 2012). Nevertheless, the industrial increase in POPs concentration has been widely observed. For example, Villa et al. (2003), while studying the European Alpine Lys glacier, have noted maximum concentrations of 20 ng L^{-1} for both α - and γ -HCHs (hexachlorocyclohexanes) and 1 ng L^{-1} of HCB (hexachlorobenzene) within the period 1955–1996, while the most recent ice core layer has contained only 1 and 0.5 ng L^{-1} , respectively (1994–1996 layer). The deposition in snow at the time their fieldwork was conducted (in 2000) was at the level of 1 and 0.03 ng L^{-1} for those compound classes. The concentration of p,p'-DDT (dichlorodiphenyl trichloroethane) has also decreased from the maximum in the ice core of 10 ng L^{-1} to 0.5 ng L^{-1} in the fresh snow collected then. The concentrations measured in the ice core and snow were equivalent to

deposition fluxes of 1.1-36.5 $\mu\text{g } \alpha\text{-HCH m}^{-2} \text{ a}^{-1}$, <1.0-33.0 $\mu\text{g } \gamma\text{-HCH m}^{-2} \text{ a}^{-1}$, 0.2-0.9 $\mu\text{g HCBs m}^{-2} \text{ a}^{-1}$ and 0.3-13.3 $\mu\text{g p,p'-DDT m}^{-2} \text{ a}^{-1}$.

Industrial maxima were also observed in a Himalayan ice core from the East Rongbuk glacier by Wang et al. (2008b), DDT flux peaking in 1974 at 2.2 $\text{ng cm}^{-2} \text{ a}^{-1}$ and $\alpha\text{-HCH}$ flux reaching 1.0 $\text{ng cm}^{-2} \text{ a}^{-1}$ in 1971. PAHs maxima were noted in the 1990s at a level of up to 4 $\text{ng cm}^{-2} \text{ a}^{-1}$ (phenanthrene). At the same field site, Kang et al. (2009) have found the dominance of $\gamma\text{-HCH}$ and $\alpha\text{-HCH}$ above the PCBs and DDTs, however PCB concentrations were non-negligible either (e.g. PCB-28 detected at concentration levels of 17 pg L^{-1} , which is 20% of the $\alpha\text{-HCH}$ concentration found there). Clear depositional patterns were detected by these authors, most probably connected to the supply from different contaminant source regions. In another Himalayan glacier, Dasuopu, X. Wang et al. (2008) have measured up to 35 $\text{pg PCB-28 cm}^{-2} \text{ a}^{-1}$ (in 2001), the most recent (2004) flux of this congener equivalent to 18 $\text{pg cm}^{-2} \text{ a}^{-1}$. The respective fluxes for ΣDDTs were 31 $\text{pg cm}^{-2} \text{ a}^{-1}$ at most (in 2000) and 16 $\text{pg cm}^{-2} \text{ a}^{-1}$ most recently (in 2004). The most abundant PAH in these ice core samples was acenaphthene, with fluxes up to 2 $\text{ng cm}^{-2} \text{ a}^{-1}$ (in 2000). By 2004, all PAHs constituent fluxes decreased below 20 $\text{pg cm}^{-2} \text{ a}^{-1}$. In the Arctic, anthropogenic ΣPCB fluxes were found in an ice core from the Lomonosovfonna ice cap in Svalbard (Garmash et al., 2013), with a peak flux of $\sim 19 \text{ pg cm}^{-2} \text{ a}^{-1}$ recorded in the layer from 1957-1966, 1974-1983, 1998-2009 and 2009-2010. In the same archipelago, on Longyearbreen glacier, deposition fluxes of PFASs (Perfluoroalkyl substances) were quantified for the first time on any glacier. These fluxes were however very small, not exceeding 1 $\text{pg m}^{-2} \text{ a}^{-1}$ for any of the compounds within this group in the layers correspondent to the years 1990-2004 (Kwok et al., 2013).

Although a useful proxy for atmospheric deposition, the fluxes calculated for the ice samples would not be representative for the initial input with snow, due to up to 90% post-depositional volatilisation losses of organic pollutants. According to Villa et al. (2003), the processes which change the final concentration of organochlorine compounds in the ice cores are, besides volatilisation, the initial photolysis, freeze-thaw and firnification processes, sorption and leaching into deep ice.

In particular, photodegradation is a potentially important chemical sink of a broad range of organic species on glaciers. However, the overall impact of this process on the organic matter in glacial snow is difficult to establish without the full composition information. The photolysis may be both source and sink to organic compounds (e.g. for HCHO, Chen et al. 2007). The photochemically active compounds are likely to have short lifetimes in the sunlit snow cover (e.g. for formaldehyde, modelled for 2.1-12.1 hours by Chen et al. (2007)). Examples of photochemically derived fluxes from snowpack to atmosphere are provided by Boudries et al. (2002) from a Canadian field campaign ALERT2000: acetaldehyde, acetone and methanol were

found to emit at rates of 26, 7.5 and 3.2×10^8 molecules $\text{cm}^{-2} \text{s}^{-1}$, respectively, during the hours of sunshine. If degassing is efficient, this would limit the lifetime of those compounds in the snow cover to 2 days. Other organic species likely to be photodegraded are CH_4 and other hydrocarbons (NMHC; Chen et al. 2007), POPs and HULIS (Voisin et al., 2012), but the rate of their decay is largely unknown. The best study so far, which estimates the net carbon removal into the atmosphere from snowpack during sunlit hours, is by Voisin et al. (2012), and their estimate amounts to a loss of 30–220 $\mu\text{g C m}^{-2} \text{h}^{-1}$ (cumulative flux of CO , CO_2 and volatile organic compounds, VOCs).

Besides deposition in snow, rainwater and windblown dust may also be a source of organic matter on glaciers, yet the studies on these factors on glaciers are virtually non-existent. The closest work done regarding the windborne material is by Šabacká et al. (2012), who have measured the aeolian POC deposition in Taylor Valley, Antarctica, but concentrated on lakes rather than glaciers. The sediment deposited there had the carbon content of $0.119 \pm 0.05 \text{mg C g}^{-1} \text{dw}$ (dry weight) and OM content of $0.25 \pm 0.06\% \text{dw}$. This resulted in variable PC fluxes for the three locations, medians amounting to between 0 and $30 \text{mg m}^{-2} \text{a}^{-1}$, and maximum annual flux exceeding $400 \text{mg m}^{-2} \text{a}^{-1}$. Among organic matter types, only the deposition of cells was estimated during the melt season in a supraglacial catchment by Irvine-Fynn et al. (2012), with a flux of $4.69 \times 10^7 \text{cells m}^{-2} \text{h}^{-1}$. This measurement is likely to represent a mixture of dry and wet deposition in the summer due to the applied methodology.

2.4.2. Organic matter removal with runoff

There are limited records of the release of OC with meltwater, from world-wide glaciers, with the highest DOC concentrations in proglacial rivers, sometimes far away from the actual glacial source. These have been measured by Bhatia et al. (2013), Downes et al. (1986), Hood and Berner (2009) and Lafrenière and Sharp (2011), and reported at mean annual concentration levels between 0.1 and 4.1 ppm DOC. Bhatia et al. (2013) have also observed an important difference between the meltwater DOC content when it originated predominantly from subglacial discharge (0.5–4.1 ppm) and when it was mainly supraglacially fed (0.1–0.6 ppm). The POC export from the Greenland Ice Sheet, on the other hand, was found to be governed by a different pattern, with concentrations ranging 4.1–13.2 ppm throughout the melt season (Bhatia et al., 2013).

The flux information for the OC release from glaciers themselves is more difficult to obtain due to constraints of measuring discharge in rapidly flowing, dynamically changing proglacial rivers. Nevertheless, the general interest in bulk quantity discharged to the downstream environment encourages estimations and extrapolations. Lawson et al. (2014) report fluxes from the Leverett Glacier of $0.56 \text{Gg DOC a}^{-1}$ in 2009 and $0.52 \text{Gg DOC a}^{-1}$ in 2010,

approximated by an area-weighted value of $0.9 \text{ g DOC m}^{-2} \text{ a}^{-1}$. These results, scaled up to the Greenland Ice Sheet size, result in a flux of $0.13\text{--}0.17 \text{ Tg DOC a}^{-1}$, which is approximately double the Bhatia et al's (2013) estimation of $0.08 \text{ Tg DOC a}^{-1}$. The respective POC flux would amount to $0.36\text{--}1.52 \text{ Tg POC a}^{-1}$, which is in line with Bhatia et al's (2013) $0.9 \text{ Tg POC a}^{-1}$ estimate. These figures quantitatively match the estimate provided by Hood et al. (2009) for the overall DOC contribution of glacially derived drainage to the Gulf of Alaska, amounting to $0.13 \pm 0.01 \text{ Tg C a}^{-1}$ (area-weighted flux of $1650 \pm 160 \text{ kg DOC km}^{-2} \text{ a}^{-1}$). The European Alpine glaciers, on the other hand, were found to contribute a similar amount to the Greenlandic Leverett Glacier alone ($0.34 \text{ Gg DOC a}^{-1}$; Singer et al. 2012). This is equivalent to $0.17 \text{ g DOC m}^{-2} \text{ a}^{-1}$, an order of magnitude smaller flux (area-weighted) than the one reported in Alaska, and about 5 times smaller than the flux reported by Lawson et al (2014) in Greenland. It is difficult to attribute this high difference in fluxes to industrial ice contamination variability, and hence further research is needed to understand this discrepancy in a glaciological context.

In some studies, concentrations or fluxes of particular organic chemicals are reported in proglacial waters, rather than, or in addition to bulk DOC. Examples include Lawson et al's (2014) estimates of free carbohydrate fluxes from the Greenland Ice Sheet of $0.041 \text{ Gg OC a}^{-1}$ in 2009 and $0.069 \text{ Gg OC a}^{-1}$ in 2010, and Kwok et al's (2013) report on PFAS concentrations in Longyearbreen proglacial river in Svalbard. In the latter study, PFOA and PFOS were found at levels below 1 ng L^{-1} , and PFBA was shown to exceed 1 ng L^{-1} in some water samples. Other PFAS were also detected, at lower concentration levels. Fluxes into lake sediment were also reported for a wide range of organic pollutants by Bogdal et al. (2009); ΣPCB , ΣDDT , dieldrin, HCB, $\gamma\text{-HCH}$, Σ synthetic musk fragrances and other POPs were all transferred into a Swiss Alpine glacier forefield at various levels between detection limit and $200 \mu\text{g m}^{-2} \text{ a}^{-1}$.

A further insight into the liberation of OM from glaciers can be gained from melt process studies conducted in snow. The best example to date is the modelling work performed by Meyer & Wania (2011), where they distinguished 4 types of elution behaviour (Fig. 2.7.). The organic species may be dissolved in meltwater (e.g. chlorothalonil), sorbed to ice interface (chlorpyrifos), sorbed to OM (PCB-180), or show a mixed behaviour (like fluorene). In case of the first type of behaviour, the chemical species is removed from snowpack early, while the compounds sorbed to OM remain in snow for longest periods. This pattern not only reveals the capacity of organic particles to accumulate the otherwise mobile chemicals, but also speaks for their own long residence time in the melting snowpack. Some of the organic particles may even be retained *in situ* after the removal of snow cover. In a glacial system, this may mean their inclusion in the supraglacial debris, or that they undergo refreezing on the glacier surface. This, however, has not been described to date in a quantitative way.

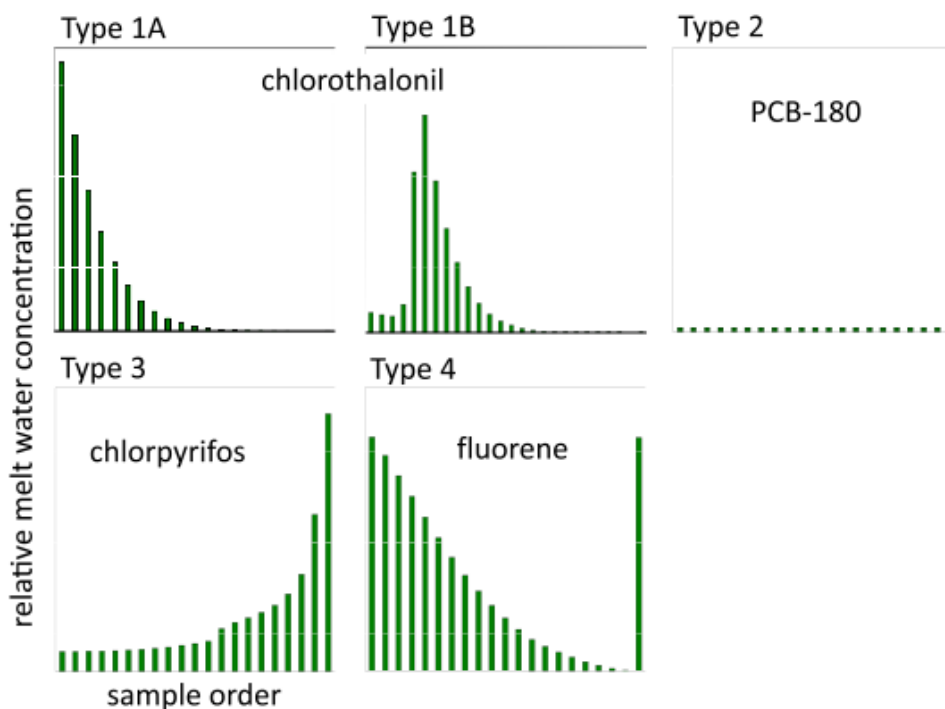


Fig. 2.7. Elution sequences for different chemicals according to Meyer and Wania (2011). Type 1 – dissolved chemicals, Type 2 – compounds associated with particle and snow grain surfaces, Type 3 – somewhat water soluble chemicals, associated with snow grain surface, Type 4 – combined enrichment type. Reprinted with permission.

2.4.3. The impact of biological activity on glaciers on the organic carbon fluxes

The supraglacial layer, which is both particle and organic-rich, is known for its intensive biological activity, both in snow (Amato et al., 2007; Takeuchi, 2001, 2004; Takeuchi et al., 2006) and the accumulated debris (Anesio et al., 2010; Sävström et al., 2002). Neighbouring this supraglacial ecosystem are the less explored englacial and subglacial ecosystems (Dong et al., 2012; Lanoil et al., 2009; Stibal et al., 2012a; Tung et al., 2005; see also Section 2.2.5). The supraglacial ecosystem provides a significant OM flux each year during the summer season, globally fixing an estimated quantity of 64 Gg C (Anesio et al., 2009). However, measurements for this ecosystem's productivity are subject to high uncertainty; Anesio et al. (2009) found 1 SD of the measured values on one glacier constituted between 6.4% and 40.9% of the average value on the respiration, and between 49.0% and 111.6% of the primary productivity measurements. Another study of the glacial ecosystem productivity rates, with measurements taken from a selection of Svalbard glaciers (Telling et al., 2010), reports a global negative flux of carbon from the microbial community there, with the average of $-1.3 \mu\text{g C g}^{-1} \text{d}^{-1}$. Hodson, Bøggild, et al. (2010) estimate the photosynthesis and respiration fluxes from the Greenland Ice Sheet for the order of magnitude of 10^1 – 10^2 Gg C a^{-1} . Despite the study result being a net source of respired carbon, the authors express reasonable doubts about the magnitude of the

photosynthesis flux. Thus, the role of glacial microbial communities in the carbon cycle remains poorly understood. It would be beneficial to apply the studies on microbial activity controls (Stibal et al., 2012b; Telling et al., 2012) in a spatial context, in order to estimate the global fluxes in a more detailed way, as did Cook et al. (2012) for GrIS. The variables important in this context are OC concentration in sediment and its layer thickness (Telling et al., 2012). Also, the comparison to other fluxes in a single glacial system would place the existing flux estimates into context.

2.4.4. Glacial storage of organic matter

The storage of OM on glaciers is the least recognised part of their OC cycle; virtually no estimations of it have been gathered to date. Hodson et al. (2007) calculated the supraglacial debris cover on Midtre Lovénbreen, using photographs acquired by UAV (unmanned aerial vehicle), obtaining 0.42% coverage (4600 kg debris km⁻²). This was upscaled using the ratio between ground-based survey results and the aerial photographs, which resulted in the final coverage of 1.23% and the dry cryoconite mass density amounting to 10600 kg km⁻². However, only the bacterial production and respiration rates were measured, but not the OC content of this sediment, and therefore the storage of OC on Midtre Lovénbreen is impossible to obtain from those data.

Telling et al. (2012) measured the respective OC content value for three other Svalbard glaciers. These were Midtre Lovénbreen, Austre and Vestre Brøggerbreen, at levels of 20.1 mg TOC g⁻¹, 17.3 and 33.9 mg TOC g⁻¹ respectively. From this, the supraglacial storage of OC on Midtre Lovénbreen can be estimated for 0.213 g TOC m⁻² (or 213 kg TOC km⁻²). However, even on the same glaciers, a variable range of OC content may be measured. For example, Telling et al. (2012) report those organic carbon contents to be in the range of 0.5-4.5%, while Edwards et al. (2011) provide the figure for organic matter content of the same set of glaciers at the level 1-16%. Elsewhere, the following organic matter fractions were reported in surface debris on Svalbard glaciers:

- 8% OM (SD ± 4.49%) and 2.03% OC (SD ± 0.53%) on Longyearbreen (Hodson et al., 2010b),
- 1.7–4.5% OC on Werenskiöldbreen (Stibal et al., 2008a),
- 4.37% OC on Austre Brøggerbreen (Takeuchi, 2002a).

On the Greenland Ice Sheet, the Kangerlussuaq marginal zone, Kangerlussuaq blue ice zone and Thule Ramp showed percentages of 1.9 ± 0.8, 7.1 ± 3.3 and 16.6 ± 3.0 respectively for OM in debris (Hodson et al., 2010a). Higher values are provided by Gerdel and Drouet (1960) for the Greenlandic supraglacial debris, amounting to 13.2–20.1% OM by dry weight. Takeuchi (2002) also describes the organic content of Himalayan and Tibetan glaciers' cryoconite, as

being 3.0-13.2% OM and 0.54-3.71% OC (in a sample of 6 glaciers). For two glaciers in the Canadian Arctic, he provides OM percentages of 11.4 and 11.6 (2.06 and 2.22% OC, respectively). On the Athabasca Glacier in the Canadian Rocky Mountains, Xu et al. (2010) report $10.4 \pm 0.3\%$ TOC in cryoconite. The Alpine cryoconite (collected in the Tyrolean Alps) contained 0.8-1.8% total carbon, with inorganic carbon contributing 0.23-0.35% of that quantity (Margesin et al., 2002). Thus, the percentages of 0.5-4.5% OC noted for Svalbard glaciers' cryoconite span a similar range to the variability described at a global scale.

Another type of storage in glaciers, that is rarely accounted for, is the englacial content of OC. This can only be based on extrapolations from ice core data, e.g. Priscu et al's (2008) global estimation of 15.4 Pg OC. Hood et al. (2015), based on a similar principle, estimate the OC storage in the Antarctic Ice Sheet for 6 Pg (or up to 8.4 Pg, depending on the method employed and input data choice). X. P. Wang et al. (2008) provide DDT and α -HCH content of all Himalayan glaciers based on this concept, equalling 414 kg of DDT and 1382 kg of α -HCH. These estimations are rarely made, and unfortunately, there is a paucity of data to base them upon, since most studies report compound concentrations in ice core layers in a detailed way, yet the layer thickness and density information is described less precisely. Therefore, our understanding of the physical properties of the sampled glaciers needs enhancing in order to obtain accurate storage calculations.

2.5. Research aims

Despite its broad and multifaceted impacts, the glacial OC cycle has been studied only fragmentarily, and therefore this research needs consolidating. In particular, no single glacier has been monitored simultaneously for the incoming and outgoing fluxes of OM, despite the potentially rewarding information on the glacial storage and residence time of OM that this would provide. The understanding of this cycle is also incomplete without the glaciological and hydrological information, which needs to be coupled to the chemical flux study. This thesis aims to fill this important research gap by a comprehensive study of two years of OC fluxes in a European High Arctic glacier. The presented thesis will be based on glaciological exploration of the Foxfonna ice cap (Svalbard), which has not been characterised in this context to date. Since the OC flux calculation is based both on the physical and biogeochemical characteristics of a system, the crucial physical overview of Foxfonna will be presented in Chapter 3. The estimated fluxes, provided in a supraglacial catchment, and their relation to one another, will then form the core of Chapter 4. The question naturally emerging is how the organic carbon fluxes interlink and where the storage of organic matter is most likely to happen on the glacier surface. This will be explored using a small-scale *in situ* experiment, and substituting time for space in Müller's (1962) supraglacial hydrological zones concept (Chapter 5). As a result, a

conceptual study on the glacial release and retention of organic matter is provided, spanning between the glacier-wide and an experimental plot scale.

It is anticipated that this thesis will help improve the understanding of organic carbon fluxes in the glacial environment. The following three research aims and detailed research objectives will lead to this result.

1. To characterise the glacial system of the small Arctic ice cap Foxfonna, to the extent which is crucial for understanding biogeochemical processes happening in this setting.

This issue will be addressed in Chapter 3, in particular:

- The mass balance of the glacier will be characterised thoroughly, providing a basis for comparison with other glaciers currently changing their thickness and extent.
- The glacier dynamics and thermal structure will be described in light of the existing data, which is also essential for understanding the type of system that this particular organic carbon study is applicable to.
- The key physical processes likely to influence the organic carbon fluxes will be identified for this setting.

2. To quantify organic carbon fluxes on the High-Arctic glacier Foxfonna, and link them to the current state of this glacier. This will be described in Chapter 4, with attention to the following points:

- Quantifying the atmospheric inputs of organic matter, with a division into fluxes in the accumulation and the ablation period.
- Estimating the outputs in riverine waters originating from glacier melt. As part of this aim, the disparity between the immediate flux from ice melt to glacier surface and from the glacier surface into its forefield will be quantified.
- Following the established balance between these two components, further possible processes will be characterised quantitatively, if needed to explain the disparity between these two factors (e.g., the role of live organisms on the glacier surface and organic matter storage in cryoconite deposits).

As a result of this work, the directions of the potential impact of OC fluxes on the glacier surface albedo change may also be characterised for the first time.

3. To characterise processes of organic carbon storage and removal in small scale, linking them to the development of the supraglacial hydrology in a vertical profile through snowpack and ice below the glacier ELA. As a result, the processes will be highlighted which are likely to remain important if more of the current glacier

surfaces shift into ablation zone. This issue, addressed in Chapter 5, will be split into the following problems.

- To describe the evolution of the glacier near-surface thermal profile and its effect on supraglacial hydrology, in particular with respect to the liquid water content of snow.
- To characterise the OC and cell content of different media on the glacier surface: pre-melt snow, wet snowpack, slush (water-saturated snow), superimposed ice and runoff waters.
- To explore the role of supraglacial hydrology in organic matter fluxes, in particular on the OM path from the atmospheric deposition to runoff waters.

The main expected research outcomes of this work are, therefore, to establish the link between the glacial system physical properties development and the organic matter fluxes in two scales: the supraglacial catchment and a point on the glacier surface. An expected outcome is a contribution to understanding the supraglacial organic carbon fluxes and the processes related to them.

Chapter 3. The glaciological characteristics of Foxfonna

Summary

Foxfonna is an ice cap located in Nordenskiöld Land, Svalbard, that has been only incidentally described in the published literature, e.g. by Liestøl (1974) and Rutter et al. (2011). Despite neighbouring an active mine corridor, the glacier appears to be hydrologically disconnected from it, in light of the limited available information. Foxfonna has experienced deeply negative mass balance in the years 1990–2012, having lost an average of 0.74 ± 0.10 m w.e. annually (data derived from direct and geodetic glaciological monitoring combined). The areas with highest mass loss were located in the lowest parts of the glacier tongue, registering locally above 1.5 m w.e. annual mass loss in the period 1990–2009, for which photogrammetric data were analysed. The surface ice velocities measured on Foxfonna indicate it to be an almost stagnant ice body, which is consistent with its predominantly cold thermal regime and small thickness. Foxfonna has therefore been found a relatively simple glacial system for supraglacial organic carbon budget monitoring, with very limited scope for possible water contact with glacier bed. A suitable surface catchment has been identified on its surface for the biogeochemical monitoring purposes.

3.1. Introduction

Foxfonna (coordinates: 78°07'-78°09'N; 16°06'-16°11'E) is an ice cap located in central Svalbard (Nordenskiöld Land, Fig. 3.1), spanning between the elevations of 304 and 808 m a. s. l. (according to elevation data from 2009). It has been, to date, mentioned incidentally in just a few scientific publications (Cameron et al., 2012a; Christiansen et al., 2005; Drewry et al., 1980; Hodgkins et al., 2004; Lysä and Lønne, 2001; Macheret and Zhuravlev, 1982), and few authors have provided glaciological data on this site. Rutter et al. (2011) have described the early mass balance measurements on this ice cap in 2007, while Liestøl (1974) reported for the first time data on the ice thicknesses, derived from boreholes and radio-echo soundings. The latter author also shows the position of the coal seam beneath the glacier (400 m a. s. l.), which has been exploited by Mine 7, in the corridor of which (running beneath Foxfonna) a temperature of -0.2°C was measured at the time.

Due to the paucity of glaciological data in the published record, understanding this field site became a core part of building the biogeochemical understanding of its organic carbon cycle. As it will be frequently stressed throughout this thesis, the glaciological background is crucial to describing biogeochemical processes in glaciers accurately, and hence, this chapter is more than a mere description of the study site. The detailed description of Foxfonna glacier that follows here subsequently forms the basis of the methodological concept for organic carbon budget construction. The contents of this chapter are therefore the crucial elements of the glacier characteristics for its biogeochemical studies: mass balance and geometry change, internal structure and thermal regime, as well as glacier dynamics and hydrology. A description of the main physical processes likely to drive the biogeochemical changes is expected to result from these considerations.

The main aims of this chapter are to characterise the physical processes present on Foxfonna glacier and to place the field site of this thesis within the spectrum of glacier changes worldwide. Specifically, the objectives of this chapter are:

- to establish a record of the recent mass balance of the small ice cap Foxfonna, using two complimentary methods, and to describe the concurrent morphology change of the site,
- to characterise thermal and dynamical properties of ice of this glacier,
- to explore the relative role played by surface and subsurface hydrology on this site.

3.2. Methods

3.2.1. Glacier mass balance

A glacier mass balance is the result of budgeting inputs and outputs of the glacial system, as described in Chapter 2 (Section 2.1). In the High Arctic, it is practical to divide the mass balance of the winter season (B_w), which is approximating the total accumulation (mass gain), from the summer season mass balance (B_s), correspondent to most of the ablation (i.e. mass loss). This makes it possible to derive valuable characteristics of mass balance components by performing two mass balance surveys per year. A total of those two terms, calculated for a balance period (usually one year), is referred to as *net mass balance* or B_n . All these values are expressed in water equivalent (w.e.), which is correspondent to the thickness of a water layer that would result from melting the gained or lost snow and ice. A water equivalent estimate therefore requires measurements of snow or ice depth (d) and density (ρ), the product of which results in the value of w.e. (Benn and Evans, 2010). An overview of mass balance measurement methods has been provided in Section 2.1. Here, both direct and geodetic methods for mass balance measurements were used, depending on the period and available data.

3.2.1.1. Direct measurements of glacier mass balance on Foxfonna

Background data for mass balance considerations consists of meteorological record of temperature and precipitation. The closest available source of a long-term meteorological record was the Svalbard Lufthavn (airport) WMO station, located 17.4 km from Foxfonna. From 2007 onwards, an AWS was installed by the University Centre in Svalbard (UNIS) on Breinosa plateau, 520 m a.s.l. and 1.7 km from Foxfonna. The data for each of the sites was collected from its respective online repository, the eKlima portal (<http://sharki.oslo.dnmi.no>) or http://www.unis.no/20_RESEARCH/2060_Online_Env_Data/weatherstations.htm (the UNIS website).

The direct mass balance measurements on Foxfonna glacier consisted of ablation surveys performed on a total of 14 aluminium stakes, as well as accumulation checks that encompassed snow d probing and ρ sampling. For all ablation measurements, 50x50 cm boards were used to avoid surface roughness interference, and an average of at least three measurements per stake was taken (following Rutter et al., 2011). Further information on the set of ablation stakes surveyed each year is presented in Table 3.1. The set of stakes installed on the ice cap (or upper part, both terms will be used interchangeably here; Fig. 3.2) of Foxfonna glacier originate from a Store Norske Spitsbergen Kulkompani AS (SNSK) monitoring initiative, founded in 2007, and led by A. Hodson. In the ablation calculations, glacial ice ρ of 0.917 g cm^{-3} (Nuth et al., 2010), superimposed ice ρ of 0.85 g cm^{-3} (Tedesco et al., 2008) and firn ρ of 0.55 g cm^{-3} was assumed (Nuth et al., 2010). The summer and net mass balance stake measurements (the latter calculated as the difference between ice surfaces in the end of consecutive ablation seasons) were extrapolated using elevation zones for the lower part of the glacier and aspect zones for the upper part, the zone boundaries being described in Table 3.2 and shown on Figures 3.2 and 3.3. The boundary between the upper and lower part of Foxfonna glacier was drawn along a bergschrund (compare to Fig. 3.7 and 3.18).

Table 3.1. Characteristics of ablation stakes on Foxfonna glacier (elevations in 2009).

Stake	Period existing	Elevation [m a. s. l.]
A1	2010–2012	451
A2	2010–2012	493
A3	2010–2012	550
A4	2010–2012	600
A5	2011–2012	624
A6	2011–2012	611
A top	2007–2013	798
A NE	2007–2013	808

A N	2007–2013	774
A NW	2007–2013	747
A SW	2007–2013	757
A S1	2007–2013	743
A S2	2007–2013	769
A SE	2007–2013	775

Table 3.2. The description of zones used for spatial mass balance calculations.

Zone	Elevation range [m a. s. l.]	Aspect	Representative stakes	Surface area [ha]
Upper Foxfonna E-NE	620-818	E-NE	A NE	21.28
Upper Foxfonna SE	620-818	SE	A SE	50.88
Upper Foxfonna S-SW	560-818	S-SW	A SW, A S1, A S2	94.96
Upper Foxfonna W	560-818	W	A top, A NW, A SW	38.60
Upper Foxfonna N-NW	620-818	N-NW	A N, A NE*, A NW*	46.13
<473.5 m	269-473.5	Mainly N, smaller areas NW, E and W	A1	30.42
473.5-528 m	473.5-528		A2	37.12
528-588 m	528-588		A3	47.61
588-618 m	588-618		A4, A6	29.22
588-691 m**	588-691		A4	90.09
618-705 m	618-705		A5	67.99
>705 or >691 m	(705 or 691)-765		A N	9.32 (with zone Lower Foxfonna 5) or 16.44 (with zone Lower Foxfonna 4a)

*Stakes positioned on the zone boundary, and therefore ascribed 0.5 weight of the main stake in the zone

**This elevation band was used instead of the bands 4 & 5, in the period when stakes A5 and A6 were not in place.

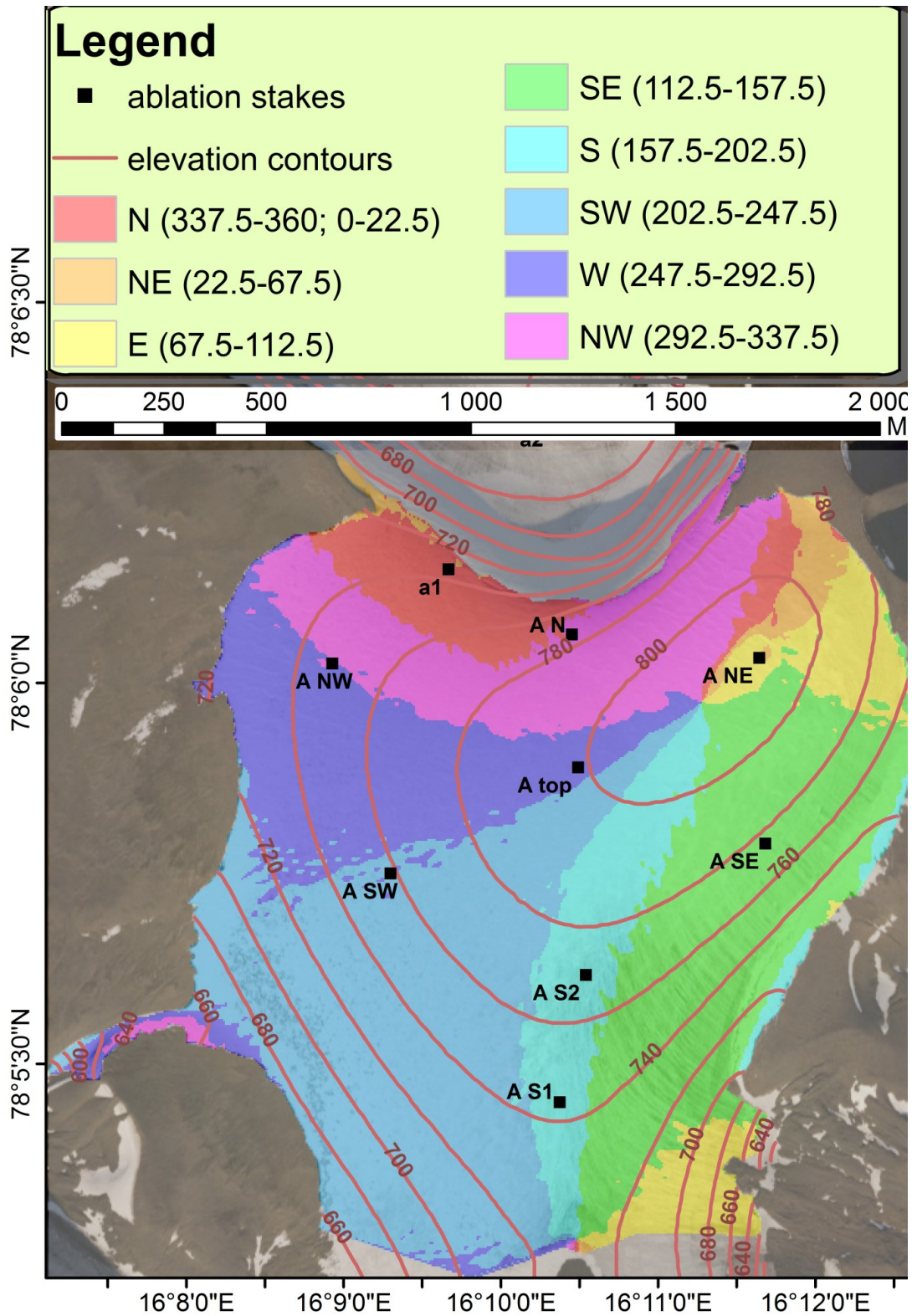


Fig. 3.2. Upper part of Foxfonna glacier, its aspect and ablation stakes.

Geodata from 2006, courtesy SNSK AS

The accumulation surveys have been performed with variable density in the years 2007–2013, most of this period covering solely the upper part of Foxfonna (2007–2009 and 2013).

These field measurements took place in April-June, depending on the annual snow conditions, and consisted of a series of snow pits for density sampling and a wider sampling of snow depth using an avalanche probe, as described in detail in Table 3.3.

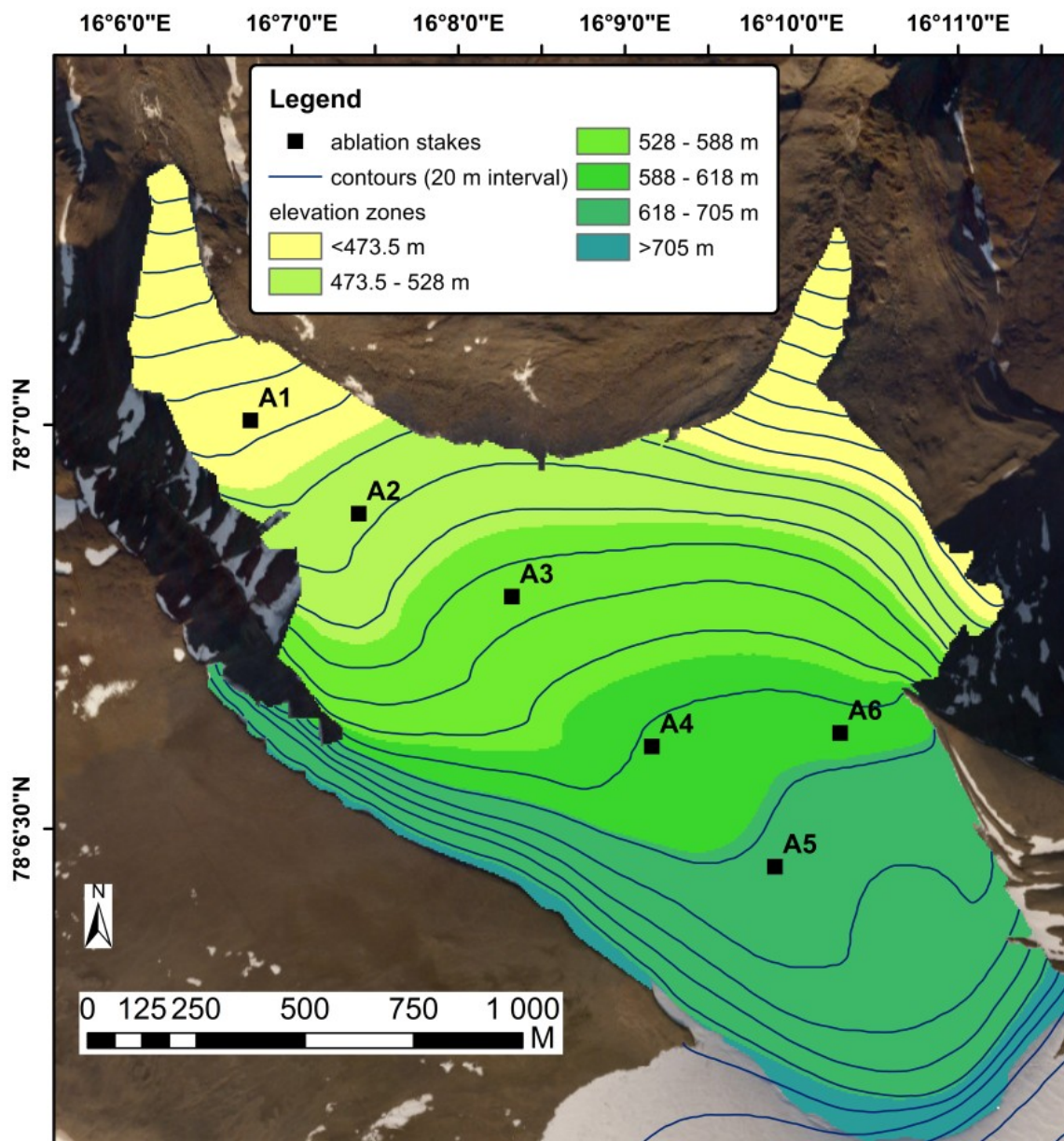


Fig. 3.3. Elevation zones of the lower part of Foxfonna glacier, for the period with all stakes A1-A6 existing.

Table 3.3. Accumulation surveys on Foxfonna glacier.

Year	Number of snowpits	Density sampler type*	Number of snow depth measurements	Dates of surveys
2007	0	T	15	May
2008	3	T	20	

2009	3	T	8	29 th May
2010	7	T	47	13 th –14 th April
2011	5	DC	31	21 st –24 th April
2012	8	T	147	Late April
2012 (2 nd survey)	5	DC	14	6–12 th June

* DC: density cutter (a 1L metal wedge), the sampling routine pictured on Figure 3.4.

T: tube (a 1L PVC tube)



Fig. 3.4. Sampling for snow water equivalent using a density cutter.

Photo by and of M. Pencarski

3.2.1.1.1. Errors in mass balance estimation using direct method

The errors involved in the estimation of glacier mass balance from direct measurements (or glaciological method) stem from three processes: the field measurement technique, representativeness of sampling points on the glacier surface, and data post-processing. The measurement errors can only be described as precision errors, and those were calculated as the average root mean square of differences between replicates in a given survey (root mean square error, RMSE). They were 0.5 cm at maximum for ablation measurements and below 5 cm for snow depth probing. Further errors in snow probing might occur due to the formation of ice lenses above the old summer surface, bending of the avalanche probe during the measurement, or due to the difficulty in detecting the old summer surface in the firn zone (Jansson, 1999). As will be shown later, the firn area of Foxfonna glacier is very small, which makes the last error type most likely negligible; the other two error sources were not possible

to account for directly, but the usually low snowpack thickness (below 1.5 m on most of the glacier surface area) is likely to have favoured obtaining high measurement accuracy (Jansson, 1999). The snow ρ , as sampled with the density cutter, was allowed a difference between the two measurements of 10%, otherwise the measurements had to be repeated. As a result, it is assumed here that the accuracy of the measurements taken on this glacier is within the error margins reported for other routine mass balance programmes, i.e. between 3 and 10% (Jansson, 1999).

Further errors could arise from the location of sampling points. Their distribution was typical for mass balance studies, and so the ablation stakes were located along the glacier centre line on the glacier tongue, with one stake representing variability in the perpendicular direction (A6; Fig. 3.3) and distributed between areas of different aspect on the ice cap (Fig. 3.2). This usually leads to a small bias towards conditions specific for the glacier centre, as opposed to margins where the accumulation locally increases, which may contribute 5-10% error into the glacier-wide mass balance estimation (Jansson, 1999). An ablation gradient is a commonly applied function for extrapolating stake data on glacier melt for the glacier-wide mass balance estimations, however this calculation yields results not significantly different from manually extrapolating stake data (Jansson, 1999), and there is a lack of other comparative methods to separate the effect of this technique on the overall mass balance error from other sources of bias. In this work, the particular ablation value was applied to elevation zones, which is an intermediate approach between the two described above.

The accumulation of snow was probed in a relatively sparse grid of points, however according to Jansson (1999) this would only introduce a bias of 7% water equivalent for the whole glacier for 18 points on the area of Storglaciären, so even on the smaller and irregularly shaped Foxfonna the errors from this bias are most probably below 10%. This is because the random errors included in each measurement are likely to equal out once all measurements are used for a glacier-wide calculation (Miller and Miller, 2005). The representativeness of snow density measurements is more problematic, since the density of sampling points is lower. Different techniques might be used to tie density properties to snow probing points; the logarithmic depth-density relationship being the most effective according to Jansson (1999). However, the same author points out that the glacier-wide mass balance estimation changes only to a small extent with the choice of a particular depth-density function type. This relationship may, however, be disturbed by wind packing and the depth hoar formation (Jansson, 1999), both of which were observed on Foxfonna. The uncertainty connected to this is, however, not quantifiable. The RMSE of the aforementioned biases in B_w is therefore assumed to be 10% at maximum.

A higher error may be connected to uneven sampling point distribution, resulting from areas excluded from sampling due to safety reasons (crevasse fields and steep slopes). Jansson (1999) accounts for this error as proportional to the total area of the inaccessible terrain, and hence on Foxfonna this will be the main error source, as the steep slopes with high avalanche risk and occasional crevasses constitute approximately 30% of its tongue (the ice cap being virtually free from this problem).

Finally, the combination of the above mentioned errors determines the accuracy of the final mass balance estimation. There are random errors, which are likely to balance one another in a spatially distributed sampling setup, and measurement biases. These all, as Jansson (1999) argues on the Storglaciären example, would not exceed 0.1 m w.e. in the final, glacier-wide net mass balance (B_n) estimate. Foxfonna is less favourable than Storglaciären for representative sampling points distribution, due to intensive snow redeposition by wind and the presence of vast steep slope areas (relative to its size) which are not safe to sample. Assuming the latter to be the main error source, which contributed a proportion of error according to its spatial coverage (Jansson, 1999), an extra 30% (± 0.3 m w.e.) was added to this error margin. This resulted in the overall mass balance error for glacier-wide estimations derived from direct measurements within ± 0.13 m w.e.

3.2.1.2. Mass balance (geodetic method) and landscape change observations

To study the extent and volume change of Foxfonna, as well as the landscape evolution, three sets of aerial photographs (1961, 1990 and 2009) and three digital elevation models (DEMs, from 1990, 2006 and 2009) of the glacier surface were compared. Aerial photographs from 1990 (22nd July) and 2009 (27th July) have been analysed by the author to produce two subsequent DEMs of the glacier, both with 5 m horizontal resolution (raster cell size), using stereoscopic photogrammetry principles applied in Erdas Imagine® 2013 software with LPS toolbox. A DEM for the year 2006, provided by SNSK, was included in the extent and volume comparison (a 5 m resolution DEM and ortophotomap based on laser scanning/LiDAR measurements and airborne photographs, taken on 30th and 31st August 2006, respectively). This LiDAR derived DEM was also treated as a reference surface for error checks of the 1990 and 2009 DEMs, because of the typical high accuracy of LiDAR data (errors ± 0.2 m or smaller; Barrand et al. 2009). As a result, two distinct periods of geodetic mass balance measurements were obtained, totalling 19 years of change. The resulting comparisons have a horizontal resolution consistent with the resolution of the 2006 reference model, i.e. 5 m, and the vertical error of the 1990 or 2009 DEM is referenced against 2006 data, as described below. In the analysis of geodetic mass balance, the approach of Nuth et al. (2010) was applied, and hence Sorge's law of firn densification was assumed to hold (Bader, 1954). Therefore, all

volume changes were assigned the density of ice, 0.917 g cm^{-3} , since if the mass change occurred in the firn area, the density profile there would remain the same.

The 1990 photo set consisted of three aerial images (copyright of the images: Norwegian Polar Institute, NPI), taken from altitudes between 8358 and 8366 m a. s. l., with a surface overlap of 60%. These were scanned with a pixel size of $14 \mu\text{m}$ for the two northernmost photographs and $30 \mu\text{m}$ for the remaining one (0.54 m and 1.64 m in the field, respectively), which is in close correspondence to picture quality ($17 \mu\text{m}$ or 0.7 m resolution) used with success for surface change on another Svalbard glacier, Austre Brøggerbreen (Pope et al. 2007). The RMSEs of the horizontal position, obtained from a sample of 27 ground control points, equalled $x_{\text{err}} = 78.52 \mu\text{m}$ and $y_{\text{err}} = 67.41 \mu\text{m}$, given the image scale of 1:54717, calculated from the flight height and focal length, this corresponds to field location errors of $x_{\text{err}} = 4.30 \text{ m}$ (easting) and $y_{\text{err}} = 3.69 \text{ m}$ (northing). The vertical accuracy checked against a stable terrain section of the LiDAR derived 2006 DEM (Breinosa plateau, an extract of 0.33 km^2 surface area) equalled 0.69 m on average (standard deviation, $\text{SD} = 0.63 \text{ m}$), while the accuracy of intersected ground control points ($n = 11$) averaged -0.58 m ($\text{SD} = 1.46 \text{ m}$).

The 2009 DEM was prepared from 14 aerial images (copyright by NPI), obtained with a multispectral digital camera with $18 \mu\text{m}$ pixel size, which corresponded to 0.70 m in the field. The photographs were taken from a flight height of 3902 m, resulting in a photo scale of 1:38826. RMSEs of this elevation model were obtained from the 512 image tie points, and amounted to $0.73 \mu\text{m}$ for x and $0.46 \mu\text{m}$ for y coordinate (0.03 m and 0.02 m in the field, respectively). The areal quality check on Breinosa plateau against the LiDAR data from 2006 (area checked 1.29 km^2) resulted in a mean elevation error of -0.45 m ($\text{SD} = 0.33 \text{ m}$). The error check area was different in 1990 and 2009 due to the different spatial extent of both DEMs on Breinosa, as well as the necessity to avoid areas of poor texture in the image. The latter were also excluded from further analysis of the glacier surface change.

The DEMs for the years 1990, 2006 and 2009 were compared in order to describe the general surface change in the region. More changes have been distinguished by visual inspection of the aerial photographs from these years and the 1961 image (taken between 23rd and 25th August; all aerial images courtesy NPI), as well as the orthophotomap from 2006. The 1961 photo was a particularly valuable source of information, as it pre-dates the opening of Mine 7 in 1976. No mining works had been conducted before 1964, when two years of initial research on the coal seam commenced. There was also a break in the mine exploration between 1978 and 1981, and after that the mine has been in use every year until now (Knudsen and Yri 2010).

3.2.1.3. Water balance in 2011 and 2012

A comparison of the water volume in runoff with the melt and rain combined was conducted for the summers of 2011 and 2012. The data contributing to this calculation originated from ablation monitoring throughout the summers of 2011 and 2012, in 4 and 5 shorter periods, respectively, as well as from the discharge records collected in those years. The ablation data were collected in the same mode as described in Section 3.2.1.1., using stakes A1-A6. The ablation within the first period of each summer was assumed to be equal to the SWE of winter accumulation across the catchment less the amount of snow remaining at the stakes on the day of the first ablation survey. This late summer snow was assumed to have a density of 0.52 g cm^{-3} , as was found consistently across measurements of snow cover density on Foxfonna glacier in the early July of 2014.

Precipitation data came from the eKlima portal (<http://sharki.oslo.dnmi.no>) and represented the WMO station Svalbard Lufthavn. The data was transformed by applying a precipitation gradient of $19\% / 100 \text{ m}$ (Nowak and Hodson, 2013) and a standard moist adiabatic lapse rate of $0.625^\circ\text{C} / 100 \text{ m}$ elevation for mean daily temperatures (Machguth et al., 2006). Following that, the precipitation was assumed to be rain if the average daily temperature exceeded 0°C at the mean elevation of the supraglacial catchment considered (575.6 m a.s.l.).

The proglacial river (Fox Gauge and B1 on Figure 3.5a., for 2011 and 2012, respectively) was also monitored for discharge. This was achieved using a Campbell logger (CR800 in 2011 and CR10 in 2012) fitted with a Druck PDCR submersible pressure transducer probe, which recorded hourly water level values. Additionally, an electric conductivity (EC) probe was fitted into the logger, which was used for salt dilution discharge gauging on 26 and 23 occasions in 2011 and 2012, respectively. These were used to construct rating curves. Multiple rating curves were used due to channel geometry changing significantly during the melt season, which consisted of between three and seven measurement points (in two isolated cases of fast changing channel properties, curves of two points were adopted for short time periods; examples of rating curves are given in Fig. 3.6.). Also, a stable gauging site was chosen in 2011 in the proglacial moraine complex, but unfortunately later on the ice-cored moraine collapsed there, forcing the water flow into an underground cavity formed nearby. This made it impossible to repeat monitoring in the same site in 2012. Instead, the most suitable channel cross-section for level monitoring was found at the icing front in 2012, which was 230 m closer to the glacier than the 2011 site (see Fig. 3.5b. for the relative location of 2011 and 2012 sites). The relative standard error (*RSE*) of the discharge estimates, i.e. the standard error of the estimation expressed as percentage of the mean (Hodgkins, 2001), were 13.9% in 2011 and 18.9% in 2012.

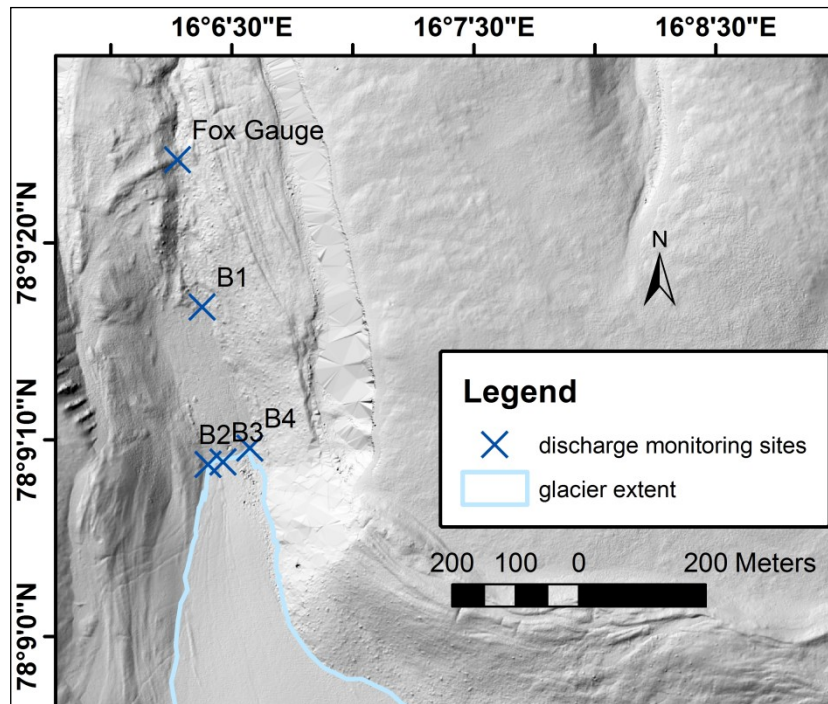


Fig. 3.5a. Location map of the discharge monitoring sites in the forefield of Foxfonna glacier.

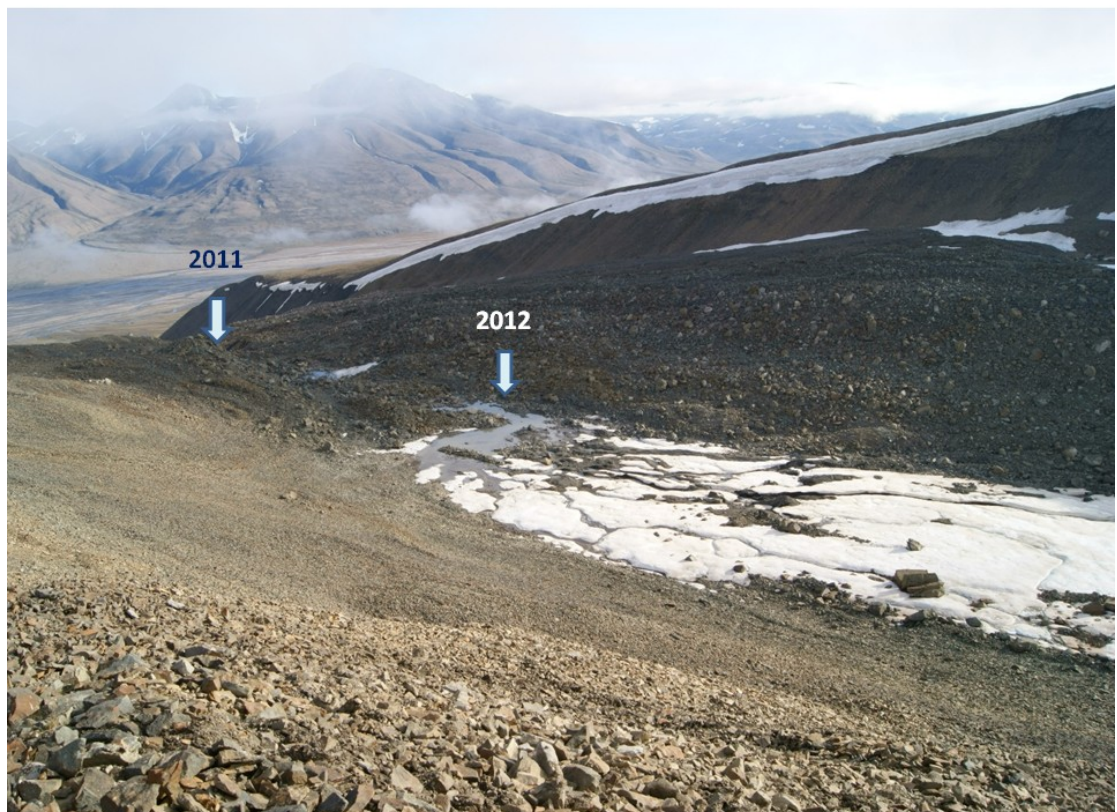


Fig. 3.5b. The discharge monitoring sites in the melt seasons of 2011 and 2012 (Fox Gauge and B1 on Fig. 3.5a., respectively).

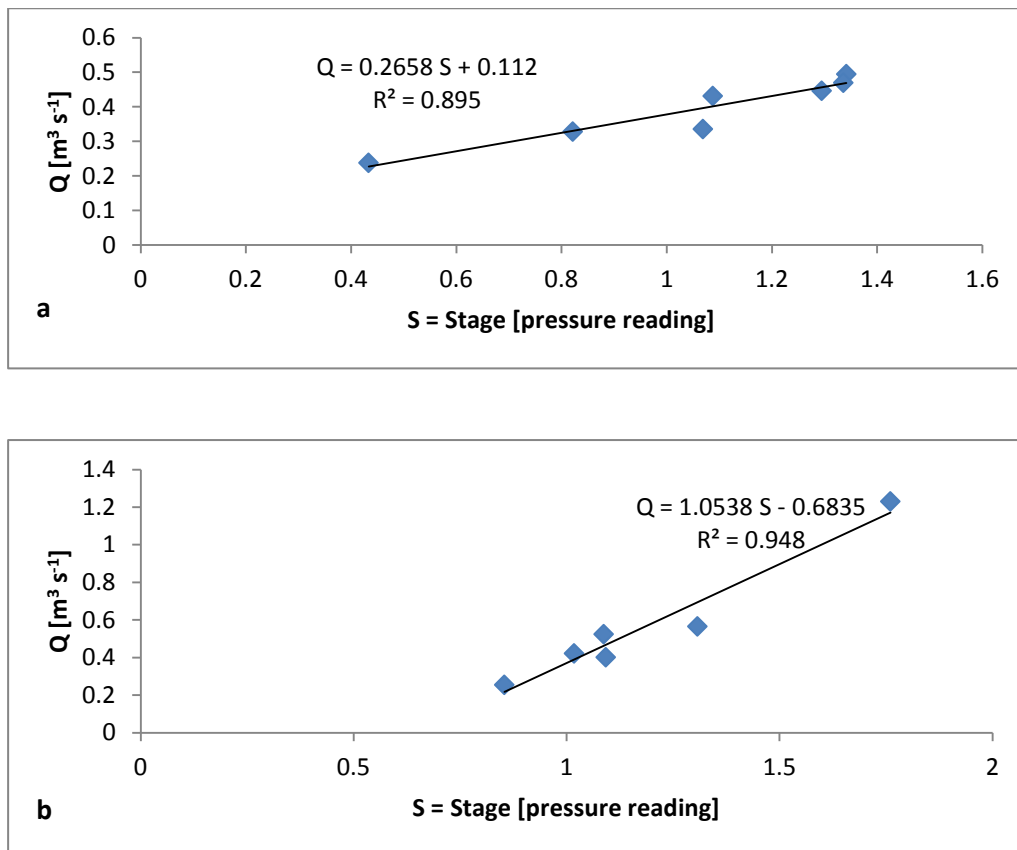


Fig. 3.6. Example rating curves from 2011 (a) and 2012 (b).

In 2012, the streams leaving the glacier snout were also monitored for discharge on each sampling occasion ($n = 10$) with the salt dilution method, using a hand-held Hanna EC-meter. For this purpose, B2 and B3 were gauged together at their confluence a few meters from the glacier snout, while B4 was measured separately (Fig. 3.5a.). The final discharge at the glacier snout was then estimated from the proportion between the sum of these discharge measurements on a given occasion to the discharge value measured downstream, at the water level gauge site. This discharge represented a catchment area delineated on Fig. 3.7.

3.2.1.4. Radar surveys of Foxfonna

The glacier thickness change was also investigated by comparing radar survey data and the archive data of Liestøl (1974). All ground-penetrating radar surveys were performed with a bistatic radar (i.e., a system comprising of two antennae: a transmitter and a receiver) with a 100 MHz frequency. The upper part of Foxfonna glacier was investigated on 21st March 2007 with pulseEKKO 100 system (Sensors & Software, 1000 V transmitter) by K. Bælum, D. Benn, A. Booth and T. Murray. Another survey, covering most of the lower Foxfonna glacier, was performed by T. Gölles and the author on 2nd March 2012 (GPR by MALÅ Geoscience, Sweden, 400 V transmitter). The general difference between the two setups was the antennae positioning (perpendicular to travel path with pulseEKKO and parallel with the MALÅ Geoscience system), and the stronger signal provided by the pulseEKKO system. The choice of

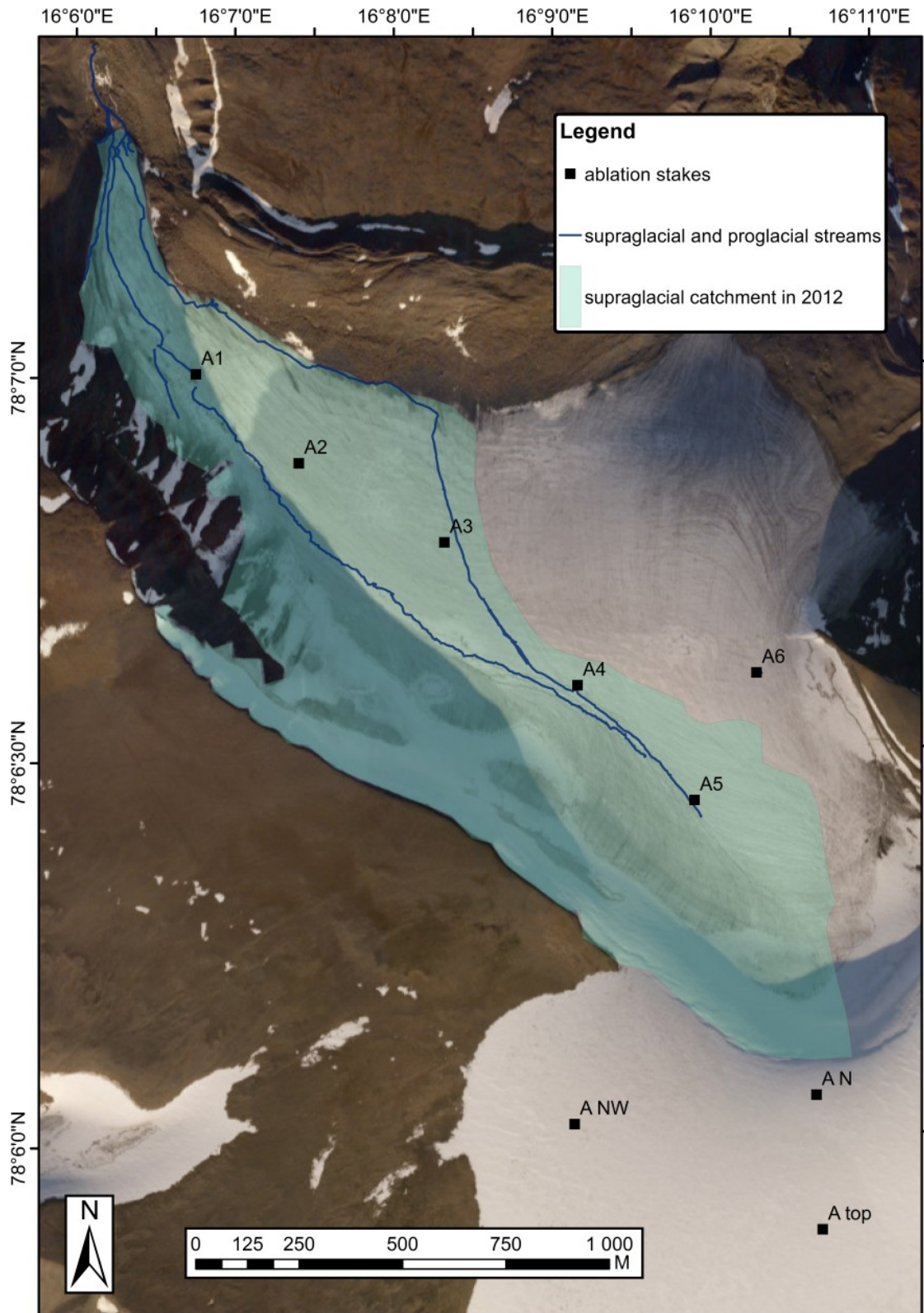


Fig. 3.7. Supraglacial catchment boundary in 2012 on Foxfonna. Supraglacial streams are shown as marked with a handheld GPS on 8th August 2012.

Source: Hodson, Unpub. Data. Background image – 2006 orthophotomap, courtesy SNSK. Fig. 3.5a. magnifies the NW corner of this map.

equipment was determined by its availability in the University Centre in Svalbard. Both surveys were processed in RadExplorer with the assumed wave velocity in ice of 16.8 cm ns^{-1} (Robin, 1975), which is typical for solid water with no liquid inclusions, and the results compared to the map derived from the 1972 borehole depths and radio-echo soundings (Liestøl, 1974).

The data from the radar survey in March 2012 were also processed using Petrel® software in order to obtain the values of relative amplitude of the bed reflector. This is a good indicator for areas where it is possible for liquid water to occur at the ice-bedrock transition, since water and wet sediment are the strongest reflecting media found in a glacial environment (Bælum and Benn, 2011). The values were generated in the following way. The raw radar data were processed in RadExplorer using Background and DC removal corrections, but no gain-related processing, and converted from two way travel time (TWT) to depth. The data were then saved in SEG-Y format, with a 100 conversion factor for horizontal coordinates (instead of 1000, which corrects a software bug). Upon import to Petrel®, the bed reflector was picked manually with an accuracy of 5 ns, which is correspondent to 0.4 m depth. Then, a surface attribute function was used to define the sum of amplitudes within the 5 ns window. The data were exported into Microsoft Excel, where they were corrected to account for the spherical divergence of radar waves, which was achieved by multiplying the amplitude sum by the bed reflector depth doubled and squared. In case of doubts about the precise distinction of the glacier bed, the strongest reflector within the layer was picked. As a result, wet bedrock and channels could be portrayed by both positive and negative relative reflectivity. However the values for environments with liquid water will produce one of the strongest possible reflections, and therefore both values above 0.5 and below -0.5 relative amplitude are interpreted here as areas with high probability of liquid water occurring. The areas with relative amplitude in the ranges (-0.5, -0.3) and (0.3, 0.5) are interpreted as those with lower likelihood of liquid water, while those with values of -0.3 to 0.3 are most likely devoid of water inclusions.

3.2.1.5. Albedo as a possible driver for mass balance changes

The albedo measurements were taken on 23rd July 2010, and the whole glacier was surveyed by two groups of students within a 48 hour time window (between 12:00 and 19:00 during two days). All measurements were performed using an Apogee SP-110 pyranometer, as a combination of five incident and five outgoing radiation fluxes in W m^{-2} , across the waveband 350-1100 nm. All measurements were taken in the vertical direction (zenith for incident and nadir for reflected), and each measurement was accompanied with marking a point with a handheld GPS. The final albedo distribution map (Fig. 3.20., Section 3.3.4) was produced by interpolation using ArcMap.

3.2.2. Glacier movement

Glacier movement was monitored with a repeated differential GPS (DGPS) measurement of the ablation stake location (both performed with Trimble R8 GNSS system, with dual frequency), over the period 14th August 2012 – 16th-18th June 2014 (two consecutive surveys undertaken on the ice cap and tongue on two days). The base station data (ETPOS type) for differential corrections were obtained upon request from SATREF® control centre (www.kartverket.no/Posisjonstjenester/ETPOS/), and came from the Longyearbyen station (coordinates 78°13'43.77230"N, 15°23'50.31623"E, elevation 495.682 m, giving a baseline length of 18.7–21.6 km, depending on a particular stake location). The horizontal coordinate precision errors in the two surveys ranged 0.012-0.084 m in 2012 (0.035 on average) and 0.010 to 0.035 m in 2014 (0.018 on average). The precision of the annual horizontal velocity measurement was estimated by totalling both measurements precisions for a particular stake and dividing by the number of years over which the measurement was undertaken.

3.3. Results

3.3.1. Glacier mass balance (direct measurements)

In the course of net mass balance measurements on the upper part of Foxfonna glacier, the influence of aspect on the annual values can be observed (Fig. 3.8.). On average, the south-east facing part has experienced the lowest B_n values in the period 2007–2013 (A SE), southern part being the second lowest (A S1 & A S2). The highest values were noted for the north-facing side of the ice cap (A N stake). Of the two stakes located on top of the ice cap (>800 m a. s. l.), the one in the area facing east and north-east (A NE) has experienced lower net balance rates than the one facing west (A top). The winter mass balance (Fig. 3.9.) was also variable with aspect, with the same pattern as net mass balance.

Once the spatial differences were incorporated into a glacier-wide mass balance estimation, using the zonation described in Section 3.2.1.1., the temporal trends were analysed. The winter mass balance on upper Foxfonna in the period 2007–2013 (Fig. 3.10.) was almost uniform temporally, with an average of 0.40 (SD \pm 0.07) m w.e. winter accumulation per annum. The differences in net mass balance are mostly driven by summer ablation variability, resulting in the average net balance of -0.28 (SD \pm 0.43) m a⁻¹ in the years 2007–2013 on the upper part of Foxfonna glacier. In the period 2007–2013, only in 2008 and 2012 were positive B_n values recorded. The lowest spatially averaged B_n was recorded in 2013, second lowest in 2009 (Fig. 3.10.). In total, during the 6 years of mass balance measurements, the upper part of Foxfonna glacier has lost 1.93 m w.e. (4.85 hm³ water; 0.32 m w.e. a⁻¹).

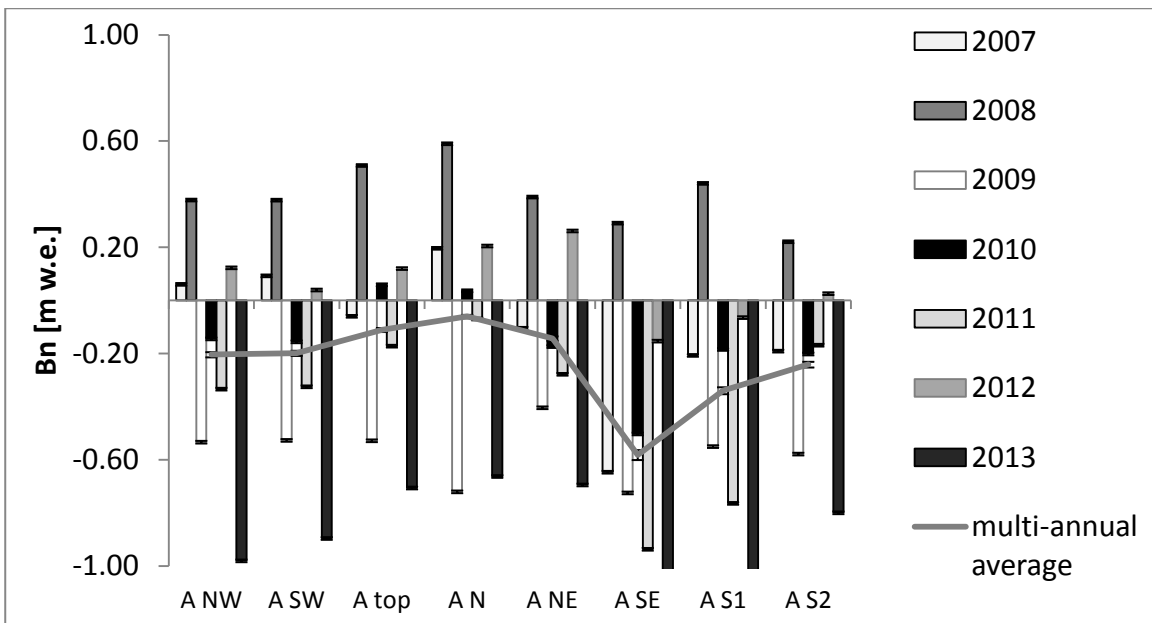


Fig. 3.8. Net annual mass balance as recorded on upper Foxfonna stakes in the period 2007–2013.

Error bars: estimated measurement precision.

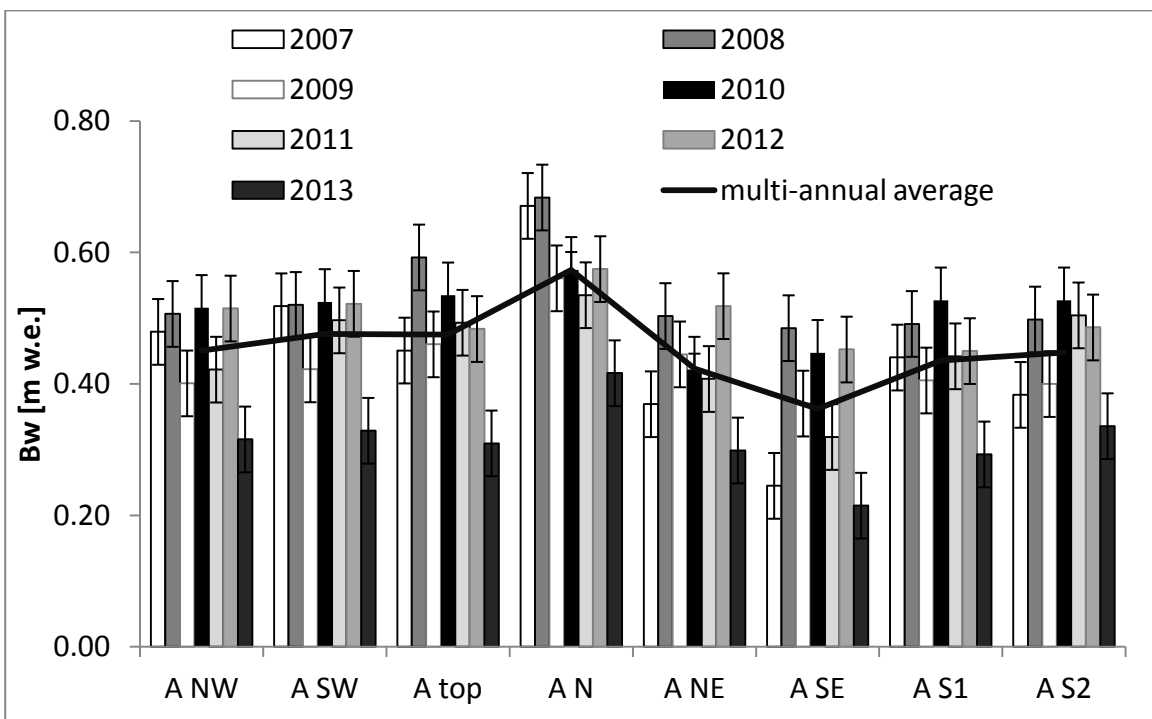


Fig. 3.9. Winter mass balance (accumulation) measured on the stakes of upper Foxfonna glacier in the period 2007–2013.

Error bars: estimated measurement precision.

The net mass balance on the lower part of Foxfonna was negative on all stakes and in the years 2010–2012 (Fig. 3.11.), with no clear elevation-related pattern, probably inherited from

Bw variability (Fig. 3.12.), as the summer mass balance has shown a weak increasing trend with elevation change (Fig. 3.13.). In the *Bw* data (Fig. 3.12.), the irregular increase of *Bw* with elevation in the lower set of stakes (up to A3 or A4) has changed into the opposite trend higher up. Foxfonna is characterised by a relatively shallow mass balance gradient, as can be seen on Fig. 3.14., which collects data from all ablation stakes in the 2012 season, when the stake network achieved the best spatial coverage. This indicates relatively small changes in mass balance conditions across the elevation span of the glacier, as compared to glaciers worldwide (Benn and Evans, 2010).

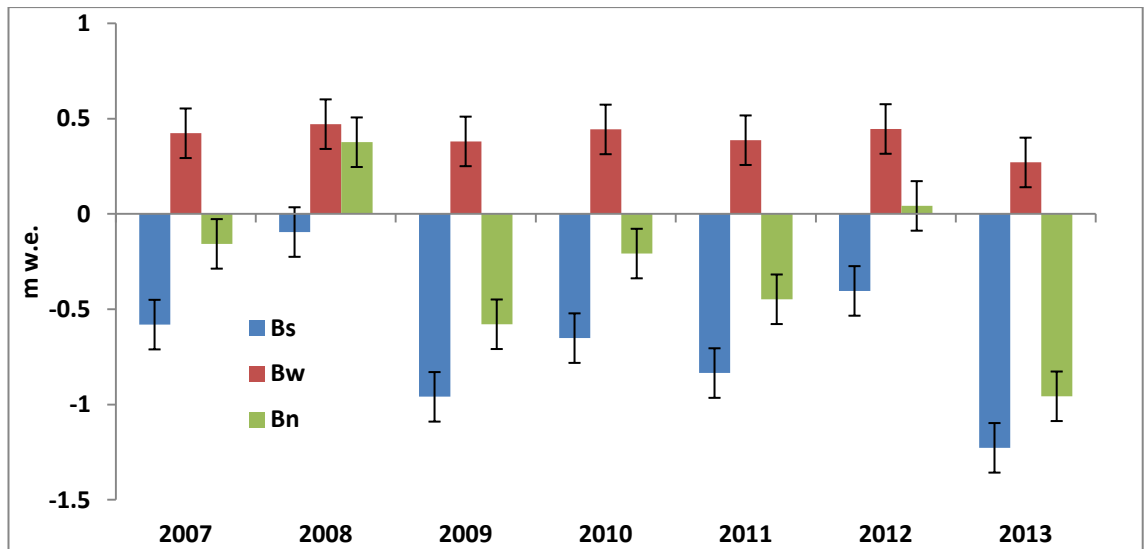


Fig. 3.10. Spatially averaged mass balance on the ice cap (upper part) of Foxfonna glacier.

Bs – summer mass balance, *Bw* – winter mass balance, *Bn* – net balance.

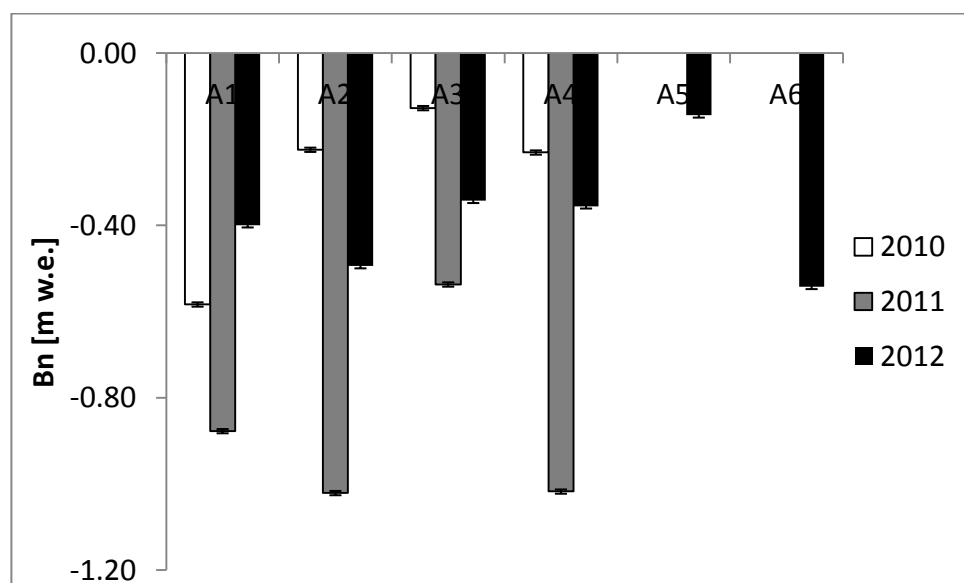


Fig. 3.11. Distribution of net mass balance on lower Foxfonna stakes (2010–2012).

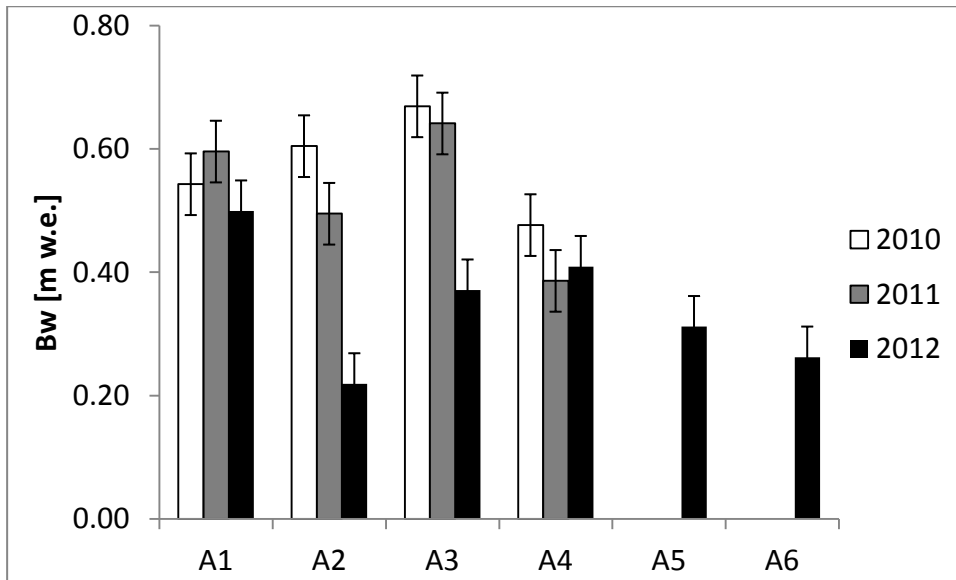


Fig. 3.12. Winter mass balance as measured on stakes of the lower Foxfonna glacier in the years 2010–2012.

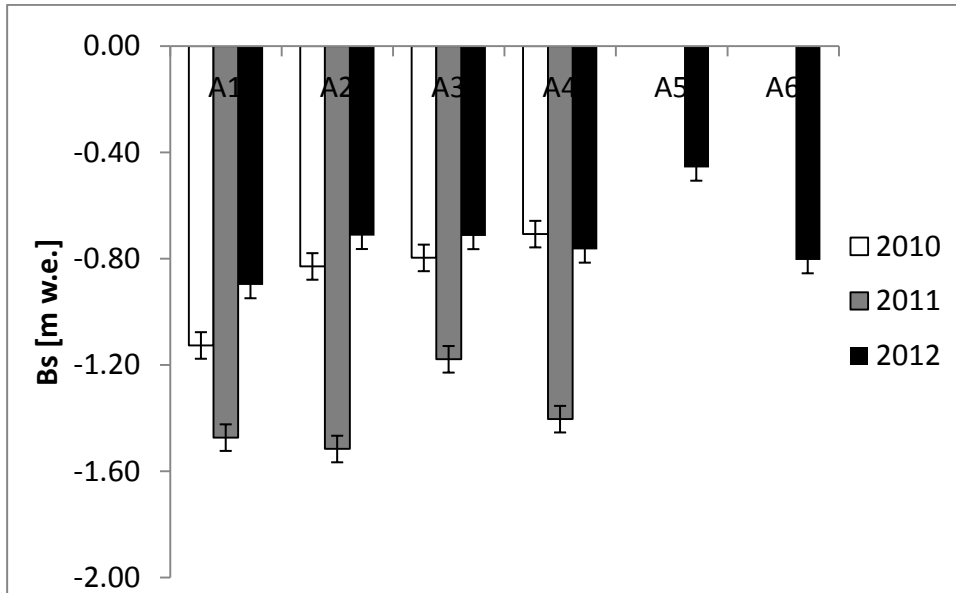


Fig. 3.13. Summer mass balance on lower Foxfonna stakes.

On the lower part of Foxfonna, mass balance was negative throughout the period 2010–2012 (Fig. 3.15.) with the lowest value in 2011 reaching -0.83 m. Similarly to the ice cap data series, B_w was much less varied than B_n ($SD \pm 0.11$ m as opposed to ± 0.32 m), and its mean value was $+0.47$ m in the years 2010–2012 ($B_n = -0.46$ m). In total, between 2010 and 2012, the lower part of Foxfonna has lost 1.37 m w.e. (3.03 hm^3 water, 0.46 m w.e. a^{-1}). The whole glacier has lost in the same period 0.97 m w.e. (4.57 hm^3 water, 0.32 m w.e. a^{-1}). More details of the annual components of Foxfonna mass balance in the years 2007–2013 are given in Table 3.5.

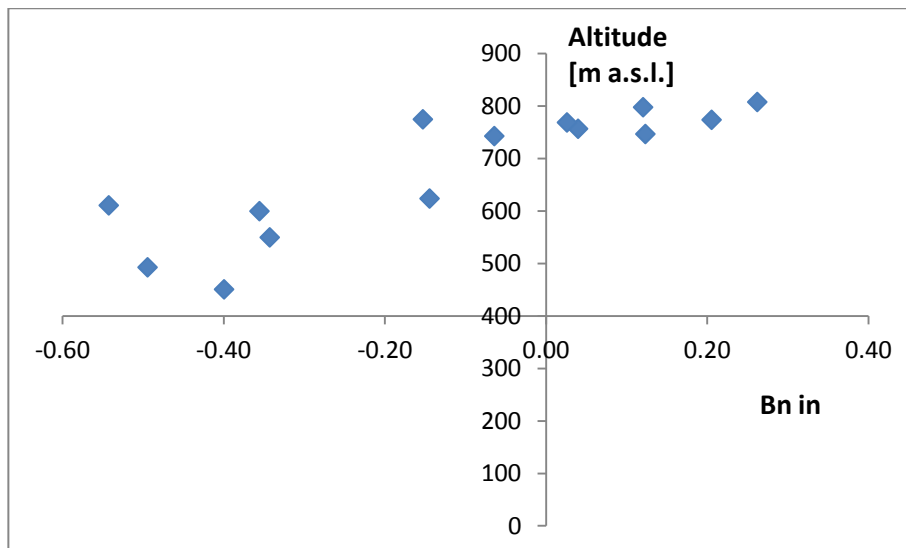


Fig. 3.14. Mass balance gradient across all stakes on Foxfonna in 2012.

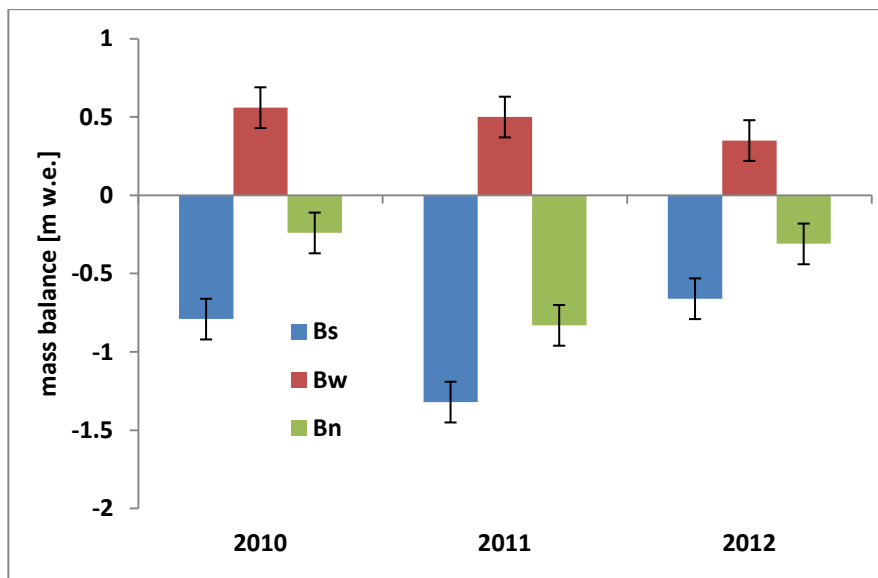


Fig. 3.15. Lower Foxfonna spatially averaged winter (*Bw*) and net (*Bn*) mass balance in the years 2010–2012 [in m w.e.].

Table 3.5. Spatially averaged annual mass balance values for parts of Foxfonna glacier included in the monitoring at the time.

m w.e.	lower Foxfonna			upper Foxfonna			whole glacier		
	<i>Bn</i>	<i>Bw</i>	<i>Bs</i>	<i>Bn</i>	<i>Bw</i>	<i>Bs</i>	<i>Bn</i>	<i>Bw</i>	<i>Bs</i>
2007				-0.16	0.42	-0.57			
2008				0.38	0.47	0.06			
2009				-0.58	0.38	-0.99			
2010	-0.24	0.56	-0.79	-0.21	0.44	-0.70	-0.22	0.50	-0.74
2011	-0.83	0.50	-1.32	-0.45	0.39	-0.86	-0.62	0.44	-1.08
2012	-0.31	0.35	-0.66	0.04	0.45	-0.45	-0.12	0.40	-0.55
2013				-0.96	0.27	-1.08			

3.3.2. Glacier mass balance (geodetic method)

The long-term mass balance data were obtained using geodetic method, from the comparison of DEMs for 1990, 2006 and 2009, for the whole glacier and separately for its lower and upper part (Table 3.6, Fig. 3.16.). The influence of the ice motion was considered negligible, due to very low surface speeds measured on the ablation stakes (see Section 3.3.6). The glacier tongue (lower Foxfonna) has systematically showed more negative mass balances than the ice cap (upper Foxfonna), but the difference between the two parts only slightly exceeded error margins. In the full 19 years studied here, the annual mass balance of Foxfonna glacier was -0.53 m w.e. per year, and this value was equal to the values reported for sub-periods 1990–2006 and 2006–2009 (within error margins).

Table 3.6. Geodetic mass balance of Foxfonna glacier in the years 1990–2009. Errors reported as the standard deviation of differences to stable terrain, divided by the number of balance years constituting a given time period.

Region	Surface area (km ²)			Mass balance (m a ⁻¹ w.e.)		
	1990	2006	2009	1990–2006	2006–2009	1990–2009
Lower Foxfonna	2.603	2.284	2.282	-0.55 ± 0.09	-0.53 ± 0.11	-0.62 ± 0.09
Upper Foxfonna	2.836	2.519	2.654	-0.44 ± 0.09	-0.39 ± 0.11	-0.45 ± 0.09
Whole glacier	5.439	4.803	4.937	-0.50 ± 0.09	-0.46 ± 0.11	-0.53 ± 0.09

The glacier extent has decreased over the period 1990–2009 and 1990–2006, while a slight increase has been noted between 2006 and 2009 (Fig. 3.16a-c). The latter change is very small, which might be partly due to the difficulty in classifying terrain as a glacier, based on photographs taken in the end of July 2009. The photographs were taken before the end of ablation season, and the glacier front has visibly receded between 2006 and 2009.

The elevation changes were mostly negative and similarly distributed in the periods 1990–2006 and 2006–2009 (Fig. 3.16b-c), maximum ice mass loss occurring:

- on the lowest part of the glacier tongue (particularly the north-eastern lobe),
- the crest of the slope flanking the glacier tongue on the south-west, and
- the southern and south-eastern areas of the ice cap.

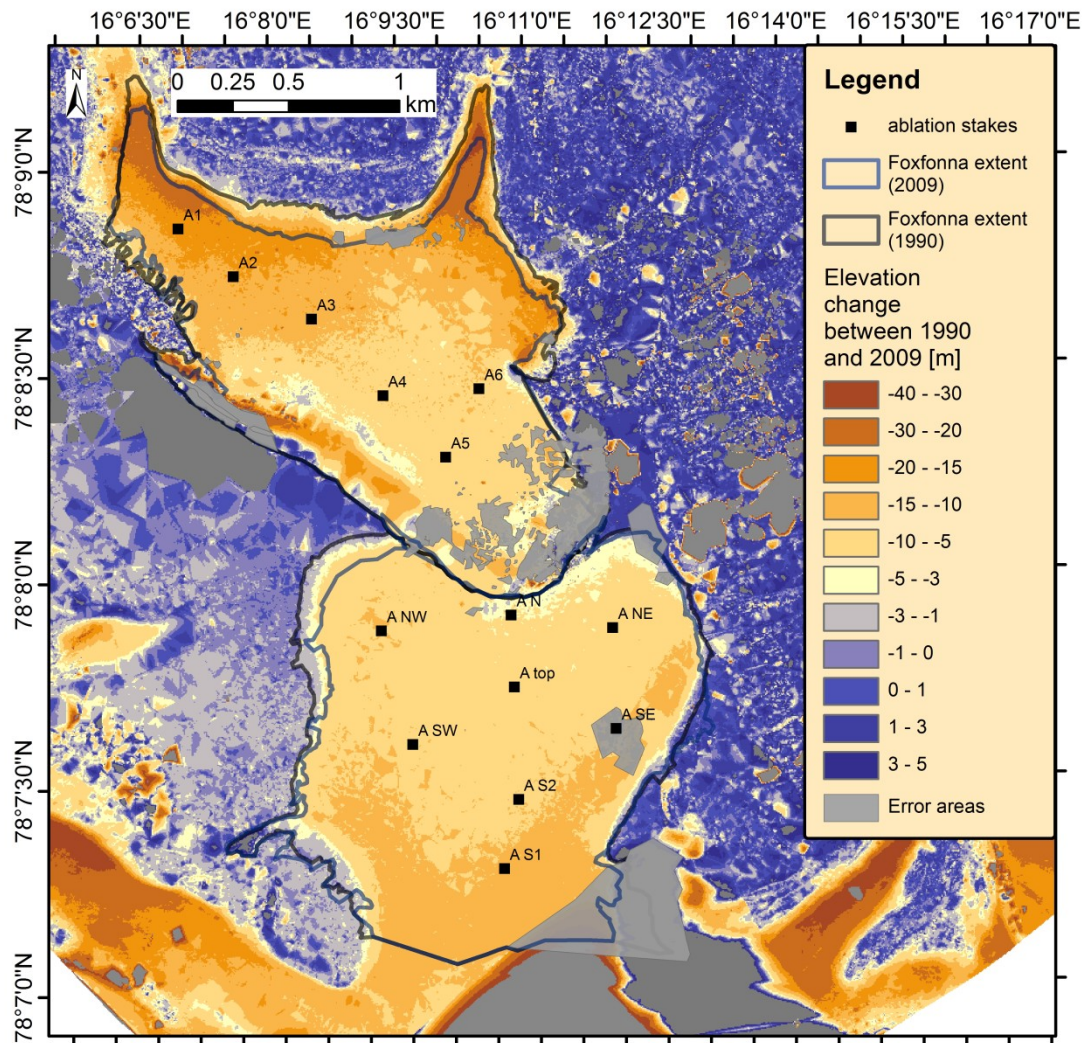


Fig. 3.16a. Map of the glacier extent and elevation change in the years 1990–2009.

Despite the altitude difference, the part of the tongue around stakes A4 and A5 showed similar mass losses to the centre of the ice cap. Ice mass gains were only noted on the north-facing slope between the upper and lower part of Foxfonna, and at the base of Foxfonna south-western flank. The distinct difference between the two shorter periods of elevation change is the behaviour of the northern part of the ice cap, which gained mass between 2006 and 2009 (Fig. 3.16c), but in the preceding 16-years period there was a pronounced mass loss (Fig. 3.16b). Also, the south-eastern ice cap has been disproportionately strongly affected by melt in years 2006–2009, in contrast to the period 1990–2006, when it was the southern ice cap that lost a thicker layer of ice among the two locations (Fig. 3.16b-c).

3.3.3. Meteorological conditions of the mass balance measurement periods

The site has been monitored for climate by a local weather station since 2007 by A. Hodson, and the record includes air temperature and humidity, wind speed and incident radiation. The nearest station measuring precipitation is the WMO weather station in Svalbard Lufthavn

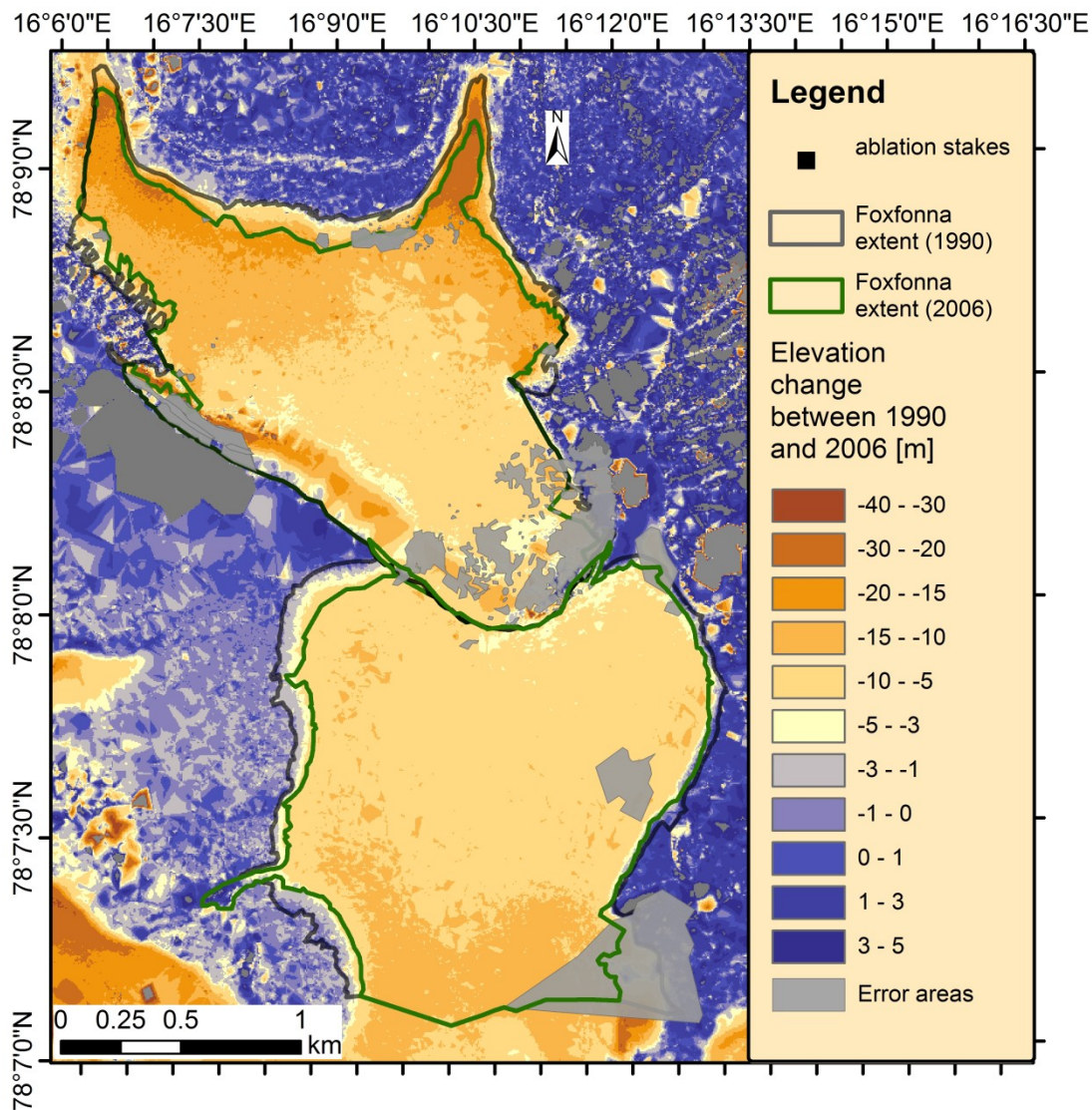


Fig. 3.16b. Map of Foxfonna glacier extent and elevation change in the years 1990–2006.

(airport), which is located 17.5 km from the glacier. Its record spans from 1912 until now, and in the years 1912-1993 the mean annual temperature of -6.3°C and the mean annual precipitation of 180.7 mm were noted there (Hanssen-Bauer and Førland, 1998). More specific meteorological conditions of the mass balance measurement periods are given in Table 3.7., indicating the period 2009-2012 to be the warmest and noting the highest sum of positive degree-days in the history of mass balance studies on Foxfonna glacier. Also, this period was characterised by the highest mean annual precipitation sum among the studied time spans.

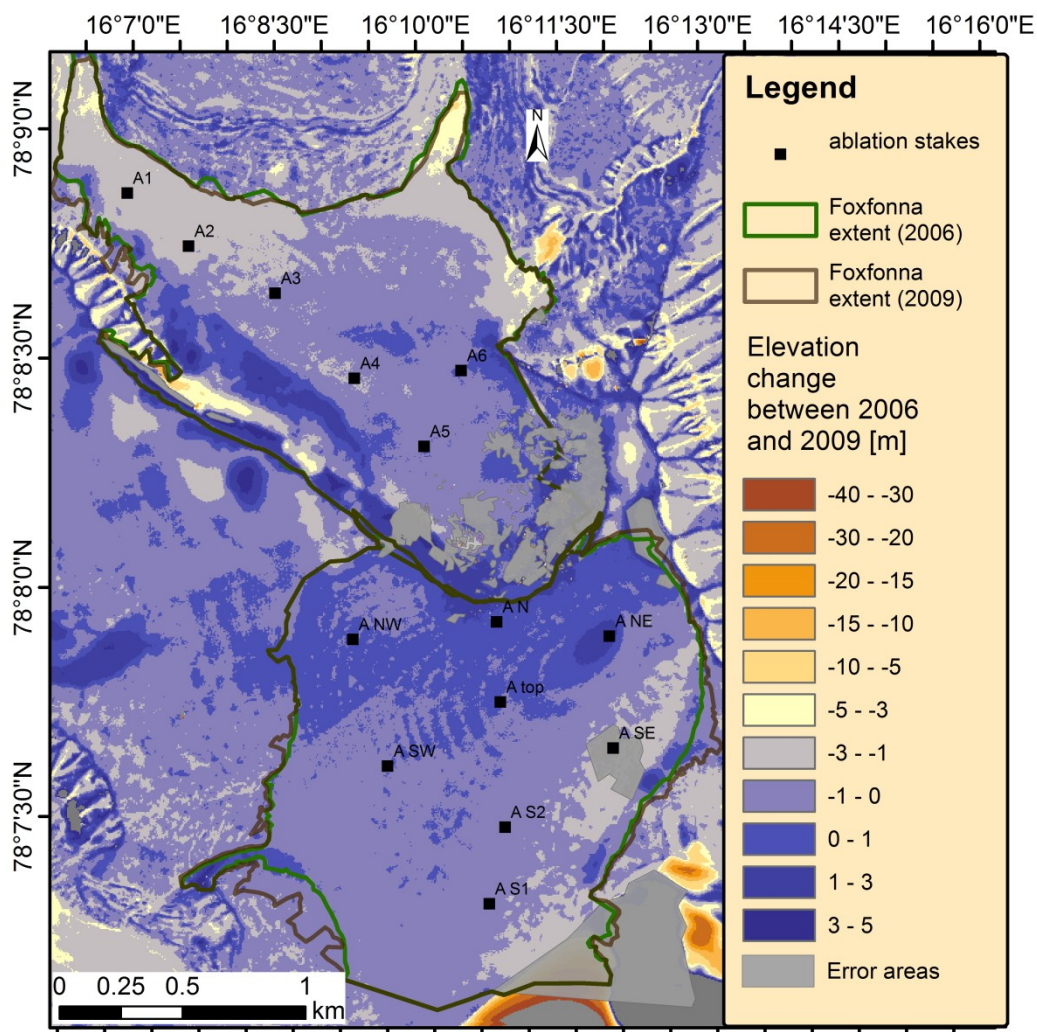


Fig. 3.16c. Map of the glacier extent and elevation change in the period 2006–2009 .

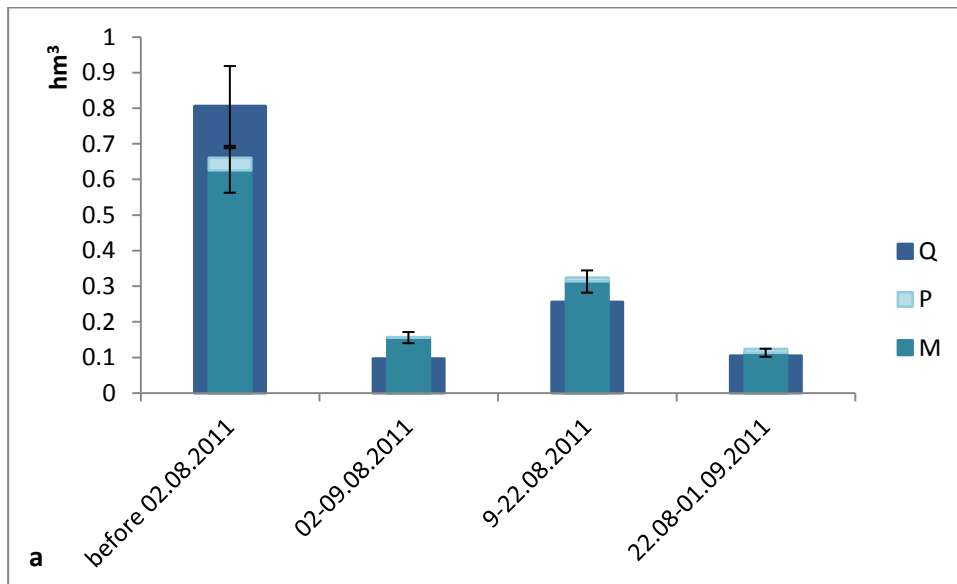
Table 3.7. Meteorological conditions in Svalbard Lufthavn station, for the three periods of geodetic mass balance measurements reported in Table 3.6, and for the period of direct mass balance measurements on the whole surface of Foxfonna (2010-2012). For comparison, data from the AWS located next to Foxfonna (on Breinosa plateau, 520 m a.s.l.) are given if available.

Period	Mean annual precipitation sum [mm]	Mean annual temperature [°C]	Mean annual sum of positive degree-days (PDD)
Sep 1990 – Aug 2006	194.3	-4.85	581
Sep 2006 – Aug 2009	173.7	-3.55	636
Sep 1990 – Aug 2009	191.0	-4.65	590

Sep 2009 – Aug 2012	211.8	-3.02	654
Sep 2009 – Aug 2012 on Breinosa		-6.73	187.6

3.3.3. Water balance of the supraglacial catchment in 2011 and 2012

The ablation with the addition of precipitation as rain was compared to the discharge sum (runoff) in shorter periods of 2011 and 2012 summers, resulting in a RSEs of 31.2% and 10.8% in 2011 and 2012, respectively (Fig. 3.17.). The highest discrepancies were found in the colder periods of the 2011 summer, when melt significantly exceeded runoff. This may be due to englacial water storage, but also due to overestimation of melt by assuming higher density of ice than was actually decaying (surface weathering crust). However, the impact of the latter factor would be balanced by the formation of cavities in deeper ice layers simultaneously with the removal of the uppermost, partly decayed ice layer. The only exception from this course of action may be long cold and cloudy periods, especially in the end of summer when further melt is impeded. Furthermore, the higher error in 2011 may be related to the fact that the ratio between the discharge at the glacier snout and in the gauging site was only determined in 2012. The close correspondence between melt combined with rain and runoff from the supraglacial catchment in 2012 is reassuring, while 2011 data need to be treated with more caution.



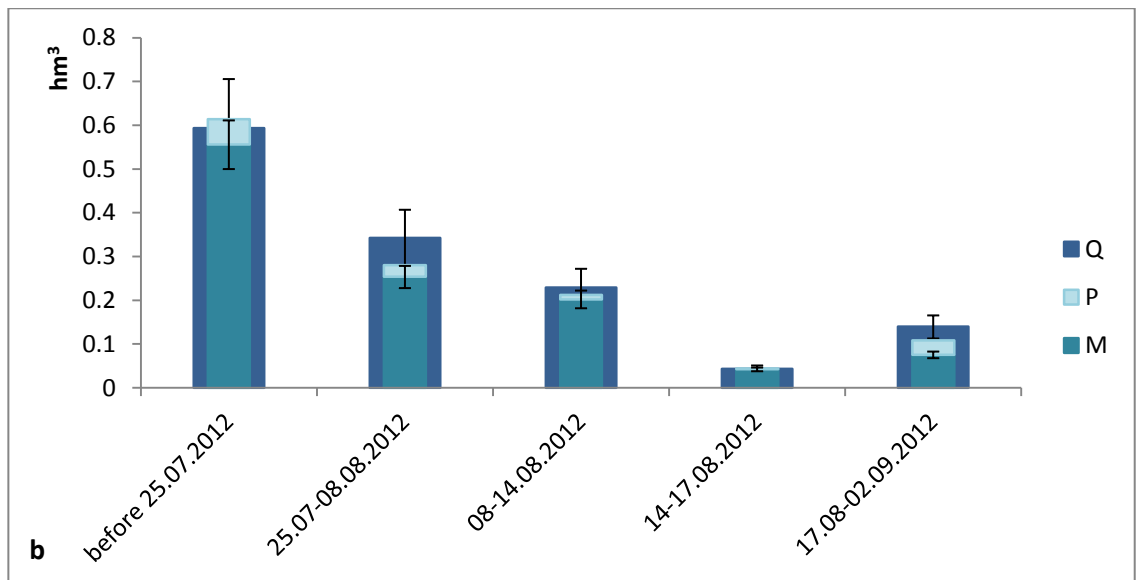


Fig. 3.17. Partial water balance for the supraglacial catchment delineated on Foxfonna glacier in 2011 (a) and 2012 (b).

The division into shorter periods is based on ablation measurement schedule in a particular season.

Q – runoff, P – precipitation as rain, M – melt.

3.3.4. Long-term glacier morphology change deduced from photogrammetric record

Along with glacier geometry changes, its surface and surroundings have altered hydrologically and geomorphologically. Small changes occurred in the hypsometry curves, especially connected to mass losses in the lower part of the glacier (Fig. 3.18).

The flow paths on the glacier surface have been considerably stable (in a glacial context) across all snapshots considered here, with the catchment occupying the western part of the tongue being the least changeable in the long term. This catchment has remained similarly shaped throughout the photogrammetric record and the field observation period in 2010–2012, and except 2006 and 2012 has been drained by one long supraglacial stream forming the main water path on the whole Foxfonna. This stream could be more precisely defined as ‘cut and closure’ type channel, with parts of the watercourse flowing englacially, as described by Gulley et al. (2009). In 2012 and 2006, an additional supraglacial stream has formed in the middle part of Foxfonna tongue, draining the part between two lobes within the same supraglacial catchment, and changing its surface area by a small amount (0.04 km²; Figure 3.18a). In 1961, there was an additional stream draining the middle part of lower Foxfonna as well, but located much further towards east than in the years 2006 and 2012.

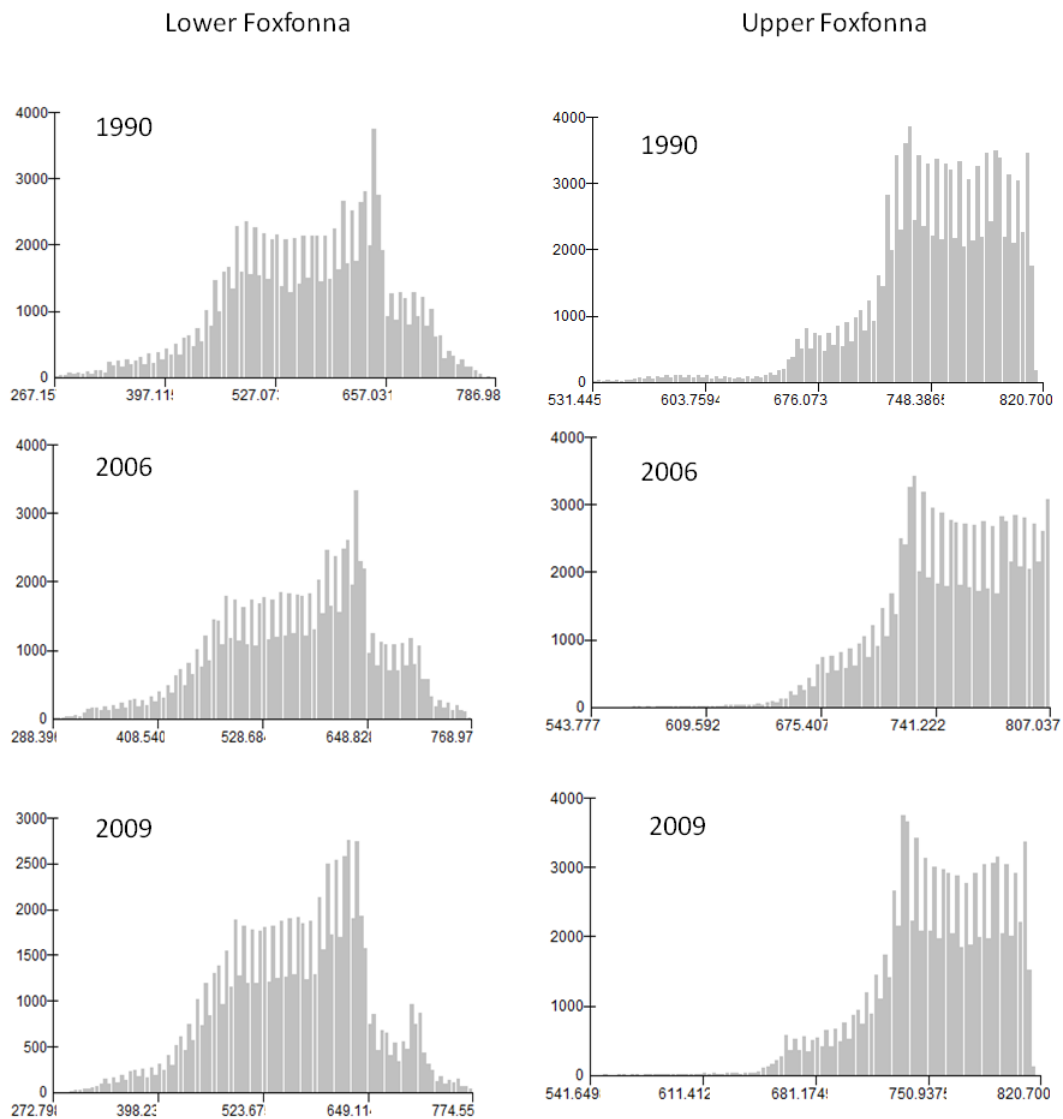


Fig. 3.18. Elevation class distribution across DEMs of Foxfonna for the years 1990, 2006 and 2009, each with a 5 m resolution.

On the Y axis frequencies of DEM cells are marked for a given elevation band.

The eastern side of the glacier was more changeable and less accessible for hydrological sampling throughout the observation on aerial images and in the field, and its importance has diminished as a result of its prominent thinning and retreat in the years 1990–2009. It has been drained by a stable small stream (existing at least since 1961), which has disappeared near the contact of Foxfonna margin with a north-west heading ridge, and was difficult to track further down (perhaps emerging again at Foxfonna’s eastern lobe). Back in 1961, there was a prominent watercourse draining the north-eastern lobe of Foxfonna, and it remained so in 1990. However, after the massive thinning exceeding 20 m ice thickness loss in the period 1990–2006, only two short streams were left instead. Due to the difficulties in accessing the patchy hydrological network of this part of the glacier, and because of the difference in

magnitude of flows between the two sides of the glacier in favour of the western part, the eastern side of Foxfonna tongue was neglected in the organic carbon budget study performed in Chapter 4.

An field of naled ice (Baranowski, 1982; Schohl and Ettema, 1986), hereafter referred to as an icing, has been seen in each of the years 1961, 1990, 2006 and 2009–2014 in front of the western lobe of Foxfonna. It has been smaller on the photographs taken in 1961 and 2006 than on the 1990 and 2009 images. This might be attributable to its slow disappearance during the melt season, which has been observed in the field in the years 2010–2012 (both 1961 and 2006 photographs have been taken about a month later in the season than those from 1990 and 2009). Also, the icing changes its location by following the tongue retreat, hence its changing extent might be topographically constrained. In any case, this record shows the existence of this feature before the mine had been opened, which suggests that the hydrological paths have not been significantly changed by the mining activities. The origin of this icing has not been resolved yet, however it may resemble the mechanism described on the neighbouring Scott Turner glacier (Hodgkins et al., 2004).

The catchment of the supraglacial stream (Fig. 3.7, compare Fig. 4.1.) running into the western lobe of Foxfonna was established by walking its boundary in accessible parts and using 2009-DEM-derived contours in inaccessible areas. There was an ambiguity connected with the bergschrund in the top part of the catchment, as to whether the water from the ice cap draining into this crevasse continues into the front of the western lobe or is redirected elsewhere. However, a dye-tracing experiment performed with 250 mL of rhodamine WT in July 2010 (Hodson, Unpub. Data) has shown no dye return at the end of the icing (data not shown). Hence, the top catchment boundary in the following years was drawn along the bergschrund (Fig. 3.7, Fig. 4.1.).

Further small changes in the glacier morphology have been observed in the years 1961–2009, but with no dramatic shifts. The most striking change observed has occurred in the eastern part of Foxfonna tongue, and this was the disappearance of a topographic depression (surrounded by crevasses) after 1961 (Figure 3.19, indicated by no. 1). In 1990, the same area was occupied by a snow patch, perhaps due to the still existent topographic sink, but crevasses were not visible any more at that time. By 2009, this area ceased to be distinguishable from its surroundings in terms of snowpack thickness. A gradual reduction in crevassing was also observed between 1961, 1990 and 2009 on the crest of the slope connecting the upper and lower Foxfonna (Fig. 3.19, no. 2, compare Fig. 3.7). The small crevasses still visible in the southern part of the ice cap in 1961 have virtually disappeared by 1990. Also between 1961 and 1990, the shattered cornices above the south-western flank of Foxfonna tongue became smaller and smoother, and have lost their northernmost section.



Fig. 3.19. A fragment of the 1961 aerial image of Foxfonna glacier.

1) the topographic depression south from the eastern lobe, 2) crevassed area at the crest of the slope dividing upper from lower part of Foxfonna. The elongated features on the lower Foxfonna are most likely supraglacial streams, since they match closely the position of streams in 2011 and 2012. Top of image is approximating north. Copyright: NPI, photograph ID s61_3088.

Finally, the moraines of the glacier have been changing as rapidly as the lowermost reaches of the glacier tongue. The elevation reduction is likely resulting from the ice core of the moraine melting, and the areas which experienced the most pronounced elevation decrease were east facing slopes in the vicinity of both glacier lobes (15-30 m in the period 1990–2009). A lowering of 5-10 m has also been observed on the north-facing slope of Foxfonna frontal moraine (its part between the two lobes) in the period 1990–2009.

3.3.5. Surface albedo survey

One of the possible factors influencing glacier thinning is surface albedo. To explore this subject, an opportunistic albedo survey, taken on 23rd July 2010, will be analysed here (Hodson, Unpub. Data). The results are presented in Fig. 3.20, and they show a striking difference between the lower and upper part of the glacier tongue, corresponding to its division into snow-covered and snow-free parts. The average albedo of the snow-covered area was 0.61 ± 0.10 (1 SD), slushy surfaces averaged at 0.40 ± 0.15 , ice showed an average value of 0.31 ± 0.11 ; the ice surface at the time was in the form of *weathering crust* sensu Müller and Keeler (1969), while surface debris depressed the albedo to 0.13 ± 0.06 .

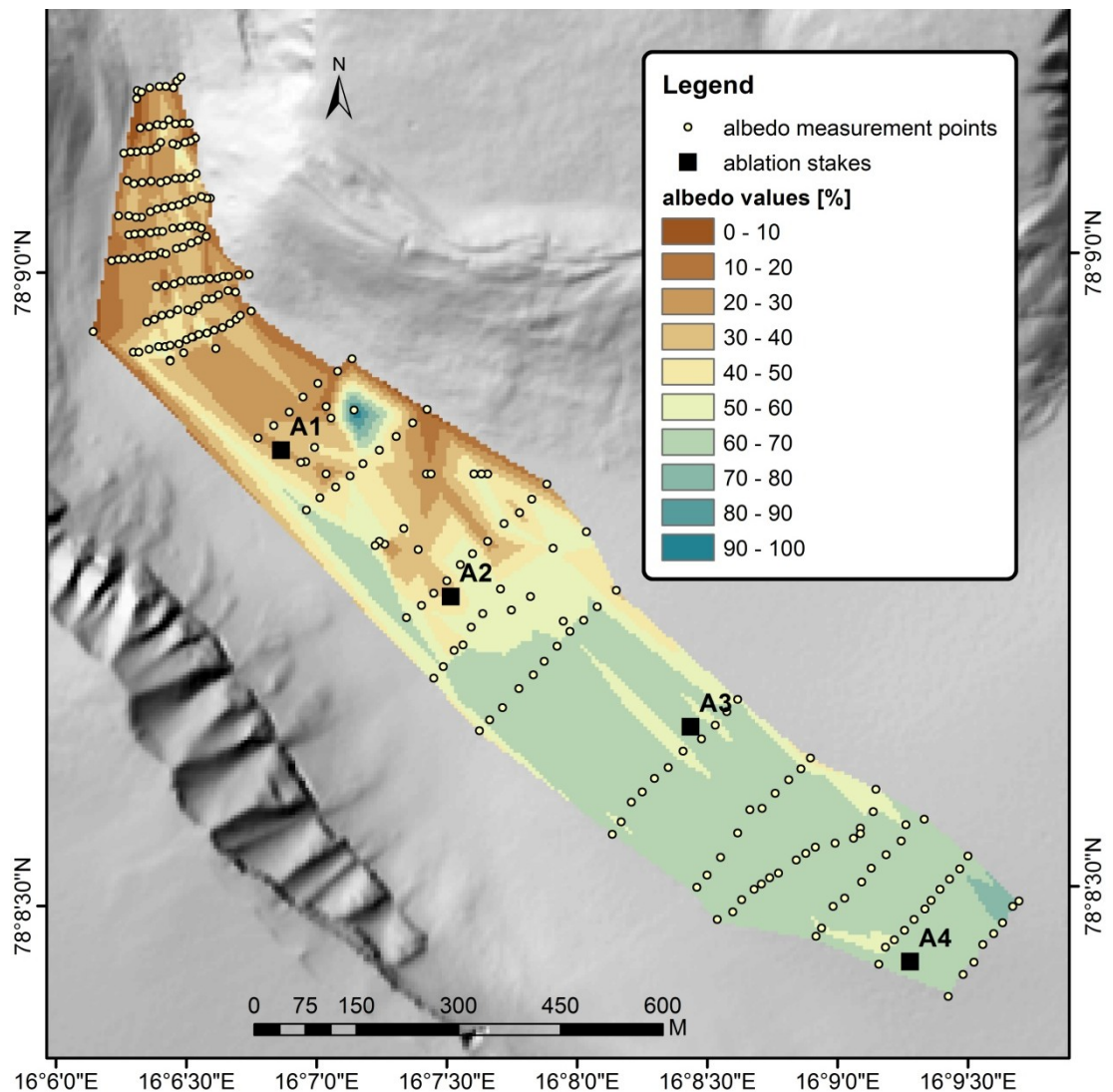


Fig. 3.20. Albedo map on 23rd July 2010.

Source: Hodson (Unpub. Data).

3.3.6. Glacier thickness change and internal structure

Upon GPR sounding, the upper part of Foxfonna glacier revealed a dome-like geometry and sloping bed topography (Fig. 3.21). The ice thickness reached 80 m in the middle of the dome,

which was surrounded by areas of thicknesses below 20 m, except streams of approximately 40-meter-thick ice to the north, south and south-east, which are aligned with the ice cap connections to Foxfonna and two other glacier tongues: Rieperbreen and Foxbreen.

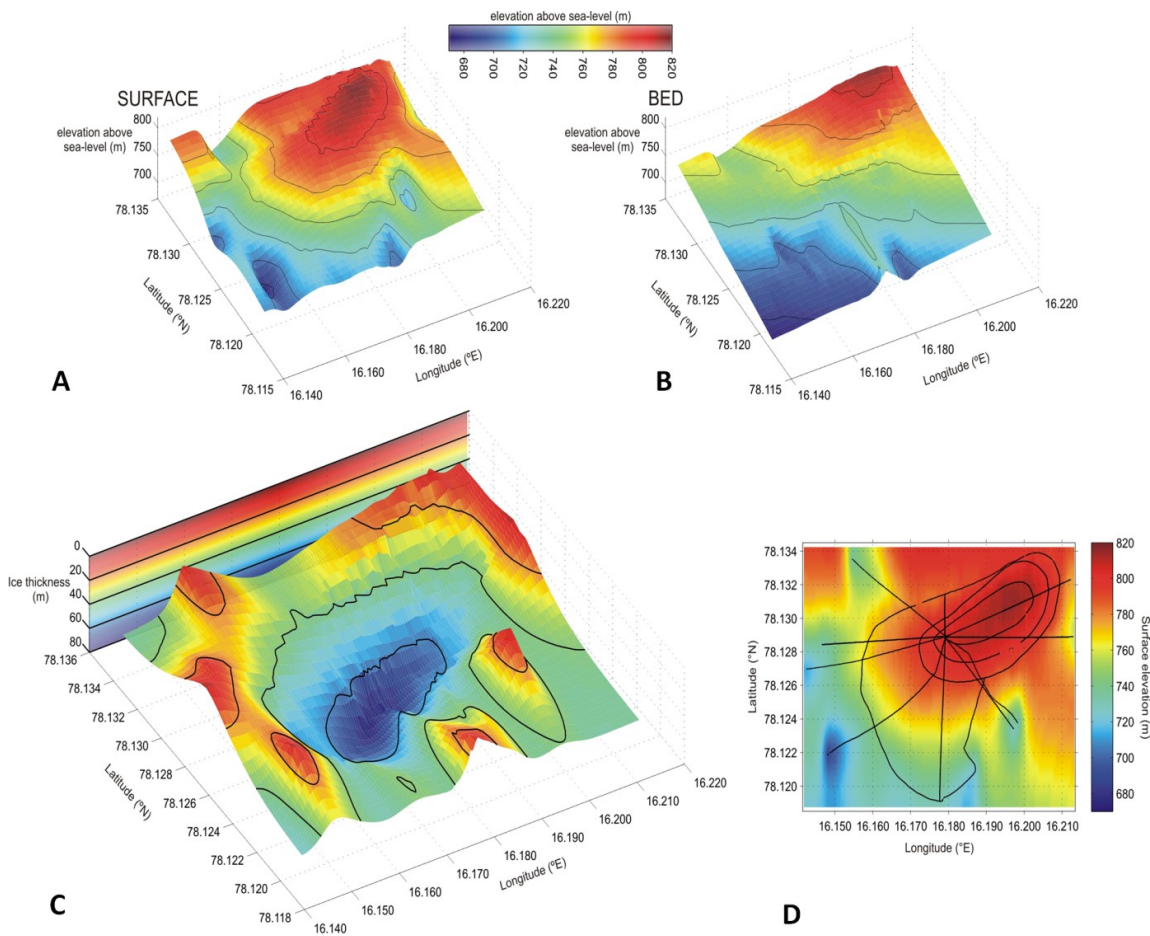
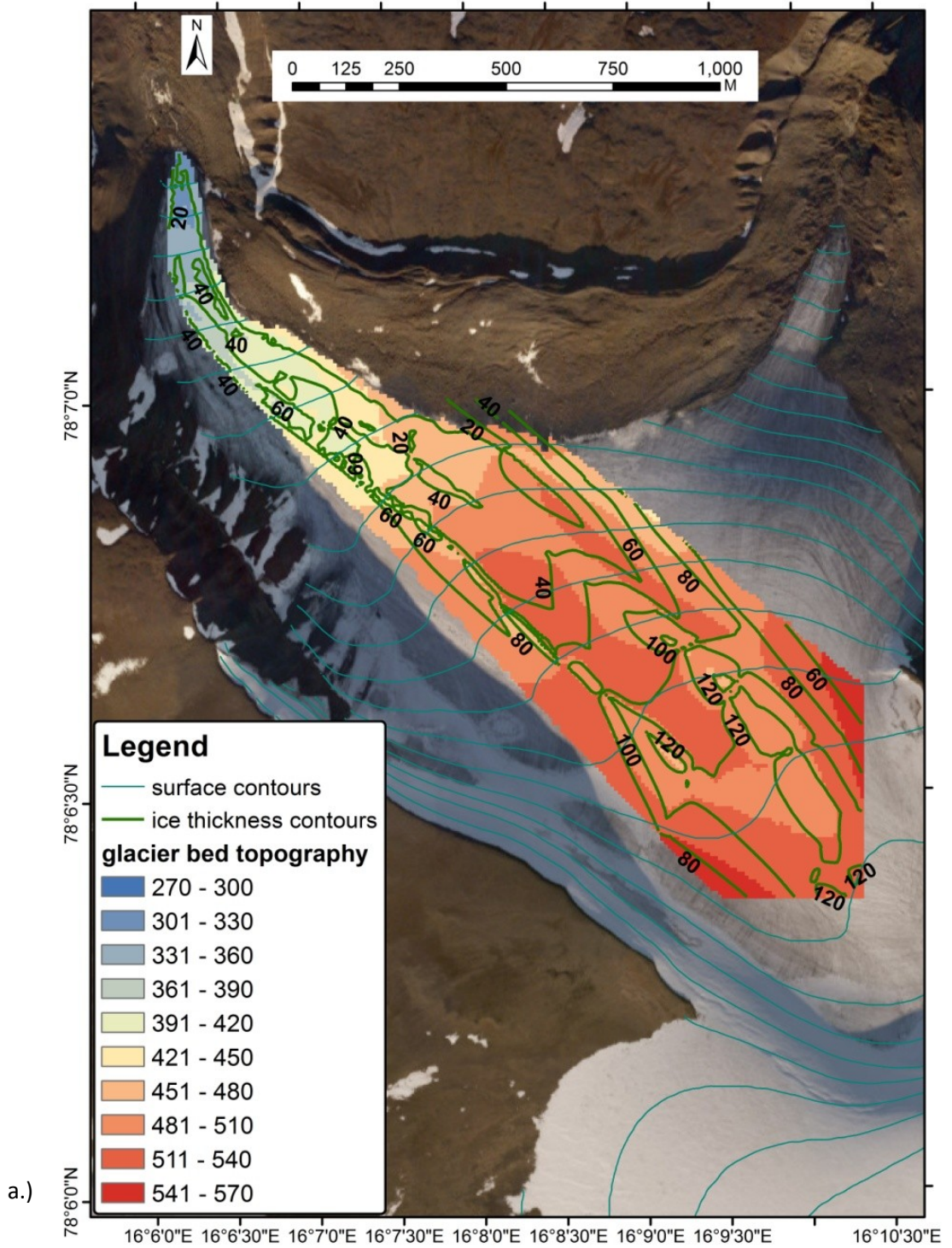


Fig. 3.21. Surface (A) and bed topography (B) of the upper part of Foxfonna glacier, ice thickness map (C) and radar sounding lines (D).

Image courtesy Adam Booth (data by T. Murray, A. Booth, K. Bælum & D. Benn).

The ice thickness on the lower part of Foxfonna glacier (Fig. 3.22), as shown by the GPR sounding in March 2012, reached 133 m in its top flat section. Towards the snout, the thickness was gradually diminishing, reaching a minimum around stake A2. The measurement of the ice thickness enabled the reconstruction of the glacier bed topography, which showed two concave features: a wide trough in the middle of the explored part of the glacier tongue and a much narrower incision to the south-west of it. Both features are located in the area with a convex ice surface, and the second one is partly aligned with the main drainage pathway, of the ‘cut and closure’ type (Gulley et al., 2009).



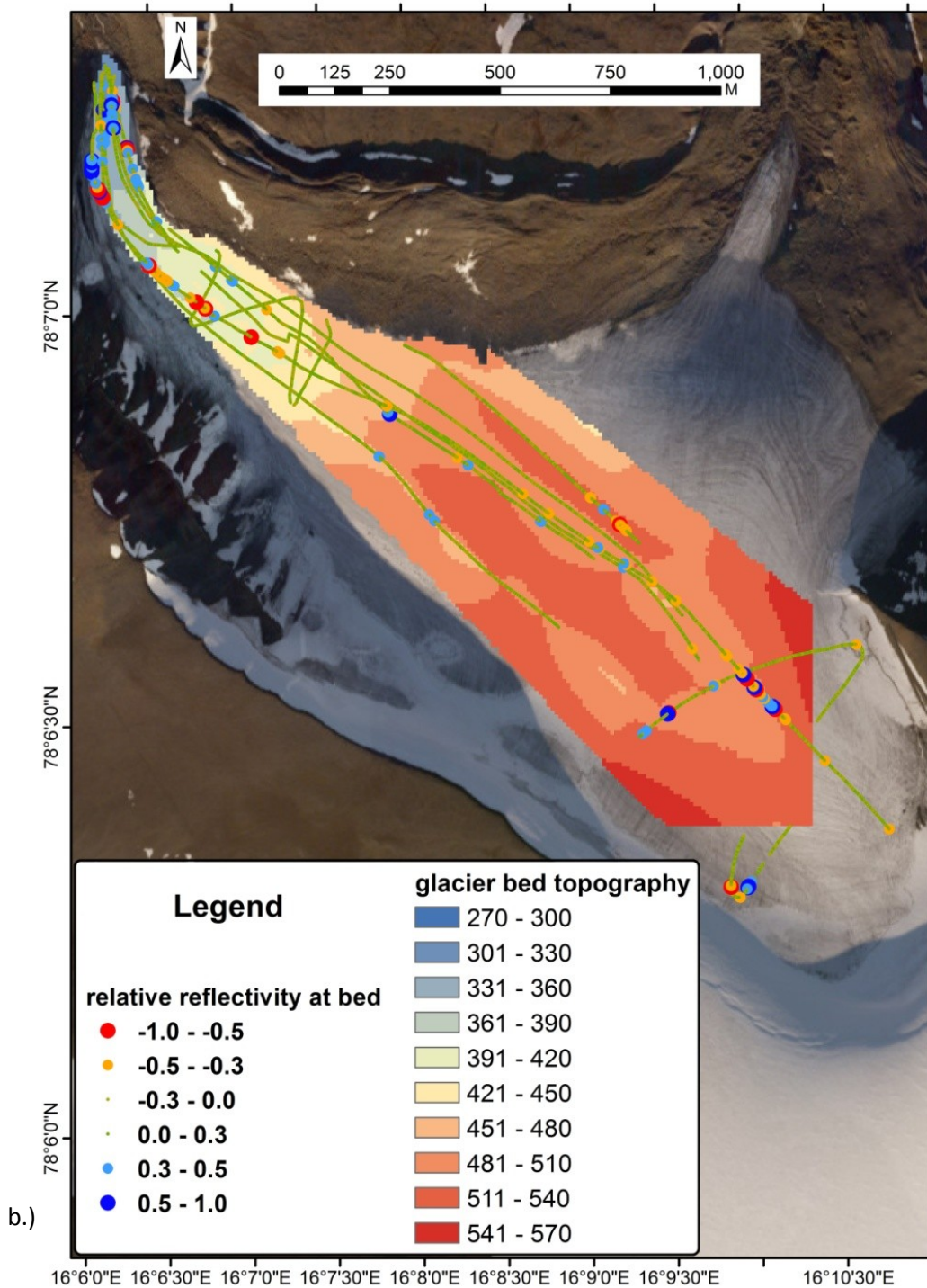


Fig. 3.22. Ice thickness and bed topography map of the lower part of Foxfonna glacier in 2012, radar-surveyed by Thomas Gölles and the author (a). Along the majority of survey lines, relative amplitude of bed reflections were also analysed (b).

Ortophotomap and DEM: courtesy Store Norske Spitsbergen Kulkompani AS.

On the radar images, information about the ice properties can also be found. The basal layer of ice shows a clear reflection profile characteristic for ice below pressure melting point, both in the upper and the lower parts of the glacier, confirming that the majority of the glacier

is cold-based (Christiansen et al., 2005; Liestøl, 1974). However, occasional hyperbolae occur in the lower part, which might be marking either entrained debris or liquid water. In the area of the north-western lobe of the glacier, the presence of cut-and-closure channel system with moulin and shallow ice (<20 m) may also promote meltwater channels bringing water to glacier bed (as was shown on Tellbreen glacier, Svalbard, by Bælum and Benn, (2011)). Hence, the possibility of liquid water occurrence at glacier bed was further explored by analysing relative amplitudes of the bed reflector. The results of this analysis are included in Figure 3.22. The strongest bed reflections were found near the thickness maximum and along the lower stretch of the 'cut and closure' stream system. Occasional strong reflections were also found in the middle of the glacier tongue and at the back wall of the cirque. An example of the line with a strong reflectivity hotspot, from the part of the glacier near its depth maximum, is shown in Figure 3.23. On the same line, it is also visible that the upper part of the ice profile in the cirque showed a layered structure, which faded between the depth of 25 and 50 m around stakes A4 and A5 (and in glacier areas below and above those points, this happened between 10 and 15 m depth).

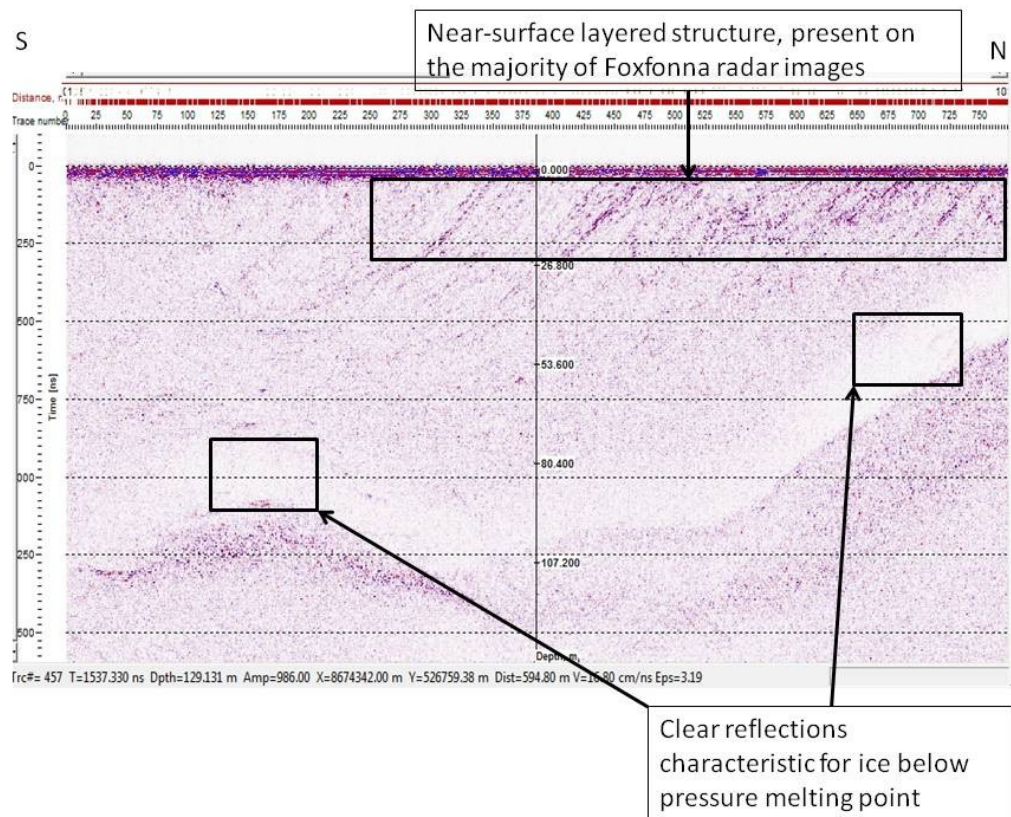


Fig. 3.23. An example radar picture taken in the vicinity of stakes A4 and A5 in March 2012.

3.3.7. Glacier movement

In Table 3.8, the measured horizontal stake speeds and movement directions for the period 2012–2014 are reported. Most of the ice cap stakes have shown very slow movement in a variety of directions, with only A SE moving by almost 1 m a^{-1} towards south-west. The lower Foxfonna stake movement have been dominated by the northward component, along with the glacier tongue direction (the more pronounced of the two lobes). The average annual translocation on the lower Foxfonna amounted to $0.33\text{--}2.79 \text{ m a}^{-1}$, while on the upper the speed values were within the range $0.00\text{--}0.99 \text{ m a}^{-1}$.

Table 3.8. Surface velocities on Foxfonna, measured in the period 14th August 2012 – 16/18th June 2014). Stake locations are shown in Figures 3.1 and 3.2.

Stake	Velocity [m a^{-1}]		Horizontal speed [m a^{-1}]	Horizontal speed error bars (range)	Direction of movement
	Northward component	Eastward component			
A1	nd	nd	nd	nd	nd
A2	2.023	-1.859	2.747	2.708–2.787	NW
A3	0.297	-0.171	0.343	0.329–0.357	NNW
A4	nd	nd	nd	nd	nd
A5	1.991	-0.747	2.127	2.087–2.167	NNW
A6	nd	nd	nd	nd	nd
A top	-0.010	-0.019	0.021	0.008–0.035	W
A NE	-0.002	0.013	0.013	0.001–0.025	E
A N	0.193	-0.097	0.216	0.160–0.271	NNW
A NW	0.075	-0.026	0.080	0.042–0.117	N
A SW	-0.175	-0.232	0.290	0.261–0.320	SW
A S1	nd	nd	nd	nd	nd
A S2	-0.116	0.033	0.120	0.100–0.141	SSE
A SE	-0.624	-0.745	0.971	0.949–0.994	SW

3.4. Discussion

3.4.1. Mass balance: multi-method comparison and spatial patterns

The mass balance of Foxfonna glacier was negative throughout the years 2007–2013, despite the glacier’s high altitude setting. This was aligned with a general thinning trend visible in the mass changes in the periods 1990–2006 and 2006–2009. The trend was consistent

between the two shorter periods, despite the error introduced into the comparison by different areas being excluded from DEMs due to shading or poor texture in snowy areas. This bias could however lead to a slight overestimation of melt, since areas with snow remaining (and hence potential accumulation or less ablation in the whole summer season) were more likely excluded. These excluded areas are shown in grey on Figure 3.16 and did not exceed 9% of the overall glacier area in any of the periods.

The spatial distribution of the mass loss was also consistent in the period 1990–2013 between the two mass balance measurement methods: geodetic and direct. However, the quantitative comparison was only possible for the period with overlapping measurements with both methods, which is 2006–2009. The results of such a comparison were inconsistent, not the least because the two datasets refer to different types of change, and so the geodetic mass balance data actually encompassed also the dynamical surface geometry change (Figure 3.24.). On the stakes A SW, A S1 and A S2 an approximately double surface lowering was recorded by the geodetic method when compared to direct measurements. This might be due to the difference between snow and ice density – the latter being assumed in geodetic mass balance calculations. Furthermore, the vertical velocities measured on those stakes, in the range (-0.01) – (-0.06) (± 0.05) m yr^{-1} , could compensate for the experienced difference. Three other stakes: A top, A NW and A N were reported to experience mass losses in the direct measurements, while the geodetic measurements were very close to zero or positive. The stakes A top and A N also experienced positive vertical velocities, which could partly account for the difference (0.09 ± 0.04) and (0.05 ± 0.06) m yr^{-1} , respectively). Hence, only the discrepancy at the stake A NW remains unexplained, since the vertical velocity measured there amounted to -0.14 ± 0.07 m yr^{-1} , while the difference direct mass balance result would suggest rather emerging velocity at that site. Finally, these three stakes (A top, A N and A NW) are likely to represent areas of gaining mass in the long term, as their locations showed snow cover persisting on both the 2006 and 2009 aerial images, and the A N stake has also been in a snow-covered area of the 1990 image with very sparse snow cover across the rest of the glacier. Hence, perhaps the mass gains were slightly underestimated there by the direct measurements, particularly as these were started by snowpit surveys in the spring of 2007 and therefore could not account for the superimposed ice accumulation in the autumn of 2006. On the other hand, the 2009 aerial image was taken at the end of July and therefore any melt after this date has not been accounted for in the geodetic dataset. Another explanation for an extra loss in the direct measurement dataset could be a localised melting accounted for by direct measurements (a cone melted around the stake due to heat conduction via aluminium pole), but this effect has been restricted by the use of ablation boards, which approximate the surface in a further distance (0.25 m) from the stake base.

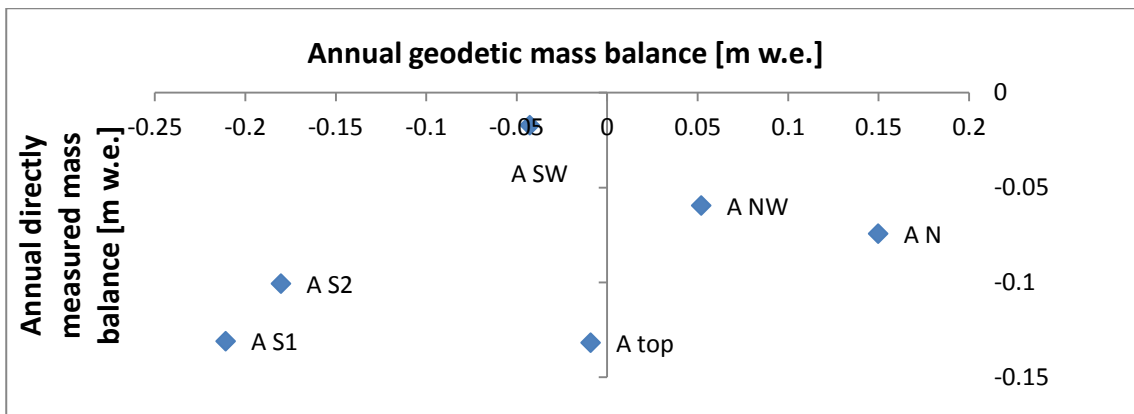


Fig. 3.24. A comparison between geodetic and direct net mass balance, as measured in the ablation stake locations for the period 2006–2009.

Taking the average of balance years 2007, 2008 and 2009 from the glaciological measurements results in a glacier-wide Bn estimate of $-0.12 \pm 0.13 \text{ m a}^{-1} \text{ w.e.}$, while the geodetic estimate is $-0.39 \pm 0.11 \text{ m a}^{-1} \text{ w.e.}$ Their discrepancy emphasises the influence of potential error sources on both values, with the direct measurements being skewed towards more positive mass balance. Part of this bias probably arises from not representing the marginal area with ablation stakes, which for an ice cap that loses mass results in an underestimation of melt.

In the years 2007–2013, as direct measurements have shown, most mass has been lost in the south-eastern part (stake A SE) and the more flat parts of the glacier tongue (stakes A2 and A4). The geodetic mass balance investigation confirmed this pattern, highlighting the location of stake A4 as losing an exceptionally high ice mass when compared to its surroundings (particularly in the years 2006–2009). The bias towards the glacier centre in the direct measurement distribution might be the reason for the higher glacier-wide mass balance estimate from direct than from geodetic method, since the spatial distribution of Bn highlights the margins as areas that are rapidly losing mass. The stake network, on the other hand, does not encompass frontal parts of Foxfonna, located below 300 m a. s. l. and characterised by a striking ice thickness loss exceeding 5 m in the period 2006–2009 and 30 m between 1990 and 2009. The areas of positive mass balance appear to have less contribution to the difference between the two methods outcomes, so the inclusion of stake AN in the lower Foxfonna mass balance estimation seems sufficient to account for possible accumulation occurring there.

The massive thinning of the lower Foxfonna lobes is likely attributable to albedo-related effects. First of all, there is a striking albedo difference between snow and ice, with the measured averages from end July 2010 contrasting by 0.30, a nearly equal value to the ice reflection coefficient itself (see Fig. 3.20). The lowermost reaches of the glacier tend to lose snow cover first. However, the difference between the time when ice is exposed at the higher

stakes is only a few days, as can be observed on frequently obtained photographs from 2011 summer season (material not shown). Still, the lowermost part of the glacier is also likely to have a lower albedo in the snow-free period due to higher cryoconite load in this area (more on this subject, including cryoconite mass distribution and its organic content, can be found in Section 4.3.6.).

Another two factors, possibly influencing Foxfonna's melt pattern, are aspect and topography, which contribute to shading of particular parts of the glacier from direct sunlight. The influence of aspect can be observed clearly on the ice cap, where the south and south-east facing parts have been losing most ice in the short and long term. On the glacier tongue, the topography plays a more important role, with an elevation gradient visible in melt intensity. The long-lasting snow cover observed on the steep slopes flanking lower Foxfonna cirque is most likely occurring due to topographic shading (Fig. 3.25), since the crests of the slopes exhibit an ice loss rate paralleled by the losses on parts of the glacier tongue below them at approximately 250 m a. s. l. (as shown on Fig. 3.16a-c). However, there are parts of the steep shaded slopes, especially on the south-western flank of Foxfonna tongue, that have experienced vast mass losses in the years 1990–2009 (and sub-periods thereof). This mass loss was accompanied by exceptionally low losses or even gains directly below these areas. This effect is likely due to avalanches occurring on this slope, which have been also observed to happen throughout the melt season in 2011 and 2012.

For the winter mass balance on Foxfonna, the main factor likely to influence the spatial variability is snow redistribution. A detailed winter accumulation mapping, conducted in April 2012 (Hodson, Unpub. Data), showed no elevation gradient in snow depth. On the contrary, an irregular pattern of snow cover thickness was observed then, with a depleted snow depth area in the middle of both the upper and the lower parts of Foxfonna (Fig. 3.26). The low accumulation on south-eastern part of the ice cap may exceed the importance of aspect in shaping the net mass balance of upper Foxfonna, however it is difficult to distinguish between the influence of the two factors. The glacier margins seem to have higher accumulation than the glacier centre, which is in accordance with the observations of Jansson (1999) taken on Storglaciären. This may be an effect of wind-packing of snow against the obstacles, e.g. the frontal moraine. Indeed, an intensive wind redeposition of snow is a well-known phenomenon in Svalbard (Grabiec et al., 2006; Jaedicke and Gauer, 2005; Sauter et al., 2013). This origin of Foxfonna's uneven snow cover is more likely than any melt-induced depletion, as the snow distribution pattern is independent of shading relief. The pattern observed, interpreted as wind-related, would indicate that the dominant wind direction in this area was from the south-east. This is consistent with the tunnelling effects of winds occurring along Adventfjord and the small valleys surrounding Foxfonna. The dominant local wind direction of SSE described for

Nordenskiöld Land (Humlum, 2002) and SE near Longyearbyen, on Gruvefjellet (Humlum et al., 2007) support this assertion. This wind direction is also close to the one modelled by Jaedicke and Gauer (2005), who predicted ESE-WNW snow redeposition pattern on Foxfonna. The local snow thickness maxima on the glacier were located on the lee-ward slope between the upper and lower part of the glacier, which can be attributed to secondary backward air circulation forming at the slope crest, as well as in front of a moraine ridge in the north, which emphasises the role of obstacles in wind deposition of snow on Foxfonna.

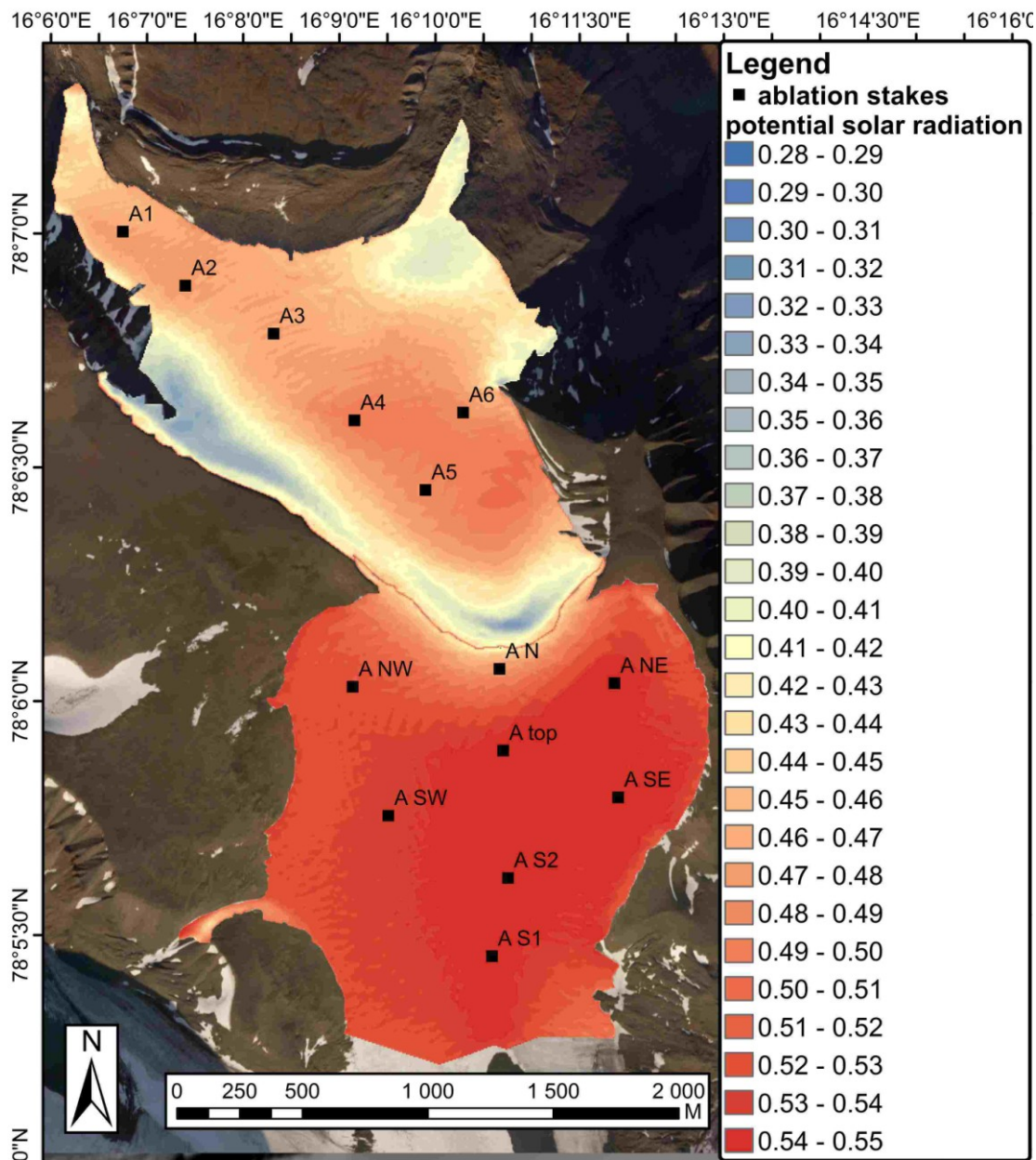


Fig. 3.25. Topographical exposure to sunlight deduced from Foxfonna DEM for 2006

The potential solar energy fluxes are expressed in $MWh\ m^{-2}\ a^{-1}$. Courtesy SNSK SA.

The map (Fig. 3.26) provides little information on the relative importance of avalanche-induced snow redistribution, but avalanche deposits were observed in the field in several

places at the base of the south-western slope of Foxfonna, which is consistent with some of the local snow depth maxima shown on the map. This snow frequently persisted until the end of the melt season in these locations. The geodetic data confirm this to be a likely occurrence, since the base of the aforesaid slope has exceptionally high net balances as compared to its surroundings.

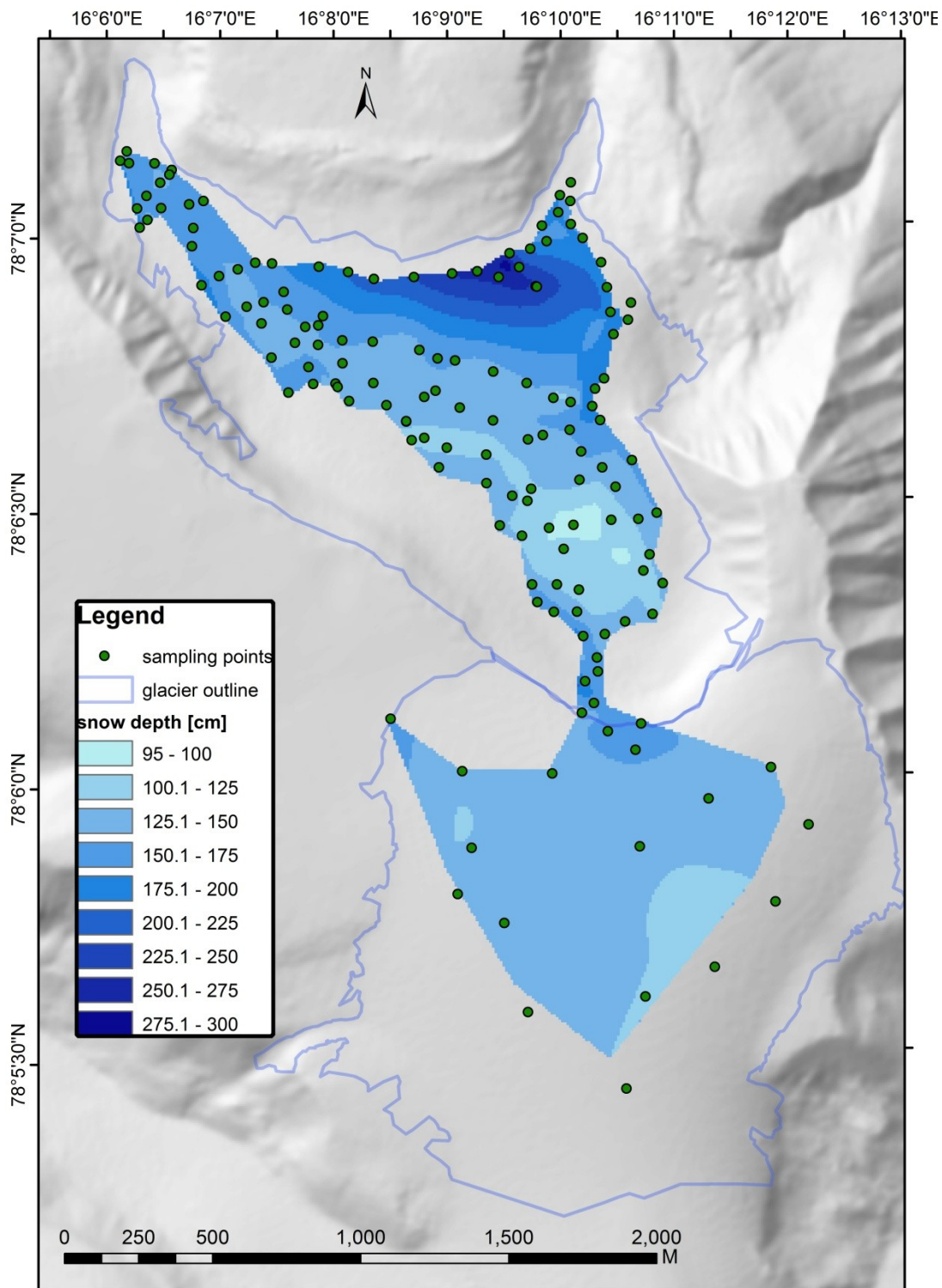


Fig. 3.26. Snow cover thickness distribution on Foxfonna in late April 2012.

Source: Hodson (Unpub. Data). Measurements by A. J. Hodson, A. Nowak, S. Smith Johnsen, I. Bakkhaug and S. Tørstad. Background: 2006 DEM of Foxfonna, courtesy SNSK.

The short-term direct mass balance monitoring has shown that the net mass balance inter-annual variability on Foxfonna was driven by the summer mass balance changes (Fig. 3.10 & 3.15). The spatial variability of B_n , on the other hand, was connected more closely to the

winter mass balance differences and the effects of wind redistribution on Foxfonna (Fig. 3.8, 3.9, 3.11, 3.12 & 3.26), as well as the observed abundance of snow cornices and avalanche deposits (Fig. 3.16). Both the summer and the winter mass balance contribute and react to the surface albedo of this glacier, and hence the albedo-related feedback is an important part of Foxfonna glaciological understanding. The accumulation of snow in winter feeds the areas of higher albedo in the summer, which are located along the steep slopes. The altitudinal pattern of mass loss, observed in the geodetic mass balance study, may stem both from snow melt patterns and the differentiation of surface albedo due to cryoconite loading. In the transition period between snow-covered and snow-free glacier, the first effect is particularly visible, leading to more scatter and generally lower albedo values in the lower part of the glacier, which becomes exposed earlier (Figure 3.20). The low-elevation fragments of the glacier are exposed to a very intensive melt, which results in the striking difference on the mass loss in the period 1990–2009 in the glacier lobe areas (Fig. 3.16).

3.4.2. Ice thickness and internal structure evolution

The sustained negative ice mass balance, as shown by the 1990–2012 data, was consistent with the thickness change between 1972 (Liestøl, 1974) and 2012 (Fig. 3.22) on the lower part of Foxfonna glacier. During the 40 years, the extent of 100 m thickness isoline has diminished, and the lower part of the tongue (below stake A2) has thinned by approximately 10 m. This is slightly less than the estimated change from geodetic mass balance in the 1990–2009 period, which would mean that the deep mass losses experienced by the glacier after 1990 were counteracted in the preceding period by years with positive mass balance. On the other hand, the data provided here have higher spatial resolution than Liestøl's (1974) interpolated depths, the shape of his isolines closely follows the shape of the glacier outline, and so the thickness estimation from that past study may be slightly exaggerated. Still, parts of the thickness pattern drawn by Liestøl (1974) are consistent with the local glacier bed topography shown in the 2012 survey, e.g. the thinning of the lower part of Foxfonna glacier towards the back wall neighbouring with the ice cap.

The detailed bed topography reported here (Fig. 3.22) needs to be interpreted with caution, but there are distinct features that require interpretation on the 2012 map. In particular, two troughs detected in the radar survey may be erosion features, time of their formation remaining unknown. However, the narrow incision feature is aligned with a cut and closure drainage system, hence the possibility of it being an artefact of lower radar wave velocity in water was checked (in case the remainder of meltwater had still been present in the englacial channels in early March 2012). The travel distance of the radar wave would then be exaggerated since the velocities ascribed to the area would be too high (specific for ice with

few liquid water pockets). Indeed, in the area some high values of bed reflection were found. However, for a thickness difference of 10 m resulting from this bias, there would have to be 2 m of liquid water somewhere within the profile, which is a rare occurrence even during summer season (it is probably limited to water-filled moulins). Another explanation would be a “delay-related” artefact, arising from the difference between signals collected on ascending and descending transects due to a delay in positioning data registration. This is unlikely, though, since data in the trough area were collected from lines of both directions. Also, interpolation techniques may contribute to bias. Therefore, the small details of bed topography shown on the map should be treated as only hypothetical, but the major features are most likely real troughs in the glacier bed. Possibly, they indicate a sequence of erosional directions at glacier bed, e.g. due to a shift in regime between the tongue being fed by ice-cap derived ice flow (which has marked a trough across the northern part of the ice cap as well) and its own independent mass transfer.

The layered structure, which was observed in the 2012 radargram (Fig. 3.23), is usually interpreted as a pattern of accumulating firn (Pälli et al., 2003), transferred with the ice flow down the glacier tongue. These features are widespread on Foxfonna, a long distance below the ELA (as observed in the field in 2011 and 2012, on the ortophotomap from 2006 and aerial images from 1990 and 2009). The layered structure of the ablation area ice was also revealed upon coring ice on the glacier surface (see Section 4.2.1.3.), and took a form of bubbly ice lenses occurring beneath the old summer surface covered with debris (cryoconite).

The main outcome of the radar investigations of Foxfonna is confirming its thinning trend by adding another observation across a 40-year-long time window (1972–2012). Based on temperature measurements in the boreholes performed by Liestøl (1974) and 2012 radar interpretation, both in 1972 and 2012 Foxfonna was cold-based in the bulk of the surveyed area. However, in very limited areas there is a possibility for liquid water to occur at the glacier bed, and these areas include the vicinity of ice thickness maximum and the active cut-and-closure drainage system in the lower part of the glacier. The latter, if following the bed reflectivity maxima derived from 2012 radar dataset, would drain subglacially into the stream located on the eastern tip of the Foxfonna lobe that ends in the icing. This is possible, given the shallow ice in the area and the ability of streams of this type to reach the glacier bed, as documented elsewhere in Svalbard (Bælum and Benn, 2011). Also, the higher suspended sediment load observed consistently in subsequent field seasons of 2011 and 2012 in this stream, as compared to the stream located on western tip on the glacier snout, corroborate with this hypothesis.

3.4.3. Glacier movement

The velocities of $0.00\text{--}2.79\text{ m a}^{-1}$, measured here, are similar to the low end of the velocities spectrum measured on other Svalbard glaciers, which is consistent with its thermal structure dominated by cold ice, as well as the shallow mass balance gradient. For example, the lowest velocity measured on Finsterwalderbreen was 1 m a^{-1} (Nuttall et al., 1997). Also, Etzelmüller et al. (1993) have measured the lowest velocities of 0.5 and 1.1 cm day^{-1} (1.83 and 4.02 m a^{-1} , respectively) along the profiles of Erikbreen and Hannabreen, respectively. All three glaciers used in this comparison have similar surface slope angles to Foxfonna (within the range $3\text{--}10^\circ$; Etzelmüller et al., 1993), but a higher range of velocities than the glacier studied here. This is in concordance not only with the reported thermal regime of Foxfonna, but also the lower ambient temperature at the higher elevation, which should limit the deformation velocity (cf. Patterson, 1994). The limitations connected to measurements taken here are however their short time span and the inclusion of only one summer season and two winters, which could cause an underestimation of the velocity measurements. Also, stake deflection could influence the movement measurements: in 2014, stakes A5 and A top were observed to tilt towards NW and N, respectively, which caused the stake top projection on the snow surface at the time to shift from the stake base by 0.36 and 0.28 m , respectively. These were corrected using basic trigonometry. However, the stake AN was also likely to deflect from vertical position, but being located on the crest of a steep slope and protruding from deep snow during measurements by only a short section, it could not be corrected for its potential tilt, contributing to an extra source of error. Nevertheless, neither of these limitations is likely to influence the general velocity range experienced on Foxfonna which is behaving like a slow-moving cold-based glacier.

3.5. Conclusion and implications for the organic carbon budget of the glacier

The final image of Foxfonna, as a result of the above considerations, is that of a relatively simple glacial system, rapidly losing mass after 1990. The glacier is currently characterised by near stagnant ice, and most of its mass has been below the ice pressure melting point both in 2012 and in 1972. There exists a very limited area, where liquid water occurrence is possible at the glacier bed, some of this water possibly derived from the 'cut and closure' channel system. The drainage pathways define a catchment in the north-western part of Foxfonna, which has shown little change in drainage morphology over a period exceeding 50 years (since 1961) and hence was found to be a suitable subject for an OC flux study (Chapter 4). Also, the very limited scope for subglacial interaction with the carbon content of discharged waters makes it an ideal site for a supraglacial OC budget monitoring. Nevertheless, it is appreciated, that even such a simple glacial system may be difficult to monitor due to water paths changing on a small

scale, as well as problems in following pathways of the cut-and-closure drainage. However, these and other difficulties are inherent to glacial systems, which are indeed very dynamic environments during the melt season, and this should not discourage flux study efforts.

Foxfonna has experienced deep mass losses in the years 1990–2013, which makes it a characteristic example for studying OC fluxes prevailing on small and thinning glaciers (provided the current climatic forcing persists). The thinning trend pervaded throughout Foxfonna's wide altitude range, and left it with a very small and non-typically located accumulation area remaining on the steep slopes in the middle of its elevation span. The thinning might have also caused the ice cap to disconnect physically from the glacier tongue; this would be consistent with the stable position of the bergschrund dividing the two parts, as well as the two erosional elongated features occurring in the lower part of Foxfonna, which can mark differently aged ice movement regimes. Also, hydrological experiment results showed no dye return at the icing from the bergschrund tracing, which hints that the two parts may be disconnected hydrologically.

Two important factors in shaping Foxfonna's mass balance are its surface albedo in the summer and wind-packing of snow in the winter. The wind redistribution of snow in the winter causes an irregular spatial pattern of the glacier mass gains, which influences the variability in net mass balance distribution. On the other hand, the temporal pattern of mass losses is more closely related to the summer ice balance, and albedo-related melt changes due to snow covered period and debris loading are likely to influence this.

The biogeochemical study based on Foxfonna glacier is, therefore, likely to be relevant to cold-based Arctic glaciers in 'poor health', rapidly losing mass, while also displaying relatively simple structure and dynamics. Hence, Foxfonna facilitates a flux study for theoretical understanding, due to no or negligible influence of such uncertainty factors as surge behaviour, pressure melting at bed or internal storage in firn areas. However, as glaciers are complex systems, interacting with their surroundings in a variety of physical and chemical processes, the system studied here is nevertheless an analytical challenge.

Chapter 4. Organic carbon fluxes on Foxfonna, a predominantly cold polythermal Arctic glacier

Summary

Arctic glaciers are rapidly responding to global warming and releasing organic carbon (OC) to downstream ecosystems. Here quantitative data on OC fluxes associated with atmospheric deposition and ice melt are budgeted against fluvial export. The explanation for discrepancies is then sought in biological growth and storage (in superimposed ice and cryoconite debris) was measured from the Foxfonna glacier system, Svalbard, over two consecutive years (2011 and 2012). Atmospheric OC input (average $0.633 \pm 0.245 \text{ Mg a}^{-1}$ total organic carbon, or TOC, and $0.396 \pm 0.217 \text{ Mg a}^{-1}$ dissolved organic carbon, or DOC) exceeded fluvial OC runoff in this glacier system (average $0.461 \pm 0.036 \text{ Mg a}^{-1}$ TOC and $0.355 \pm 0.028 \text{ Mg a}^{-1}$ DOC). Early in the summer, an average amount of $0.107 \pm 0.039 \text{ Mg a}^{-1}$ TOC and $0.086 \pm 0.034 \text{ Mg a}^{-1}$ DOC, released through snowmelt, was temporarily stored in a superimposed ice layer on the glacier. This fraction represented up to 28.5% of the total runoff OC flux (in 2012). Thereafter, large quantities of OC were liberated from this and the underlying glacier ice by summer melting. Biological production in cryoconite deposits represented the smallest OC fraction from all the fluxes quantified here (average $0.026 \pm 0.083 \text{ Mg a}^{-1}$ TOC). If an OC budget is constructed using these fluxes, an excess of inputs over outputs will be revealed (average $0.646 \pm 0.121 \text{ Mg a}^{-1}$ TOC and $0.279 \pm 0.103 \text{ Mg a}^{-1}$ DOC), resulting in a net retention of OC on the glacier surface at a rate that would require c. 3 years to account for the OC stored as cryoconite debris.

4.1. Introduction

Glaciers store aeolian dusts rich in organic carbon (OC) and host active microbial cells (Anesio et al., 2009; Hodson et al., 2008), factors which are likely contributing to the darkening of glacier surfaces (Lutz et al., 2014; Warren and Wiscombe, 1980). Whilst recognized as important for the concentration and properties of the surface debris, and hence also the albedo of glaciers and ice sheets (e.g. Stibal et al., 2010; Takeuchi, 2002), the processes of OC input, storage and release in glacial systems are yet to be quantified. A better understanding of OC dynamics is crucial for two key reasons. Firstly, Arctic glaciers are losing mass at an increasing rate (Gardner et al., 2011; Moholdt et al., 2010b) and so the accumulation of atmospheric OC inputs, including natural and anthropogenic aerosols, could further increase the rate of mass loss due to ice surface darkening (e.g. Bøggild et al., 2010; Hodson, 2014). Secondly, the interaction of this biogeochemically reactive OC store with meltwater can influence downstream ecosystems during summer (e.g. Fellman et al., 2010; Hood et al., 2009;

Stubbins et al., 2012), by supplying biolabile organic matter for decomposition at the base of the food chain.

Previous studies in organic matter deposition on glaciers have focussed on anthropogenic pollution, in particular in elemental carbon (e.g. Xu et al., 2009), organic acids (e.g. Li et al., 2001) and persistent organic pollutants (e.g. Bogdal et al., 2010; review by Kozak et al., 2013). In addition, previous research has demonstrated that glaciers act as organic matter storage, and complex microbial communities have been identified in snow (e.g. Amato et al., 2007; Takeuchi, 2001), in supraglacial debris (Anesio et al., 2009; Hodson et al., 2010a), and trapped within the ice (Tung et al., 2005), potentially contributing to OC production and consumption. The fluvial export of OC from glaciers has also been documented in recent years (e.g. Singer et al., 2012; Stubbins et al., 2012). Some studies have also considered the wider implications of glacier biotic activity in regional and global carbon cycles (Anesio et al., 2009; Cook et al., 2012; Hodson et al., 2010b; Stibal et al., 2008a, 2010). However, whilst these studies collectively show active carbon transformation in glacier systems, they rely upon limited field data, which can be attributed to the vast scale of the systems studied (e.g. the Alaskan ice field, Stubbins et al., 2012) or the large sample volume needed to analyse particular compounds (e.g., Garmash et al., 2013). More importantly, no study has yet directly compared carbon inputs and outputs, despite input/output balances being essential to explain OC residence time and cycling in glaciers.

To address this knowledge gap, a detailed and spatially intensive investigation of glacial OC fluxes is presented here for the first time. This study was conducted for two consecutive years (2011–2012). Initially, the OC flux budget was based on the water balance between melt and runoff, as described in Section 3.2.1.3, following the Equation 4.1.:

$$(4.1.) \quad Mc = Qc,$$

where Mc is the release of organic carbon from melting snowpack, superimposed ice or glacial ice with ablation, while Qc is the fluvial OC export to the proglacial region, gauged at the glacier front. However, the strong imbalance between those two components, has led to reframing the problem into a more complex budget study, with the glacial storage of OC in a balance year derived from the Equation 4.2 (see also conceptual model in Fig. 2.6.):

$$(4.2.) \quad \Delta SOC = A + Ic - Qc \pm \Delta bio,$$

where:

- ΔSOC represents the change of OC storage on the glacier surface (in supraglacial debris and near-surface ice), during a balance year. However, this parameter will include an unknown variability introduced by the fluxes not accounted for in this work.

- A is net atmospheric deposition (from aeolian, pluvial and nival sources).
- I_c stands for OC release from legacy ice melting.
- Δbio is the net biological production (positive) or oxidation (negative) of OC, considered in supraglacial debris (cryoconite). A potentially important flux linked to algal blooms is also very challenging to measure in this glacier system and therefore it is not considered in ΔSOC calculation.

Hence, this study is the first attempt to estimate the OC budget for a glacial system, beyond the typically conducted runoff export measurements and a single OC source. Emphasis is placed upon ice surface processes, as this is where the most dynamic OC cycling occurs in High Arctic glacial ecosystems, except perhaps for biological activity in subglacial hotspots. The role of the subglacial ecosystem in the OC cycle is, however, ultimately negligible as climate-driven glacial thinning and mass loss increasing the number of Arctic glaciers that are becoming frozen to their beds (Bælum and Benn, 2011; Hodson et al., 2008).

4.2. Materials and methods

The study was conducted on Foxfonna glacier (for a thorough description of the field site, see Chapter 3), in a small supraglacial catchment representing almost the entire elevation range of the glacier (Fig. 4.1.). The surface area of the catchment varied slightly between investigated years, amounting to 1.27 km² in 2011 (Fig. 4.1.) and 1.31 km² in 2012 (Fig. 3.7.). In both years, the catchment was drained by two lateral marginal streams and a smaller supraglacial stream, all of which flowed into a proglacial icing field. The remaining part of the glacier outside the catchment boundary could not be monitored, since it was impossible to access the runoff for sampling purposes.

4.2.1. Field sampling

Fieldwork was conducted in the spring (April) and summer (June–August) of 2011 and 2012. Specific sampling dates in each year varied due to inter-annual seasonal variation; the 2012 winter was extraordinary because of low snowfall and warm episodes in January–February, which was then compensated by a high snowfall in May. The melt season therefore started later in 2012 than in 2011. Since the snow cover was thicker in early June 2012 than in late April, snow sampling for organic carbon content was performed at the beginning of June in 2012, rather than in April as was the case in 2011.

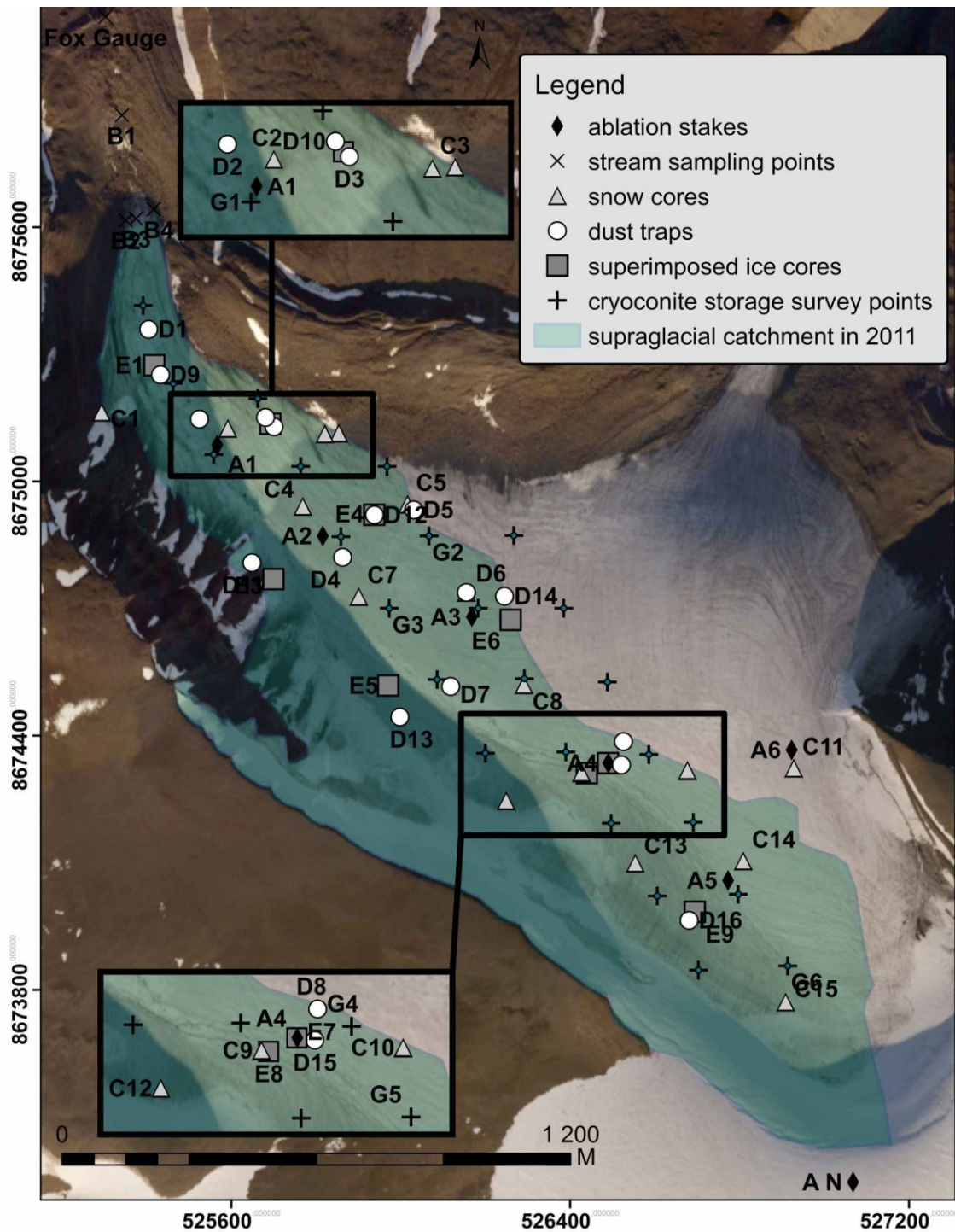


Fig. 4.1. Sampling points on Foxfonna glacier included in 2011 or 2012 field programme.

Labels are provided for: ablation stakes (A1-6, A N), stream sampling locations (B1-4), accumulation season deposition in snow cores (C1-15), ablation season deposition in dust traps (D1-16), superimposed ice sampling points (E1-9) and glacial ice cores (G1-6). Fox Gauge denotes the location of 2011 discharge monitoring station, and the catchment area drawn applies to 2011 (see Fig. 3.7 for 2012 catchment boundary). Orthophotomap (2006) in the background: courtesy of Store Norske Spitsbergen Kulkompani AS.

4.2.1.1. Fluvial export (Q_c) and melt release of OC (M_c) estimation

For Q_c , meltwater runoff was sampled every 2–3 days for most of the melt season on the proglacial stream (Site B1 on Fig. 4.1.), for organic carbon concentration. Every other measurement was accompanied by sampling the streams on the glacier snout (B2, B3 & B4 on Fig. 4.1.). All stream water samples were collected using pre-rinsed centrifuge tubes and frozen at -20°C upon return from the field.

Additionally, in 2012 bigger water samples were taken into 1 L HDPE bottles to estimate the TOC content of the sediment carried at the glacier snout (B2+B3, B4) and downstream (B1); sampling of these started when the streams were visibly sediment-laden. The volume taken was filtered through a $0.7\ \mu\text{m}$ GF/F Whatman filter paper, the filtrate analysed for DOC and the suspended sediment for TOC.

The release from melt, that was compared the fluvial export, required the determination of OC concentrations in snow, superimposed ice and glacial ice.

Pre-melt snow-depth surveys were undertaken at 10 and 14 points during 2011 and 2012, respectively (Fig. 4.1), and were accompanied by snow core collection for measurement of the depth-integrated OC content of the snowpack at each point. Snow water equivalent (SWE) was also measured at several snowpit sites, where between 4 and 6 samples were taken from the different stratigraphic layers for OC analysis. These sites were in the vicinity of the ablation stakes (A1–A4; A3 excluded in 2011) and also at an additional location in 2012 (C15; Fig. 4.1.).

The superimposed ice was sampled at a time coincident with its maximum observed thickness in 2011 and 2012. Samples were taken at the end of July in both seasons using a Kovacs corer with a 9 cm core barrel, coupled to a Stihl two-stroke engine. Manual coring would be impossible with the existent time constraints due to the high water content slowing down the drilling. Cores were collected from 9 locations in 2012, but just one location in 2011 (E7 in Fig. 4.1., where 3 cores were taken). Therefore, the 2011 estimate was scaled up using the ratio between deposition measured at this point and the spatial average of deposition in 2012.

The OC concentration of glacial ice was estimated from 6 shallow sampling profiles (Fig. 4.1.) of surface ice collected at the end of summer 2011 using a stainless steel Kovacs ice auger, which enabled quick and efficient sampling. In each case, a 1-m long glacier ice section was sampled at 20 cm intervals by collecting ice chips with clean, powder-free gloves. The drill was rinsed with $18\ \text{M}\Omega$ deionised water between and prior to measurements.

All snow and ice samples were collected into pre-cleaned plastic zip-lock bags and were allowed to melt in those at a low temperature ($<10^{\circ}\text{C}$) and in the dark. Sample aliquots for OC analysis were taken into plastic centrifuge tubes and frozen in -20°C upon return from the field (after up to 5 days of low temperature storage).

4.2.1.2. Atmospheric deposition (A), supplied with snow or in other forms

Following the determination of the OC release from melting snow, other forms of atmospheric deposition were included in the study, and the sums of all its fluxes will be hereafter described as net atmospheric deposition (A). Different methodological approaches were required to reflect seasonal differences in its dominant inputs, and hence the A term was conceptualised as the sum of deposition from inputs in the accumulation and ablation seasons (Equation 4.3.):

$$(4.3.) \quad A = A^{acc} + A^{abl},$$

where A^{acc} is net OC deposition in pre-melt snowpack, as sampled at its maximum thickness (in the end of accumulation season), and A^{abl} is the ablation season deposition of OC, summarised from shorter sampling periods during summer.

The A^{acc} term was determined by sampling snow prior to the commencement of melt, as was detailed in Section 4.2.1.1. In the accumulation season, snowpack was assumed to be a bulk reservoir for the atmospheric OC supplied by clouds it originated from, scavenged from underlying air, and trapped from dryfall and wetfall afterwards. Here, the term *dryfall* encompasses aeolian dust deposition and gas exchange with the ambient atmosphere, while *wetfall* describes the wet deposition with fog, dew or hoarfrost (see Schlesinger and Bernhardt, 2013).

During the ablation season, any freshly deposited OC could be removed from the glacier immediately, so a different sampling strategy was required. During the summer, atmospheric supply collectors ('dust traps'), were installed to estimate A^{abl} , following an inverted frisbee design by Hall and Upton (1988), modified by installing a drain into a 1L HDPE bottle to collect precipitation. The frisbee part was filled with glass marbles, to improve dry deposition gauging. The collectors were emptied and washed with 18 M Ω deionised water every 7–10 days during the sampling period. Traps were lined with aluminium foil to avoid OC leaching. Since plastic elements were used for sampling, full procedural blanks were quantified and subtracted from sample analysis results. Whilst it is recognised that plastics (even when thoroughly pre-cleaned) can contribute to the OC content of samples, it would be impractical to leave heavy and fragile glassware on the glacier in sub-freezing temperatures. The use of glass would also hinder the completion of a spatially and temporally intensive sampling essential for this project.

The storage procedure was uniform for all atmospheric deposition samples, and followed the protocol from Section 4.2.1.1.

4.2.1.3. Net glacier mass balance contribution (I_c) and the role of superimposed ice (SI) in the OC budget

In the expanded budget, the I_c term represents the transfer of OC from inside the glacier to its surface through ice ablation, and hence it incorporates the glacial ice concentration data, as well as the superimposed ice concentrations (both described in the Section 4.2.1.1.). The amount of melted ice was estimated from an annual net glacier mass balance survey conducted on ablation stakes A1–5 (Fig. 4.1.) on 2nd September each year (for details on the measurements and their precision, see Chapter 3).

The superimposed ice may or may not be included in the glacial OC budget, depending on the extent of the ablation in a given year. This type of ice forms during early summer due to refreezing at the base of the snowpack, which process might delay the OC removal by runoff within the ablation season or precede its incorporation into glacier ice by accumulation (and hence result in the OC storage beyond one balance year). As a result, the SI flux is a separate term from the I_c flux, which will be reflected in the data analysis that follows.

4.2.1.4. Biological production (Δbio)

Another additional input or output in the expanded OC budget of a glacier (Equation 4.2.) is the biological activity on its surface. In Svalbard, the rapid ablation of the snowpack means that biological activity is most pronounced in cryoconite debris on the glacier surface (Hodson et al., 2008). The net ecosystem production (NEP) and respiration (R) rates of cryoconite were therefore measured by means of *in situ* 24 hour incubations of cryoconite following the methodology of Hodson et al. (2010b), but using 300 mL sterile Whirlpak® bags as incubation vessels instead of fragile glass bottles. Biological production (Δbio) was assumed to be equivalent to NEP , and the primary productivity (PP) was calculated from Equation 4.4, in order to facilitate comparison with other glacial ecosystem productivity studies:

$$(4.4.) \quad \Delta bio = NEP = PP - R.$$

Five sets of six incubations were prepared in 2011 and three sets of six incubations in 2012, using three locations at different elevations (A1, A2 and A4 in Fig. 4.1.). NEP was obtained from changes in total dissolved inorganic carbon (TDIC) using the headspace method after its transformation into CO_2 and injection into a PP-Systems EGM4 infra-red CO_2 analyser. The respiration rate, R , was taken from dissolved oxygen (DO) concentration measurements using a Hach HQ30d portable meter with LDO101 optical DO probe, after incubation in the dark (in a Whirlpak® bag wrapped in aluminium foil). The molar ratio of used O_2 to respired CO_2 was assumed to be 1:1. Corrections for carbonate dissolution in all incubations were made by assuming that increases in Ca^{2+} and Mg^{2+} concentrations during the incubations came solely from weathering of carbonates (Hodson et al., 2010b). The ion analysis necessary for this

correction procedure was undertaken using a Dionex ICS 90 ion chromatograph, under operating conditions described by Hodson et al. (2010b) and with a precision error $\leq 5\%$.

Estimates of *NEP* (i.e. Δbio), *PP* and *R* from Equation 4.4 were expressed as $\mu\text{g C g}^{-1}$ cryoconite day^{-1} (per dry weight) and employed in a basic seasonal production model described in Section 4.2.3. The Δbio estimates are only presented as TOC fluxes here because the relative importance of DOC and POC (or biomass) in the *PP* or *R* fluxes was impossible to determine using the adopted method.

4.2.1.5. Storage in supraglacial debris (SOC)

OC storage in cryoconite was assumed to be the dominant component of particulate SOC within the supraglacial ecosystem on account of there being no significant medial moraines on the glacier. Cryoconite was therefore systematically surveyed by photographing the glacier surface and collecting samples for OC content analysis at 24 locations at 200 m distance intervals (Fig. 4.1.). The grid of GPS points used for sampling was prepared prior to the field survey to avoid human bias towards areas rich in cryoconite. At each location, a minimum of 16 pictures were taken using a Sony DSLR-A390 digital camera with a fixed focal length and from similar height (about 1.0 m) above the ice surface, producing images of c. 0.145 m^2 (± 0.040 , 1 SD). The survey was conducted at the end of 2011 summer season but was not repeated in 2012 due to early snowfalls. Photos were processed using ImageJ software, following Irvine-Fynn et al. (2010), with manual threshold selection to account for spatial differences in sediment hue. Once the areal extent of the cryoconite was determined, a transfer function was used to estimate the mass (see Section 4.2.3.).

4.2.2. Laboratory analysis

All samples were stored in -20°C prior to analyses. Total organic carbon (TOC) and dissolved organic carbon (DOC) analysis were conducted on freshly melted samples using a Sievers 900 TOC Analyzer. DOC was defined as the $0.7 \mu\text{m}$ Whatman GF/F filtrate of the sample. TOC and DOC measurements in the laboratory gave very low and repeatable analytical blanks (0.029 ± 0.009 ppm, 1 SD), while the operational blanks ranged from 0.088 to 0.099 ppm and are given in Table 4.1. For comparison, the blank-corrected concentration values and their variability are provided in Table 4.2. The visual inspection of samples showed that this could cause a problem in runoff, and hence in 2012 the opportunistically taken 1 L samples were analysed for the TOC content of the suspended sediment above $0.7 \mu\text{m}$, hereafter called TOC_{SSC} . This was analysed using the loss on ignition technique at 400°C for 16 hours (Nelson and Sommers, 1996).

In the case of the cryoconite samples, a chemical digestion method was employed after detecting significant mass loss due to clay particle loss through use of the LOI method. The organic matter content of the cryoconite samples was established gravimetrically following

chemical digestion with 1M KOH. From the mass loss, the OC content was estimated using an OC to organic matter mass ratio of 0.254, which was found in cryoconite on Longyearbreen, a glacier located within 20 km radius from Foxfonna (Hodson et al., 2010b).

Table 4.1. Procedural blanks for OC sampling and analysis (± 1 SD)^a.

Procedure/blank type	TOC [ppm]
P _{b1} : 18 M Ω deionised water	0.029 ^b (\pm 0.009) n = 27
P _{b2} : Regular sampling (triple rinse with sample, collection into 60 mL centrifuge tube)	0.098 (\pm 0.012) n = 5
P _{b3} : A, <i>lc</i> and <i>SI</i> sampling (collection into zip-lock bags, triple-rinsed with 18 M Ω deionised water)	0.088 (\pm 0.013) n = 5
P _{b4} : Dust trap field blank (a combination of aluminium foil and collector bottle blanks, corrected for 18 M Ω wash water concentration)	0.099 (\pm 0.026) ^c n = 8
P _{b5} : Dust trap initial blank (ppm TOC) obtained from 18 M Ω wash after triple rinsing and single autoclaving of a glass marble portion; initial blanks were applied individually to applicable datasets	0.099 (\pm 0.070) n = 7
P _{b6} : Filtration for DOC determination (18 M Ω water rinse of total volume of 800 mL, final 20 mL rinse analysed as blank)	0.092 (\pm 0.044) n = 300

^aThe combined procedural blanks for each flux were:

- 1) for A^{abl} : P_{b2} + P_{b3} + P_{b4} + P_{b5},
- 2) for A^{acc} , *lc* and *SI*: P_{b2} + P_{b3},
- 3) for Qc : P_{b2},
- 4) for the DOC content, P_{b7} was added to the blank calculated as above.

^bAll blank values reported in this table have been corrected for the deionised water OC content reported here.

^cThe standard deviation was pooled as described by Rogerson (2010).

Table 4.2. Blank corrected average sample concentrations (± 1 SD) of TOC and DOC.

Sample type		TOC [ppm]	DOC [ppm]
<i>A</i>	A^{abl}	1.071 (\pm 0.624)	0.776 (\pm 0.559)
	A^{acc}	0.441 (\pm 0.304)	0.178 (\pm 0.253)
<i>lc</i>		0.515 (\pm 0.354)	0.288 (\pm 0.208)
<i>Qc</i>		0.285 (\pm 0.131)	0.214 (\pm 0.113)
<i>SI</i>		0.649 (\pm 0.307)	0.555 (\pm 0.283)

4.2.3. Budget calculations

For consistency, all total annual fluxes were expressed in Mg a^{-1} for the whole glacial catchment area, and the partial, sub-annual fluxes were expressed in Mg in a given period. All concentration terms in the following equations were subject to operational blank correction.

On the basis of the calculated partial water budgets for the 4 and 5 periods of the summer season in 2011 and 2012, respectively, the sub-annual organic carbon budgets were devised, that included only the release of organic carbon with melt and its export in runoff (Equation 4.1.). The determination of mean concentrations for flux calculation mirrored that applied to full seasonal fluxes, and the application of snow, superimposed ice or glacial ice concentrations to the melt flux depended on the observed predominant nature of ablation in the given period. In particular, the water fluxes were calculated in the manner described in the Section 3.2.1.3. For Q_c , the OC concentrations were averaged between specific measurements taken across these periods. The snow and ice OC concentrations were averaged spatially. While data from snow cores and superimposed ice sampling lacked vertical resolution for a particular sampling location, it was assumed in the calculations of Mc that the concentrations were vertically uniformly distributed. For glacial ice, the 20 cm vertical distribution of measurements was incorporated into Mc estimation.

The expanded OC budget calculations led to solving Equation 4.2 for ΔSOC in the following manner. Winter deposition (A^{acc}) was estimated from the arithmetic mean loading of the individual snow cores (see Equation 4.5.):

$$(4.5) \quad A^{acc} = \overline{(SWE \times k_s \times OC^{snow})} \times A_c,$$

where SWE is snow water equivalent, OC^{snow} is the concentration of TOC or DOC in the snow cores, k_s is a factor applied to cases where the full depth of the snowpack could not be sampled using the corer (derived from the vertical OC gradient in snowpits) and A_c is the catchment area. A sensitivity test was run to explore the influence of both spatial variability and the correction in OC content to adjust for full depth in some cores. This was performed by removing each 2 snow cores from the record. This resulted in RSEs for TOC of 40.9% and 7.3% in 2011 and 2012, respectively. For DOC, the correspondent values of RSE were 16.3% and 15.0% in the subsequent years.

Summer deposition (A^{abl}) was also calculated as an arithmetic mean, following Equation 4.6:

$$(4.6.) \quad A^{abl} = \frac{1}{d_A} \sum_n \overline{V \times OC^{DT} \times a \times k_{DT}} \times A_c,$$

where d_A is the proportion of the total ablation period encompassed by dust trap monitoring, n is the number of separate short periods (7-10 days), for which the A^{abl} was estimated, and V and OC^{DT} are the volume of water and OC concentration measurements collected at each dust

trap. The terms a and k_{DT} represent the trap area (0.0397 m^2) and an efficiency factor as described by Sow et al. (2006), which employs average wind speed observations taken from the automatic weather station installed at stake A4 (Fig. 4.1.; compare to Irvine-Fynn et al., 2012). If there was an incomplete set of samples during any particular interval, the average glacier-wide estimates were scaled up or down according to the ratios between the incomplete datasets and the complete datasets from other periods. Again, a sensitivity analysis was performed to test the impact of the incomplete spatial record on glacier-wide flux estimates. To do so, the dust traps absent in some periods were removed from the average flux estimations for the periods with complete spatial coverage, and the new estimates were produced from incomplete datasets and compared to original ones. This resulted in TOC flux *RSEs* of 8.3% in 2011 and 10.3% in 2012. For DOC, the correspondent *RSE* values were 12.7 % in 2011 and 12.9% in 2012. Hence, the spatial variability is considered here a significant error source in both atmospheric flux calculations, however not to the extent which would change the direction or order of magnitude of the flux.

The calculation of the annual fluvial export (Q_c) followed Equation 4.7:

$$(4.7.) \quad Q_c = 1/d_Q \times Q_{obs} \times \overline{OC},$$

where d_Q is the proportion of all days with positive temperature in the ablation season that have been monitored for discharge, Q_{obs} is the total observed water flux (determined from Q measurements at the glacier snout, as described in Section 3.2.1.3) and \overline{OC} the arithmetic mean of DOC or TOC concentration, respectively. The arithmetic mean was found suitable for the total flux calculation because of the lack of interdependence between discharge and any of the OC concentrations. The OC concentration values were deduced from the streams at the glacier snout (B2, B3 and B4 sites). To estimate the total runoff from the glacier surface only, the sum of discharge at sites B2, B3 and B4 was calculated from the 2012 salt dilution gauging performed on those streams on 10 occasions. This total was expressed as a proportion of the total discharge measured on the same occasions at site B1. In doing so, a complete hourly discharge record was tied to the glacier front discharge dataset, and this relationship was assumed to hold unchanged in 2011, when the discharge measurements at the glacier snout were not collected.

The release of OC from glacier ice (I_c) was calculated using Equation 4.8:

$$(4.8.) \quad I_c = \sum_i (Bn_i \times \overline{OC}^{GI}_i \times A_{Z_i}),$$

where \overline{OC}^{GI}_i is the depth-weighted mean OC content of melted glacier ice, estimated from the drilled samples; the total depth of melt was deduced from the annual net mass balance measurement (Bn_i), for a given elevation zone of surface area A_{Z_i} (see Chapter 3 for full

methodology of B_n estimation). It should be noted that this equation simplifies the variability of mass balance losses in the forms of firn, superimposed ice and glacial ice by assuming all three components to have the concentration of OC found in glacial ice. This simplification is justified here by the very small accumulation area of the glacier (Chapter 3, see also Section 4.3.3.) and therefore also a small contribution of the firn or superimposed ice to the otherwise vast mass losses experienced by Foxfonna in 2011 and 2012.

It should be emphasised, that the transient OC store in superimposed ice (SI) is not included in budget calculations, and has been estimated separately from the I_c flux. Given the spatial uniformity of superimposed ice layer thickness and the lack of observed spatial pattern in OC concentration, this transient store was quantified using arithmetic mean of concentrations in ice cores, multiplied by: mean layer depth, assumed density of 0.85 g cm^{-3} , and the catchment area.

Estimates of Δbio assumed that the rate of NEP was constant in time and equal to the average of measured values in a given year ($\overline{NEP_d}$). This is admittedly a simplification, but the distribution of measurements across most of the glacier's altitude range was likely to reflect the high natural variability. Also, the timing of the survey in the middle of the melt season means that if the estimation is biased, it is most probably towards too high values. The spatial coverage of cryoconite activity was calculated following the model developed by Hodson et al. (2010a), which incorporates the surface variability in time (Equation 4.9.):

$$(4.9.) \quad \Delta bio = \overline{NEP_d} \times \sum_{i=1}^n (d \times a \times c \times M_d),$$

where d is the number of days when a particular fraction of the glacier surface was not snow-covered; c is the mean proportion of area a that is covered by cryoconite and M_d is a cryoconite area to dry mass conversion factor derived from the complete sampling of ten cryoconite holes of known surface area (0.059 g cm^{-2}). This function was built using the concept developed by Cook et al. (2010). The term d was estimated from oblique photos of the glacier surface taken every 1–4 days (n being the number of those periods), while c was deduced from the 2011 photographic survey across the glacier.

4.2.3.1. Error estimation for the OC fluxes

Error estimations were calculated for all the measured fluxes in Equation 4.2, as well as for the flux into superimposed ice, with the exception of Δbio . This is because the small sample size prevented a fully informed error analysis in this case. If an approach of combining error contribution from different data collection aspects was taken, uncertainties would occur in Δbio that were impossible to account for numerically (such as the dependence of cell metabolism upon environmental factors, which is unknown). However, the Δbio term will be also shown to be a trivial flux in the overall mass budget, which is another reason for

neglecting errors in its estimation. For the final budget, the assumed uncertainty in Δbio was equal to the one estimated by Hodson et al. (2010b). This was further justified by the values reported here corresponding to the levels of those described in literature, and hence the high uncertainty boundaries adopted from Hodson et al's (2010b) study are likely to encompass the variability experienced on Foxfonna.

The overall error of each flux was assumed to be equal to sampling error from the population; therefore we expressed it as 95% confidence intervals of the mean (Quinn and Keough, 2007). Since the datasets were non-parametric, bootstrap resampling was applied to the calculation of confidence intervals with R software (Canty and Ripley, 2012; Davison and Hinkley, 1997; R Core Team, 2012).

For storage in cryoconite estimation, error of area computation with ImageJ was derived in the way described for manual picture processing by Irvine-Fynn et al. (2010) (and equalled 16.6%), and then combined with the RSE of 30.9% for area to mass conversion curve and the 1.5% analytical error for chemical digestion method (following equation 4.10; Rogerson, 2010; Statsoft, 2013):

$$(4.10.) \quad RMS = \sqrt{\frac{\sum_{i=1}^n (a_i)^2}{n}}.$$

RMS denotes here the root mean square combined error type, a_i is the error of the i -th aspect of data collection, and n is the number of those aspects. The same equation (4.10.) was used for combining the errors of budget components to obtain the final error value for ΔSOC , and for combining discharge estimation and OC concentration errors in the sub-seasonal flux estimations (Equation 4.1.).

4.3. Results

4.3.1. Partial OC budgets based on the water balance of the catchment

The release of organic carbon with melt differed significantly from its export in proglacial waters, especially in the beginning of the summer of 2011 (before 02.08.2011) and during the ice ablation period in 2012 (after 08.08.2012; Fig. 4.2.). The snow ablation period of 2011 was characterised by an excess of both DOC and POC removal over release from melt, indicating the possibility of additional OC inputs to the system at that time. The opposite situation persisted throughout most of the ice ablation period of both years.

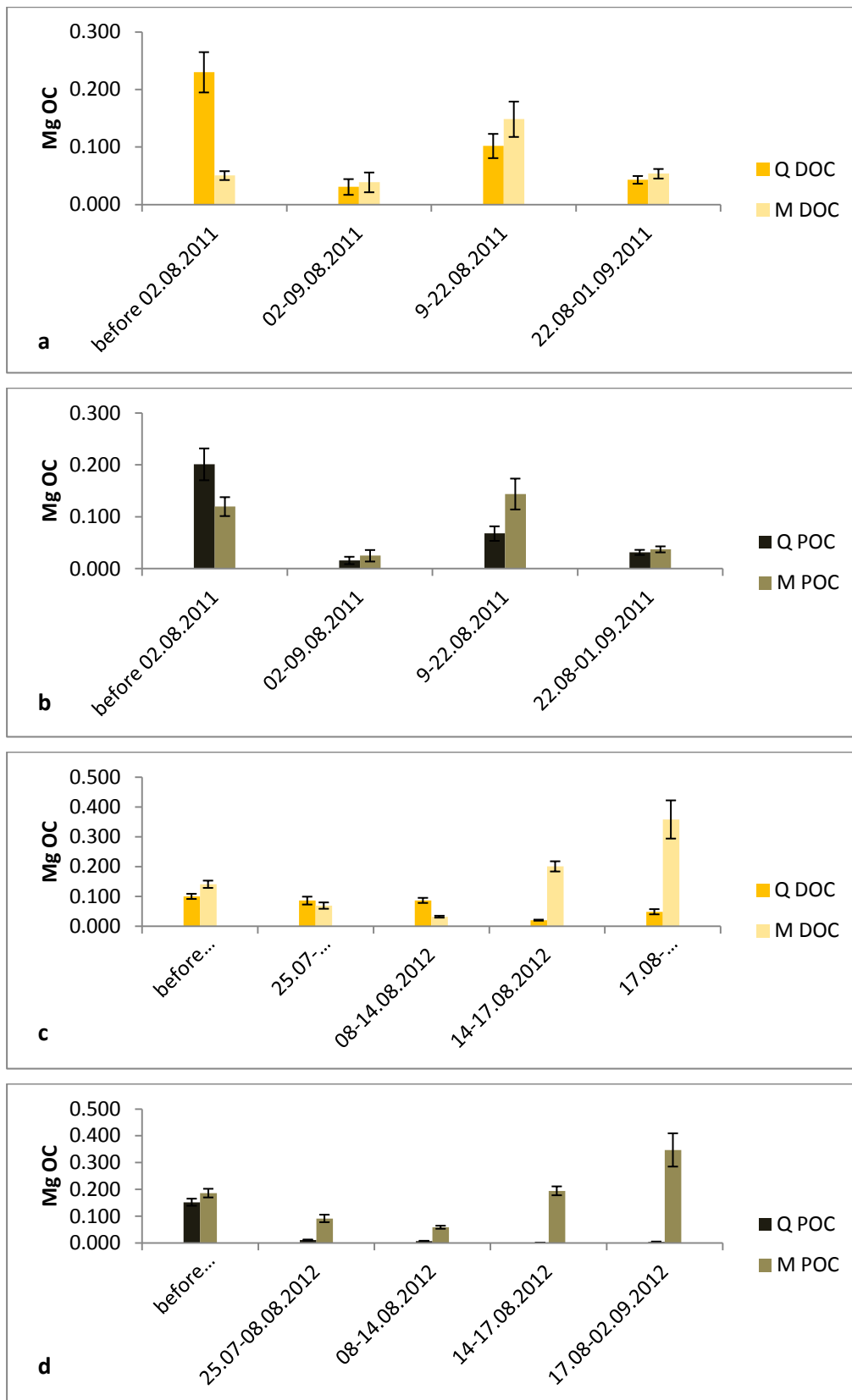


Fig. 4.2. Partial organic carbon flux balances across the summers of 2011 (a & b) and 2012 (c & d).

Q DOC – runoff flux of dissolved organic carbon (DOC), M DOC – melt-related flux of DOC, Q POC – riverine export of particulate organic carbon (POC), M POC – melt release of POC.

4.3.2. Atmospheric deposition (A)

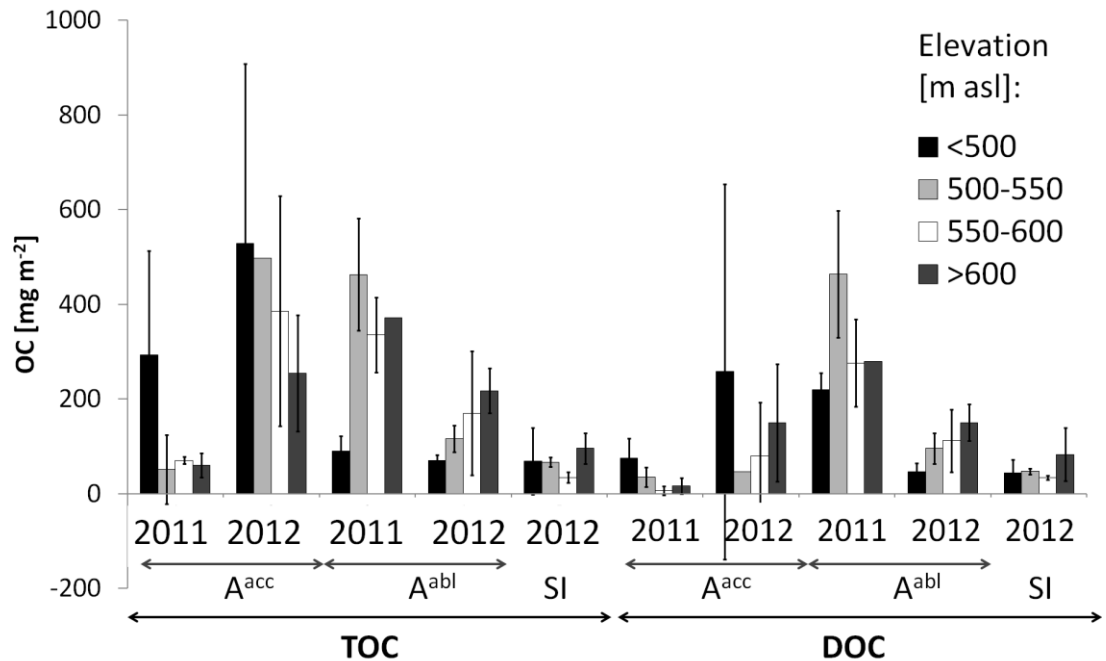


Fig. 4.3. Variability of atmospheric deposition of OC in the accumulation (A^{acc}) and ablation season (A^{abl}) and the amount stored in superimposed ice (SI) in 50 m elevation zones on Foxfonna glacier.

Where more than one value contributed to the mean, 1 SD error bars are shown.

Figure 4.3. and Table 4.3 show that deposition of OC exhibited great spatial and temporal variability between seasons and years. A^{acc} TOC in 2011 ($0.138 \pm 0.051 \text{ Mg a}^{-1}$) was much smaller than in 2012 ($0.484 \pm 0.219 \text{ Mg a}^{-1}$), whilst the opposite was the case for A^{abl} TOC ($0.473 \pm 0.171 \text{ Mg a}^{-1}$ in 2011 and $0.172 \pm 0.048 \text{ Mg a}^{-1}$ in 2012). In the winter of 2012, the distribution of DOC in snow was uneven, with the middle part of the glacier (500–550 m elevation band) showing the lowest DOC flux. Conversely, in the winter of 2011 the upper elevation bands contained less DOC than the lower part of the glacier (Fig. 4.2.). Otherwise, TOC concentration variability was closely connected to SWE changes (Spearman rank correlation $r = 0.482$, $p < 0.018$), unlike DOC concentrations (no significant correlation). The DOC:TOC ratios in snow equalled to 0.27 in 2011 and 0.48 in 2012.

4.3.3. Organic carbon transport by meltwater runoff (Qc)

The discharge in the proglacial river in 2011 (Fig. 4.4a) was generally less variable than in 2012 (Fig. 4.4b), although a snowfall event in August caused a sudden decrease in discharges from 10–12 August 2011. This was followed by warming and an associated rise in runoff on 14 August. Low, stable discharges, indicative of the end of the ablation season, occurred after 27

August 2011. The second half of August 2012 was characterised by similar low discharges. The high flows during each year were linked to snow or ice melt in July, sometimes combined with heavy rainfall (7, 11 and 14 July 2011 and around 8 August 2012). The importance of melt was emphasised by a significant correlation between discharge and temperature across both years (Spearman rank $r = 0.475$, $p < 0.001$).

Table 4.3. Organic carbon (OC) budget components [$Mg a^{-1}$] of Foxfonna glacier in 2011 and 2012. Ic and ΔSOC for 2011 highlighted in grey as these values are based on assumption that the OC concentration in glacial ice remained constant between sampled years.

Year		2011		2012	
Flux		TOC	DOC	TOC	DOC
Budget components					
A	A^{acc}	0.138 (± 0.051)	0.037 (± 0.050)	0.484 (± 0.219)	0.233 (± 0.196)
	A^{abl}	0.473 (± 0.171)	0.377 (± 0.142)	0.172 (± 0.048)	0.145 (± 0.046)
Q_c		0.522 (± 0.040)	0.351 (± 0.027)	0.401 (± 0.032)	0.358 (± 0.029)
Ic		0.513 (± 0.174)	0.259 (± 0.112)	0.382 (± 0.130)	0.216 (± 0.094)
Δbio		0.030 (± 0.095)	-	0.023 (± 0.071)	-
ΔSOC		0.632 (± 0.121)	0.322 (± 0.095)	0.660 (± 0.121)	0.236 (± 0.112)
Temporary storage ^a					
SI		0.099 (± 0.037)	0.070 (± 0.028)	0.114 (± 0.042)	0.101 (± 0.040)

^a This denotes superimposed ice at the maximum of its formation (late July). This term is not a part of the expanded budget sum since ablation in both years exceeded the refrozen layer thickness.

DOC concentrations in runoff (Fig. 4.4.) showed little fluctuation, and no significant correlation with discharge nor time of the day was found for either DOC or TOC in the two years combined (for Q , $r = -0.219$, $p > 0.05$ for DOC and $r = 0.272$, $p > 0.05$ for TOC; for diurnal cycle, $r = -0.192$, $p > 0.05$ for DOC and $r = -0.108$, $p > 0.05$ for TOC; all data merged for 2011 and 2012). There was, however, a significant progressive increase in both TOC and DOC concentrations over time across both melt seasons ($r = 0.565$, $p < 0.001$ for DOC and $r = 0.389$, $p < 0.02$ for TOC). In the Q_c fluxes (Table 4.3), DOC represented the largest fraction of the TOC runoff yield in both years (67.2 ± 6.6 and $89.5 \pm 7.7\%$ in 2011 and 2012, respectively).

The Q_c TOC_{SSC} flux was compared for B1, B2, B3 and B4 streams in 2012 (Fig. 4.5.), and showed a 25% difference between the sum of snout streams (B2, B3 and B4) and the stream arising from their confluence after a 250 m long distance covered in an icing area surrounded

by ice-cored moraines. Also, there was a significant difference noted between the two snout streams Q_c in TOC_{SSC} , despite their similar discharges.

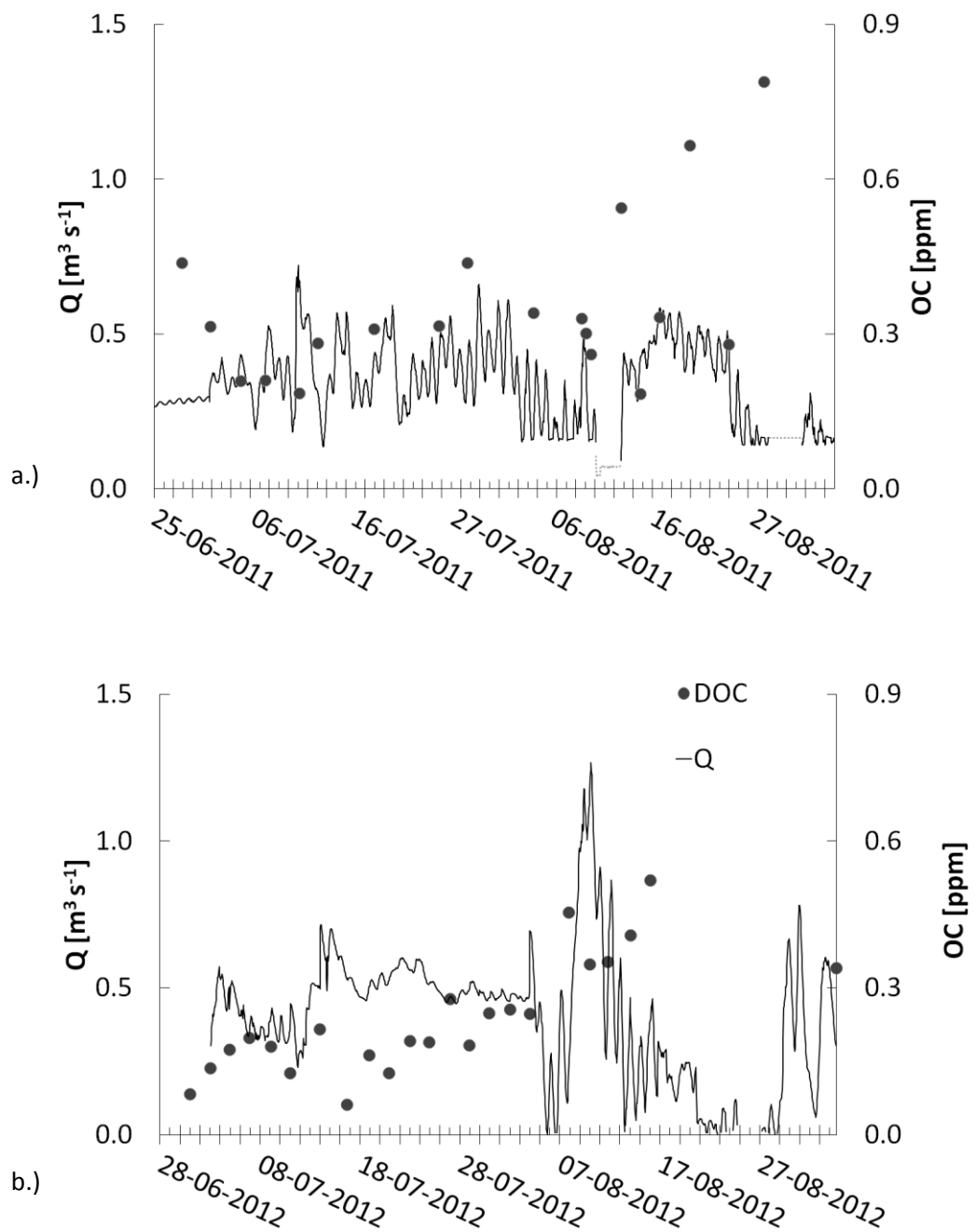


Fig. 4.4. Discharge curve for 2011 (a) and 2012 (b) with DOC concentrations in B1 site marked.

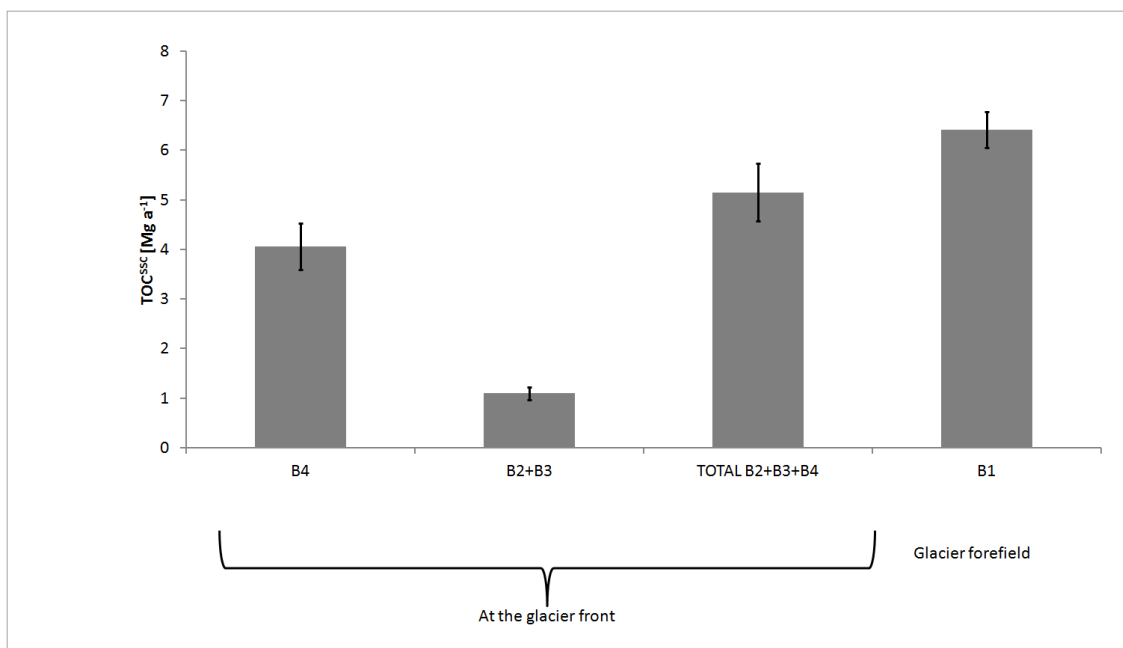


Fig. 4.5. Q_c flux connected to suspended sediment (TOC_{SSC}) in the glacier forefield in 2012.

4.3.4. Glacial ice melt (I_c) and the transient store of OC in the superimposed ice (SI)

During 2011 and 2012, the net mass balance in the studied catchment was estimated for -0.89 and -0.42 $m a^{-1}$, respectively. No superimposed ice accumulation was observed at the end of either summer, although there is likely to have been some refreezing within the firn-covered area where crevasses and steep slopes prevented its investigation. However, even if present, the limited firn covered area (<0.3 km^2) and its steep topography facilitating water runoff mean that the quantity of OC stored there was likely trivial (compare Chapter 5). Therefore, the estimated I_c fluxes (Table 4.3 and Figure 4.6.) were solely based on B_n and the glacial ice OC concentrations, and the 26% difference between the annual TOC fluxes for 2011 and 2012 stemmed mainly from the net mass balance variability. The difference was, however, smaller than the B_n difference of 53% due to a high OC concentration in the upper 20 cm layer, which contributed (in 2012) 55% of TOC and 49% of DOC content in the annual I_c flux.

Due to the net ablation exceeding the superimposed ice thickness in both years, the superimposed ice is analysed here only as a transient store, in the interest of its effects on temporal patterns in the OC release from Foxfonna. The maximum superimposed ice layer thicknesses during July 2011 and 2012 were $21 (\pm 2, 1SD)$ cm and $18 (\pm 2, 1SD)$ cm, respectively, indicating a broadly similar quantity of snowmelt refreezing on the glacier surface during the early ablation seasons. This maximum refrozen ice layer was found to represent a flux capturing 0.115 ± 0.042 $Mg a^{-1}$ TOC and 0.081 ± 0.032 $Mg a^{-1}$ DOC in 2011, and 0.129 ± 0.048 $Mg a^{-1}$ TOC and 0.114 ± 0.045 $Mg a^{-1}$ DOC in 2012. The values for 2011, therefore, show that the temporary storage of OC in SI can be the same order of magnitude as the A^{occ} (Table

4.3). Furthermore, the storage in *SI* was also spatially variable (Figure 4.3.), although less so than snow inputs to the system.

4.3.5. Biological activity (Δbio)

Table 4.4 shows that the *NEP* was on average $10.96 (\pm 5.31 \text{ 1SD}) \mu\text{g C g}^{-1} \text{ day}^{-1}$ in 2011 and $23.43 (\pm 7.17 \text{ 1SD}) \mu\text{g C g}^{-1} \text{ day}^{-1}$ in 2012, implying that the ecosystem was therefore net autotrophic. This is in agreement with the results of incubations conducted in 2009 (Hodson, Unpub. Data; locations A2 and A4). Both *R* and *PP* increased with elevation in 2011 and 2012 (data not shown). The final budget contribution of Δbio was, however, small: $0.030 \pm 0.095 \text{ Mg a}^{-1} \text{ TOC}$ in 2011 and $0.023 \pm 0.071 \text{ Mg a}^{-1} \text{ TOC}$ in 2012.

Table 4.4. Components of biological growth (equation 4.4.) in $\mu\text{g C g}^{-1} \text{ sediment day}^{-1}$ ($\pm 1 \text{ SD}$).

<i>Δbio</i> component	2011	2012
<i>NEP</i>	10.96 ± 5.31	23.43 ± 7.17
<i>PP</i>	24.14 ± 4.90	36.30 ± 10.09
<i>R</i>	13.19 ± 1.96	12.87 ± 5.98

4.3.5. Long-term storage on the glacier surface (*SOC*) and the organic carbon budget

The average cryoconite coverage on the glacier was estimated from the image analysis to be 8.25%, with a debris mass of $56.4 \pm 14.0 \text{ Mg}$ according to the mass conversion (and taking into account the ablation area in 2011). The corresponding TOC store in the supraglacial debris was therefore $1.14 \pm 0.23 \text{ Mg}$ in the end of summer 2011. The lower part of the glacier had both the greatest proportion of its surface covered with cryoconite and the highest OC mass per unit area gathered in this debris layer (Fig. 4.7., Fig. 4.8.).

The combined OC budget calculations produced positive estimates for ΔSOC during both years (Figure 4.6. and Table 4.3). The total atmospheric deposition input slightly exceeded the fluvial export, and the biological component was small compared to the other fluxes in both years. As a result, ΔSOC was quantitatively similar to *Ic* in both years.

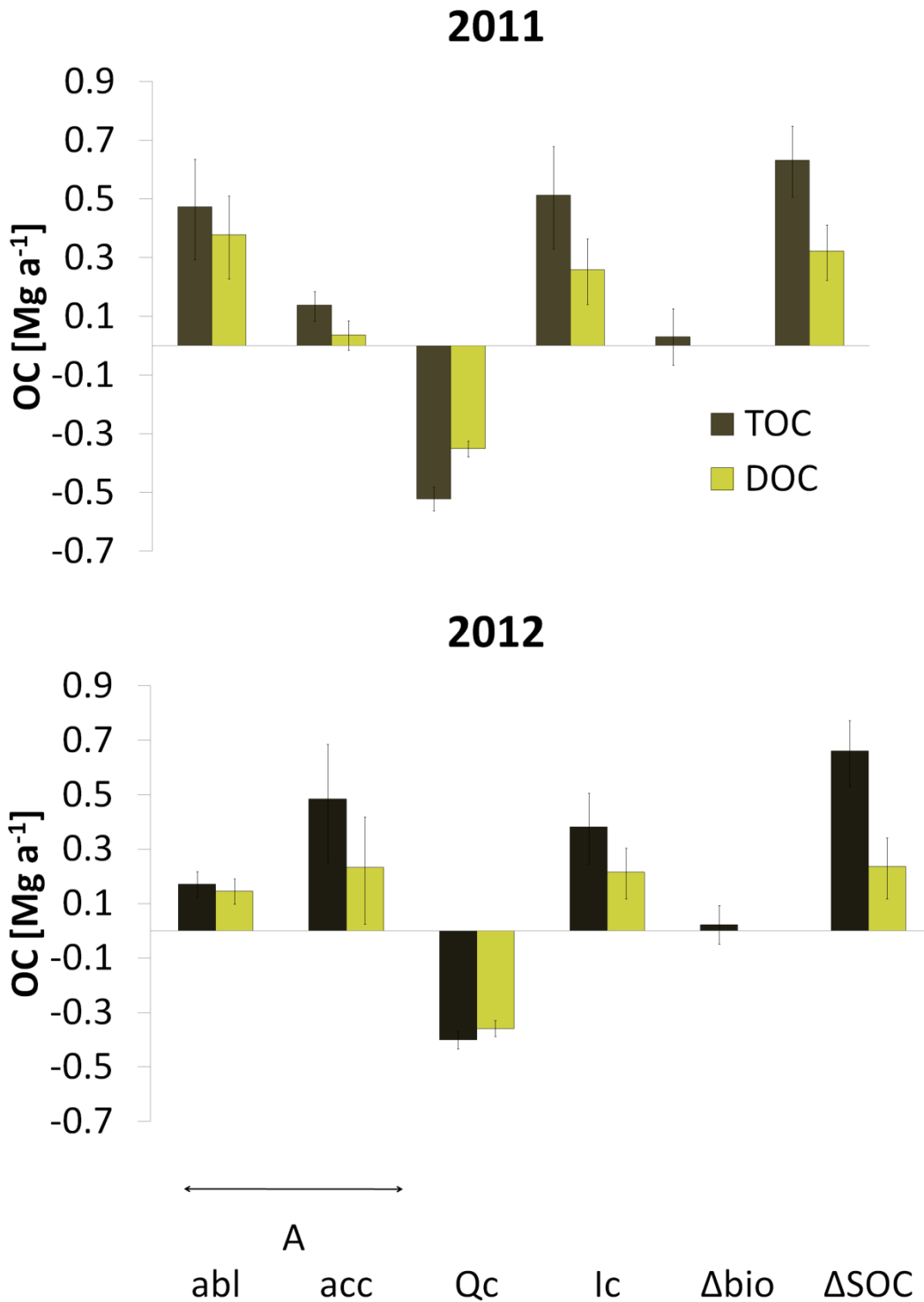


Fig. 4.6. The expanded organic carbon budget of Foxfonna glacier for 2011 and 2012.

Abbreviations: abl = A^{abl} = net atmospheric deposition, in the ablation season, acc = A^{acc} = ditto, in the accumulation season, Qc = fluvial export of OC from the glacier, Ic = OC release from the legacy ice melting, Δbio = net biological production (positive) or oxidation (negative) of OC, considered in supraglacial debris (cryoconite), ΔSOC = the change of OC storage on the glacier surface.

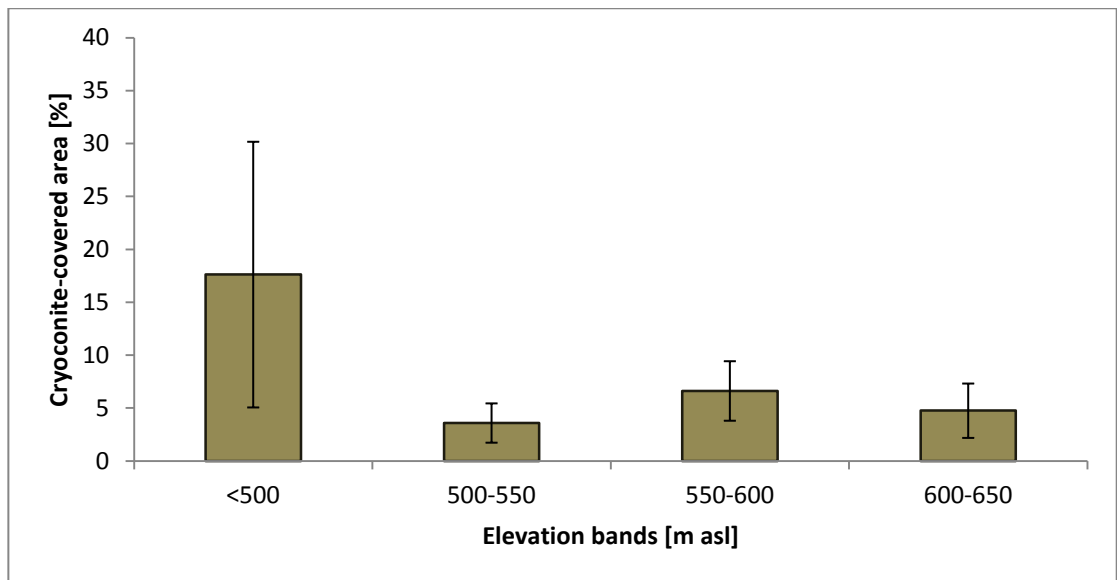


Fig. 4.7. Cryoconite surface coverage in 50 m elevation bands of Foxfonna glacier, as surveyed on 25th August 2011.

Error bars given as 1 SD of samples collected in a particular elevation zone.

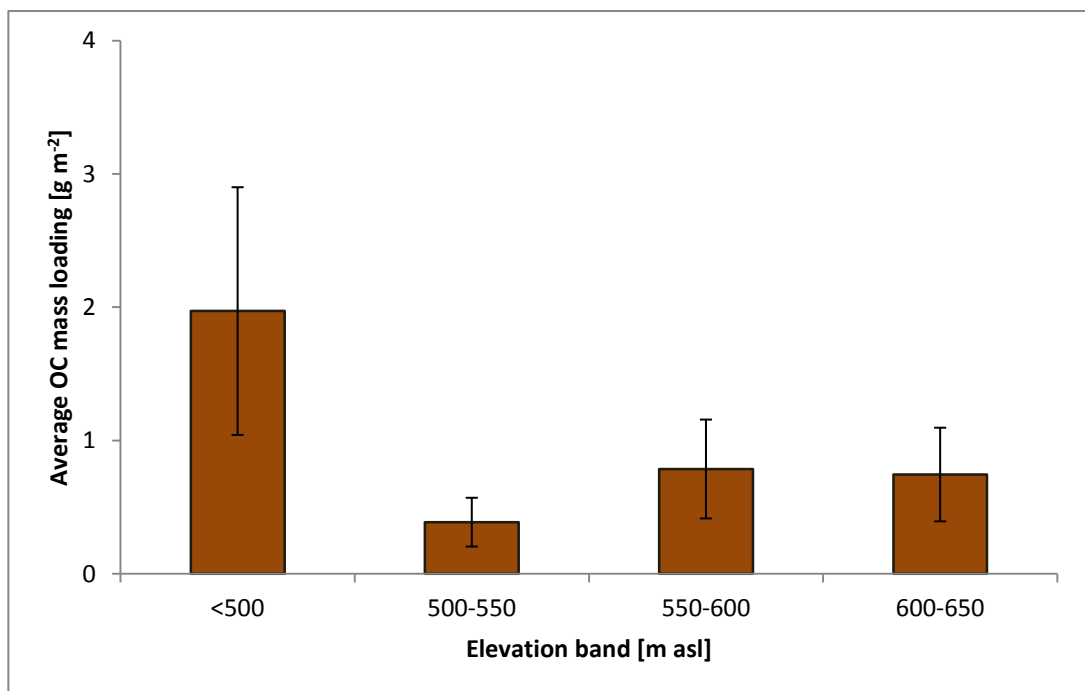


Fig. 4.8. Supraglacial storage of OC and its distribution across elevation zones of Foxfonna (on 25th August 2011).

Error bars as 1 SD (spatial variability).

4.4. Discussion

The initial attempt at budgeting OC melt and runoff resulted in disparities which could not be explained by measurement errors alone. The most likely cause for the negative differences

between the OC release from melt and the export in riverine waters were additional, unaccounted for inputs from rain and dry deposition (especially in early July 2011, when an extreme rain episode took place on Foxfonna; see also the section below). On the other hand, both late summer seasons of 2011 and 2012 experienced an excess of melt release of POC and DOC over their export in runoff. This points to the possible presence of a mechanism capturing this excess OC, which requires further exploration. Therefore, the discussion below will concern the expanded TOC and DOC budgets, as devised in Equation 4.2. The OC deposition, storage and export of a single glacial system have been measured here in two budget years for the first time, resulting in the most detailed description of a flux and storage scheme in such a system to date. This information will be placed here in the context of the known, more incidental reports on glacial OC concentrations and fluxes.

4.4.1. Atmospheric inputs

The observed OC concentrations in the snow were highly variable, and averaged 290 ppb TOC (including 70 ppb DOC) in 2011 and 570 ppb TOC (242 ppb DOC) in 2012. These findings are similar to those reported elsewhere. For example, Xu et al. (2006) analysed the OC content of snow in Tibet, obtaining averages of 87.5 ppb (parts per billion) in fresh snow and 195.5 ppb in 2-day old snow, while the more mature snowpacks on Foxfonna have shown moderately higher TOC levels. The DOC content of mature snow was quantified in a partly glaciated catchment by Lafrenière and Sharp (2011), who observed mean concentrations of DOC in non-melting snow samples between 280 ppb (meadow setting) to 410 ppb (forested site). These values exceed the average DOC in Foxfonna snow, suggesting that the OC content of lower latitude snow might be greater than in the High Arctic, at least when more vegetation is present in the catchment. The connection between the presence of vegetation and OC content of snow is also concordant with the general pattern of mostly allochthonous OC sources on small glaciers (see Section 2.4.1.) and the observations of macroscopic plant fragments on the surface of Foxfonna. It is likely that the windborne transport is also important, given the intensive wind redeposition of snow observed in this site (Section 3.4.1.) and the interdependence of TOC concentration and SWE (Section 4.3.1.). However, this latter relationship may be partly invoked by the scavenging of OC during snowfall (Kang et al., 2009).

The contribution of winter snow to the annual OC budget may be reduced by post-depositional processes (including photo-oxidation) during the spring and summer season (Grannas et al., 2004). This problem has not yet been addressed quantitatively for any glacier and was beyond the capacity of the current research project, however its influence was diminished by the collection of snow samples shortly before the melt commenced. Hence, the only discussion of the subject can be based on a published estimate of photodegradational loss

of organic matter from Arctic snowpack of 0.480-4.08 mg C m⁻² d⁻¹ (Voisin et al., 2012). This value shows a potentially important, but highly variable factor, which is likely dependent on the organic matter composition, the snowpack characteristics and ambient meteorological conditions. The measurement of this flux is still a challenge in glacial settings, and so more research is needed in this context.

A striking feature of atmospheric OC deposition rates at Foxfonna was the high spatial and temporal variability. Temporal variation between the two years of monitoring (Table 4.3 and Figure 4.6.) is attributed to the different meteorological conditions during the sampling periods. In July 2011, 16mm of rainfall fell over the catchment in a single week, and contributed very significantly to A^{abl} (Fig. 4.2.). Unseasonal, major events were also notable in winter 2012, including rainfall in January and a large snowfall event in late May 2012. High precipitation events like these are usually associated with warm air inflow to Svalbard from southerly latitudes, where industrial pollution sources contribute to their chemical composition which in turn may dominate atmospheric solute inputs in Svalbard. This is certainly the case with respect to ionic constituents (e.g. Hodson et al., 2009; Krawczyk et al., 2008; Kühnel et al., 2013). The importance of the rainfall events was also compared against a counter-hypothesis that bacterial production within the dust sampler contributed a significant error to those measurements. However, in the conditions described, *in situ* bacterial uptake rates are unlikely to be significant compared to experienced OC concentration levels within a 7-10 day period, given those uptake rates and cell concentrations reported in literature (following Coveney, 1982; Irvine-Fynn et al., 2012). This means that only a minor impact of biological cells on the A^{abl} flux is possible. Nevertheless, the experienced variability in the summer season atmospheric deposition of OC has emphasised the difficulties connected to its sampling, and developing more appropriate means of establishing this flux would be beneficial in the future.

4.4.2. Fluvial export

Estimates of fluvial export of TOC and DOC from the glacier surface were comparable between years (Table 4.3). The Q_c flux for DOC (0.27 g m⁻² yr⁻¹ in both years) was also close to Singer et al.'s (2012) estimate of 0.17 g C m⁻² yr⁻¹ for glaciers in the European Alps, however its higher value on Foxfonna may raise questions about the origin of this OC, for example the local pollution sources, or the relative proportions of accumulation to ablation zones on the glaciers in Singer et al.'s (2012) study as contrasted to Foxfonna. Given the very small accumulation zone in the supraglacial catchment studied here and the significant inputs from the melting glacial ice, the Q_c flux per unit area may depend on the accumulation area ratio (AAR) of the glacier.

The DOC concentrations in runoff reported here are also similar to those found in other studies (Bhatia et al., 2013; Downes et al., 1986; Hood et al., 2009; Lafrenière and Sharp, 2011) which showed mean annual concentrations of 0.1–4.1 ppm DOC. The findings from Foxfonna of 0.35 ppm (2011) and 0.25 ppm (2012) are at the lower end of this range, along with values reported as characteristic for runoff dominated by surface meltwater from the Greenland Ice Sheet (Bhatia et al., 2013). The higher values reported in other studies may result from subglacial contributions (Bhatia et al., 2013) or processes occurring in the glacier forefield (Downes et al., 1986; Hood et al., 2009).

The progressive increase in TOC and DOC over time that was observed in Foxfonna proglacial waters may be connected to a shift in hydrological regime. This shift was most obvious in 2012, seen as a change in runoff amplitudes after 28th July (Fig. 4.3b.) which coincided with the supraglacial catchment losing most of its snow cover. This might have exposed sources of OC in the supraglacial debris, but possibly also those directly contained in superimposed ice (see Chapter 5). Such a factor would be reflected in the outlet stream OC concentrations as a gradual change over time, because the subsequent elevation zones are liberated from under the snow cover at subsequent time points in the melt season.

When the downstream flux of TOC was considered, the impact of suspended sediment upon the TOC content of runoff was marked (Fig. 4.4.). The striking differences in Q_c estimates for TOC_{SSC} between the snout streams and their confluence just 250 m distance further, as well as between the snout streams themselves, indicate a source that is independent of water volume. This strongly suggests a source different from glacial ice and snow cover melt. A likely explanation is particle contributions from moraines (both side-moraines and perhaps also basal material in the case of B4 flux, since Fig. 3.22 suggests this stream may have a short subglacial stretch). The difference is unsurprising given the description of microbial communities and clay particles in these features (e.g. Edwards et al. 2013; Laybourn-Parry et al. 2011), as well as the differentiation of OC flux regimes between supraglacially and subglacially derived waters of GrIS (Bhatia et al., 2013). These considerations lead to the conclusion that the sediment-bound OC flux is most probably derived from sources which are disconnected from the glacier surface in a time scale of annual budget.

4.4.3. Liberation of OC from melting ice and the supraglacial biological activity

The concentrations of OC found in Foxfonna glacial ice were higher than values of 14.6–66.3 ppb reported by Jenk et al. (2009) in a deep Alpine ice core, averaging 933 ppb TOC in the upper 20 cm of the profile and 410 ppb in the rest of the 1 m section sampled. A strong down-core gradient in OC was therefore found in the present study, which suggests that the upper ice profile of the glacier might in fact represent a store of OC supplied by meltwater

percolation. Since Foxfonna is a predominantly cold polythermal glacier, the melting isotherm is often very close to the surface, so only the upper ice layer acts as a shallow aquifer through which OC can be transported. This is often referred to as the *weathering crust* or *ablation crust* and a further description of its hydrological properties is given by Irvine-Fynn et al. (2011).

It cannot be excluded here that biological activity in the surface layer of ice is the source of some of this elevated concentration. Further research is therefore required to assess the dynamics of OC enrichment in the upper layer of the glacier surface. It might be that the OC is derived entirely from the leaching of cryoconite, or that the ablation crust represents a distinct habitat in its own right, similar to the Greenlandic grey ice (Lutz et al., 2014). It can only be established here that the surface layer of glacial ice (i.e. the upper 20 cm, where enhanced concentrations were found) is a small store of OC compared to the 1.14 ± 0.23 Mg TOC stored in cryoconite, amounting to 0.21 ± 0.13 Mg TOC and 0.11 ± 0.07 Mg DOC in the end of 2011 (errors reported as CV from spatially distributed samples). Hence, even if all the carbon stored in the uppermost glacial ice was produced in situ, the flux related to biological production there would still be an order of magnitude smaller than glacier-wide supraglacial carbon storage. Moreover, the biological origin of the OC contained in upper glacial ice would imply a more active ecosystem in this layer than that contained in cryoconite (and described here by the Δbio flux), with *NEPs* an order of magnitude higher.

The magnitude of surface OC storage in cryoconite suggests that probably the most important biological OC flux is related to this debris. The *NEP* values obtained for Foxfonna cryoconite are high compared to those from other glaciers in the area, where a net heterotrophic system ($R > PP$) has been reported (Stibal et al., 2008a; Telling et al., 2010). Stibal et al. (2008) measured *PP* on Werenskiöld glacier, Svalbard, to be c. $4.3 \mu\text{g C g}^{-1} \text{ yr}^{-1}$, whilst Telling et al. (2010) reported *PP* rates of $17.3 \mu\text{g C g}^{-1} \text{ d}^{-1}$, a mean *R* of $20.1 \mu\text{g C g}^{-1} \text{ d}^{-1}$ and *NEP* of $-1.3 \mu\text{g C g}^{-1} \text{ d}^{-1}$ for three Svalbard glaciers located near Ny Ålesund. Although it is unclear whether cryoconite ecosystems are mostly net autotrophic or net heterotrophic, the finding from this study that the Δbio connected to cryoconite is a very small component of the entire OC budget is important. Furthermore, since the *NEP* values found on Foxfonna are an order of magnitude higher than on other Svalbard glaciers, it is likely that the flux is also negligible in other, similar settings.

The likely source for a higher flux related to biological activity is algal blooms found on snow or ice surface. In Greenland these were found to promote net autotrophy both on the GrIS and the Mittivakat glacier, independent of high debris cover (Lutz et al., 2014; Yallop et al., 2012), contributing to the ice surface darkening. However, such intense blooms do not occur on Foxfonna and they are not at all widespread on Svalbard glaciers. Occasional snow algal blooms, with moderate biomass, do result in red colouration of the snow surface, and

usually correspond to the periods and areas where snow is in the form of slush. This poses certain logistical difficulties in the sampling, including the possible human bias towards areas of higher cell concentration. Furthermore, the highly changeable distribution of the small area of algal blooms challenges the estimation of its glacier-wide impact, unless a detailed photographic record of the glacier surface across the snow melt season is collected. The processing of such a record would also require a satisfactory calibration of bloom coloration to its biological activity rates. Hence, this may represent a project in its own right and is considered outside the scope of the current work, and treated as an unknown and a possible error source to the final calculation of ΔSOC . If there is any significant biological activity in the snow, then most likely the input from a net autotrophic ecosystem into the glacial OC budget is underestimated here. In such a case the true retention of OC upon Foxfonna would also be higher than calculated in this work.

4.4.4. The relation between OC fluxes and its long-term storage

Since the accumulation and ablation conditions during 2011 and 2012 were significantly different, and the budget calculation leads to similar results for both years, it is proposed here that the net retention of OC implied by the positive ΔSOC in this study is a typical scenario for this glacier and others like it. This is supported by studies of microbial cell abundance in atmospheric deposition and runoff on Midtre Lovénbreen, another Svalbard glacier (Björkman et al., 2014; Irvine-Fynn et al., 2012). In order to consider whether cryoconite debris represents the most likely sink for the particulate component of ΔSOC , this particulate OC storage change (ΔSOC^{POC}) was estimated using Equation 4.11:

$$(4.11.) \quad \Delta SOC^{POC} = \Delta SOC^{TOC} - \Delta SOC^{DOC}.$$

The calculations suggest that ΔSOC^{POC} was $0.310 \pm 0.109 \text{ Mg a}^{-1}$ POC in 2011 and $0.424 \pm 0.117 \text{ Mg a}^{-1}$ POC in 2012. With this being the case, ΔSOC^{POC} requires c. 3 years to account for the cryoconite SOC store ($1.14 \pm 0.23 \text{ Mg}$). This seems reasonable given the longevity of many cryoconite deposits observed on the glacier during the research conducted there (A. Hodson, personal communication on his observations since 2006) and so cryoconite is a plausible sink for the excess OC in both annual budgets. The turnover time corresponds to the average age estimate of 3.5 years for cryoconite debris particles upon Glacier No. 1 in China, examined by Takeuchi et al. (2010). This study, and others from Svalbard (Hodson et al., 2010b; Langford et al., 2010), also show how the internal structure of cryoconite debris resembles an aggregation of mineral particles (including clays), allochthonous organic matter and autochthonous microbial biomass. Indeed, the organic component of the cryoconite established here averaged only 8.0%. The role of biological activity, however quantitatively small, may contribute positively to the cryoconite aggregation (Hodson et al., 2010b), as well as their

darkening (Takeuchi, 2002b; Takeuchi et al., 2001b). The magnitude of the ΔSOC^{POC} flux indicates that most likely the general mass of cryoconite stored on the glacier surface was increasing. However, without the general cryoconite mass change, this flux would be increasing the TOC concentration in the supraglacial debris by 27%-37% per annum, resulting in an OC content in 2012 and 2013 of approximately 2.6% and 3.5%, respectively. This is a possible value in light of the aforementioned typical OC concentrations in cryoconite (see Section 2.4.4.), however it would indicate an extraordinarily rapid change in the system, which is unlikely. Therefore, cryoconite mass increase is a more plausible explanation of the effect of the ΔSOC^{POC} flux.

Cryoconite appears to be a major store for the positive ΔSOC , and hence the processes responsible for its removal will regulate the residence time of the supraglacial OC. These processes will also govern the impact of OC storage upon the glacier surface albedo (e.g. Bøggild et al., 2010; Hodson, 2014). Beyond the fluvial export estimations provided here, two additional mechanisms of OC removal are recommended as a subject for future research here:

1. Washout of particles from the glacier surface during extreme melt events or heavy rains, and
2. Internal storage of debris transported down crevasses and through deeply incised meltwater channels.

However, if none of the proposed or unknown removal processes is as efficient as the flux concentrating organic carbon on the glacier surface, the organic layer volume is expected to increase. This may lead either to increased cryoconite coverage on the glacier surface or to the formation of organic debris hotspots, e.g. by its concentration in melt ponds or supraglacial kames. The features likely to represent the latter deposition form have been observed in the lowest part of Foxfonna, and other intensively melting glaciers, for example on Leverett Glacier in Greenland (Stibal et al., 2010), and on Svalbard on Werenskiöldbreen (Stibal et al., 2006) or Bungebreen (J. Dudek, personal communication). Also, the relative concentration of debris in the lowest elevation band (Fig. 4.7.), as well as its higher OC mass loading (Fig. 4.8.), support this argument.

An important part of the glacial OC fluxes is the dissolved form of organic matter, which comprises 63% of the atmospheric flux, 53% of the release from ice melt, and only 43% in the storage change calculated from the budget (51% in 2011 and 36% in 2012). Compared to the identified OC supplying fluxes, the supraglacial riverine OC is enriched in dissolved fraction (77% DOC), and so is the superimposed ice (with the average content of DOC at 80% of TOC). The DOC is therefore likely to be transferred to the glacier forefields more efficiently than POC, and its impacts on the downstream ecosystems, as highlighted by Hood et al. (2009), may happen as an immediate consequence of enhanced melt. However, a variable proportion of

the supplied DOC (48% in 2011 and 40% in 2012) has been shown to remain in the supraglacial system each year, and hence the impact on the downstream ecosystems is likely to be overestimated if the OC which melts out of the glacial ice is assumed to be fully discharged. The ways in which glacier surfaces are capable of storing DOC are therefore worth investigating. The process likely contributing to this phenomenon is the meltwater refreezing, as the refrozen layer has been shown here to contain a high proportion of DOC. The fate of the atmospheric supply will be, therefore, explored further in the next chapter of this thesis, especially regarding its links to refrozen basal ice and meltwater runoff.

4.5. Conclusions

This study provides details on the development of the first organic carbon (OC) budget for an Arctic glacier surface, represented by two budget years of data. The variability of glaciological conditions between the two investigated periods, and their consistency in the estimation of the resulting OC storage, show that net retention of OC is most likely a common occurrence on glaciers like Foxfonna. This is predominantly caused by the physical retention of both allochthonous inputs of atmospheric OC and the OC released from the uppermost layers of ice by extensive melt. The observed rates of storage of particulate OC (POC) were consistent across the two years and represent enough OC to supply the amount of carbon associated with cryoconite debris within c. 3 years. This surface carbon is likely to contribute to glacier surface darkening, raising the pressing need to better understand the long-term fate of supraglacially stored OC, and its feedback to melt processes.

The processes leading to apparent organic carbon concentration on the glacier surface need to be balanced by a yet unknown process in the long-term, or else the supraglacial layer of POC would be increasing infinitely. Therefore, two potentially important processes involved in the removal of POC from the glacier surface are proposed here: organic-rich debris erosion during extreme melt and rainfall events and POC transfer to internal storage within the glacier. The former process would drive irregular supplies of OC to the glacial forefield and therefore needs further attention from the perspective of nutrient supply to ecosystems. The latter would increase the lag between OC release from melting ice and its removal from the site, and it could also lead to multiple cycles of the same particle being buried and re-emerging on the glacier surface. Studying these processes is a major challenge due to their likely irregular, non-linear nature; however, it would help understanding of the feedback mechanisms linking the release of carbonaceous particles from melting ice and their impact on the glacier albedo.

The processes leading to OC retention are active also for dissolved organic species, despite these are removed more rapidly from the glacier surface than POC. The highest ratio of dissolved to total organic carbon was found in the refrozen meltwaters (superimposed ice) and

the supraglacial runoff, and hence the superimposed ice is proposed here as a storage medium for dissolved OC. Yet, it is unclear how this storage medium obtains and releases its OC content, and this information is crucial to establish the spatial and temporal variability introduced to the supraglacial OC cycle by the occurrence of basal refreezing. Hence, the formation of the superimposed ice OC storage, and its connection to supplies and sinks, will be investigated further in Chapter 5 of this thesis.

Chapter 5. Thermal and hydrological controls over organic matter distribution in the supraglacial environment

Summary

Cells and organic carbon (OC) are vital components of the supraglacial ecosystem and their distribution changes rapidly as glaciers melt. A small-scale experiment was conducted to elaborate their fate during melting and refreezing on Foxfonna. This led to a conceptual understanding of the co-evolution of the thermal, hydrological and biochemical state of the snowpack and surface ice, which was found to develop in three stages:

(1) Melting front penetration into the cold snowpack, leading to intensive OC removal from snow and its capture as a superimposed ice layer on the glacier surface (early stage); later on, following melt water inundation of the snowpack, the majority of cells were also eluted from any remaining snow and captured in the refrozen layer

(2) An isothermal snow and superimposed ice profile development, during which time the OC and cell removal in streams was marked

(3) Superimposed ice ablation, which was followed by an intensive release of cells and OC into runoff after this refrozen layer decayed.

The effect of rapid warming on OC transfer to supraglacial and downstream ecosystems was therefore found to be buffered by superimposed ice zone development, delaying the release of both nutrients and cells. In this study, the superimposed ice accumulated $0.096 \pm 0.011 \text{ g m}^{-2}$ TOC (total OC), 87% of which was DOC (dissolved OC), and $265 \pm 27 \times 10^7 \text{ cells m}^{-2}$. The cells were released rapidly after the superimposed ice was exposed and decayed, with a single meltwater pulse discharging fourteen times the cell concentration of that of the original snowpack. However, a simple OC budget showed net retention of $0.134 \pm 0.033 \text{ g m}^{-2}$ TOC and $0.040 \pm 0.019 \text{ g m}^{-2}$ DOC, whilst the cell concentrations showed a negative budget of $-144 \pm 55 \times 10^7 \text{ cells m}^{-2}$, and therefore they were entirely released by the time the glacial ice became exposed.

5.1. Introduction

Due to their ongoing rapid mass change, glaciers have become secondary sources of bioavailable organic carbon (OC) (Fellman et al., 2010; Hood et al., 2009) and living cells (Irvine-Fynn et al., 2012) to downstream environments. These processes are usually studied from a watershed perspective, e.g. by studying a proglacial river discharging into the sea (Hood et al., 2009). However, it is yet unclear which part of the glacial system these chemical and biological components originate from. Explaining this is crucial for understanding their future

release, as glaciers and glacial ecosystems undergo a complex set of changes (Hodson et al., 2008) that is not driven by melting and meltwater runoff alone. In particular, refreezing processes play a hitherto underexplored role in partitioning and delaying OC and cell fluxes. In this chapter, the focus will therefore be on processes of melting and refreezing, and their impact on biochemical changes and fluxes from glaciers that are experiencing increased ambient temperatures.

The existing data on the behaviour of nutrients and cells in glacial settings are more abundant for melting than for refreezing processes. They suggest a behaviour of solutes called preferential elution, which is a phenomenon of sequential relative enrichment and dilution of a certain compound in meltwater derived from the snowpack (Bales et al., 1993; Brimblecombe et al., 1985, 1987; Tranter et al., 1986). In particular, the ionic constituents in snowpacks are usually recognised to elute in the order $\text{SO}_4^{2-} > \text{NO}_3^- > \text{NH}_4^+ > \text{K}^+ > \text{Ca}^{2+} > \text{Mg}^{2+} > \text{H}^+ > \text{Na}^+ > \text{Cl}^-$ (Brimblecombe et al., 1985) or else $\text{SO}_4^{2-} > \text{NO}_3^- > \text{Cl}^-$ for anions and $\text{K}^+ = \text{Mg}^{2+} > \text{Na}^+$ for cations (Brimblecombe et al., 1987). This sequence, recognised in snow in the Scottish Highlands, is not uniform world-wide though. For example, Li et al. (2006) report a pattern $\text{SO}_4^{2-} > \text{Ca}^{2+} > \text{Na}^+ > \text{NO}_3^- > \text{Cl}^- > \text{K}^+ > \text{Mg}^{2+} > \text{NH}_4^+$ occurring at the Úrúmqi glacier in Tien Shan, China. The relative enrichment of particular compounds was found to be independent of snow grain affinity to ions at the time (a chromatographic effect was therefore excluded). Instead, the preferential elution was found to be a legacy of the snowpack history, and to follow the relative enrichment of solutes in snow grain coats formed during snow metamorphosis (Cragin et al., 1993, 1996). It also depends on the depositional sequence, with solutes on the top of the snow column eluting first (Bales et al., 1989; Davis et al., 1995). Long melt-freeze cycles, followed by the formation of basal ice, are also contributing to the relative enrichment of solutes at the snowpack base (Davis et al., 1995; Lilbæk and Pomeroy, 2008), and this ice has also been shown to produce pulses of enriched solutes during melt (Brimblecombe et al., 1988). The preferential elution of ions is capable of increasing their concentration to 1.3-1.6 times the concentration expected if leaching was uniform (Williams and Melack, 1991). On glaciers, the elution processes lead to the redistribution of ionic compounds in firn relative to their original depositional pattern (Holdsworth et al., 1988), especially the more mobile ions, such as nitrate (Zhao et al., 2006). Additionally, these elution processes modify the chemical composition of runoff (Hodgkins and Tranter, 1998).

The complexity of elution processes for organic compounds in snow has only recently been considered (Meyer et al. 2009a; Meyer et al. 2009b, see Chapter 2.4.2), and the only studies documenting OC capture in the refrozen layers concern sea ice (Kattner et al., 2004). This phenomenon has been observed on glaciers for the first time by the author (Chapter 4) of this work, and its significance for the ecosystem located there deserves further attention in this

thesis. As glacial settings are known to produce bioavailable organic matter (Hood et al., 2009; Singer et al., 2012), it is valuable to explore the core processes associated with this organic matter production and storage. To contribute to this research problem, it is deemed important here to study the distribution of dissolved organic carbon (DOC) and its relationship to total organic carbon (TOC) in the initial snowpack, refrozen ice and meltwater. As a result, the processes of organic matter transfer from fresh snowpack to ablating ice surface may be tracked and the origin of the bioavailable OC on glaciers revealed.

The location of cells in the glacier near-surface layer is crucial for the potential *in situ* production of bioavailable OC, but data describing processes related to cell dynamics there are scarce. Until recently data has been limited to studies on snow (Hell et al., 2013; Müller et al., 2001), a budget of one supraglacial catchment (Irvine-Fynn et al., 2012) and algae-based ice core stratigraphic studies (Uetake et al., 2006). Whilst bacterial cells have been found to differ in concentration in ice core layers, possibly relating to changes in the depositional environment (Zhang et al., 2010), their relative abundance still lacks process-related explanation. Research into snow microbial communities highlights the importance of depositional processes (Hell et al., 2013; Irvine-Fynn et al., 2012; Zhang et al., 2010), as well as finds the motility of algal cells to be limited in both location and displacement extent (Grinde, 1983; Müller et al., 2001).

A recent addition to the studies on cell behaviour in snowpacks is the paper by Björkman et al. (2014). This study compared the elution behaviour of ions and cells to conclude that cells undergo longer retention in snowpack than inorganic solutes. Specifically, 50% of the fast-eluting ions were removed from the snowpack once 20-25% of its water equivalent has melted. The corresponding proportion for 50% removal of ions with intermediate mobility occurred after 30-45% SWE removal. Cells, on the other hand, persisted above 50% of total load in the initial snowpack until the removal of 70% of SWE occurred. Björkman et al. (2014) also argued against atmospheric dry deposition, in particular by aeolian dust, being important in determining the heterogeneity in initial cell distribution within the glacial snowpack. However, they did emphasise the potential importance of fresh cell inputs with precipitation, and highlighted the role of precipitation events in initial snowpack heterogeneity. This early-season distribution may then be, however, modified by wind redistribution of snow, leading to a more homogeneous snowpack structure at the onset of melt due to mixing. There are clearly gaps remaining in the understanding of snowpack cell distribution, in particular regarding the role of refreezing at the snowpack base, which could not be captured in Björkman et al's (2014) study due to its experimental design. If the role of basal ice is similar for biological as it is for inorganic chemical constituents, this may be a major factor in modifying cell runoff from glaciers. Also, the relative importance of different depositional pathways for cell in High Arctic

snowpacks is still unknown, and its further exploration is needed. Many studies omit the slush stage of snowpack development, since it is difficult to sample, yet it can be especially important role for the cell community due to its abundant water content. In fact, it has already been shown to host a distinct bacterial community to the one in its initial snowpack (Hell et al., 2013).

To address the aforementioned research gaps and gain insight into how melting and refreezing impact OC and cell dynamics on warming glaciers, a small-scale study was designed on the surface of Foxfonna glacier.

The objectives of the study were:

- to build a reliable model of the thermal and hydrological development of the melting glacier surface before the exposure of cryoconite deposits, which can be linked to biogeochemical processes there,
- to establish the temporal pattern of the processes of organic matter elution and recapture, in the context of physical (thermal) and hydrological changes on the glacier,
- to quantify OC and cell fluxes in the melting snowpack, and establish their partitioning between the free flowing water in supraglacial streams and the ice formed by refreezing.

5.2. Methods

5.2.1. Fieldwork

All fieldwork for this study was conducted within a partial catchment of the supraglacial stream described in Chapter 4 (namely, the catchment of its upper reach, Fig 5.1.), hereafter called a subcatchment (de Jong et al., 2005). The supraglacial catchment approach of Irvine-Fynn et al (2012) was followed but the present study also included the early season snow cover dynamics for the first time. The fieldwork involved thermistor string installation and sampling across the air-snow-ice boundaries. In this way the seasonal change in the biogeochemical composition of snow, slush and superimposed ice was established and linked to temperature changes. Thermal characteristics of the surface ice and snow were obtained with the use of thermistor strings installed in the vicinity of the sampling locations. Data describing OC export processes were then obtained from repeated stream water sampling at the outflow from the subcatchment.

The two thermistor strings consisted of 10 resistance sensors each, reaching approximately 2 m into the ice, and extending approximately 1 m into the air. The strings were installed on the glacier two years before the study period, 50 m apart from one another. Temperature data was logged between 1st June and 8th August 2012 at hourly intervals. The main measurement

site in this study is T2 (which corresponds to sites I2 and S8 for biochemical characteristics; Fig. 5.1), as a continuous data series was obtained there, while site T1 was affected by a data gap between 17th June and 11th July 2012 due to a power supply error. Within 5 m distance from the T1 thermistor pole (Fig. 5.1), an automatic weather station (AWS) was recording hourly data on air temperature, incident radiation, wind speed, air humidity, and distance to the glacier surface with a sonic ranger. The latter was calibrated with a set of 22 manual distance measurements, spanning the period 6th June – 8th August 2012. The ablation in mm w.e. was derived from this dataset, assuming a uniform density of snow of 0.52 g cm⁻³, as measured in the field for aged snow that was not saturated with water. After 28th July 2012, when the superimposed ice became exposed, the density assumption was changed to 0.85 g cm⁻³ (Tedesco et al., 2008). The detailed characteristics of the physical state of snowpack and top ice layer were obtained by repeated measurements (Table 5.1). The final superimposed ice survey was taken, when nearly all snow had disappeared from the vicinity of the thermistor; the refrozen ice layer thickness was expected to be close to maximum at this time (Bøggild, 2007).

It is appreciated here that the installation of thermistors can disturb the temperature readings due to heat conduction through the pole, and thermistors in snowpack might occasionally show higher temperatures than the surrounding snowpack due to absorption of radiative heat (Brandt and Warren, 1997, 1993). For the latter reason, care was taken to increase albedo of the measurement equipment by coating it in reflective material (white tape). The most probable errors in temperature measurements occurred near to the snow surface due to sun cup formation around the thermistor pole, and hence the interpretation of those was avoided. This was the likely cause of noise in the 0°C isotherm signal, when it was occurring in the upper layers of snowpack, and therefore this noise was manually removed by smoothing changes higher than 0.5°C in a few hours. All the aforementioned limitations may alter the absolute timing of the threshold changes noted in this chapter. Nevertheless, the temporal pattern of processes is very unlikely to be influenced by this effect.

The biogeochemical conditions and (re)distribution of OC was tracked in a series of 4 snow samplings, a single superimposed ice survey (28th July 2012) and stream water collection combined with salt dilution discharge measurements on 7 occasions (25th July – 16th August 2012). At the onset of snow melt (6th June 2012), the S1 snowpit was sampled for OC and cell content by representing each distinct layer by a 10 cm sample. Subsequently (3rd July 2012 and 11th July 2012), the sampling was repeated in snowpits at S1 and S8 (Fig. 5.1). Additionally, on 12th June 2012, snow cores were collected in 7 points across the subcatchment (sites S1-S7, Fig. 5.1) to measure their snow water equivalent (SWE), cell and OC content. The hydrological

and biogeochemical budgets were calculated using sampling locations S1-S7 for snow and I1-I3 for superimposed ice.

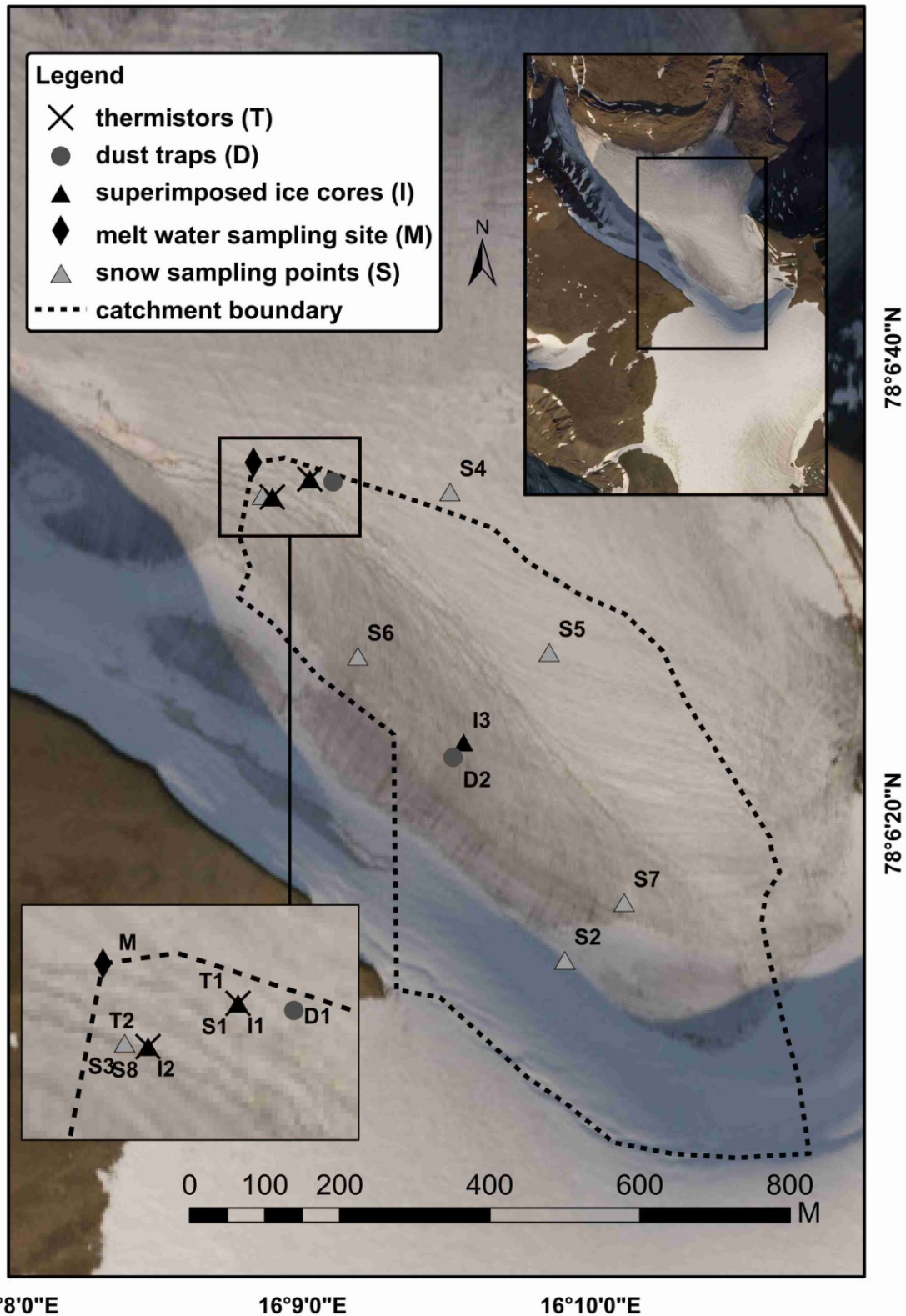


Fig. 5.1. Location of the subcatchment, which is the upper part of the catchment presented on Fig. 4.1.

Orthophotomap for 2006 - courtesy of Store Norske Spitsbergen Kulkompani AS.

Table.5.1. Summary of field measurements to describe the physical state of the glacier surface at Site T2.

Element measured	Dates	Number of direct measurements	Number of measurements at site T1 used for extrapolation	Measurement method	Comments
Snow density	6-06-2012 3-07-2012 11-07-2012		3	Snowpits, 10 cm layers sampled with a density cutter	Average of 2 samples per layer, allowed difference between both measurements: <10%
Snow depth	5 – 21-07-2012	7	9	Avalanche probe measurement in snowpits (site T2) or probing from snow surface (site T1)	Average of 4 measurements at each occasion, except 9 th July for superimposed ice (1 measurement then)
Water level	5 – 21-07-2012	7		Avalanche probe measurement in snowpits (capillary fringe surface)	
Superimposed ice thickness	5 – 21-07-2012	4		Depth of the hole drilled with Kovacs ice auger (to the cryoconite layer)	
	28-07-2012	1		Depth to the cryoconite layer in the hole from which an ice core was retrieved (taken using a 9 cm Kovacs ice corer)	

All OC and sampling in the field was performed in the way described in Section 4.2.1., and the aliquots for cell analysis were taken as aliquots of agitated melted samples for snow and ice, and were taken directly from the stream into sterile centrifuge tubes. For field equipment washes, 18 M Ω deionised water was used, with a cell content $0.332 \pm 0.331 \times 10^6$ counts L⁻¹ (error reported as 1 SD). All cell samples were frozen and stored in -80°C upon return from the field (after a maximum period of 12 hours from sampling), and analysed in Department of Geography, University of Sheffield.

5.2.2. Chemical and biological analysis

The laboratory analysis of TOC and DOC was performed in the way described in Section 4.2.2., including the operational definition of DOC as the TOC content of the 0.7 μ m sample filtrate (on Whatman GF/F filters). All values were blank-corrected, as has been described in Table 4.1.

For cell counts, a Partec CyFlow[®] SL flow cytometer, fitted with a 20 mW, 488 nm argon ion laser was used. The cytometry staining procedure followed (Van Nevel et al., 2013), a result of optimisation performed by Hammes et al. (2012), with the use of SybrGreen II stain. Cells were defined as particles fluorescing in the waveband 536/40 nm (FL1) when stained, with a minimum signal intensity equal to 0.001 of the intensity recorded for 3 μ m beads. This boundary for noise signal was chosen following manufacturer's (Partec) recommendations, based on the cytometer performance. Furthermore, the runs of this waveband were cross-checked against 18 M Ω water blanks (stained), which showed cell counts of 0.211 ± 0.097 (1 SD, n = 11) L⁻¹. This amount was further interpreted as the background level for the laboratory conditions (the facility is not a sealed clean room, so a small contamination with cells may occur in sample runs), and used for blank-correction of all obtained cell counts. The accuracy of the absolute counting procedure was monitored using CountCheck[®] beads by Partec in the low and medium concentration range, obtaining an RSE of 9.3% from n = 7 independent measurements (24.850×10^6 counts L⁻¹ and 82.660×10^6 counts L⁻¹, respectively).

5.2.3. Computation of water balance

Calculation of the subcatchment hydrological budget followed Equation 5.1:

$$(5.1.) \quad P + M + C - Q - I = \Delta S,$$

where:

P – liquid precipitation input during the study period,

M – water inputs from melt of the snow and ice within the subcatchment,

C – net balance between condensation and evaporation,

Q – runoff from the subcatchment within a supraglacial stream,

I – storage as superimposed ice,

ΔS – liquid water storage in snowpack and error.

The precipitation data were obtained from the Norwegian Meteorological Institute website (Norwegian Meteorological Institute, 2013) for the station in Longyearbyen (Svalbard Airport), 17.5 km from Foxfonna glacier. To account for the increase in rain and snowfall with altitude, a gradient of 19% per 100 m was adopted, based on water balance calculations in Bayelva catchment, Svalbard (Nowak and Hodson, 2013). Precipitation occurring on days with negative air temperatures was assumed to result in accumulation of snow, which would contribute to the budget as meltwater at a later stage, thus solid precipitation was excluded from the budget, based on the mean daily temperature record, as calculated from the local AWS data.

To estimate melt parameters for the snow/ice surface, the Brock & Arnold energy balance melt model (Brock and Arnold, 2000) was employed for the period 1st June – 8th August 2012 at the point location of the AWS (T1). Vapour pressure was calculated from air temperature using the Antoine equation (Thomson, 1946). The albedo was set at 0.6 in the model, as this was the average value measured for snow-covered areas of Foxfonna in 2010 (see Section 3.3.3.). Modelled melt was corrected for the subsurface heat flux which is not accounted for in the original parameterisation, and was estimated using equation 2.5. using thermistor measurements nearest to the top and bottom of the snowpack at a particular point in time (see Section 2.2.2.). The model performance was then validated against the water equivalent change derived from sonic ranger measurements, which indicated a -3.1% error in total melt in the period 6th June – 8th August 2012 (Fig. 5.2.). The Brock and Arnold (2000) model run provided also a C budget component estimation, from the latent heat flux and the value for proportion between the latent heat of ice melt and latent heat of vaporisation at 0.1336 (cf. Hock, 2005).

A continuously monitored record of discharge from the proglacial river draining the north-western lobe of Foxfonna glacier (Section 4.2.1.2.) was compared to the discharge measured at a corresponding time point (± 1 hour) at the M site (Fig. 5.1.) between 25th July and 16th August 2012, using salt dilution method. Unfortunately, no direct discharge measurement at the site M could be taken before 25th July 2012, since early in the season the stream was impossible to approach safely due to slush. Therefore, a record of hourly discharges at the site M was modelled, beginning on 5th July 2012, when the stream was first observed there, by assuming that the relationship established between these sites during the period of simultaneous records (a logarithmic one, $R^2 = 0.638$) was invariant in time. Daily runoff values at M were expressed in mm (subcatchment surface area equalling 0.383 km²).

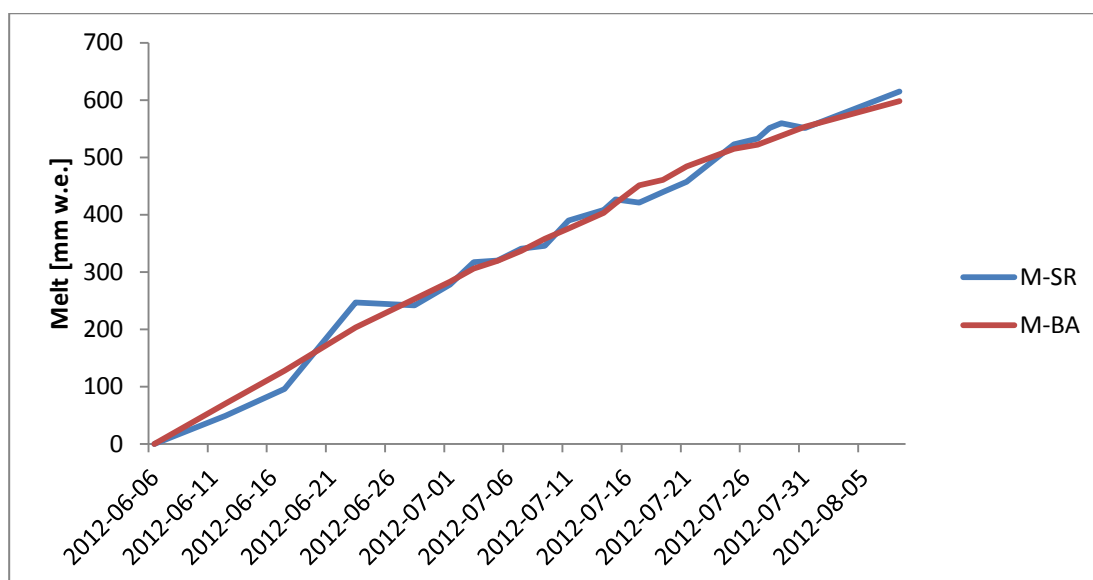


Fig. 5.2. The comparison of cumulative melt estimates given by applying density assumptions to surface lowering registered by a sonic ranger (M-SR) and the Brock & Arnold energy balance melt modelling (M-BA, Brock and Arnold 2000), corrected for subsurface heat flux.

Snow densities were measured as part of each sampling for the respective 10 cm layers, or the full depth in the case of core extraction. The superimposed ice water equivalent was obtained from surveying the thickness of superimposed ice layers, assuming a mean ice density of 0.85 g cm^{-3} (Tedesco et al., 2008). The glacial ice density was assumed to be 0.916 g cm^{-3} (Nuth et al., 2010).

Biases in the hydrological budget were possible due to the use of meteorological data and surface measurements from the lowest point of the subcatchment, because melt decreases with altitude, whilst refreezing increases. The discharge estimates might be also biased because runoff in the subcatchment (minimum elevation 600 m a. s. l.) was estimated from limited data, which were extrapolated using a relationship with continuous proglacial runoff records (lowest point at 336 m a. s. l., see Section 4.2.1.2.). A small bias in the onset of runoff and the total runoff magnitude is therefore possible. However, a major part of the catchment area is within $\pm 60 \text{ m}$ altitude difference from the AWS location, and the average temperature difference between the periods with measured and extrapolated discharges at the site M was -0.6°C . Hence, these biases seem unlikely to be sufficient to undermine the total water storage change estimated in Section 5.3.2.

5.2.4. Estimation of organic carbon and cell fluxes

In order to explore relationships between OC and cell fluxes within the subcatchment, including atmospheric deposition, removal by runoff, and the storage change (especially due

to the superimposed ice layer formation), a budget was devised (equation 5.2.). To fully account for the role of superimposed ice as a storage media, all budget terms were calculated for a single time point at its maximum extent (28th July 2012).

$$(5.2.) \quad S_{OC/cell} + D_{OC/cell} - Q_{OC/cell} = I_{OC/cell} + \Delta R_{OC/cell},$$

Here:

- $S_{OC/cell}$ is net atmospheric deposition of OC or cells over the entire winter, captured by snow sampling.
- $D_{OC/cell}$ is the summer wet and dry deposition of OC/cells, measured using 'dust traps' (cf. Section 4.2.1.1.).
- $Q_{OC/cell}$ represents removal of OC/cells from the catchment with meltwater in the supraglacial stream.
- $I_{OC/cell}$ is OC/cell storage in superimposed ice at its maximum formation, and
- $\Delta R_{OC/cell}$ is the change of OC/cell retention (storage) on the glacier surface in other forms than superimposed ice, plus all errors associated with the estimation of other fluxes.

The budget terms described here were calculated in a similar way to those in Chapter 4, in particular:

- $S_{OC/cell}$ was calculated using the same approach as A^{acc} (equation 4.4), from 7 snow cores distributed across the subcatchment area (S1-S7, Fig. 5.1.).
- $D_{OC/cell}$ calculation followed equation 4.5 for A^{abl} , and used data for three collection periods from two dust traps shown on Fig. 5.1 (D1-2).
- $Q_{OC/cell}$ corresponded directly to Q_c estimation (equation 4.6.) with the substitution of the discharge from the hydrological balance of the subcatchment (Q , Section 5.2.3.) for the Q_{obs} extrapolated in time.
- $I_{OC/cell}$ was estimated using the same principles as for the SI flux in Section 4.2.3., with the use of 3 core locations (I1-3, Fig. 5.1.)
- The equation 5.2. was then solved for $\Delta R_{OC/cell}$.

5.3. Results

5.3.1. Physical processes in the snowpack

The temperature changes at the T2 site can be divided into three distinct periods (Fig. 5.3):

1. Melting front penetration into a cold snowpack (phase 1a ending on 18th June 2012 and phase 1b lasting until 16th July 2012).
2. The development of isothermal snow and superimposed ice temperatures at 0°C (between 16th July and 26th July 2012).
3. Superimposed ice ablation period (after 26th July 2012).

Period 1 can also be described as the time of superimposed ice formation, with the growth from 0 to approximately 60 mm w.e. having happened in an initial phase (1a, between 9th and 18th June), and the next 90 mm w.e. formed at a slower pace, in phase 1b. Period 2, on the other hand, showed fluctuations of superimposed ice thickness, with a magnitude of approximately 30 mm w.e. Period 3 experienced superimposed ice thinning, resulting in its final w.e. value of 147 mm in the end of thermistor measurement period (8th August 2012). This change also involved the 0°C isotherm penetrating the glacial ice layer beneath. Throughout the melt season, a progressive decrease in temperature amplitudes and daily melt rates also occurred. The highest level of snow saturation by meltwater ponding was observed on 11th July 2012, which coincided with a period of lower melt.

5.3.2. Hydrological budget of the subcatchment

Figure 5.4. shows that in the Period 1a of melting front propagation, the meltwater produced was mainly stored *in situ*, contributing to storage of water in the form of ice or capillary moisture. Period 1b was characterised by meltwater storage, and the majority of refreezing happened then. The water storage, as calculated from the hydrological balance, was slowly increasing in this period, reaching 227 mm w.e. towards its end. Mid-way through Period 1b, runoff commenced, however it was not until Period 2 that it experienced a marked increase, at the expense of water storage. Also in Period 2, the highest input of precipitation water was noted, amounting to 11.3 mm w.e. (on 4th July 2012), while the second highest rainfall of 6.5 mm w.e. occurred towards the end of Period 1a, on 15th June. Both the runoff and the remaining water storage became more stable in Period 3. Already during Period 2, storage change became negative, reaching -195 mm w.e in the end of the monitoring period.

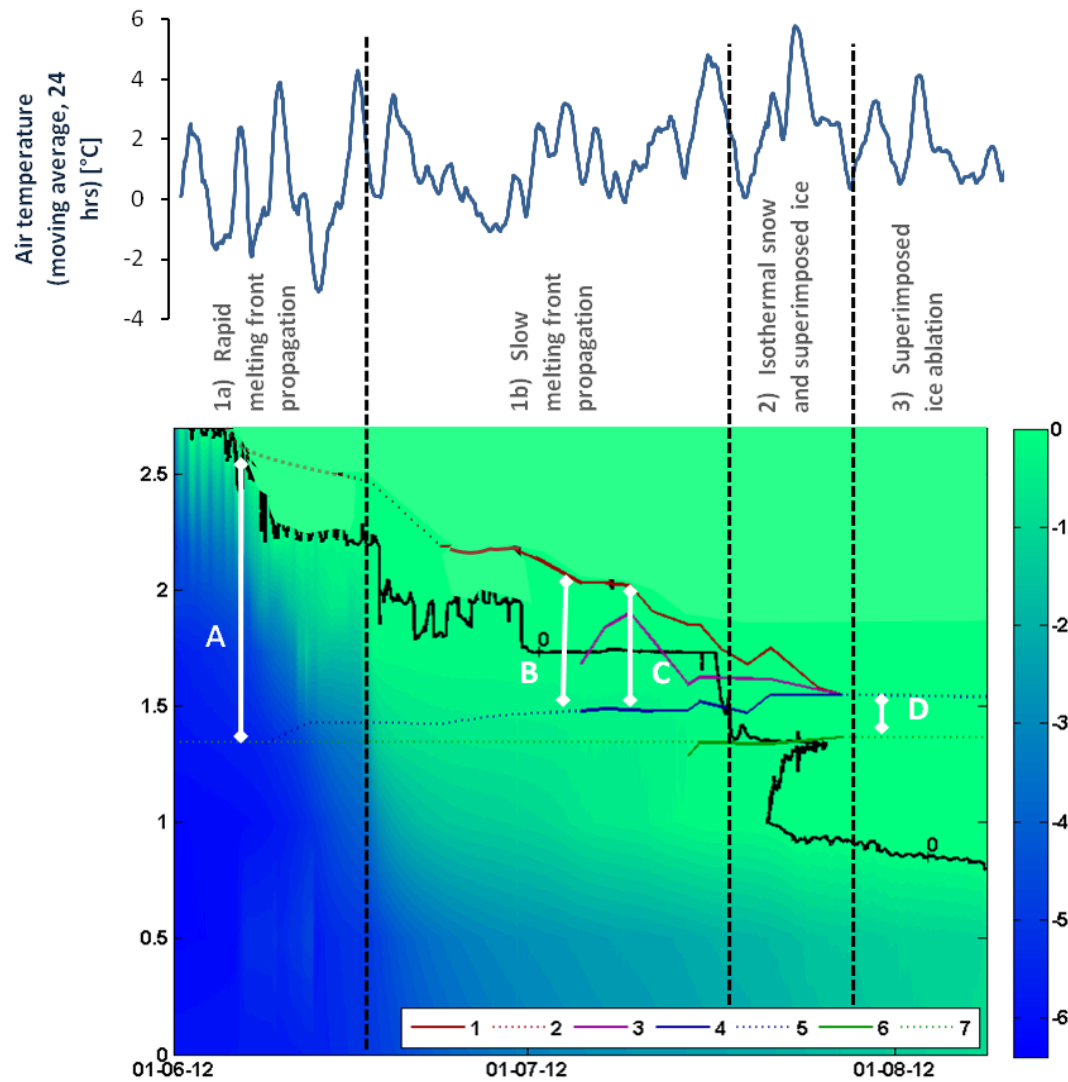


Fig. 5.3. Temperature-related changes at the snow-ice interface in the melt season.

a – 24 hour moving average of air temperature registered by the local AWS, b – temperature profile in T2 site during the melt season of 2012. Superimposed on the graph are the following boundaries: (1) top of snowpack: measured, (2) top of snowpack, extrapolated based on a record from T1 site, (3) water level in snow (capillary fringe surface), (4) superimposed ice surface: measured, (5) superimposed ice surface: extrapolated from T1 site measurements, (6) glacial ice surface: measured, and (7) glacial ice surface: extrapolated as constant during the season. A, B, C and D indicate the times of snow or superimposed ice profile sampling (Fig. 5.5).

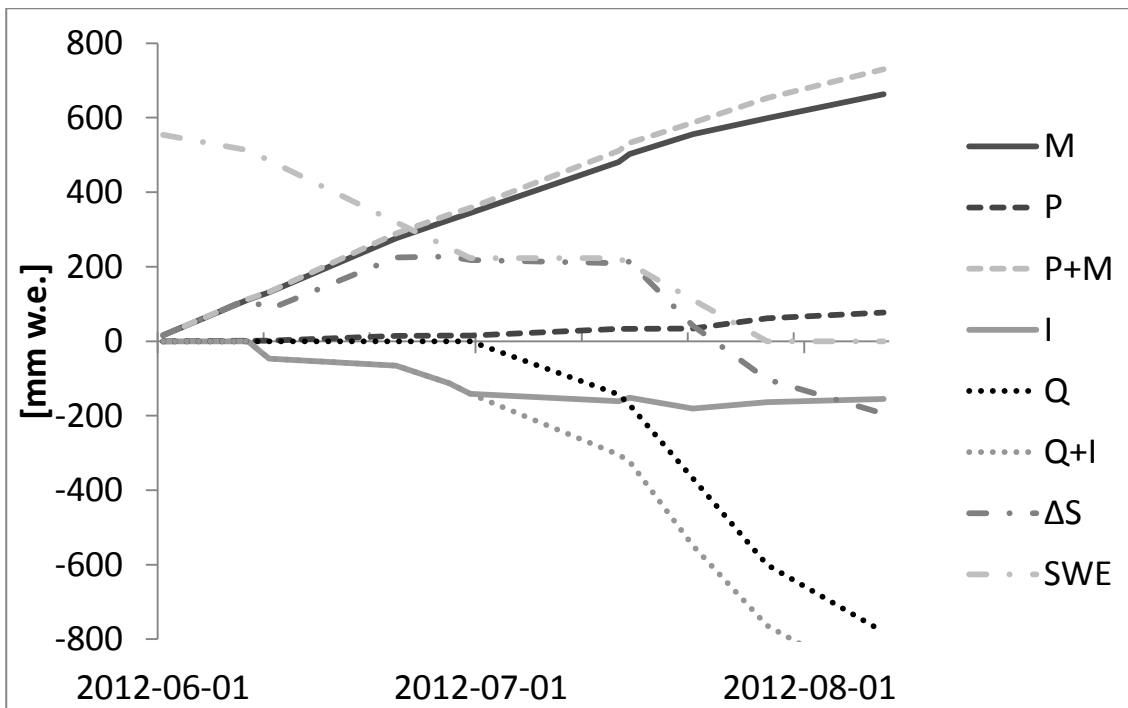


Fig. 5.4. Hydrological balance of the studied subcatchment (see Fig. 5.1).

All curves represent cumulative values from the start of the season. *M* – melt, *P* – precipitation, *I* – superimposed ice, *Q* – total runoff. Sources and sinks merged as curves (*P+M*) and (*Q+I*), respectively. ΔS denotes the sum of the water budget, which accounts for liquid water storage change and errors. Net condensation/evaporation was omitted due to its negligible sum in the season (1.4 mm), as estimated from latent heat flux in Brock and Arnold's (2000) energy balance model. To facilitate interpretation in the context of snowpack lifetime, the snow water equivalent (*SWE*), as measured at the catchment outlet, was added to the graph.

The ΔS term, which was calculated from the budget (Equation 5.1), followed the same temporal pattern as the wet snow level monitored at the site T2 (Fig. 5.3 & 5.4). This water storage component equalled melt before 9th June 2012, when the superimposed ice started forming. Initially, this curve followed the trend of the melt curve closely, then diverged in late June and remained stable or increased slightly until mid-July. Before 20th July 2012, the storage was rapidly reduced, reaching another stable level in the first week of August. The first stabilisation of water storage level coincided with the temporary slowdown in SWE depletion, while the level of the final part of the monitored period corresponded to a situation devoid of snow at the weather station area in the lower part of the subcatchment.

5.3.3. Organic carbon and cell transfer

In the snowpack, initially both OC and cells were distributed in layers of variable composition: on 6th June 2012 (Period 1a), there was between 4 and 30 mg m⁻² DOC in each 10 cm layer (on average 10 mg m⁻² ± 13%), 24–66 mg m⁻² for TOC (averaging 47 mg m⁻² ± 13%) and

59–732 × 10⁶ counts m⁻² for cells (average equal to 263 × 10⁶ counts m⁻² ± 11%; Fig. 5.5A). As the melt proceeded towards the end of Period 1, the snow profile became depleted of OC. At the same time, there was a relative enrichment of cells near the snow surface (from 150 × 10⁶ counts m⁻² to 4727 × 10⁶ counts m⁻² in the upper 10 cm layer; Fig. 5.5B). Following this, most of the cells were removed from the profile (between 3rd and 11th July 2012), leaving the surface layer with a cell content of 366 × 10⁶ counts m⁻² towards the end of Period 1 (Fig. 5.5C). The cell depletion coincided with a rise in the liquid water level, which was observed to reach its maximum at Site T2 on 9th July 2012. The unsaturated snow zone had virtually disappeared by 14th July.

Once all snow had been melted, the superimposed ice layer remained, and contained on average 41.2 mg m⁻² DOC, 53.4 mg m⁻² TOC and 916 × 10⁶ cell counts m⁻² in each 10 cm layer (Fig. 5.5D). It was enriched in DOC and cells by a factor of 4.1 and 3.4 respectively, while TOC concentration was only 1.1 times that of the initial snowpack (as collected on 6th June 2012).

In runoff at Site M (Fig. 5.6), there was a sharp increase in both OC and cell concentrations during Period 3, when the superimposed ice disappeared from the vicinity of the gauging site and glacial ice melt started providing most meltwater. For example, on 25th July 2012 the discharge (Q) was c. 0.135 m³ s⁻¹, whilst the TOC concentration was 175 ppb, DOC was 105 ppb and the cell count was 3.9 × 10⁶ L⁻¹. On 12th August 2012, with a very similar discharge (Q = 0.132 m³ s⁻¹), TOC concentration was 1.6 times higher (275 ppb), DOC concentration increased 1.9 times (to 200 ppb) and cell count exceeded the initial value more than 14 times (amounting to 58.1 × 10⁶ L⁻¹).

The OC budget in the subcatchment showed the atmospheric inputs to be the dominant process, providing 279 ± 49 mg m⁻² TOC (of which 156 ± 28 mg m⁻² was DOC) as snow and further 78 ± 25 mg m⁻² TOC and 44 ± 14 mg m⁻² DOC in the precipitation and dry deposition in the summer (Fig. 5.7.). The superimposed ice, at its maximum thickness, stored 27% of this TOC (and 41% of the atmospheric DOC supply). Another 128 ± 32 mg m⁻² TOC (of which 60% was DOC) was removed by the supraglacial stream. For the cell fluxes, storage in the superimposed ice was even more important, since it stored 73% of the winter atmospheric inputs (93 ± 15 × 10⁷ cells m⁻² in snow and 269 ± 87 × 10⁷ cells m⁻² in the summer deposition, compared to 265 ± 27 × 10⁷ cells m⁻² in refrozen ice at the snowpack base). For both DOC and cells, the partitioning between superimposed ice and stream removal was approximately equal. In the case of DOC, 77 ± 19 mg m⁻² was removed in the stream and 83 ± 9 mg m⁻² was stored by refreezing; for cells, the corresponding fluxes were 240 ± 59 × 10⁷ cells m⁻² and 265 ± 27 × 10⁷ cells m⁻², respectively.

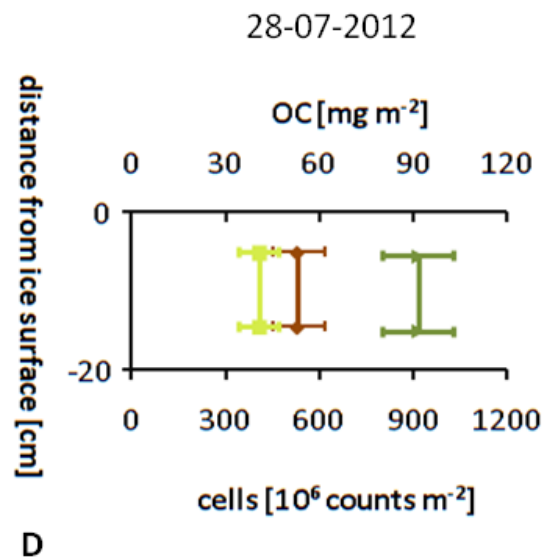
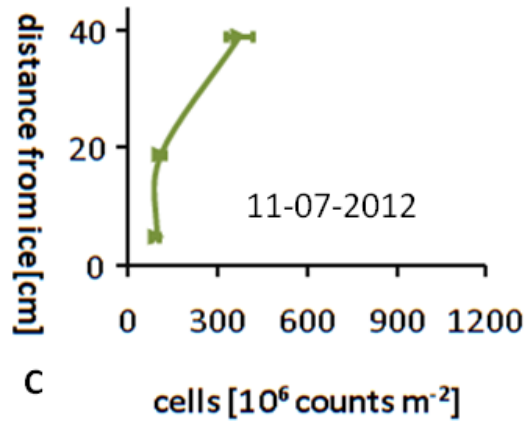
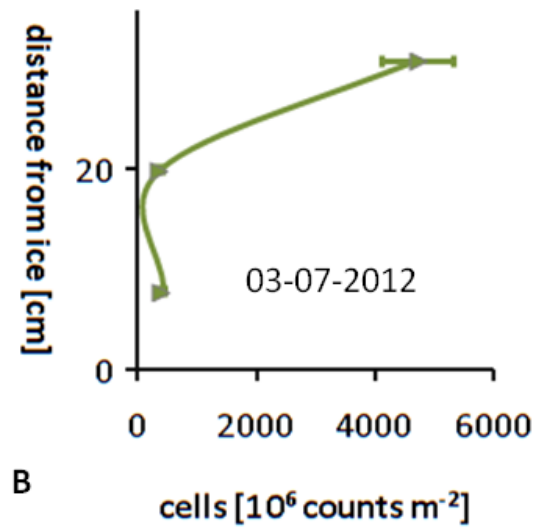
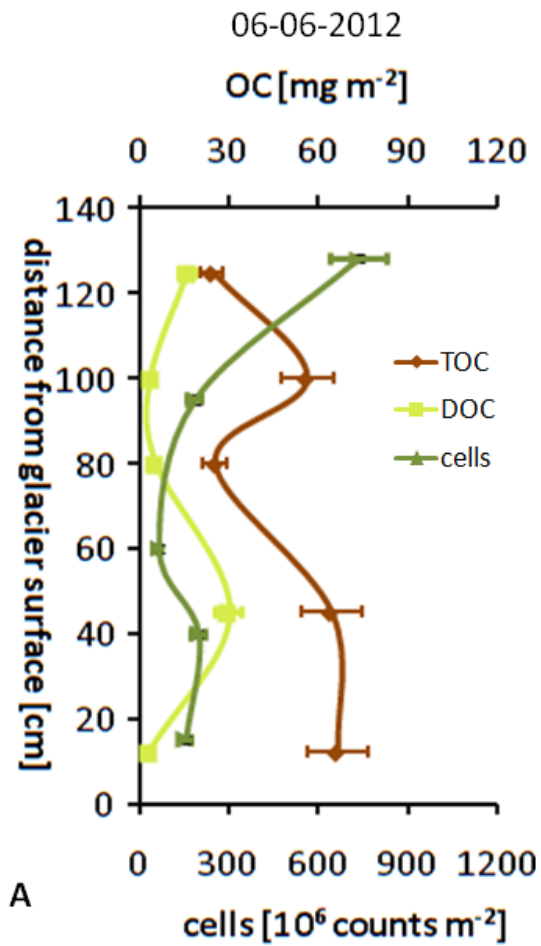


Fig. 5.5. Organic carbon (OC) and cells in 10 cm snowpit layers.

1 – TOC, 2 – DOC, 3 – cells. A, B, C and D denote times shown on Fig. 5.3. Please note the change in horizontal scale on graph B, and the difference in vertical scales.

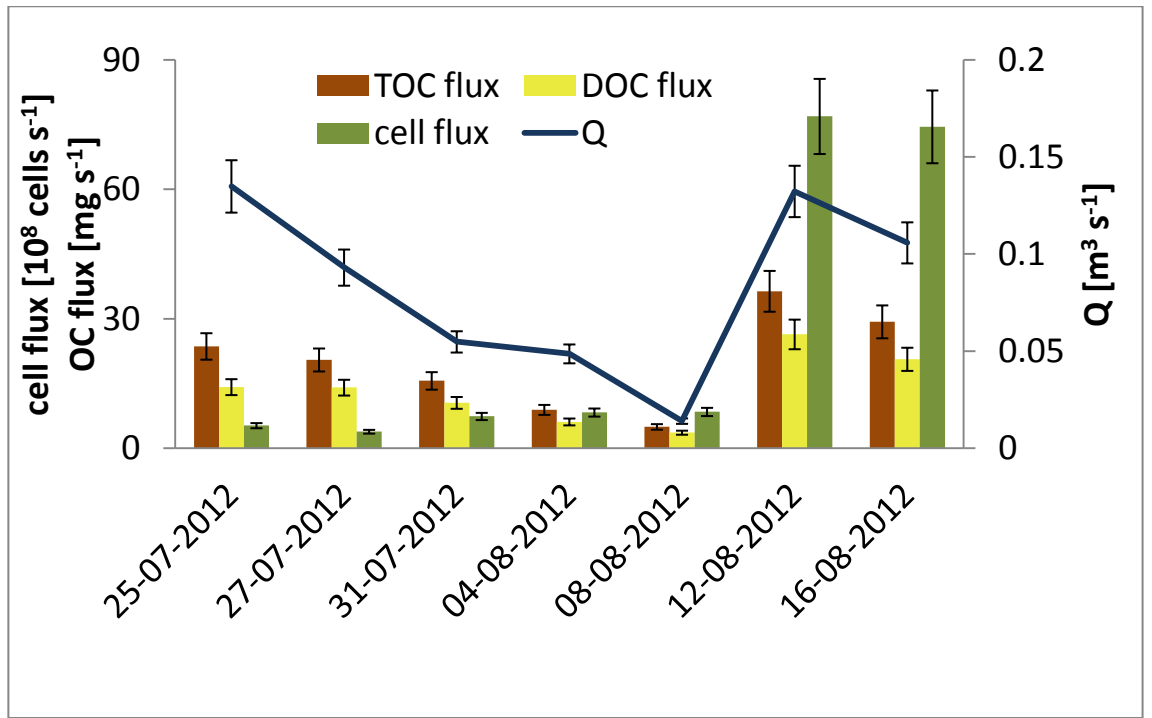


Fig. 5.6. OC and cell flux in the supraglacial stream at the basin outlet (M point on the location map).

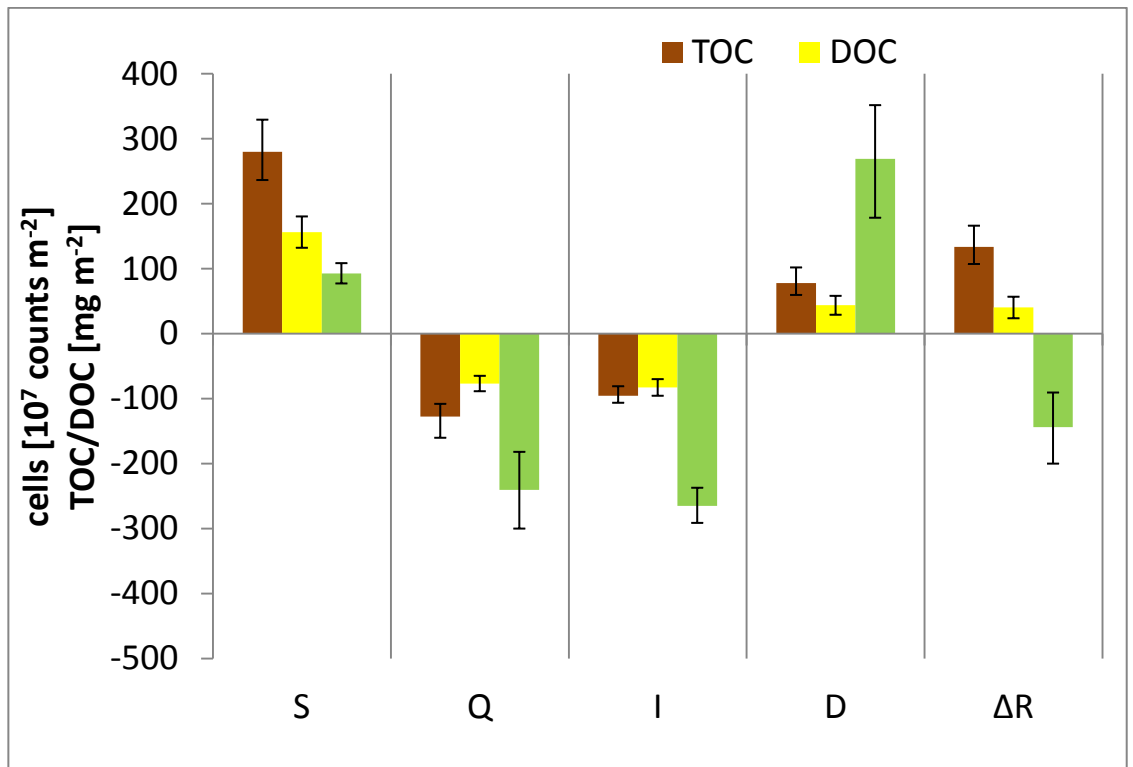


Fig. 5.7. Subcatchment budgets of OC and cells, calculated for 28th July 2012 (superimposed ice sampling day).

Terms as in equation 5.2.

5.4. Discussion

5.4.1. Hydrological evolution of the near-surface part of the glacier

The thermal evolution of snowpack on the glacier surface unfolds in three main periods, corresponding to its hydrological development (Table 5.2.). These are influential for the biogeochemical profile of the supraglacial environment.

The general hydrological evolution presented here is in tune with other studies, e.g. Bøggild's (2007) model of superimposed ice formation. Most of the hydrological changes appear to be directly temperature-driven, with the exception of snowpack inundation, which also requires favourable local topography to occur (compare Hodgkins, 2001). The inundated snow may also cause additional water removal, in the form of slush flows. These were observed on Foxfonna, especially in the period of study (around 5th July 2012 and 26th July 2012), but impossible to capture in the hydrological budget or to sample for biogeochemical composition due to their rapid movement. The reduction in water storage, as calculated for 8th August 2012, may be attributed to firn melt observed in the upper part of the catchment.

5.4.2. Biogeochemical changes in the supraglacial environment

The changes in surface energy balance and hydrology shown here are capable of influencing the biogeochemical fate of cells and nutrients. Figures 5.3 and 5.5 show evidence of both OC and cells being eluted from snowpack at clearly defined stages of the hydrological evolution of the glacier surface.

Moreover, the behaviour of DOC and cells closely corresponds to the theoretical elution expected from their general characteristics. DOC, which contains hydrophilic organic molecules, is removed early, according to Meyer and Wania's (2011) enrichment Type 1. Cells, on the other hand, were present in the profile until the point of snow inundation with meltwater, and concentrated in top layers of melting snowpack. This is consistent with the Type 3 enrichment (Meyer and Wania, 2011), characteristic for substances associated with snow grain surfaces. Indeed, cells have been observed to associate with water-surfaces of snow grains (Grinde, 1983). The long cells retention in snow corroborates also with the empirical pattern of their elution observed in a Svalbard snowpack lysimeter study by Björkman et al. (2014).

Both cells and DOC showed high enrichment factors in the refrozen layer. The timing of the most important phase of superimposed ice formation is consistent with the inferred moment of maximum DOC elution, while the slower superimposed ice formation coincides with the maximum cell leaching from melting snow. Hence, the elution phenomena could contribute to the composition of the superimposed ice layer. This layer not only acts as a

storage media for both DOC and cells, but also postpones the exposure of glacial ice surface after snowpack melts. The final removal of the superimposed ice layer results in a regime shift in supraglacial runoff of organic matter, increasing the concentrations of DOC and cells. This shift can be described with a classic hysteresis loop, and is especially pronounced in the case of cells (Fig. 5.8).

A puzzling result is the uniform behaviour of DOC and TOC, seen between the Period 1a and 1b snow profiles. TOC can be split into two mutually exclusive fractions, i.e. the DOC and POC (particulate organic carbon), which theoretically correspond to two end members of elution behaviour. While DOC is expected to elute early, similarly to organic compounds showing affinity to liquid water in the model by Meyer and Wania (2011), particle-bound organic chemicals are usually the least mobile phase in snowpack (Type 2 enrichment). Hence POC would be expected to behave accordingly and accumulate on the snowpack surface, similarly to hydrophobic soot-derived organics observed by Doherty et al. (2010, 2013).

In order to explore the agreement between this theory and empirical results from snow profiles on Foxfonna, the concentration of POC was calculated according to equation 5.3:

$$(5.3.) X_{\text{POC}} = X_{\text{TOC}} - X_{\text{DOC}},$$

where X is an OC-type concentration in a particular environmental component. Whilst the behaviour of DOC was found to be concordant with its expected elution, the POC in the snow profile seemed to have been removed before cells, instead of concentrating on the snow surface. POC was therefore eluted in a manner more akin to DOC than to cells, despite cells being part of the POC pool, if classified by size. Both DOC and POC have virtually disappeared from the snow column before the profile on 3rd July 2012 was sampled (Fig. 5.5.). On the other hand, the superimposed ice showed a relatively small storage of POC, indicating a different behaviour from the dissolved fraction, at least in the extent of refreezing. The possible explanations of these observations are:

- 1) a sampling bias, resulting from the thin surface layer of snowpack being omitted during profile surveys in the end of Period 1b (and hence the actual fate of POC involving its concentration in the surface layer and later removal),
- 2) POC concentrating on the snowpack surface during melt and decay of snowpack profile, but being subject to a removal mechanism washing off the uppermost layer of snowpack,
- 3) the majority of POC being eluted before cells, and travelling down the snow profile with percolating water, but accumulating at snow-ice interface,
- 4) POC being co-eluted with DOC, but being excluded from refreezing, and leaching further into the cryoconite layer beneath.

Of these, option 1 can be excluded based on the post-sampling photograph taken upon sampling profile B (Fig. 5.9, cf. Fig. 5.3, Fig. 5.5B.), which documents the inclusion of the uppermost snow layer and the lack of visible dirt cones or BC-like deposits on its surface. Option 2 is also very unlikely, since the only mechanism observed to remove snow from the site, except meltwater percolation, was slush flows. These are rapid movements mobilising the full snowpack profile and occur once it is saturated, so the probability of them selectively removing the uppermost layer of snow is near zero. Options 3 and 4 require POC to behave like a relatively mobile phase compared to hydrophobic particulates similar to BC. This is plausible, since some types of POC (e.g. macromolecules of starch) may form colloidal dispersions in water, especially in waters of low ionic strength. This is, for example, the case with high-molecular-weight acids in soils, which maintain mobility in percolating water (McSween et al., 2003). A further insight into the likelihood of options 3 and 4 occurring could be gained from the subcatchment OC budget construction, which will be performed in the next section.

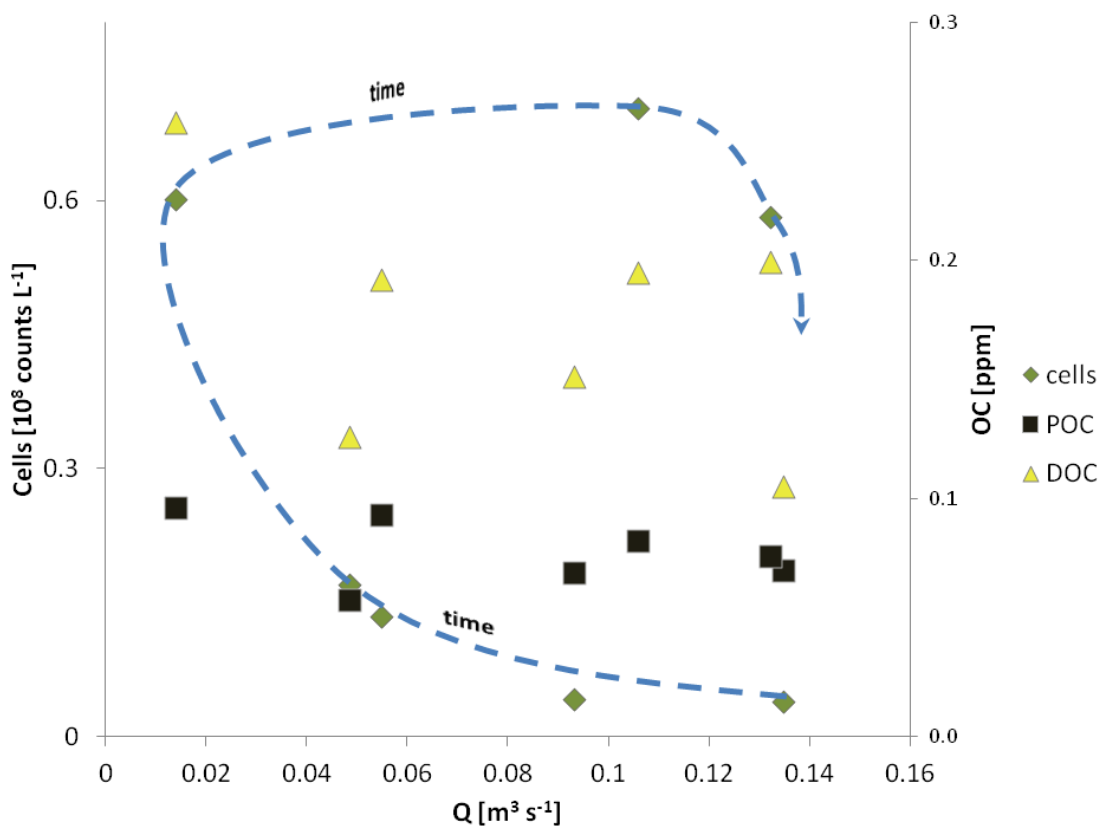


Fig. 5.8. A hysteresis behaviour observed in the cell runoff (M site).

An interpretation of the pattern presented on Fig. 5.6.



Fig. 5.9. Photo taken after sampling the snowpack profile on 3rd July 2012.

Photo by Emma Brown.

A further insight of the POC behaviour analysis is its general dissimilarity to cells, despite the size limits for POC encompassing the typical algal cell size (Vézina and Vincent, 1997). This can be confirmed by the small and non-significant correlation coefficients between the POC and cell concentrations in snow, ice and stream water samples (Spearman rank $r = -0.212$ in snow; $r = 0.358$ in superimposed ice and $r = 0.500$ in the supraglacial stream samples; all p values exceeding 0.05), and will be further explored in the context of OC and cell fluxes (see below).

As a result of the above considerations, physical processes emerge as powerful factors in shaping the fate of OC and cells in the near-surface environment of glaciers, perhaps even sufficient to describe major distributional features of OC and cell abundance in ice and runoff. The opposing idea, however, is that the biological activity of cells themselves contributes significantly to the patterns. Algal blooms are indeed known from glacial snowpacks (Lutz et al., 2014; Remias et al., 2005; Takeuchi et al., 2006), but their role in the glacial OC cycle has yet to be assessed. These were not widespread on Foxfonna, and the incidental high cell concentration measured in the upper snow layer on 3rd July 2012 produced no detectable OC peak in this layer or within the snow column (Fig. 5.5). To further explore this issue, the role of biological production is estimated here using a flux balance approach, performed in the

following section. This will include an estimation of the proportion contributed by cells to the POC fraction of TOC.

5.4.3. Organic carbon and cell fluxes

When the inputs and outputs of organic matter were budgeted against each other (Fig. 5.7, Equation 5.2), a positive ΔR for both DOC and TOC resulted, with a DOC:TOC mass ratio of 0.30. This ratio was lower than those noted in the budget terms, 0.56 in both S_{OC} and D_{OC} , 0.60 in Q_{OC} , and 0.87 in I_{OC} , indicating a POC enrichment in ΔR_{OC} . Hence, the term corresponds to a fugitive sink of POC or the presence of storage media preferentially retaining POC. However, the cells budget showed ΔR_{cell} of $-144 \pm 55 \times 10^7$ cells m^{-2} (Fig. 5.7), implying either a missing source in the described system, or the overestimation of cell removal fluxes. This again confirmed the dissimilar behaviour of POC and cells in the system.

In Section 5.3.2., the water balance showed that hydrological storage had actually decreased in the catchment by 28th July 2012, suggesting that water movement out of the catchment is a plausible explanation of the negative cell budget discussed above. Also, this suggests the interpretation of the positive ΔR_{OC} as a relative enrichment phenomenon rather than a net water retention. Furthermore, it seems unlikely for a large water output to remain unaccounted for, while the calculated hydrological budget for the subcatchment closes with a negative storage change. Therefore, the zones of relative POC enrichment were sought, using the DOC:TOC ratios of full catchment flux data discussed in Chapter 4. The lowest DOC:TOC ratios were found in accumulation season snowpack (0.44), surface glacial ice (0.53) and storage change (0.43), which corroborates with the hypothesis that POC may be accumulating on ice surfaces, including refrozen layers in firn area. The DOC:TOC ratio in cryoconite debris was not established, but it is a plausible final sink for the POC leaching from snow, due to its capacity and structure. This is further supported by the runoff flux of POC during the superimposed ice ablation period accounting only for a similar amount to that stored in superimposed ice (14.2 mg POC m^{-2} compared to 12.9 mg POC m^{-2}). Both superimposed ice and glacial ice are less permeable to water than snow, and the small size of ice veins (tens of micrometers at most, see Dani et al., 2012; Price, 2000) may prevent bigger size fractions of colloids from penetrating through. However, upon ice melt, POC may still penetrate the ice to reach cryoconite deposits, especially if the superimposed ice melt is non-uniform and forms *weathering crust* (Irvine-Fynn et al., 2011; Müller and Keeler, 1969), i.e. a pattern of fractured ice forming a shallow aquifer.

Both TOC and DOC budgets (Fig. 5.7) yield positive ΔR s (134 ± 33 and 40 ± 19 mg C m^{-2} , respectively), which imply an excess of inputs over outputs, beyond the superimposed ice retention already accounted for. The biological contributions to these changes can be

calculated assuming data presented by other researchers. Using metabolic rates taken from Stibal et al. (2012), all cells deposited in the subcatchment area, during the study period, can be estimated to respire and incorporate $(-3.1) \times 10^{-5} \text{ mg C m}^{-2}$. Furthermore, if the cell OC content is computed following Felip et al. (2007), then the OC store in all cells remaining in the end of the study period amounted to 0.98 mg C m^{-2} , a mere 0.4% of the TOC stored, and also a small proportion of the overall POC remaining in the subcatchment (0.9%). That makes the biological production fluxes unimportant in the OC flux balance of the subcatchment. They were also an unimportant part of the POC pool, amounting to 1.9% of POC in atmospheric deposition and 3.8% in runoff, only in superimposed ice reaching as much as 16.6% of POC (all estimations of cell OC computed as described above).

For both cells and DOC, superimposed ice is the most important store in the constructed budget. The cell storage was quantitatively similar to their estimated summer atmospheric input, while for DOC, superimposed ice stored an amount equal to half of the winter deposition supply (and exceeded the summer atmospheric input). The presence of this store significantly delays the export of both these organic matter types from the point on the glacier surface where they were deposited. During the period of superimposed ice melt (28th July 2012 – 8th August 2012), only c. 45 mg TOC m^{-2} (of which 31 mg m^{-2} was DOC) were removed, which implies that part of the superimposed ice OC content remained on the glacier surface beyond this period, and was only released in the major removal event after the glacial ice surface was revealed by ablation (12th and 16th August 2012 on Fig. 5.6.). In the case of cell removal, the runoff flux between 28th July 2012 and 8th July 2012 can be estimated for $371 \times 10^7 \text{ cells m}^{-2}$, which exceeds the superimposed ice cell store estimated here, whereas the cell flux in the supraglacial stream increased greatly after the glacial ice had been exposed. This single event changed the cell runoff regime significantly, causing the classic hysteresis behaviour shown in Fig. 5.8. A smaller effect was observed also in the case of DOC, while POC was not observed to display such a pattern.

The negative ΔR_{cell} on 28th July 2012, as well as Q_{cell} in the superimposed ice ablation period exceeding I_{cell} for 28th July, may account for their net loss from the subcatchment. This is consistent with the negative hydrological storage change (Section 5.3.2.) and the possibility of intensive cell removal in runoff (Fig. 5.6.). However, the influence of the biological cell source should be also considered, as an alternative source of this budget outcome. An attempt at its estimation will be made here, using published data. These are, however, sparse; there is a paucity of reports on *in situ* reproduction rates of bacteria and algae in snow and slush. One of the few studies that report algal reproduction is Hoham et al. (2000), where cell population change rates of up to 23% in a life cycle (7-10 days) are reported for *Chloromonas sp.* algae, in 24h daylight conditions. If all cells in this study were reproducing at that rate, and the cycle

was 7 days long, then this could exceed the negative budget sum found from the above considerations (301×10^7 cells m^{-2} by reproduction). However, it is highly unlikely for all cells to belong to the *Chloromonas sp* and reproducing that efficiently, not least because the environment is very likely oligotrophic (e.g. Hodson et al., 2007; Mindl et al., 2007; Stibal and Tranter, 2007). Furthermore, the *Chlamydomonas* algae were observed to produce new cells only in the dark period (Hoham et al., 2000), which makes the application of these results to a 24-hour daylight study rather problematic. For bacterial cells, only cultivability data are available (e.g. Møller et al. (2013) report 12% cultivability in High-Arctic snow), which is not directly informing about the rate of cell reproduction. Hence, the cell counts could be changed significantly by biological reproduction, but the influence of this factor is moderate at most.

5.4.4. Conceptual model

The processes described above can be presented in a conceptual model (Fig. 5.10), which links the evolution of the melt zones on the glacier surface (see Müller, 1962) to the changes in the water, OC and cell fluxes. The measurements conducted here represent a time sequence, but they can also be applied spatially across glacier hydrological zones (see Section 2.2.3). Highlighted are different temporal patterns characteristic for OC and cells, the former being a mobile species, quickly removed from the snow and locked in superimposed ice. The cells, on the other hand, behave more like chemical substances associated to snow grains (Meyer & Wania elution Type 3), remaining in the snow profile until inundation with liquid water, and also experiencing increased concentrations in meltwater runoff after the superimposed ice has melted.

The exact mechanism and timing of organic matter trapping by superimposed ice is ambiguous, however OC seems to be both refrozen and released earlier than cells (cells being removed more uniformly during superimposed ice melt). The supply of cells to the refrozen layer peaks at the end of this ice formation, and hence, the bottom layers of superimposed ice would be expected to be relatively enriched in DOC, while the top layers would be proportionally more enriched in cells (Section 5.4.1). Since this does not correspond to the sequence of their removal from superimposed ice, it is proposed here that further biogeochemical processes differentiate the output from this layer (e.g., it is subject to preferential elution such as that in the snow profile), however the exact nature of these requires further research.

The effects described here might be disturbed by events of summer deposition with high organic matter content, which have been observed in the record presented in Section 4.3.1 (see also Section 4.4.1). In the firn zone, where the water level never reaches the top of the snowpack, wet snow surface layer enrichment in cells would persist throughout the summer,

however there might be secondary concentration maxima in refrozen layers in firn. Therefore, the careful interpretation of ice cores containing algae-rich layers (e.g. Uetake et al., 2006) is required, in order to distinguish between the two effects and not attribute them to separate summer seasons.

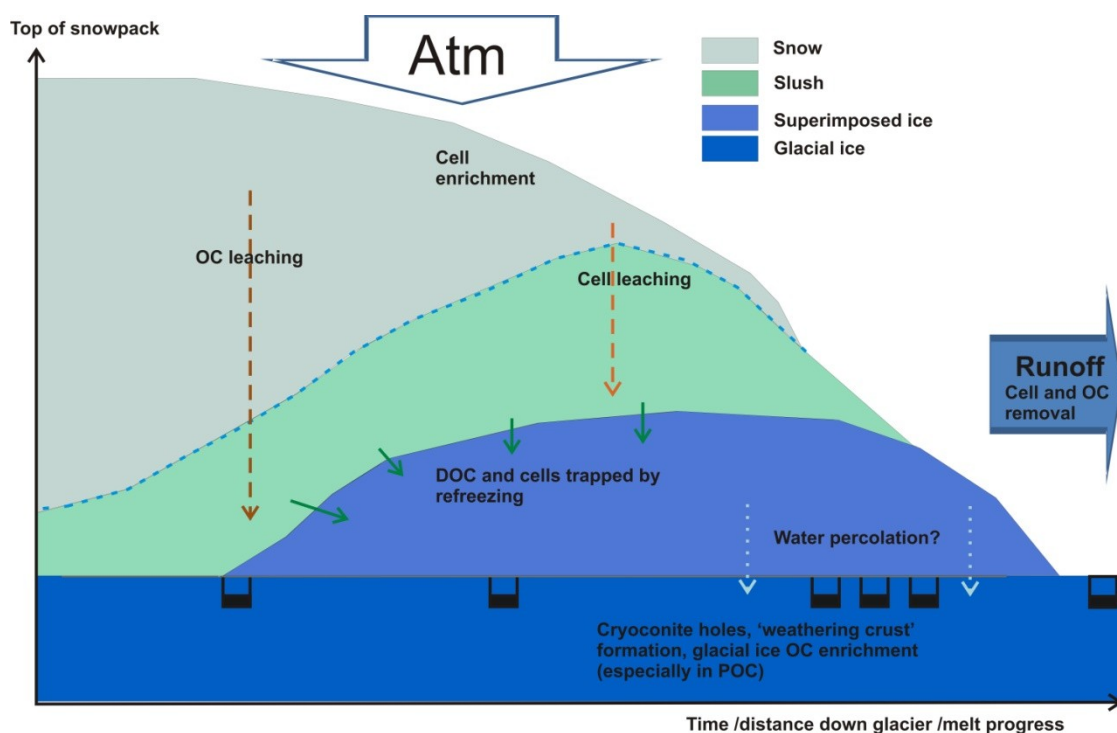


Fig. 5.10. Conceptual model for organic matter behaviour in snow, slush and superimposed ice zones on the glacier surface.

Cells distinguished from general organic matter pool. Abbreviations: OC – organic carbon, Atm – atmospheric deposition of cells and OC.

5.5. Conclusions

This chapter shows a conceptual understanding of temporal patterns in cell and organic carbon (OC) removal from glaciers, in particular by highlighting periods of thermal and hydrological importance, that influence the supraglacial biogeochemistry. These are:

1a. A period of rapid melt front penetration and basal refreezing, which is decisive for DOC removal from the snow profile and its subsequent storage in the refrozen layer.

1b. Further melting front propagation into snow, followed by snow profile inundation and the release of runoff, which drives cell removal from snowpack into superimposed ice, which is their dominant store on the glacier surface.

2. Isothermal snow and superimposed ice, a period of increased runoff and commencement of OC removal in streams.

3. Superimposed ice ablation, which releases the majority of DOC and cells stored in this layer. Its removal reveals glacial ice surface, which results in a strong outgoing flux of OC and cells, and causes a classic hysteresis behaviour especially in the case of cells runoff.

The second half of the melt season is therefore likely to witness an increased release of DOC, due to its short-term storage in superimposed ice. However, a positive storage change was found for both DOC and the other part of TOC, i.e. particulate organic carbon (POC), in the subcatchment. This could neither be attributed to water balance, which noted a negative storage change, nor to biological factors, whose quantitative contribution was most likely small. The majority of POC, despite its size limits encompassing cells, was behaving different from them and was partly mobile, at least in the snow profile. Hence, a zone enriched in high-molecular-size OC ($>0.7 \mu\text{m}$) was sought. It is proposed here that this POC is enriching cryoconite and surface glacial ice in the late melt season, however the exact mechanism of this enrichment needs further exploration.

Chapter 6. Discussion

6.1. Research aims revisited

The provenance, composition and fate of organic carbon (OC) on Arctic glaciers have been, to date, only fragmentarily explored. The question of glacial organic matter origin has been given a range answers, likely depending on the setting, its climate and topography. For example, the organic matter of the Greenland and Antarctic Ice Sheets (GrIS and AIS) has been reported as dominated by the products of local biological activity (Pautler et al., 2011; Stibal et al., 2010), however Stibal et al. (2010) point out the possibility for some microbial organic matter to be supplied by aeolian processes. On the other hand, Stibal et al. (2008) show in the example of Werenskiöld glacier in Svalbard, that vast deposits of organic matter in cryoconite found there could not be accumulated by the small biological production rates observed, and hence the OC in them is predominately allochthonous. To date, there has been no synthesis on the origin of this organic matter, neither have there been any that would show a global pattern in its abundance or composition.

The further fate of organic matter upon its deposition or production, i.e. its redistribution on glaciers and the final removal, after a certain time lag, have been addressed from different perspectives, e.g. in studies oriented on biolabile organic matter supply to downstream ecosystems (Bhatia et al., 2013; Hood et al., 2009; Lawson et al., 2014). Many studies also addressed the morphology of supraglacial ecosystems (Hodson et al., 2008), their spatial variability (Langford et al., 2014; Telling et al., 2012) and their role in the global carbon cycle (Anesio et al., 2009). However, no study has yet quantified organic carbon fluxes, even for a single glacier and time period, which would help enormously by indicating their relative importance. Furthermore, in order to understand the long-term or spatially distributed impact of OC fluxes, an understanding of dynamics across a spectrum of study sites is crucial. Hence, it became an objective of this study to picture a set of OC fluxes in two subsequent balance years, in conjunction with a thorough geographical understanding of the field site, by placing its mass balance changes within the context provided by a world-wide inventory of glacier changes. By understanding not only its OC cycle, but also the recent glaciological history of Foxfonna glacier, it is possible to present this work as a benchmark study. Furthermore, the OC flux observations on this glacier were integrated within hydrological zonation described by Müller (1962), which is a transferable framework for comparing glaciers at various stages of spatio-temporal evolution. The flux study was expanded here by comparing labile, dissolved OC (DOC), to cells and the total pool of organic matter (TOC) at a small scale. The difference

between TOC and DOC (in concentrations and fluxes) was interpreted as particulate organic carbon (POC).

6.2. The summary and interpretation of main findings

The results of this study underline the close correspondence between accelerating cryospheric change and the biogeochemical state of ice masses. They fit into the trend of recent discoveries of the ice masses' potential to sustain life and interact with their surroundings by exchanging nutrients and living cells (e.g. Anesio and Laybourn-Parry, 2012; Hodson et al., 2008; Hood et al., 2009; Irvine-Fynn et al., 2012; Singer et al., 2012). In particular, they add to the understanding of feedback mechanisms that link melt processes and the organic matter distribution to the fluxes that export this organic matter to downstream environments. The main findings of the thesis are summarised and discussed below.

Foxfonna is a High Arctic glacier that may be described as a non-steady-state, rapidly decaying ice mass. It consists of an ice cap and a tongue, and both its parts witnessed net mass loss in the period 1990–2009, as well as each year in the period 2010–2012. Hence, the contemporary accumulation area of the glacier is very small, mostly located on the north-facing part of the ice cap and the slope below it on the tongue. In the study catchment, the accumulation zone consisted <10% of its surface area, while steady-state glaciers have accumulation areas consisting 50–80% of their overall spatial extent (Benn and Evans, 2010). Hence, this study can be interpreted as a testimony of the biogeochemical processes of a glacier in 'poor health', i.e. rapidly losing mass. This is likely to be the fate of many small glaciers within the next century, if the current predictions for future glacier mass balance hold (Meier et al., 2007; Radić and Hock, 2011; Raper and Braithwaite, 2006; see Section 2.2.1). The net glacier mass balance in the period 1990–2009 amounted to $-0.53 \text{ m w.e. a}^{-1}$, and the glacier tongue was characterised by a mean value of $-0.62 \text{ m w.e. a}^{-1}$. The catchment subject to the OC fluxes investigation conducted in Chapter 4 (Fig. 4.1.) was characterised by net mass balance of -0.89 m w.e. in 2011 and -0.42 m w.e. in 2012. These values fit well with the record of negative net mass balances measured on Svalbard glaciers since 1960s and 1970s, in several areas of the archipelago (Hagen et al., 2003; Jania and Hagen, 1996). They also exceed the mass losses experienced across the archipelago in the years 2003–2008 of $-0.12 \pm 0.04 \text{ m w.e. a}^{-1}$ (in a more spatially representative study by Moholdt et al., 2010), and represented values correspondent to those noted in the north-west of Svalbard, where glaciers were losing mass the most rapidly in that period at $-0.54 \pm 0.10 \text{ m w.e. a}^{-1}$ (Moholdt et al., 2010b).

The thermal structure of the glacier is predominantly cold (below pressure melting point), as can be seen on radar profiles. This not only limits significantly the possibility of liquid water

to occur at glacier bed, but also promotes very slow ice movement. The horizontal surface velocities of ice on Foxfonna glacier ranged from below measurement error to 2.79 m a^{-1} , which is at the low end of the spectrum of published velocity estimates in Svalbard archipelago (Etzelmüller et al., 1993; Nuttall et al., 1997). There are limited areas at the glacier bed where liquid water may occur, either as a result of supraglacial meltwater penetration, or, in a very limited area under Foxfonna's thickness maximum, perhaps also by the occurrence of ice at pressure melting point (Fig. 3.22). Hence, the role of the processes occurring at the glacier bed is very limited in Foxfonna's OC cycle and decoupled from the meltwaters exporting organic matter downstream (as is also the role of englacial processes). Therefore, the glacier surface became the main focus of the OC flux study.

A range of processes were identified as likely contributors to the supraglacial OC cycle of Foxfonna. Due to the consistently negative mass balance of the glacier and its small accumulation area, the release of OC from glacier ice was identified as one of the key processes in the cycle. Supraglacial drainage was seen to be predominate on the glacier; parts of the stream were enclosed in cut-and-closure type channels, possibly reaching the glacier bed on a very limited proportion of their path, and relatively close to the glacier snout. This was likely to result in mechanical enrichment of the suspended sediment, but left little time for chemical reactions on the water – sediment interface. As a result, the streams sampled at the glacier snout would represent net OC sinks in the supraglacial cycle, provided the fluxes related to suspended sediment are excluded. A wind-redistributed snow cover was observed in the accumulation season: this was identified as a likely reservoir of both aeolian and cloud-derived organic matter brought onto the glacier during the accumulation season. These sources supplied organic matter throughout the year. Therefore, a technique for their sampling in the summer was found – that is, using modified dust samplers which collected also precipitation water (cf. Irvine-Fynn et al., 2012). Finally, the glacier surface had been observed to host microbial communities in cryoconite debris (A. Hodson, personal communication; Cameron et al., 2012), and so the biological activity connected to this environment was also placed within the OC cycle scheme.

The physical processes were found to dominate in the overall picture of OC fluxes on Foxfonna, with ice melt, runoff and atmospheric supply ranging from 0.4 to $0.7 \text{ Mg TOC a}^{-1}$, of which $0.2 - 0.4 \text{ Mg a}^{-1}$ was DOC. The flux connected to the biological activity of cryoconite was an order of magnitude smaller. Hence, the role of the biological activity in shaping supraglacial organic matter storage is qualitative rather than quantitative on Foxfonna and similar glaciers. This can be expressed by the microorganisms binding the mineral and organic particles into aggregates, especially through producing extracellular polymeric substances (EPS; Hodson et al., 2010; Langford et al., 2010). Also, they can be changing light-absorbing properties of

organic carbon by transforming plant litter into humic substances, and hence changing the albedo of cryoconite deposits (Takeuchi, 2002a). However, quantitatively, the majority of the organic matter added each year to the surface OC storage on Foxfonna and similar glaciers comes from allochthonous sources, and as such are not produced by local biological activity.

A strong coupling was observed between the glacial mass balance and the TOC fluxes connected to runoff and ice melt (Table 4.3.), which changed significantly between years in the direction observed for net glacier mass losses. Thus, it is proposed here that glacier mass balance drives the supply and release of OC on glacier surfaces, at least in short time scales of interannual variability. Since the storage change was consistent between the two years of majorly different mass balance characteristics and weather conditions, it is likely to be independent of short term changes, but perhaps more dependent on the longer-term properties of the glacier surface, e.g. surface roughness providing storage spaces for cryoconite debris. The glacier surfaces have been recognised to develop a pattern of surface roughness, called the *weathering crust* (Müller and Keeler, 1969), the occurrence of which is partly dependent on the abundance of cryoconite debris (Irvine-Fynn et al., 2011, and citations therein). This *weathering crust* forms a shallow aquifer near the glacier surface and therefore may contribute to the redistribution of organic matter in the uppermost layers of the ice profile, and also act as local storage media. Its role does need further exploration; nevertheless it was shown here that the surface layer of approximately 20 cm of ice is enriched in both TOC and DOC (Section 4.3.3.). This layer has also been observed to turn into temperate ice by the end of summer season (Fig 5.3.).

The OC fluxes on Foxfonna were described both in respect to their magnitude (Fig. 6.1.) and variability. For example, the atmospheric input of OC to glacier surface has shown major temporal (between seasons and years) and spatial differences. The DOC:TOC ratio was also variable between seasons (amounting to 0.44 in accumulation season and 0.81 in ablation season, averaged across both budget years). In total, the atmospheric flux amounted to $0.633 \pm 0.245 \text{ Mg TOC a}^{-1}$ (of which $0.396 \pm 0.217 \text{ Mg a}^{-1}$ was DOC), and exceeded the supply to the glacier surface from underlying ice melt of $0.448 \pm 0.152 \text{ Mg TOC a}^{-1}$ ($0.237 \pm 0.103 \text{ Mg DOC a}^{-1}$). In 2012, 55% of the TOC from glacial ice melt originated from the uppermost 20 cm of the ice profile. The elevated concentration of OC in the top part of glacial ice, together with the budget outcome of net storage increase in both balance years, support the interpretation that this ice layer, as well as the surface, is a reservoir for organic carbon. Following on from that interpretation, an additional supraglacial storage of $0.21 \pm 0.13 \text{ Mg TOC}$ and $0.11 \pm 0.07 \text{ Mg DOC}$ was found in the end of 2011 ablation season. Furthermore, part of this TOC pool might have been 'recycled' in 2012, i.e. it may have remained in the near-surface layer instead of being liberated into supraglacial runoff.

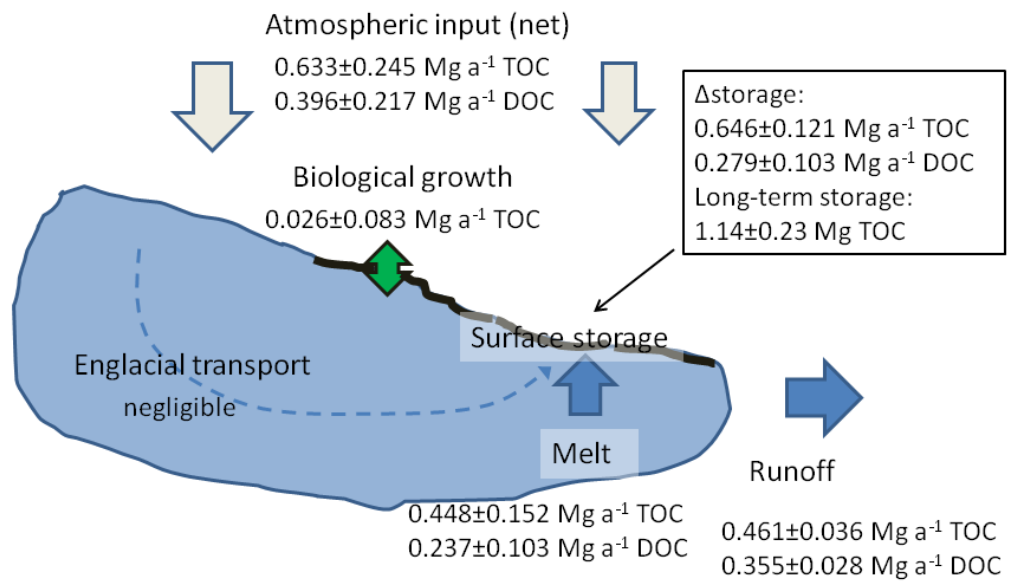


Fig. 6.1. The summary of OC fluxes on Foxfonna glacier, averaged across the balance years 2011 and 2012.

The annual OC flux in runoff was estimated for an average of $0.461 \pm 0.036 \text{ Mg TOC a}^{-1}$ (of which $0.355 \pm 0.028 \text{ Mg a}^{-1}$ was DOC). The OC concentrations in runoff were at the lower end of the published spectrum of proglacial waters concentrations (Bhatia et al., 2013; Downes et al., 1986; Hood et al., 2009; Lafrenière and Sharp, 2011), alongside the runoff from GrIS dominated by supraglacial meltwater. This may indicate that the majority of bioavailable organic matter, measured in proglacial rivers (e.g. in Hood et al's 2009 study) might be of subglacial or proglacial origin. In the forefield of Foxfonna, a major increase in sediment-bound TOC was found in a short stretch of proglacial river, which confirms the notion that glacial forefields play an important role in producing riverine OC fluxes.

Budgeting the fluxes produced similar outcomes in both years, resulting in an average net storage increase of $0.646 \pm 0.121 \text{ Mg TOC a}^{-1}$ and $0.279 \pm 0.103 \text{ Mg DOC a}^{-1}$. At the same time, the glacier-wide supraglacial storage in cryoconite was estimated for $1.142 \pm 0.231 \text{ Mg TOC}$ at the end of 2011. Assuming the main source of this cryoconite matter is POC estimated from the quantified fluxes, the average residence time of cryoconite granules on the glacier surface of Foxfonna would be c. 3 years, a value not unexpected if compared to the sparse data on cryoconite age from elsewhere (Hodson et al., 2010b; Stibal et al., 2008a; Takeuchi et al., 2010).

As a result of the flux study, superimposed ice was identified as a significant temporary OC store (with an average of 0.107 ± 0.039 Mg TOC captured at its maximum extent), especially in the dissolved form (0.086 ± 0.034 Mg of the TOC mentioned above was DOC). The formation of this layer was studied in respect to the thermal and hydrological development of the glacier surface in the early ablation season. In doing so, the thermal and hydrological processes were shown to define four distinct periods of the glacier surface development, which had an impact on the fate of OC and cells on the glacier surface. These periods were: 1a) intensive melting front propagation into the snowpack, associated with superimposed ice formation, and trapping of the DOC leached from snowpack into this refrozen layer; 1b) slower melting front propagation, which was assisted by further basal refreezing and gradual saturation of snowpack with liquid water, up to a point of inundation which rapidly decreased cell concentration in the uppermost layer of snowpack; 2) isothermal near-surface profile, when the drainage intensifies (having commenced during the former stage) and the remainder of snowpack is removed, which is assisted by relatively slow removal of all organic matter types; finally, 3) superimposed ice ablation, which results in glacier surface exposure and an increase in DOC and cell runoff, causing a hysteresis behaviour especially in the case of the latter component. The increase in the DOC flux may even be responsible for the regime shift observed in its removal at the glacier snout (Section 4.4.2).

In this study, the OC and cell content of a wide suite of different media on the surface of the same glacier was characterised for the first time. To look at it chronologically, in pre-melt snow, each 10 cm layer was found to contain between 24 and 66 mg m^{-2} of TOC ($\pm 13\%$), $4\text{--}30 \text{ mg m}^{-2}$ DOC ($\pm 13\%$) and $59\text{--}732 \times 10^6 \text{ cells m}^{-2}$ ($\pm 11\%$). As a result of meltwater percolation, wet snowpack was quickly deprived of OC, while the cells concentrated in a layer close to its surface at concentrations exceeding $4700 \times 10^6 \text{ cells m}^{-2}$. The water-saturated snow, known also as slush, has been much less abundant in cells than the prior stage of snowpack development, reaching $366 \times 10^6 \text{ cells m}^{-2}$ in its uppermost layer, and hence still exceeding the initial average concentration in the full snowpack column. Whether the maximum concentration in the uppermost layers of wet snowpack occurred as a result of cell reproduction, atmospheric input or horizontal displacement and local concentration, is beyond evaluation in light of the collected data. However, the preferential concentration of cells in the upper part of the profile is visible throughout the measurement period and complies with the observations of Grinde (1983) on the algal cells' behaviour in snowpack which may be interpreted as phototaxis despite the algae using an external process (affinity to water-surfaces of snow grains) rather than flagella for transport in snowpack. This location certainly provides good condition for algal growth, in contrast to the buried superimposed ice. This refrozen layer has been shown to trap cells and DOC at respective concentrations of

916×10^6 cells m^{-2} and 41 mg DOC m^{-2} in an averaged 10 cm layer, while the respective TOC content was 53 mg m^{-2} . The high cell content in superimposed ice poses questions about the ability of algae to photosynthesise in this environment, which has only recently been explored on Mittivakkat glacier (Lutz et al., 2014) and will hopefully be given more attention in the future. The runoff showed highly variable cell concentrations, and less diverse OC content, at the respective levels of $3.9-70.4 \times 10^6$ cells L^{-1} and 0.175-0.354 TOC (of which 0.105-0.258 DOC) mg L^{-1} , it was especially rich in cells when glacial ice was revealed from underneath the superimposed ice layer.

If the OC and cell fluxes, as related to physical processes on the glacier surface, are calculated for a small catchment at the time of maximum superimposed ice extent, the following picture emerges. DOC, TOC and cells were differently partitioned between fluxes. In the case of TOC and DOC, the atmospheric deposition in snow was the largest flux noted, at 280 ± 49 and 156 ± 28 mg m^{-2} , respectively. Most of this TOC was transferred into the supraglacial stream (128 ± 32 mg m^{-2}) or the inferred storage outside superimposed ice (134 ± 33 mg m^{-2}). DOC, on the other hand, was mostly captured by superimposed ice (83 ± 9 mg m^{-2}) and removed in runoff (77 ± 19 mg m^{-2}). For cells, the ablation season deposition was more important than the initial supply in the snowpack, the two amounting to 2690 ± 866 and $927 \pm 156 \times 10^6$ cells m^{-2} , respectively. The main outputs for cells was temporary storage in refrozen ice ($2650 \pm 270 \times 10^6$ cells m^{-2}) and removal in runoff ($2400 \pm 590 \times 10^6$ cells m^{-2}), similarly to DOC. Unlike for TOC and DOC, the biological component could have been moderately important in their distribution, particularly for their enrichment in the upper layer of snowpack. Hence, the negative storage change resulting from the cell budget may also be identified as evidence of a missing input in the flux study (perhaps cell reproduction), but more likely it was associated with the negative storage change found in the water budget of this small catchment. Finally, upon budgeting all the quantified TOC and DOC fluxes, an apparent storage of both OC types resulted. This storage was relatively enriched in POC (since the excess of TOC over DOC storage amounted to 93 ± 26 mg m^{-2}). The plausible locations for the POC-enrichment were therefore sought, with the likely candidates being the firn zone (perhaps on ice surfaces resulting from internal refreezing) and cryoconite deposits.

The above considerations show DOC to be the most mobile of the three OC types examined, corresponding to Type 1 enrichment in the meltwater elution study by Meyer and Wania (2011). The cells, on the other hand, behaved closer to the modelled Type 3 enrichment (Meyer and Wania, 2011), corresponding to snow-grain associated chemicals. This pattern was, however, slightly modified by the existence of further cell elution beyond the moment of their maximum leaching when the snow profile was completely inundated by meltwater and became slush. The elution sequence for POC was more difficult to establish, due to the

contradiction between the observed removal of this component from the initial snowpack before cells, and its greatest retention of all organic matter types in the budgets calculations of both Chapters 4 and 5. Also, the POC was relatively less abundant in refrozen layers than the other two organic matter types. Hence, it is proposed here that the POC in the snow is relatively mobile, in a manner resembling high-molecular-weight acids found in soils, and forming colloidal dispersions in meltwater (cf. McSween et al., 2003). However, there is as yet unclear mechanism preventing POC from being incorporated into superimposed ice efficiently. Instead, POC may have concentrated on the ice surface, and ultimately enrich cryoconite deposits and the surface layer of glacial ice. However, a further study into the behaviour of POC upon water percolation through snowpack is needed to establish an unequivocal conclusion. On the other hand, the behaviour of the two other organic matter species is rather non-controversial. The elution of cells observed here is coherent with the observations of Björkman et al. (2014), who showed them to be removed from snowpack with far greater delay than mono and bivalent inorganic ions. Also, despite refreezing effects not being directly studied in their research design, the distribution of cells in the initial snowpack used for Björkman et al's (2014) experiment showed elevated cell concentrations in the vicinity of ice lenses and denser snow layers in the profile.

Björkman et al. (2014) claim that summer atmospheric deposition is an unlikely source of cells during their experiment, which is a major difference to what was found on Foxfonna. However, they were referring largely to the efficacy of dry deposition, whilst other researchers have commented upon large atmospheric inputs via wet and dry deposition combined (e.g. Irvine-Fynn et al. 2012). Therefore, the rates of summer deposition of organic matter reported here are plausible when the precipitation events that were observed during the study are considered.

6.3. Conceptual understanding of organic carbon fluxes and storage in the context of a glacier's development

The overarching research outcome in this work is the classification of the various OC storage mechanisms on glaciers, which determine the spatial location of certain organic matter types, as well as the timing of their release. Figure 6.2. shows a conceptual model of these biogeochemical zones of a glacier. They are shown on a glacier cross-section at the end of the ablation season, however a space for time substitution of these zones allows this to be proposed for any point during the melt season. The biogeochemical zones distinguished here may correspond to the ecological zones described on Mittivakkat glacier by Lutz et al. (2014). Due to cell enrichment in upper snow layers, the percolation zone may have formed *green snow* and *red snow* zones on Mittivakkat. Furthermore, *clean snow* in their study is likely to

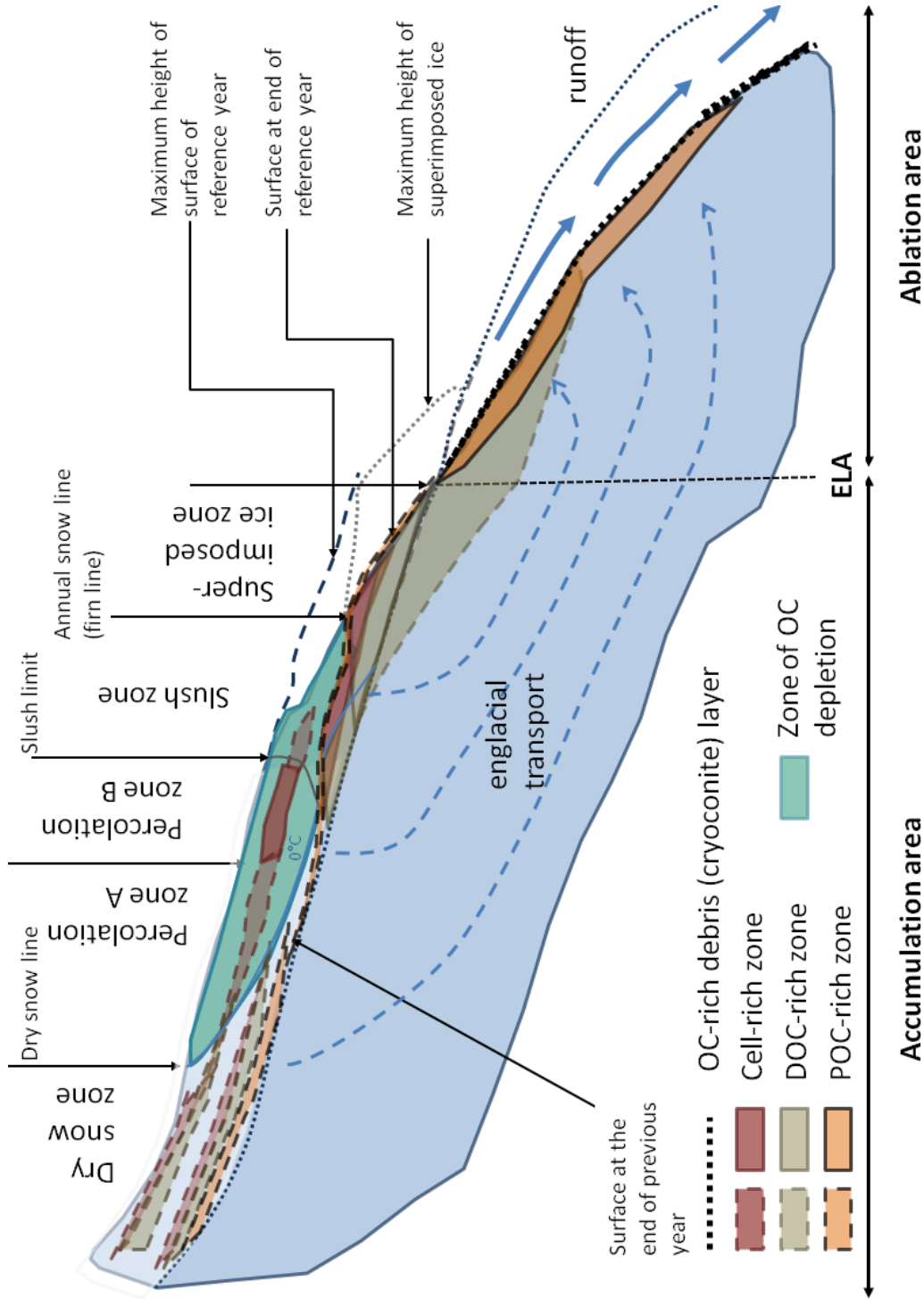
correspond to the dry snow zone of Müller's (1962), where cells and OC are confined to layers inherited from the biogeochemical history of precipitation. Biofilm is most likely to form in the slush stage, while it is possible that the cell-enriched superimposed ice forms the grey ice zone.

Since the OC store contained in living cells on Foxfonna was relatively small compared to the overall OC content on the glacier surface (see Section 5.4.3.) and the biological production flux was also estimated to be an order of magnitude smaller than the hydrologically determined fluxes (Section 4.3.5., Table 4.3.), the importance of physical processes is emphasised. Among these, refreezing emerges as a particularly important process for DOC storage, although POC storage within the surface layer of the ablating glacier ice also becomes important later on. Both may be supplied by the initial snowpack, since the elution study has shown POC to be retained in the catchment for a surprisingly long time. Another source of POC on the surface of glacier ice is the incorporation of particles melting out from the underlying ice layers, and becoming incorporated into cryoconite debris, the biggest store present in the near-surface environment of the glacier. An interaction with the shallow aquifer in a *weathering crust* (Irvine-Fynn et al., 2011) may promote further enrichment. Since the debris cover obtains significant inputs from melting glacier ice, the state of cryoconite cover on a glacier might be tightly coupled to the mass balance state of the glacier. This concept will be further explored below with reference to other published data.

If the debris cover on Foxfonna is the result of multi-annual supply and retention of OC, then it should represent a different situation to glaciers with positive mass balance which are thus undergoing mass increase. Published estimates of debris coverage are, however, very limited, and so a comparison of the debris cover through time and space is not possible at the time of writing. However, on Midtre Lovén glacier it is possible to estimate the magnitude of the supraglacial storage of OC in cryoconite, by combining data on debris loading (in g cm^{-2}) from Hodson et al. (2007) with estimates in Telling et al (2012) of the organic content (in $\mu\text{g g}^{-1}$). The estimated storage amounts to $0.213 \text{ Mg TOC km}^{-2}$, which is approximately 4.6 times less than on Foxfonna ($0.986 \text{ Mg TOC km}^{-2}$). Midtre Lovénbreen has an accumulation area ratio (AAR; the ratio between the glacier's accumulation area and its overall surface area) of approximately 0.3 (Irvine-Fynn et al., 2014), while Foxfonna's AAR is below 0.10. These accumulation area ratios are long-term averages derived from glacial mass balance trends. Hence, this comparison corroborates the postulated interdependence between intensive glacier melt and increasing supraglacial TOC loads. However, more studies are certainly needed to draw meaningful conclusions about other glaciers and the prolonged effects of negative mass balance upon OC storage in near-surface glacier ice. Such studies also need to account for the spatial variability in debris coverage and its OC content.

Fig. 6.2. Conceptual diagram of glacial biogeochemical zones, in respect to the nature of organic matter contained within them.

The picture shows a glacier cross-section, with an exaggerated area covered by supraglacial hydrological zones sensu Müller (1962). Since the cell behaviour in the ablation zone was not investigated in this work, there is no information on them contained in the diagram. ELA may be substituted for transient superimposed ice limit to show glacier surface state at any point in the ablation season.



Another argument for a sustained increase in the surface and near-surface storage of OC on Foxfonna and other rapidly melting glaciers like it is the high TOC load in its lowermost elevation band (Fig. 4.8.), which is also the area that showed the highest ice mass loss in the period 1990–2009 (Fig. 3.16a). The phenomenon of increasing debris concentration on the lower elevation bands of glaciers, perhaps as a result of enhanced melt, has been noted in literature before. For example, Hock and Holmgren (2005) took this effect into account when modelling spatial distribution of albedo on Storglaciären, by reducing the albedo by 0.03 per 100 m elevation decrease. In extreme cases, it may lead to emergence of debris-covered glaciers (Benn and Lehmkuhl, 2000; Bolch et al., 2007; Paul et al., 2004). However, there might be different reasons for the greater debris cover on the frontal part of the glacier surface, e.g. entrainment of bed sediments as a result of thrusting (Bennett et al., 1996; Hambrey et al., 1997) or supraglacial sediment concentration in crevasses (Goodsell et al., 2005). Still, there is at least one published example of documented feedback between glacial ice darkening and enhanced melt, where in a season of intensive melt the ice albedo was depressed to 0.15, a value typical for debris-rich ice, and this change was noted further up on the glacier than its snout area (Paul et al., 2005).

The chemical composition of the debris may play an important role in its influence on the glacier melt, since particular types of organic chemicals have strong light-absorbing properties, which is especially the case for soot and humic substances. Therefore, the composition of these deposits requires a detailed study, so that their concentration trends may be established. Here, by building upon the understanding emerging from the research into OC fluxes, assumptions about the likely composition of this debris can be made. The results from Foxfonna show that the OC in supraglacial debris is mostly derived from allochthonous organic matter. The supraglacial waters transport this organic matter downslope, but their efficiency in particle removal is limited, contributing to the c. 3 years average residence time of the supraglacial OC. Hence, the cryoconite aggregates in the lower reaches of the glacier are likely to have been on its surface for a longer period. This, in turn, would have led to their more mature biogeochemical structure, perhaps of the kind seen in proto-soils, as opposed to the deposits in the upper part of the glacier which are more likely to contain freshly deposited, less decomposed organics. An even stronger contrast between these locations would be seen on glaciers with large ablation zones, where the distance covered by supraglacial transport needs to be longer. Hence, a development of humic-rich cryoconite would be more likely: 1) towards glacier snouts, 2) on glaciers with thickening organic carbon cover, i.e. those losing mass rapidly, with smaller AARs. The results of Langford et al. (2010), who describe the development of cryoconite aggregates from 'marine-snow-like' structures to those more akin to soil aggregates later on, support the connection between cryoconite residence time and structure

inferred above. Since the more humic cryoconite would promote lower albedos, the organic carbon cycle on glaciers may thereby exert an influence on glacier melt, and that would happen by shaping the distribution of different organic matter types. Nevertheless, the links outlined above are an emerging concept and need thorough examination.

Furthermore, the connection between the glacier AAR and its OC biogeochemistry can carry wider implications: Foxfonna's example provides a reference point at the low extreme of the AAR spectrum, showing a biogeochemical state of a glacier close to its terminal phase of development. The rapid melt of glacial ice causes a strong incoming flux of OC towards the glacier surface, which cannot be balanced by the burial of OC in the accumulation zone. However, on a glacier that is in steady-state a higher proportion of the atmospheric supply of OC would be stored and the melting superimposed ice layer would maintain a steady supply of dissolved organic carbon throughout the summer, providing organic substrate for the supraglacial ecosystem. If that indeed is the case, then the biogeochemical composition and structure of cryoconite would be linked to the glacier's mass balance. There is little published data to prove or disprove this concept, yet in Langford et al.'s (2010) work, the organic content of various cryoconite deposits seemed to correspond to the glacial mass balance state in a group of three Svalbard glaciers. The maximum organic content was found in cryoconite from Vestfonna at 6.07%, which is an ice cap with a positive mass balance of $+0.05 \pm 0.17 \text{ m a}^{-1}$ (1990–2005; Nuth et al., 2010). Smaller organic contents were noted on the aforementioned Midtre Lovénbreen at 3.76%, with mass balance of $-0.35 \text{ m w.e. a}^{-1}$ (1967-1993; Jania and Hagen, 1996) or $-0.30 \text{ m w.e. a}^{-1}$ (1971-1999, Hagen et al., 2003). Finally, Longyearbreen showed 2.76% OC in cryoconite, while being characterised the most negative mass balance of $-0.55 \text{ m w.e. a}^{-1}$ (1993-1999; Hagen et al., 2003). Foxfonna, with its mass balance in the catchment area of $-0.66 \text{ m w.e. a}^{-1}$ (average between 2011 and 2012; in the periods 1990–2009 and 2006–2009 this area noted net mass balances of -0.34 and $-0.50 \text{ m w.e. a}^{-1}$, respectively), ranks at the lowest end of the OC content spectrum presented here with a mean OC concentration of 2.03%. The data are, admittedly, too sparse to prove any pattern but these limited values speak of a decreasing gradient in OC content of cryoconite on Svalbard glaciers with their decrease in AAR, which is a concept worth investigation in the future.

A similar dependence may occur in transects along the ablation zones of large glaciers and ice sheets, due to the respective proximity of sources of DOC and cells in the accumulation zone and POC and mineral debris increasing with melt in the ablation zone. The pattern of decreasing OC concentration in cryoconite debris closer and closer to the ice margin was observed on the GrIS by Stibal et al. (2010) and interpreted as a result of balance between aeolian inputs, wash-away by runoff, and biological activity. Here, it is proposed that the

intensity of surface melt is an important factor in shaping the organic content of cryoconite debris, and it should be included in future studies of ablation zones.

In brief, it is proposed here that both OC fluxes and the cryoconite debris undergo evolution on glacier surfaces in conjunction with changes in the glacier mass balance state. The end-member of a dwindling glacier with a very small AAR may be represented by Foxfonna. It is a glacier with relatively low organic content of cryoconite particles, dense cryoconite debris cover, and likely a high humic substance proportion in the OC content of the debris, which is expressed by its dark hue. The other end of the spectrum will be glaciers and ice caps with high AARs, less abundant marine-snow-like cryoconite aggregates with lower humic substance proportion, less mineral material and a greater proportion of DOC and cells. These two organic matter types seem to be removed from the glacier rapidly upon the commencement of glacier ice melt, following a period of temporary retention in refrozen layers. Hence, it is proposed here that there is a direct relationship between the physical condition of a glacier and its surface OC abundance and composition.

6.4. Unexpected findings

In the context of the impact of supraglacial ecosystems on the global carbon cycle reported by Anesio et al. (2009), the finding here that biological activity in cryoconite was negligible compared to other OC fluxes is puzzling. However, the global NEP of 64 Gg C estimated by those authors is based on values from a total of 5 glaciers, and each of the values used is subject to high uncertainty due to internal variability of datasets. Therefore, it is difficult to incorporate observations from other parts of the world. Nevertheless, Hood et al. (2009) estimate the DOC runoff flux from glaciers draining into the Gulf of Alaska at 130 Gg DOC a⁻¹, which is double the global estimate for the carbon flux fixed by photosynthesis according to Anesio et al. (2009). Furthermore, the OC flux magnitude is likely to be subject to regional variability, thus studies on organic matter cycling on glaciers and ice sheets should continue until a wide coverage of data points is achieved. The unimportance of the biological OC flux was, for example, described on the Werenskiöld glacier in Svalbard (Stibal et al., 2008a), which is closer to Foxfonna in terms of glacial mass balance, location and glacier structure than any of the ice sheets or even valley glaciers in the European Alps.

Another unexpected result was the relative mobility of POC, the substantial majority of which has been observed to elute from snowpack before cells and in doing so exhibited entirely different behavior to the hydrophobic carbonaceous particles described by Doherty et al. (2010, 2013). Also, the POC in the Foxfonna snowpack, superimposed ice and streams was found to have a very different distribution pattern to cells, despite the overlapping size limits for those organic matter fractions. Furthermore, the estimated contribution of cell carbon to

overall POC mass was negligible (Section 5.4.3). However, the spectrum of potential organic matter types that may be removed by a 0.7 μm pore size filter is rather wide and encompasses starches (Hoover, 2001) and aquatic humic substances, which arrange into μm -sized groups (Plaschke et al., 1999). Humic substances are particularly known to exhibit greater mobility in aqueous environments, especially in waters of low ionic strength (McSween et al., 2003). Furthermore, humic-like substances have also been found in relative abundance in Arctic snow (Voisin et al., 2009, 2012) and in glacier ice from the European Alps (Legrand et al., 2007). Thus, it is also a likely component of snowpack on Foxfonna, while cells have been estimated to contribute a negligible (quantitatively) amount of POC in the surveyed snow profiles.

6.5. Limitations of the current work

There are several limitations to this research, stemming from the adopted research design, methods used in the study, as well as the specifics of the collected datasets. For example, the study framework prevented the inclusion of subglacial or englacial processes into the flux calculations, however on some glaciers these may play an important role in organic carbon cycling. In particular the subglacial environment has been shown to host active microbial communities (e.g. Kaštovská et al., 2007; Lanoil et al., 2009; Skidmore et al., 2000) and interact biogeochemically with the runoff from glaciers and ice sheets that is confined to subglacial drainage networks (e.g. Anderson et al., 2003; Tranter et al., 1996). However, this environment needs very different methods of exploration to those applied in the supraglacial zone, and is a vast area of study in its own right. Furthermore, the elimination of basal melting that follows glacier thinning in the Arctic (Bælum and Benn, 2011; Dowdeswell et al., 1995) is likely to reduce the importance of subglacial processes in the organic carbon cycle of small and shrinking glaciers. Hence, the work conducted here is most relevant to small Arctic glaciers, while its application to ice sheets would require major uncertainties to be overcome.

Furthermore, a mixture of sampling and laboratory methods was applied here, which in some cases places constraints on data interpretation. Especially, all the geomorphological processes connecting the glacier to the rock slopes and moraines had to be excluded from further investigation due to the exclusion of sediment-bound organic carbon (except supraglacial debris cover and the additional runoff sampling in 2012, which revealed dependence on ice-marginal inputs). These fluxes are likely to be a major influence upon the fate of OC in the glacier forefield and at glacier beds (Section 4.3.2).

Another aspect of field sampling, which may impose limits on the interpretation of the results, is the natural variability and the inaccessibility of glacier surface sections causing high error estimations in the reported fluxes. However, such variability, especially in the atmospheric deposition, is inherent to the nature of this phenomenon, even more so if the

role of wind is added to the picture. Moreover, atmospheric precipitation gauging is problematic in Svalbard, as it suffers from 50% or more gauge under-catch, even in the measurements taken by the WMO stations (Førland and Hanssen-Bauer, 2000). In the current study a relatively dense grid of summer deposition collectors was set up, and hence the random errors in the independent measurements in them were likely to cancel out. This statement generally applies to all glacier-wide flux calculations here, since there was a higher probability of obtaining a correct flux estimate from the inherently variable processes being measured in multiple locations (Miller and Miller, 2005). Otherwise, single values for time points and locations should be treated with more caution than overall flux estimates.

Finally, there was also a chemical flux which was beyond the scope of the research conducted here namely the photooxidation of glacial organic matter. This problem, however, deserves full attention as a project in its own right, due to the likely spatial and temporal variability and the implications for the chemical composition of organic matter on glaciers. Moreover, this process is less likely to impact the overall organic carbon quantity on the glacier, since in many cases it decomposes organic chemicals to different molecules which would still be included in the total OC estimations. However, after a time lag it will lead to OC loss as it degrades to CO₂ (Grannas et al., 2007). Its effects were also further limited by the fact that net photolytic transformation of snowpack OC was already incorporated into the snow sampling strategy, since it was conducted just prior to the onset of melt. However, it cannot be discounted that a small proportion of the apparent storage resulting from the OC budgets calculated in Chapters 4 and 5 was actually depleted by the light-induced chemical degradation. Also, some of the organic matter initially deposited as POC might have been transferred into DOC phase due to photooxidation. Therefore, the small changes in glacial OC storage were not treated as important.

6.6. Implications for the fate of supraglacial ecosystems on Arctic glaciers

Hodson et al. (2008) proposed the impacts of climate change on Arctic supraglacial ecosystems in the future, which can be revised or refined on the grounds of this study, with focus on glaciers rather than ice sheets. The first impact proposed was increased snowpack productivity following increased melt. This research provides some arguments against this notion, as with increased melt the OC content of snowpack is likely to be removed faster, therefore removing the substrate for bacterial cells. However, if the OC fluxes related to cells are generally small compared to overall OC turnover on glaciers, as is inferred here, then they might sustain their productivity even after the majority of DOC has been eluted. Furthermore, autotrophic cells are highly likely to remain and proliferate in the upper part of the profile, and their retention on the glacier surface will depend on when the snow profile inundation

happens, which is the point when the snowpack depletes the majority of its cell content. Since inundation is favoured by level topography, this will have important spatial variability. The increased melt results in the transient snow line, slush and superimposed ice zones shifting upwards, and on a steady-state glacier topography is usually convex near the ELA. Hence, the initial change connected to ELA shift will lead to a wider area covered by these transient zones in the future melt seasons, and a wider area of DOC and cell storage. That may lead to a more diversified organic matter supply downstream, as the effects of OC and cell trapping in superimposed ice and the hysteresis in runoff are enhanced. In the long term, however, the role of temporary storage in refrozen layers might subside, if air temperatures increase significantly and limit the superimposed ice formation (Woodward et al., 1997), and the shift of the ELA proceeds towards steeper parts in the upper reaches of glaciers, where their area and storage capacity of DOC and cell-enriched zones will decrease.

The upward shift will also apply to end-of-summer snowlines, decreasing the relative importance of the snow ecosystem in favour of cryoconite ecosystem, and high melt could threaten the cryoconite 'niche stability', claim Hodson et al. (2008). An important insight from this study is the relative paucity of cells in saturated snowpacks and their immediate removal in runoff originating from superimposed ice, which means that the cell supply to these cryoconite ecosystems might be limited. A further, more marked period of cell removal was also observed at the point when the glacier ice surface became exposed, which shows that cryoconite was likely a source of cells to runoff. Further, the supraglacial catchment seems to be enriched in POC according to the fluxes shown in Section 5.4.3. Therefore, a shift towards a more and more allochthonous organic matter storage on glaciers might be observed.

The third impact listed by Hodson et al. (2008), which is the resuscitation of cells liberated from recently melted ice, is beyond evaluation in light of this study. If occurring, this would counteract the effects on cryoconite cell supply exerted by the efficient removal of cells from recently deposited snow and contribute to the proliferation of the cryoconite ecosystem on warmer glaciers. However, a strong outgoing cell flux in meltwater streams has been noted here, and hence the balance of the glacial ice input and runoff cell output needs establishing.

On a final note, the effect of warmer climate on the organic matter cycling in glaciers would most probably be a liberation of vast amounts of OC and cells stored in glacier ice. The superimposed ice layer would continue to act as a buffer and net storage medium for DOC and cells, as the cryoconite debris does for TOC (see Section 4.4.3). However, the release of cells is very rapid at the point of glacial surface ice exposure. In this study, a fourteenfold increase in cell concentration was found in stream water between days with similar discharge (as compared to a twofold increase for OC then) when the superimposed ice melting was superseded by glacial ice melting.

6.7. Recommendations for future research

The understanding of the glacial OC fluxes and the nature of the organic matter storage would benefit beyond the conclusions drawn here if further research were conducted. Since physical processes were shown to be a powerful factor in shaping the organic carbon cycle on Foxfonna, the further connection between geomorphology and organic matter storage and release would be an important subject of a future study. Several processes were not addressed here, either due to their relatively small extent on Foxfonna, or their rapid and irregular nature preventing representative sampling. These are:

- the interaction between rock slopes or moraines and the glacier surface, in particular through avalanching and landsliding,
- the occurrence of avalanches on the glacier surface, including slush avalanches (known also as slush flows),
- the interaction of the glacier bed with its surface, by means of thrusting or other debris entrainment processes, water drainage penetrating to bed and water emerging on the glacier surface from pressurised subglacial channels,
 - the transfer of sediment into crevasses, moulins and englacial channels,
 - the erosion of the supraglacial debris layer by extreme flows, including it being unsettled by rain splash.

In particular, the last factor requires more research due to its possible counter effect upon supraglacial storage according to the results of the current study. The impact of rain events is particularly interesting also due to the likely high OC supply in extreme rain events, as has been inferred from the high summer atmospheric OC deposition in 2011 (the majority of which was DOC), as well as its capacity to wash the glacier surface and thus export the older OC stored in cryoconite. Furthermore, there is a need for more data from other glaciers to help prove or disprove the hypothesis postulated about the connections between the biogeochemical composition of supraglacial sediment and glacier mass balance.

A further recommendation for future research is the chemical flux, that may contribute to part of the OC storage found in this study to be actually depleted before the end of the light season. This flux would be the degradation of organic matter due to photooxidation, which has been studied to a very limited extent to date. By comparison to the published estimate from high latitude snowpack by Voisin et al. (2012), it was pointed out here as a potentially important quantitatively flux of OC in glacial environment. However, this cited estimate was based on the physical characteristics of the collected snowpack. The actual *in situ* measurements, including chemical analysis of the volatile OC emitted, still need to be conducted. Furthermore, the role of photodegradation transformation may also be important

qualitatively, particularly by counteracting the production of high mass organic molecules, and hence counteracting the snow and ice surface darkening caused by the deposition of atmospheric HULIS or brown carbon and the *in situ* development of humic substance. Since photodegradation leads to the production of relatively volatile, low mass compounds, it may contribute to the biolabile organic matter flux found by Hood et al. (2009). Also, perhaps it may counteract the future release of harmful organic compounds by their decomposition, however it may also produce poisonous organic compounds, especially formaldehyde.

Finally, the chemical speciation of the glacial OC fluxes needs more research efforts. The concentration of both harmful substances and bioavailable OC types on the glacier surface could be established with more detail then. This would especially help the prediction of future release of persistent organic pollutants, the distribution of which in the glacial system still needs constraining. Therefore, the main recommendations for future research resulting from this study are the further exploration of the connection between glacial geomorphology and OC fluxes, the examination of the impact of photolytic processes and the establishment of the chemical partitioning of OC found in glacial environments.

6.8. Major conclusions

As a result of the current study, a close connection between physical processes and OC fluxes can be drawn, and their impact on the glacier surfaces can be further characterised. The biological processes happening in the supraglacial debris were an order of magnitude less important than the fluxes connected to melt, runoff of atmospheric deposition. While the role of biota may still be important to the quality of organic matter, the vast amount of organic-rich debris on Foxfonna is best interpreted as a result of intensive melt and the imbalance of OC fluxes resulting in surface storage of this chemical species. Several types of supraglacial OC storage were identified, in particular in the superimposed ice enriched in DOC and in cryoconite debris, the largest store found, whose size would require c. 3 years of the experienced OC budget sums to persist, while no removal processes were counteracting except the regular runoff measured here. Moreover, the uppermost layer of glacier ice has been identified to contain elevated concentrations of both DOC and TOC. Cells were behaving differently to TOC and DOC, since at first they became concentrated in the upper layers of snowpack, then removed into superimposed ice upon snow profile inundation with liquid water, and finally experienced rapid removal in runoff once the glacial ice surface became exposed. Still, their location on the glacier could also be linked to particular hydrological zones on the glacier surface. Therefore, the major conclusion of this study is the direct linkage between glacial hydrology, mass balance and the supraglacial organic carbon storage. This link

is likely to influence the biogeochemical development of the surfaces of glaciers as they decrease their thickness and AARs.

Chapter 7. Conclusions

7.1. Organic matter on glaciers in the context of global change

Recently, a major change has been experienced by the global cryosphere, and further impacts on these ice masses are predicted (Hanna et al., 2013; Jacob et al., 2012; Radić and Hock, 2011). Besides being vast freshwater reservoirs, glaciers host live and dormant microbes, and contain a multitude of organic substances as a result of the atmospheric deposition history and post-depositional processes. Just like a living organism in good health, a steady-state glacier maintains homeostasis as its exchanges with the outside environment are balanced. However, the current cryosphere experiences a major forcing, which unsettles this dynamic balance, and affects glaciers on many levels, including their biogeochemical state.

The variety of organic substances and their roles in the environment, even a relatively simple glacial one, complicates the task of recognising the directions of change in the carbon cycle. This is probably the reason why the understanding of glacial carbon cycling is still fragmented. The research on glacial organic matter furthers the understanding of both extremophilic organisms and chemical tracers of events occurring prior to the human history. These are all connected to glacier melt, yet its impact on the glacial organic carbon (OC) cycle remains, surprisingly, affected by vast knowledge gaps. This very field certainly needs expanding and strengthening, particularly if the actual impacts of climate change on glacial biogeochemistry are to be predicted.

Many important steps have been made that provide valuable starting points for future predictions, without which the knowledge about OC dynamics on glaciers would indeed be very limited. The glacial ecosystems have been observed in terms of carbon sequestration potential (Anesio et al., 2009), as a carbon store (Priscu et al., 2008), and foremost as a vast variety of habitats and organisms therein, not only on ice surfaces (Hodson et al., 2010a, 2010b; Säwström et al., 2002; Telling et al., 2010), but also at glacier beds (Kaštovská et al., 2007; Lanoil et al., 2009), and even liquid water veins deep within the ice mass (Mader et al., 2006; Price, 2000). Recently, world's glaciers were recognised as a biome (Anesio and Laybourn-Parry, 2012), the knowledge about their ecosystems became more systematic (Hodson et al., 2008; Margesin et al., 2007) and links between the living organisms and the abiotic environment became better constrained (Stibal et al., 2012b; Telling et al., 2012). Furthermore, the impacts of those ecosystems on the glacier melt are being explored, either in the context of darkening by humic substance (Takeuchi, 2002b), microbial biomass growth (Cook et al., 2012), or snow and ice surfaces colouration by active cells (Lutz et al., 2014; Takeuchi, 2002b, 2009).

Furthermore, a range of recent discoveries suggest wide impacts of glacial melt on downstream waters. The organic matter in glacial runoff has especially been shown to be abundant and mostly biolabile (Fellman et al., 2010; Hood et al., 2009). This organic matter has been shown by Pautler et al. (2012) and Singer et al. (2012) to contain products of *in situ* microbial activity, however a proportion of ancient but not recalcitrant organic matter can be ascribed to anthropogenic emissions (Stubbins et al., 2012). That, unfortunately, also implies the presence of harmful pollutants among glacial organic matter types. Persistent organic pollutants, including PCBs (polychlorinated biphenyls) and DDT (dichlorodiphenyl trichloroethane), were found to accumulate in proglacial lake sediments in the European Alps (Bogdal et al., 2009, 2010a, 2010b). These have a long residence time in the food chain, undergo biomagnification, and were inferred to affect penguin populations in the Southern Ocean due to the release from the Antarctic Ice Sheet (AIS; Geisz et al., 2008). Furthermore, aerosols accumulating on glacier surfaces may contain substances originating from fossil fuel and biomass combustion, which influence the surface reflectivity by darkening snow, especially as they concentrate on the snow surface during melt (Doherty et al., 2010, 2013).

Whilst the biological and chemical components of the research considered above are indeed important, these are highly dependent on the physical characteristics of the environment. Long-range atmospheric transport is capable of bringing pollutants even to Greenland and Antarctica (Fuoco et al., 2012; Kallenborn et al., 2013; Legrand and Angelis, 1996; Masclat et al., 2000), and this is also a possible path for cell transport (Price and Bay, 2012). Moreover, once upon the glacier, these undergo various changes connected to melt and transport in aqueous suspension. For example, the organic chemicals and cells undergo elution processes in snowpack (Björkman et al., 2014; Meyer and Wania, 2011) and both these organic matter types are liberated from melting glacier ice (Bogdal et al., 2010a; Irvine-Fynn et al., 2012). Following that, they may contribute to the vast outgoing fluxes of organic matter in glacial catchments (Bhatia et al., 2013; Hood et al., 2009; Lawson et al., 2014). Glaciers have also been recognised as important for organic matter storage (Priscu et al., 2008; Wang et al., 2008b), which can be effectively used for ice core dating (Jenk et al., 2009; Sigl et al., 2009; Uetake et al., 2006; Yoshimura et al., 2006). The importance of physical processes has been found to be important in the formation of organic-rich debris deposits on glacier surfaces (known as cryoconite; by Stibal et al., 2008), the spatial distribution of supraglacial OC (Stibal et al., 2010), microbial abundance and activity (Stibal et al., 2012b).

7.2. Contribution of the current work: The fate of organic carbon on glacier surface upon melt

The multiple OC fluxes in a glacial setting were constrained here simultaneously for the first time (in Chapter 4), showing an example of the supraglacial OC cycle on a glacier rapidly losing mass (described in Chapter 3). As a result of the concurrent observation of the glacier's physical characteristics and biogeochemical fluxes on a variety of scales (Chapters 4 and 5), the following improvements to the understanding of OC cycle on glaciers have been made:

The atmospheric inputs of OC to glaciers are highly variable both temporally and spatially, which may be linked to the influence of wind action on snow cover (see Section 4.4.1.). Extreme precipitation events may also contribute to this effect, as has already been observed for the respective fluxes of inorganic solutes (Hodson et al., 2009; Kühnel et al., 2013). The highest variability among all studied OC fluxes was inherent to those connected to aeolian and precipitation-related inputs, and these caused higher error limits assigned to these OC budget components (Section 4.3.5.).

The interannual variability of two OC fluxes, related to the melt of surface ice and the stream runoff, follows variability in the net mass balance of the glacier (see Section 6.2.). The variability experienced in atmospheric deposition measurements has little effect on runoff, where concentrations of OC are strongly connected to the progress of the melt season instead (as has been shown in Sections 4.3.2. and 4.4.2.). This work has shown that during snowpack melt, post-depositional processes (i.e. preferential elution and refreezing, cf. Björkman et al., 2014; Meyer and Wania, 2011) segregate organic matter types, especially by capturing dissolved OC (DOC) and cells in superimposed ice (see Sections 5.3.3. and 5.4.3). This contributes to a delay in DOC and cell release, which results in a hysteresis behaviour of those in runoff (which is best expressed in the case of cells, as has been described in Section 5.4.2.). Hence, the net ablation periods and zones on the glacier play a crucial role in the OC export from glaciers, while the water percolation in the accumulation zone differentiates the storage of organic matter types (Section 6.3.). By the same token, the physical characteristics of a glacier may be important in predicting its OC export rates, particularly its mass balance and accumulation area ratio.

On a glacier that is rapidly losing mass, the OC flux related to biological activity in supraglacial debris is relatively small in comparison to the fluxes resulting from melting ice, the atmospheric deposition or runoff (see Sections 4.3.5. and 6.2.). These three physical processes caused transfers of 0.4 – 0.7 Mg TOC a⁻¹ each (including between 0.2 and 0.4 Mg DOC a⁻¹), and the storage change implied by budgeting them was of the same order of magnitude (all measured in supraglacial catchment of 1.3 km²). At the same time, the biological production

contributed to the glacier surface an order of magnitude smaller amount of TOC. Admittedly, in some glacial environments algal blooms may promote high rates of biological OC production (Lutz et al., 2014; Takeuchi, 2009), however the shrinking wet snow zones, as well as scarce nutrient supplies on glacier surfaces (Takeuchi, 2004) considerably limit this effect. On these glaciers with sparse algal blooms, biological growth is unlikely to produce considerable DOC fluxes in the snowpack, and nor is it likely to form a quantitatively important proportion of particulate OC (Section 5.4.3.). Hence, the importance of the glacial ecosystem in the OC cycle of small and shrinking glaciers is qualitative, since it can rework organic matter to change structure and properties of supraglacial organic-rich debris (Langford et al., 2010; Takeuchi, 2002a; Takeuchi et al., 2001b). This is in concordance with the observation of Stibal et al. (2008), who deemed improbably high the estimated 15-40 years residence time of cryoconite that resulted from comparing the net biological carbon production and the supraglacial OC storage in this debris on Werenskiöld glacier, Svalbard. On the contrary, the flux-derived estimates from Foxfonna indicate a cryoconite residence time of c. 3 years (Section 4.4.4.), which compares well with the estimates of cryoconite granule age of Takeuchi et al. (2010) and Hodson et al. (2010b), that were obtained with independent methods on other glaciers.

The dominant feature of the multiple OC-related processes is the formation of various organic matter retention zones on the glacier surface (Section 6.3.). These differentiate the location of organic matter types, e.g. the superimposed ice preferentially stores DOC and cells (see Sections 5.3.3. and 5.4.3.). The superimposed ice contained at its maximum extent c. 0.1 Mg TOC, of which 80% was DOC and 2% was cells. Cell enrichment was also observed in the uppermost layers of wet but not saturated snowpack, and hence a rapid transfer of these was observed at the point of snow profile inundation with meltwater (as has been shown in Sections 5.3.3. and 5.4.2.). The zones of particulate OC enrichment are the uppermost layers of glacial ice (the upper 20 cm containing 0.2 Mg TOC a⁻¹, of which 51% was DOC) and most likely also cryoconite, the largest organic matter store on the glacier surface, where 1.1 Mg TOC was retained beyond one balance year (see Sections 4.3.3. and 4.3.5.). Still, the proceeding melt and supply of material from underlying ice may lead to relative enrichment in the mineral fraction of cryoconite, resulting in denser cryoconite cover but with smaller organic content than on the glaciers experiencing less intensive melt (Section 6.3.).

Therefore, there exist strong links between the physical processes on glaciers and their organic matter cycle, especially in the influence exerted by the extensive melt. Moreover, the supraglacial hydrological zones (Müller, 1962) correspond to varying biogeochemical properties of the glacier surface, promoting enrichment of different organic matter types. The movement of these zones controls the timing of organic matter release to the supraglacial debris and downstream ecosystems. Probably the strongest factor found to influence the OC

cycle on rapidly shrinking glaciers was their net mass balance, but an important role may also be played by glacier topography, snow accumulation regime and drainage patterns.

7.3. Implications of the current study: From sea level rise to biogeochemical change

Glaciers contain a variety of organic matter types which are not only passively stored, but are also reworked, transported and fractionated in concordance with the physical and biological processes, all of which depend strongly on the presence of liquid water. More melt happening on the glaciers worldwide and their growing ablation zones are likely to intensify the supraglacial release of OC from ablation, which being temporarily stored on the glacier surface, would cause its darkening and a positive feedback to melt (especially if it becomes more humic towards glacier snouts; cf. Section 6.3.). Furthermore, the sustained melt will contribute to a change in the biogeochemical state of glacier surfaces, ultimately reducing the area occupied by live cells and increasing the area in particulate organic matter (cf. Section 6.3. and 6.6.). The physical characteristics of glacial environments, especially mass balance, but also glacier dynamics or thermal regime, are likely to play their role in driving the direction and extent of this change (cf. Sections 6.2–6.3.). A special role in delaying the effect of organic matter release will be played by refreezing processes.

In this thesis, an example of a small and shrinking glacier was characterised for OC fluxes. This example is of importance for the fact that small glaciers and ice caps are predicted to dominate the sea level rise contributions within the next century (Meier et al., 2007; Raper and Braithwaite, 2006). Furthermore, the benchmark glacier used in this thesis is located on the archipelago of Svalbard, an important contributor to the forecasted ice mass loss (Radić et al., 2014). Hence, some features of OC cycle encountered on Foxfonna are likely to be widespread in a few decades. The vast ablation zone area seems to result not only in a greater cryoconite coverage, but also in its composition shift towards a smaller proportion of organic material (see Section 6.3.), which is also mostly allochthonous (i.e. has not been produced by the ecosystem *in situ*). These changes will contribute to the future darkening of small glaciers, and likely enhanced melt, unless a debris thickness threshold is reached that will insulate the ice surface instead (Nakawo and Rana, 1999; Reznichenko et al., 2010). Hence, the OC cycle is likely to participate in a positive feedback with melt, the extent of which may be controlled by the counteracting geomorphological processes that would be capable of removing the supraglacial debris (see Sections 4.4.4. and 6.3). Furthermore, the melt enhancement due to cryoconite cover may be magnified if the melt season becomes longer due to the warming of ‘shoulder months’ experienced (i.e. margins of the melt season becoming wider; see trends

observed by Førland et al. (2011) for spring and autumn temperatures). This is because then the cryoconite layer will be exposed for a longer period from under the snow cover.

Since the glacial melt is also contributing to a strong outgoing flux of OC (Sections 4.3.5., 4.4.2 and 6.2.), especially when dissolved, from the glacier surface, such a feedback loop would result in even faster removal of the most labile fraction of organic matter contained near the surface of these glaciers. This might be experienced as a concentrated DOC runoff in the proglacial areas, where it may be either utilised by freshwater and riparian ecosystems, transferred into sediment-bound form and deposited, or transferred into the final sink in the marine environment. This DOC is likely to be assisted by cells, being stored and released in a somewhat similar fashion to DOC, i.e. enriched in superimposed ice and removed rapidly upon its melt (see Sections 5.3.3. and 5.4.2.). The DOC and cell export would thus be intensified as the melt season becomes longer.

7.4. Future research suggestions: Geomorphological processes and chemical fluxes

Despite the intensive focus on glaciers and their biogeochemistry in the recent past, many aspects of the influence of physical processes such as melting upon OC quantity and quality remain underexplored. While the current study has shown the impact of sustained melt, supraglacial runoff and atmospheric deposition on the supply and removal of OC on a glacier surface, it would be beneficial to expand this with the understanding of the role of more rapid and episodic processes, such as extreme rainfall and avalanches. The impact of extreme rain events needs exploring in particular, as the frequency of those events is likely to increase with the warming in Svalbard (Førland et al., 2011; Niedźwiedź, 2003). Also the interaction between the glacier beds and surfaces, as well as the possibilities for repeated OC entrainment into glacial ice, need exploring. This is for two reasons: first, to explore the possibility for some of the dark supraglacial organic matter being excluded from enhancing melt (e.g. by being buried or concentrated into thick insulating layers); and secondly, to discover the fate of OC entering the glacier.

Of particular importance for the proglacial soils, ecosystems and river water quality is the chemical composition of the organic matter exported from glaciers. Hence, the speciation of the OC fluxes connected to glaciers, especially in respect to nutrients and harmful substances (poisons, hormone disruptors, carcinogens and others), needs urgent exploration. The presence of supraglacial storage of particular organic compounds may also affect the supraglacial ecosystems. In particular, the stored organic matter may undergo further chemical changes, including the photodegradation, which is an underexplored process possibly leading to the production of more labile organic compounds. Finally, glacial runoff worldwide is used by numerous groups of people for consumption. For example, the

Himalayan glacial melt feeds drinking and irrigation water to approximately 1.3 billion people (Jianchu et al., 2009). Hence, the recognition of the potential pollutant load in these waters appears crucial also in the context of the current challenge in providing clean drinking water and food to the growing global population.

References

- Amato P, Hennebelle R, Magand O, Sancelme M, Delort A-M, Barbante C, Boutron C, Ferrari C. 2007. Bacterial characterization of the snow cover at Spitzberg, Svalbard. *FEMS Microbiology Ecology* **59** : 255–64. DOI: 10.1111/j.1574-6941.2006.00198.x
- Anderson SP. 2007. Biogeochemistry of Glacial Landscape Systems. *Annual Review of Earth and Planetary Sciences* **35** : 375–399. DOI: 10.1146/annurev.earth.35.031306.140033
- Anderson SP, Longacre SA, Kraal ER. 2003. Patterns of water chemistry and discharge in the glacier-fed Kennicott River, Alaska: evidence for subglacial water storage cycles. *Chemical Geology* **202** : 297–312. DOI: 10.1016/j.chemgeo.2003.01.001
- Andreassen LM, van den Broeke MR, Giesen RH, Oerlemans J. 2008. A 5 year record of surface energy and mass balance from the ablation zone of Storbreen, Norway. *Journal of Glaciology* **54** : 245–258.
- Anesio A, Mindl B, Laybourn-Parry J, Sattler B. 2007. Virus dynamics on a high Arctic glacier (Svalbard). *Journal of Geophysical Research* **112** : G04S31. DOI: doi:10.1029/2006JG000350
- Anesio AM, Hodson AJ, Fritz A, Psenner R, Sattler B. 2009. High microbial activity on glaciers: importance to the global carbon cycle. *Global Change Biology* **15** : 955–960. DOI: 10.1111/j.1365-2486.2008.01758.x
- Anesio AM, Laybourn-Parry J. 2012. Glaciers and ice sheets as a biome. *Trends in Ecology & Evolution* **27** : 219–225. DOI: 10.1016/j.tree.2011.09.012
- Anesio AM, Sattler B, Foreman C, Telling J, Hodson A, Tranter M, Psenner R. 2010. Carbon fluxes through bacterial communities on glacier surfaces. *Annals of Glaciology* **51** : 32–40. DOI: 10.3189/172756411795932092
- Bader H. 1954. Sorge's law of densification of snow on high polar glaciers. *Journal of Glaciology* **2** : 319–323.
- Bælum K, Benn DI. 2011. Thermal structure and drainage system of a small valley glacier (Tellbreen, Svalbard), investigated by ground penetrating radar. *The Cryosphere* **5** : 139–149. DOI: 10.5194/tc-5-139-2011
- Bahadur R, Praveen PS, Xu Y, Ramanathan V. 2012. Solar absorption by elemental and brown carbon determined from spectral observations. *Proceedings of the National Academy of Sciences of the United States of America* **109** : 17366–71. DOI: 10.1073/pnas.1205910109
- Bales RC, Davis RE, Stanley DA. 1989. Ion Elution Through Shallow Homogeneous Snow. *Water Resources Research* **25** : 1869–1877.
- Bales RC, Davis RE, Williams MW. 1993. Tracer release in melting snow: diurnal and seasonal patterns. *Hydrological Processes* **7** : 389–401.
- Baranowski S. 1982. Naled ice in front of some Spitsbergen glaciers. *Journal of Glaciology* **28** : 211–214.

Barcena TG, Yde JC, Finster KW. 2010. Methane flux and high-affinity methanotrophic diversity along the chronosequence of a receding glacier in Greenland. *Annals of Glaciology* **51** : 23–31.

Bardgett RD et al. 2007. Heterotrophic microbial communities use ancient carbon following glacial retreat. *Biology Letters* **3** : 487–90. DOI: 10.1098/rsbl.2007.0242

Barker JD, Klassen JL, Sharp MJ, Fitzsimons SJ, Turner RJ. 2010. Detecting biogeochemical activity in basal ice using fluorescence spectroscopy. *Annals of Glaciology* **51** : 47–55. DOI: 10.3189/172756411795931967

Barker JD, Sharp MJ, Fitzsimons SJ, Turner RJ. 2006. Abundance and Dynamics of Dissolved Organic Carbon in Glacier Systems. *Arctic, Antarctic, and Alpine Research* **38** : 163–172.

Barker JD, Sharp MJ, Turner RJ. 2009. Using synchronous fluorescence spectroscopy and principal components analysis to monitor dissolved organic matter dynamics in a glacier system. *Hydrological Processes* **23** : 1487–1500. DOI: 10.1002/hyp

Barrand NE, Murray T, James TD, Barr SL, Mills JP. 2009. Optimizing photogrammetric DEMs for glacier volume change assessment using laser-scanning derived ground-control points. *Journal of Glaciology* **55** : 106–116.

Benn DI, Evans DJA. 2010. *Glaciers and Glaciation*. 2nd ed. Routledge: London & New York

Benn DI, Lehmkuhl F. 2000. Mass balance and equilibrium-line altitudes of glaciers in high-mountain environments. *Quaternary International* **65/66** : 15–29.

Bennett MR, Huddart D, Hambrey MJ, Ghienne JF. 1996. Moraine development at the High-Arctic valley glacier Pedersenbreen, Svalbard. *Geografiska Annaler. Series A, Physical Geography* **78** : 209–222.

Benson CS. 1962. Stratigraphic studies in the snow and firn of the Greenland Ice Sheet

Bernasconi SM et al. 2011. Chemical and Biological Gradients along the Damma Glacier Soil Chronosequence, Switzerland. *Vadose Zone Journal* **10** : 867–883. DOI: 10.2136/vzj2010.0129

Bhatia M, Sharp M, Foght J. 2006. Distinct bacterial communities exist beneath a high Arctic polythermal glacier. *Applied and environmental microbiology* **72** : 5838–45. DOI: 10.1128/AEM.00595-06

Bhatia MP, Das SB, Longnecker K, Charette MA, Kujawinski EB. 2010. Molecular characterization of dissolved organic matter associated with the Greenland ice sheet. *Geochimica et Cosmochimica Acta* **74** : 3768–3784. DOI: 10.1016/j.gca.2010.03.035

Bhatia MP, Das SB, Xu L, Charette MA, Wadham JL, Kujawinski EB. 2013. Organic carbon export from the Greenland ice sheet. *Geochimica et Cosmochimica Acta* **109** : 329–344. DOI: 10.1016/j.gca.2013.02.006

Bianchi TS. 2011. The role of terrestrially derived organic carbon in the coastal ocean: A changing paradigm and the priming effect. *Proceedings of the National Academy of Sciences* **108** : 19473–19481. DOI: 10.1073/pnas.1017982108

Bidleman TF, Jantunen LM, Binnur Kurt-Karakus P, Wong F, Hung H, Ma J, Stern G, Rosenberg B. 2013. Chiral chemicals as tracers of atmospheric sources and fate processes in a world of changing climate. *Mass spectrometry (Tokyo, Japan)* **2** : S0019. DOI: 10.5702/massspectrometry.S0019

Björkman MP, Zarsky JD, Kühnel R, Hodson A, Sattler B, Psenner R. 2014. Microbial Cell Retention in a Melting High Arctic Snowpack , Svalbard Microbial Cell Retention in a Melting High Arctic. *Arctic, Antarctic and Alpine Research* **46** : 471–482.

Blankenship DD, Morse DL, Finn CA, Bell RE, Peters ME, Kempf SD, Hodge SM, Studinger M, Behrendt JC, Brozena JM. 2001. Geologic controls on the initiation of rapid basal movement for West Antarctic ice streams: a geophysical perspective including new airborne radar sounding and laser altimetry results. *The West Antarctic Ice Sheet: behavior and environment Antarctic research series* **77** : 105–121.

Bogdal C, Nikolic D, Lüthi MP, Schenker U, Scheringer M, Hungerbühler K. 2010a. Release of legacy pollutants from melting glaciers: model evidence and conceptual understanding. *Environmental Science & Technology* **44** : 4063–9. DOI: 10.1021/es903007h

Bogdal C, Scheringer M, Schmid P, Bläuenstein M, Kohler M, Hungerbühler K. 2010b. Levels, fluxes and time trends of persistent organic pollutants in Lake Thun, Switzerland: Combining trace analysis and multimedia modeling. *The Science of the Total Environment* **408** : 3654–63. DOI: 10.1016/j.scitotenv.2010.04.038

Bogdal C, Schmid P, Kohler M, Müller CE, Iozza S, Bucheli TD, Scheringer M, Hungerbühler K. 2008. Sediment record and atmospheric deposition of brominated flame retardants and organochlorine compounds in Lake Thun, Switzerland: lessons from the past and evaluation of the present. *Environmental Science & Technology* **42** : 6817–22.

Bogdal C, Schmid P, Zennegg M, Anselmetti FS, Scheringer M, Hungerbühler K. 2009. Blast from the past: melting glaciers as a relevant source for persistent organic pollutants. *Environmental Science & Technology* **43** : 8173–7. DOI: 10.1021/es901628x

Bøggild CE. 2007. Simulation and parameterization of superimposed ice formation. *Hydrological Processes* **21** : 1561–1566. DOI: DOI: 10.1002/hyp.6718

Bøggild CE, Brandt RE, Brown KJ, Warren SG. 2010. The ablation zone in northeast Greenland: ice types, albedos and impurities. *Journal of Glaciology* **56** : 101–113. DOI: 10.3189/002214310791190776

Bolch T, Buchroithner MF, Kunert A, Kamp U. 2007. Automated delineation of debris-covered glaciers based on ASTER data. In *Geoinformation in Europe* , Gomasca MA (ed). Millpress; 403–410.

Bond TC, Habib G, Bergstrom RW. 2006. Limitations in the enhancement of visible light absorption due to mixing state. *Journal of Geophysical Research* **111** : D20211. DOI: 10.1029/2006JD007315

Boudries H, Bottenheim JW, Guimbaud C, Grannas a. M, Shepson PB, Houdier S, Perrier S, Dominé F. 2002. Distribution and trends of oxygenated hydrocarbons in the high Arctic derived from measurements in the atmospheric boundary layer and interstitial snow air during the ALERT2000 field campaign. *Atmospheric Environment* **36** : 2573–2583. DOI: 10.1016/S1352-2310(02)00122-X

- Brandt RE, Warren. 1997. Temperature measurements and heat transfer in near-surface snow at the South Pole. *Journal of Glaciology* **43** : 339–351.
- Brandt RE, Warren SG. 1993. Solar-heating rates and temperature profiles in Antarctic snow and ice. *Journal of Glaciology* **39** : 99–110.
- Brimblecombe P, Clegg SL, Davies TD, Shooter D, Tranter M. 1987. Observations of the preferential loss of major ions from melting snow and laboratory ice. *Water Research* **21** : 1279–1286.
- Brimblecombe P, Clegg SL, Davies TD, Shooter D, Tranter M. 1988. The loss of halide and sulphate ions from melting ice. *Water Research* **22** : 693–700.
- Brimblecombe P, Tranter M, Abrahams PW, Blackwood I, Davies TD, Vincent CE. 1985. Relocation and preferential elution of acidic colute through the snowpack of a small, remote, high-altitude Scottish catchment. *Annals of Glaciology* **7** : 141–147.
- Brock BW, Arnold NS. 2000. A spreadsheet-based (Microsoft Excel) point surface energy balance model for glacier and snow melt studies. *Earth Surface Processes and Landforms* **25** : 649–658.
- Brock BW, Willis IC, Sharp MJ. 2000. Measurement and parameterization of albedo variations at Haut Glacier d’Arolla, Switzerland. *Journal of Glaciology* **46** : 675–688.
- Bromwich DH, Nicolas JP, Monaghan AJ, Lazzara MA, Keller LM, Weidner GA, Wilson & AB. 2013. Central West Antarctica among the most rapidly warming regions on Earth. *Nature Geoscience* **6** : 139–145. DOI: 10.1038/ngeo1671
- Cameron KA, Hodson AJ, Osborn AM. 2012a. Carbon and nitrogen biogeochemical cycling potentials of supraglacial cryoconite communities. *Polar Biology* **35** : 1375–1393. DOI: 10.1007/s00300-012-1178-3
- Cameron KA, Hodson AJ, Osborn MA. 2012b. Structure and diversity of bacterial, eukaryotic and archaeal communities in glacial cryoconite holes from the Arctic and the Antarctic. *FEMS microbiology ecology* **82** : 254–67. DOI: 10.1111/j.1574-6941.2011.01277.x
- Canty A, Ripley B. 2012. boot: Bootstrap R (S-Plus) Functions.
- Carlsson P, Cornelissen G, Bøggild CE, Rysgaard S, Mortensen J, Kallenborn R. 2012. Hydrology-linked spatial distribution of pesticides in a fjord system in Greenland. *Journal of Environmental Monitoring* : *JEM* **14** : 1437–43. DOI: 10.1039/c2em30068k
- Cazenave A, Llovel W. 2010. Contemporary sea level rise. *Annual Review of Marine Science* **2** : 145–73. DOI: 10.1146/annurev-marine-120308-081105
- Chen G et al. 2007. An assessment of the polar HOx photochemical budget based on 2003 Summit Greenland field observations. *Atmospheric Environment* **41** : 7806–7820. DOI: 10.1016/j.atmosenv.2007.06.014
- Chen W, Westerhoff P, Leenheer JA, Booksh K. 2003. Fluorescence excitation-emission matrix regional integration to quantify spectra for dissolved organic matter. *Environmental science & technology* **37** : 5701–10.

Christiansen HH, French HM, Humlum O. 2005. Permafrost in the Gruve-7 mine, Adventdalen, Svalbard. *Norsk Geografisk Tidsskrift - Norwegian Journal of Geography* **59** : 109–115. DOI: 10.1080/00291950510020592

Cogley JG. 2009. Geodetic and direct mass-balance measurements: comparison and joint analysis. *Annals of Glaciology* **50** : 96–100.

Considine GD (ed). 2005. Van Nostrand's Encyclopedia of Chemistry . 5th ed. Wiley-Interscience

Cook J, Hodson A, Telling J, Anesio A, Irvine-Fynn TD, Bellas C. 2010. The mass–area relationship within cryoconite holes and its implications for primary production. *Annals of Glaciology* **51** : 106–110. DOI: 10.3189/172756411795932038

Cook JM, Hodson AJ, Anesio AM, Hanna E, Yallop M, Stibal M, Telling J, Huybrechts P. 2012. An improved estimate of microbially mediated carbon fluxes from the Greenland ice sheet. *Journal of Glaciology* **58** : 1398–1408. DOI: 10.3189/2012JoG12J001

Coveney MF. 1982. Bacterial uptake of photosynthetic carbon from freshwater phytoplankton. *Oikos* **38** : 8–20.

Cragin JH, Hewitt AD, Colbeck SC. 1993. Elution of ions from melting snow. Chromatographic versus metamorphic mechanisms

Cragin JH, Hewitt AD, Colbeck SC. 1996. Grian-scale mechanisms influencing the elution of ions from snow. *Atmopsheric Environment* **30** : 119–127.

Dani KGS, Mader HM, Wolff EW, Wadham JL. 2012. Modelling the liquid-water vein system within polar ice sheets as a potential microbial habitat. *Earth and Planetary Science Letters* **333-334** : 238–249. DOI: 10.1016/j.epsl.2012.04.009

Davis RE, Petersen CE, Bales RC. 1995. Ion flux through a shallow snowpack: effects of initial conditions and melt sequences. 115–126 pp.

Davison AC, Hinkley D V. 1997. Bootstrap Methods and Their Applications . Cambridge University Press: Cambridge

Doherty SJ, Grenfell TC, Forsström S, Hegg DL, Brandt RE, Warren SG. 2013. Observed vertical redistribution of black carbon and other insoluble light-absorbing particles in melting snow. *Journal of Geophysical Research: Atmospheres* **118** : 5553–5569. DOI: 10.1002/jgrd.50235

Doherty SJ, Warren SG, Grenfell TC, Clarke a. D, Brandt RE. 2010. Light-absorbing impurities in Arctic snow. *Atmospheric Chemistry and Physics Discussions* **10** : 18807–18878. DOI: 10.5194/acpd-10-18807-2010

Dong K, Liu H, Zhang J, Zhou Y, Xin Y. 2012. *Flavobacterium xueshanense* sp. nov. and *Flavobacterium urumqiense* sp. nov., two psychrophilic bacteria isolated from glacier ice. *IJSEM* **62** : 1151–1157.

Dowdeswell JA, Hodgkins R, Nuttall A, Hagen JO, Hamilton GS. 1995. Mass balance change as a control on the frequency and occurrence of glacier surges in Svalbard, Norwegian High Arctic. *Geophysical Research Letters* **22** : 2909–2912.

- Downes MT, Howard-Williams C, Vincent WF. 1986. Sources of organic nitrogen, phosphorus and carbon in Antarctic streams. *Hydrobiologia* **134** : 215–225.
- Drewry DJ, Liestøl O, Neal CS, Orheim O, Wold B. 1980. Airborne Radio Echo Sounding of Glaciers in Svalbard. *Polar Record* **20** : 261–275.
- Dubnick A, Barker J, Sharp M, Wadham J, Lis G, Telling J, Fitzsimons S, Jackson M. 2010. Characterization of dissolved organic matter (DOM) from glacial environments using total fluorescence spectroscopy and parallel factor analysis. *Annals of Glaciology* **51** : 111–122. DOI: 10.3189/172756411795931912
- Edwards A, Anesio AM, Rassner SM, Sattler B, Hubbard B, Perkins WT, Young M, Griffith GW. 2011. Possible interactions between bacterial diversity, microbial activity and supraglacial hydrology of cryoconite holes in Svalbard. *The ISME journal* **5** : 150–160. DOI: 10.1038/ismej.2010.100
- Edwards A, Rassner SME, Anesio AM, Worgan HJ, Irvine-Fynn TDL, Williams HW, Sattler B, Griffith GW. 2013. Contrasts between the cryoconite and ice-marginal bacterial communities of Svalbard glaciers. *Polar Research* **32** : 19468. DOI: <http://dx.doi.org/10.3402/polar.v32i0.19468>
- Etzel Müller B, Vatne G, Ødegård RS, Sollid JL. 1993. Dynamics of Two Subpolar Valley Glaciers. Erikbreen and Hannabreen, Liefdefjorden, Northern Spitsbergen. *Geografiska Annaler. Series A, Physical Geography* **75 A** : 41–54.
- Felip M, Andreatta S, Sommaruga R, Straskrábová V, Catalan J. 2007. Suitability of flow cytometry for estimating bacterial biovolume in natural plankton samples: comparison with microscopy data. *Applied and Environmental Microbiology* **73** : 4508–14. DOI: 10.1128/AEM.00733-07
- Fellman JB, Spencer RGM, Hernes PJ, Edwards RT, D'Amore D V., Hood E. 2010. The impact of glacier runoff on the biodegradability and biochemical composition of terrigenous dissolved organic matter in near-shore marine ecosystems. *Marine Chemistry* **121** : 112–122. DOI: 10.1016/j.marchem.2010.03.009
- Fischer A. 2011. Comparison of direct and geodetic mass balances on a multi-annual time scale. *The Cryosphere* **5** : 107–124. DOI: 10.5194/tc-5-107-2011
- Flanner MG. 2013. Arctic climate sensitivity to local black carbon. *Journal of Geophysical Research: Atmospheres* **118** : 1840–1851. DOI: 10.1002/jgrd.50176
- Flanner MG, Zender CS, Hess PG, Mahowald NM, Painter TH, Ramanathan V, Rasch PJ. 2009. Springtime warming and reduced snow cover from carbonaceous particles. *Atmospheric Chemistry and Physics* **9** : 2481–2497.
- Flanner MG, Zender CS, Randerson JT, Rasch PJ. 2007. Present-day climate forcing and response from black carbon in snow. *Journal of Geophysical Research* **112** : D11202. DOI: 10.1029/2006JD008003
- Flato GM, Boer GJ. 2001. Warming asymmetry in climate change simulations. *Geophysical Research Letters* **28** : 195–198.

Førland EJ, Benestad R, Hanssen-Bauer I, Haugen JE, Skaugen TE. 2011. Temperature and Precipitation Development at Svalbard 1900–2100. *Advances in Meteorology* **2011** : 1–14. DOI: 10.1155/2011/893790

Førland EJ, Hanssen-Bauer I. 2000. Increased precipitation in the Norwegian Arctic: true or false? *Climatic Change* **46** : 485–509.

Fuoco R, Giannarelli S, Onor M, Ghimenti S, Abete C, Termine M, Francesconi S. 2012. A snow/firn four-century record of polycyclic aromatic hydrocarbons (PAHs) and polychlorobiphenyls (PCBs) at Talos Dome (Antarctica). *Microchemical Journal* **105** : 133–141. DOI: 10.1016/j.microc.2012.05.018

Gardner AS et al. 2013. A reconciled estimate of glacier contributions to sea level rise: 2003 to 2009. *Science (New York, N.Y.)* **340** : 852–7. DOI: 10.1126/science.1234532

Gardner AS, Moholdt G, Wouters B, Wolken GJ, Burgess DO, Sharp MJ, Cogley JG, Braun C, Labine C. 2011. Sharply increased mass loss from glaciers and ice caps in the Canadian Arctic Archipelago. *Nature* **473** : 357–60. DOI: 10.1038/nature10089

Gardner AS, Sharp MJ. 2010. A review of snow and ice albedo and the development of a new physically based broadband albedo parameterization. *Journal of Geophysical Research* **115** : F01009. DOI: 10.1029/2009JF001444

Garmash O, Hermanson MH, Isaksson E, Schwikowski M, Divine D, Teixeira C, Muir DCG. 2013. Deposition History of Polychlorinated Biphenyls to the Lomonosovfonna Glacier, Svalbard: A 209 Congener Analysis. *Environmental Science & Technology* **47** : 12064–12072. DOI: 10.1021/es402430t

Gašparović B, Plavšić M, Čosović B, Saliot A. 2007. Organic matter characterization in the sea surface microlayers in the subarctic Norwegian fjords region. *Marine Chemistry* **105** : 1–14. DOI: 10.1016/j.marchem.2006.12.010

Geisz HN, Dickhut RM, Cochran M a, Fraser WR, Ducklow HW. 2008. Melting glaciers: a probable source of DDT to the Antarctic marine ecosystem. *Environmental Science & Technology* **42** : 3958–62.

Gerdel R. W., Drouet F. 1960. The Cryoconite of the Thule Area, Greenland. *Transactions of the American Microscopical Society* **79** : 256–272.

Giesen RH, Oerlemans J. 2013. Climate-model induced differences in the 21st century global and regional glacier contributions to sea-level rise. *Climate Dynamics* **41** : 3283–3300. DOI: 10.1007/s00382-013-1743-7

Goodsell B, Hambrey MJ, Glasser NF. 2005. Debris transport in a temperate valley glacier: Haut Glacier d’Arolla, Valais, Switzerland. *Journal of Glaciology* **51** : 139–146.

Grabiec M, Leszkiewicz J, Głowacki P, Jania J. 2006. Distribution of snow accumulation on some glaciers of Spitsbergen. *Polish Polar Research* **27** : 309–326.

Grannas AM et al. 2007. An overview of snow photochemistry: evidence, mechanisms and impacts. *Atmospheric Chemistry and Physics* **7** : 4329–4373.

Grannas AM et al. 2013. The role of the global cryosphere in the fate of organic contaminants. *Atmospheric Chemistry and Physics* **13** : 3271–3305. DOI: 10.5194/acp-13-3271-2013

Grannas AM, Hockaday WC, Hatcher PG, Thompson LG, Mosley-Thompson E. 2006. New revelations on the nature of organic matter in ice cores. *Journal of Geophysical Research* **111** : D04304. DOI: 10.1029/2005JD006251

Grannas AM, Shepson PB, Filley TR. 2004. Photochemistry and nature of organic matter in Arctic and Antarctic snow. *Global Biogeochemical Cycles* **18** DOI: 10.1029/2003GB002133

Grinde B. 1983. Vertical distribution of the snow alga *Chlamydomonas nivalis* (Chlorophyta, Volvocales). *Polar Biology* **2** : 159–162.

Gulley JD, Benn DI, Müller D, Luckman A. 2009. A cut-and-closure origin for englacial conduits in uncrevassed regions of polythermal glaciers. *Journal of Glaciology* **55** : 66–80. DOI: 10.3189/002214309788608930

Guzzella L, Poma G, De Paolis A, Roscioli C, Viviano G. 2011. Organic persistent toxic substances in soils, waters and sediments along an altitudinal gradient at Mt. Sagarmatha, Himalayas, Nepal. *Environmental Pollution* **159** : 2552–64. DOI: 10.1016/j.envpol.2011.06.015

Hagen JO, Melvold K, Pinglot F, Dowdeswell JA. 2003. On the Net Mass Balance of the Glaciers and Ice Caps in Svalbard, Norwegian Arctic. *Arctic, Antarctic, and Alpine Research* **35** : 264–270.

Hall D, Upton S. 1988. A wind tunnel study of the particle collection efficiency of an inverted Frisbee used as a dust deposition gauge. *Atmospheric Environment* **22** : 1383–1394.

Hambrey MJ, Huddart D, Bennett MR, Glasser NF. 1997. Genesis of “hummocky moraines” by thrusting in glacier ice: evidence from Svalbard and Britain. *Journal of the Geological Society* **154** : 623–632. DOI: 10.1144/gsjgs.154.4.0623

Hammes F, Broger T, Weilenmann H-U, Vital M, Helbing J, Bosshart U, Huber P, Odermatt RP, Sonnleitner B. 2012. Development and laboratory-scale testing of a fully automated online flow cytometer for drinking water analysis. *Cytometry Part A : The Journal of the International Society for Advancement of Cytometry* **81A** : 508–16. DOI: 10.1002/cyto.a.22048

Hanna E et al. 2013. Ice mass balance and climate change. *Nature* **498** : 51–59. DOI: dx.doi.org/10.1038/nature12238

Hansen J, Nazarenko L. 2004. Soot climate forcing via snow and ice albedos. *Proceedings of the National Academy of Sciences of the United States of America* **101** : 423–8. DOI: 10.1073/pnas.2237157100

Hansen J, Ruedy R, Sato M, Lo K. 2010. Global surface temperature change. *Reviews of Geophysics* **48** : 1–29. DOI: 8755-1209/10/2010RG000345

Hanssen-Bauer I, Førland EJ. 1998. Long-term trends in precipitation and temperature in the Norwegian Arctic: can they be explained by changes in atmospheric circulation patterns? *Climatological Research* **10** : 143–153.

Hell K, Edwards A, Zarsky J, Podmirseg S, Girdwood S, Pachebat J, Insam H, Sattler B. 2013. The dynamic bacterial communities of a melting High Arctic glacier snowpack. *ISME J* **7** : 1814–26. DOI: 10.1038/ismej.2013.51

Hock R. 2005. Glacier melt: a review of processes and their modelling. *Progress in Physical Geography* **29** : 362–391. DOI: 10.1191/0309133305pp453ra

Hock R, Holmgren B. 2005. A distributed surface energy-balance model for complex topography and its application to Storglaciaren, Sweden. *Journal of Glaciology* **51** : 25–36.

Hodgkins R. 2001. Seasonal evolution of meltwater generation, storage and discharge at a non-temperate glacier in Svalbard. *Hydrological Processes* **15** : 441–460.

Hodgkins R, Tranter M. 1998. Solute in High Arctic glacier snow cover and its impact on runoff chemistry. *Annals of Glaciology* **26** : 156–160.

Hodgkins R, Tranter M, Dowdeswell JA. 2004. The Characteristics and Formation of a High-Arctic Proglacial Icing. *Geografiska Annaler, Series A: Physical Geography* **86** : 265–275.

Hodson A, Mumford P, Lister D. 2004. Suspended sediment and phosphorus in proglacial rivers: bioavailability and potential impacts upon the P status of ice-marginal receiving waters. *Hydrological Processes* **18** : 2409–2422. DOI: 10.1002/hyp.1471

Hodson A, Roberts TJ, Engvall A-C, Holmén K, Mumford P. 2009. Glacier ecosystem response to episodic nitrogen enrichment in Svalbard, European High Arctic. *Biogeochemistry* **98** : 171–184. DOI: 10.1007/s10533-009-9384-y

Hodson AAJ, Anesio AM, Tranter M, Fountain A, Osborn M, Priscu JC, Laybourn-Parry J, Sattler B. 2008. Glacial ecosystems. *Ecological Monographs* **78** : 41–67. DOI: 10.1890/07-0187.1

Hodson AJ et al. 2007. A glacier respire?: Quantifying the distribution and respiration CO₂ flux of cryoconite across an entire Arctic supraglacial ecosystem. **112** : 1–9. DOI: 10.1029/2007JG000452

Hodson AJ. 2014. Understanding the dynamics of black carbon and associated contaminants in glacial systems. *WIREs: Water* **1** : 1–9. DOI: 10.1002/wat2.1016

Hodson AJ, Bøggild C, Hanna E, Huybrechts P, Langford H, Cameron K, Houldsworth A. 2010a. The cryoconite ecosystem on the Greenland ice sheet. *Annals of Glaciology* **51** : 123–129. DOI: 10.3189/172756411795931985

Hodson AJ, Cameron K, Bøggild C, Irvine-Fynn T, Langford H, Pearce D, Banwart S. 2010b. The structure, biological activity and biogeochemistry of cryoconite aggregates upon an Arctic valley glacier: Longyearbreen, Svalbard. *Journal of Glaciology* **56** : 349–362. DOI: 10.3189/002214310791968403

Hodson AJ, Mumford PN, Kohler J, Wynn PM. 2005. The High Arctic glacial ecosystem: new insights from nutrient budgets. *Biogeochemistry* **72** : 233–256. DOI: 10.1007/s10533-004-0362-0

Hoham RW, Marcarelli AM, Rogers HS, Ragan MD, Petre BM, Ungerer MD, Barnes JM, Francis DO. 2000. The importance of light and photoperiod in sexual reproduction and

geographical distribution in the green snow alga, *Chloromonas* sp. -D (Chlorophyceae, Volvocales). *Hydrological Processes* **14** : 3309–3321.

Holdsworth G, Krouse HR, Peake E. 1988. Trace-acid ion content of shallow snow and ice cores from mountain sites in Western Canada. *Annals of Glaciology* **10** : 57–62.

Hood E, Battin TJ, Fellman J, O'Neel S, Spencer RGM. 2015. Storage and release of organic carbon from glaciers and ice sheets. *Nature Geoscience* : 1–6. DOI: 10.1038/ngeo2331

Hood E, Berner L. 2009. Effects of changing glacial coverage on the physical and biogeochemical properties of coastal streams in southeastern Alaska. *Journal of Geophysical Research* **114** : G03001. DOI: 10.1029/2009JG000971

Hood E, Fellman J, Spencer RGM, Hernes PJ, Edwards R, D'Amore D, Scott D. 2009. Glaciers as a source of ancient and labile organic matter to the marine environment. *Nature* **462** : 1044–1048. DOI: 10.1038/nature08580

Hoover R. 2001. Composition, molecular structure, and physicochemical properties of tuber and root starches: a review. *Carbohydrate Polymers* **45** : 253–267. DOI: 10.1016/S0144-8617(00)00260-5

Horton BP, Rahmstorf S, Engelhart SE, Kemp AC. 2014. Expert assessment of sea-level rise by AD 2100 and AD 2300. *Quaternary Science Reviews* **84** : 1–6. DOI: 10.1016/j.quascirev.2013.11.002

Humlum O. 2002. Modelling late 20th-century precipitation in Nordenskiöld Land, Svalbard, by geomorphic means. *Norsk Geografisk Tidsskrift–Norwegian Journal of Geography* **56** : 96–103.

Humlum O, Christiansen HH, Juliussen H. 2007. Avalanche-derived Rock Glaciers in Svalbard. *Permafrost and Periglacial Processes* **18** : 75–88. DOI: DOI: 10.1002/ppp.580

Huss M, Bauder A, Funk M. 2009. Homogenization of long-term mass-balance time series. *Annals of Glaciology* **50** : 198–206. DOI: 10.3189/172756409787769627

Iken A. 1981. The effect of the subglacial water pressure on the sliding velocity of a glacier in an idealized numerical model. *Journal of Glaciology* **27** : 407–421.

IPCC. 2014. Climate Change 2014: Synthesis Report. Contribution of Working Groups I, II and III to the Fifth Assessment Report of the Intergovernmental Panel on Climate Change. Geneva, Switzerland

Irvine-Fynn TD., Bridge JW, Hodson AJ. 2010. Rapid quantification of cryoconite: granule geometry and in situ supraglacial extents, using examples from Svalbard and Greenland. *Journal of Glaciology* **56** : 297–308. DOI: 10.3189/002214310791968421

Irvine-Fynn TDL, Edwards A, Newton S, Langford H, Rassner SM, Telling J, Anesio AM, Hodson AJ. 2012. Microbial cell budgets of an Arctic glacier surface quantified using flow cytometry. *Environmental microbiology* **14** : 2998–3012. DOI: 10.1111/j.1462-2920.2012.02876.x

Irvine-Fynn TDL, Hanna E, Barrand NE, Porter PR, Kohler J, Hodson AJ. 2014. Examination of a physically based, high-resolution, distributed Arctic temperature-index melt model, on Midtre Lovénbreen, Svalbard. *Hydrological Processes* **28** : 134–149. DOI: 10.1002/hyp.9526

Irvine-Fynn TDL, Hodson AJ, Moorman BJ, Vatne G, Hubbard AL. 2011. Polythermal glacier hydrology: a review. *Reviews of Geophysics* **49** : 1–37. DOI: 10.1029/2010RG000350

Jacob T, Wahr J, Pfeffer WT, Swenson S. 2012. Recent contributions of glaciers and ice caps to sea level rise. *Nature* **482** : 514–8. DOI: 10.1038/nature10847

Jaedicke C, Gauer P. 2005. The influence of drifting snow on the location of glaciers on western Spitsbergen, Svalbard. *Annals of Glaciology* **42** : 237–242.

Jaffrezo JL, Clain MP, Masclat P. 1994. Polycyclic Aromatic Hydrocarbons in the polar ice of Greenland. Geochemical use of these atmospheric tracers. *Atmospheric Environment* **28** : 1139–1145.

Jania J. 1997. *Glacjologia* . PWN: Warszawa

Jania JA, Hagen JO (eds). 1996. *Mass Balance of Arctic Glaciers* . University of Silesia: Sosnowiec-Oslo

Jansson P. 1999. Effect of Uncertainties in Measured Variables on the Calculated Mass Balance of Storglaciären. *Geografiska Annaler. Series A, Physical Geography* **81** : 633–642.

Jenk TM, Szidat S, Bolius D, Sigl M, Gäggeler HW, Wacker L, Ruff M, Barbante C, Boutron CF, Schwikowski M. 2009. A novel radiocarbon dating technique applied to an ice core from the Alps indicating late Pleistocene ages. *Journal of Geophysical Research* **114** : D14305. DOI: 10.1029/2009JD011860

Jianchu X, Shrestha A, Eriksson M. 2009. Climate change and its impacts on glaciers and water resource management in the Himalayan Region. 44–54 pp.

De Jong C, Collins D, Ranzi R (eds). 2005. *Climate and Hydrology in Mountain Areas* . John Wiley & Sons Ltd: Chichester

Jonsell U, Hock R, Holmgren B. 2003. Spatial and temporal variations in albedo on Storglaciären, Sweden. *Journal of Glaciology* **49** : 59–68.

Joshi M, Hawkins E, Sutton R, Lowe J, Frame & D. 2011. Projections of when temperature change will exceed 2°C above pre-industrial levels. *Nature Climate Change* **1** : 407–412. DOI: doi:10.1038/nclimate1261

Kallenborn R, Breivik K, Eckhardt S, Lunder CR, Manø S, Schlabach M, Stohl A. 2013. Long-term monitoring of persistent organic pollutants (POPs) at the Norwegian Troll station in Dronning Maud Land, Antarctica. *Atmospheric Chemistry and Physics* **13** : 6983–6992. DOI: 10.5194/acp-13-6983-2013

Kang J-H, Choi S-D, Park H, Baek S-Y, Hong S, Chang Y-S. 2009. Atmospheric deposition of persistent organic pollutants to the East Rongbuk Glacier in the Himalayas. *The Science of the Total Environment* **408** : 57–63. DOI: 10.1016/j.scitotenv.2009.09.015

Kaštovská K, Stibal M, Šabacká M, Černá B, Šantrůčková H, Elster J. 2007. Microbial community structure and ecology of subglacial sediments in two polythermal Svalbard glaciers characterized by epifluorescence microscopy and PLFA. *Polar Biology* **30** : 277–287. DOI: 10.1007/s00300-006-0181-y

Kattner G, Thomas DN, Haas C, Kennedy H, Dieckmann GS. 2004. Surface ice and gap layers in Antarctic sea ice: highly productive habitats. *Marine Ecology Progress Series* **277** : 1–12. DOI: 10.3354/meps277001

Kawamura K, Izawa Y, Mochida M, Shiraiwa T. 2012a. Ice core records of biomass burning tracers (levoglucosan and dehydroabietic, vanillic and p-hydroxybenzoic acids) and total organic carbon for past 300 years in the Kamchatka Peninsula, Northeast Asia. *Geochimica et Cosmochimica Acta* **99** : 317–329. DOI: 10.1016/j.gca.2012.08.006

Kawamura K, Matsumoto K, Tachibana E, Aoki K. 2012b. Low molecular weight (C1–C10) monocarboxylic acids, dissolved organic carbon and major inorganic ions in alpine snow pit sequence from a high mountain site, central Japan. *Atmospheric Environment* **62** : 272–280. DOI: 10.1016/j.atmosenv.2012.08.018

Kawamura K, Yokoyama K, Fujii Y. 1992. Vertical profiles of total organic carbon and polar organic compounds in the ice core from Site-J, Greenland. *Proceedings of NIPR Symposium on Polar Meteorology and Glaciology* **6** : 99–105.

Knudsen E, Yri HT. 2010. Teknisk industrielle kulturminner i Longyearbyen med omegn. Verneverdi og forvaltning . Longyearbyen

Kozak K, Polkowska Ż, Ruman M, Koziół K, Namieśnik J. 2013. Analytical studies on the environmental state of the Svalbard Archipelago provide a critical source of information about anthropogenic global impact. *TrAC Trends in Analytical Chemistry* **50** : 107–126. DOI: 10.1016/j.trac.2013.04.016

Krawczyk WE, Bartoszewski SA, Siwek K. 2008. Rain water chemistry at Calypsobyen, Svalbard. *Polish Polar Research* **29** : 149–162.

Kühnel R, Björkman MP, Vega CP, Hodson AJ, Isaksson E, Ström J. 2013. Reactive nitrogen and sulphate wet deposition at Zeppelin Station, Ny-Ålesund, Svalbard. *Polar Research* **32** : 19136. DOI: <http://dx.doi.org/10.3402/polar.v32i0.19136>

Kwok KY et al. 2013. Transport of perfluoroalkyl substances (PFAS) from an arctic glacier to downstream locations: implications for sources. *The Science of the total environment* **447** : 46–55. DOI: 10.1016/j.scitotenv.2012.10.091

Lack DA, Cappa CD. 2010. Impact of brown and clear carbon on light absorption enhancement, single scatter albedo and absorption wavelength dependence of black carbon. *Atmospheric Chemistry and Physics* **10** : 4207–4220. DOI: 10.5194/acp-10-4207-2010

Lack DA, Langridge JM, Bahreini R, Cappa CD, Middlebrook AM, Schwarz JP. 2012. Brown carbon and internal mixing in biomass burning particles. *Proceedings of the National Academy of Sciences of the United States of America* **109** : 14802–14807. DOI: 10.1073/pnas.1206575109/-
/DCSupplemental.www.pnas.org/cgi/doi/10.1073/pnas.1206575109

Lafrenière MJ, Sharp MJ. 2011. The Concentration and Fluorescence of Dissolved Organic Carbon (DOC) in Glacial and Nonglacial Catchments: Interpreting Hydrological Flow Routing and DOC Sources. *Arctic, Antarctic and Alpine Research* **36** : 156–165.

Langford H, Hodson A, Banwart S, Bøggild C. 2010. The microstructure and biogeochemistry of Arctic cryoconite granules. *Annals of Glaciology* **51** : 87–94. DOI: 10.3189/172756411795932083

Langford HJ, Irvine-Fynn TDL, Edwards A, Banwart SA, Hodson AJ. 2014. A spatial investigation of the environmental controls over cryoconite aggregation on Longyearbreen glacier, Svalbard. *Biogeosciences Discussions* **11** : 3423–3463. DOI: 10.5194/bgd-11-3423-2014

Lanoil B, Skidmore M, Priscu JC, Han S, Foo W, Vogel SW, Tulaczyk S, Engelhardt H. 2009. Bacteria beneath the West Antarctic ice sheet. *Environmental microbiology* **11** : 609–15. DOI: 10.1111/j.1462-2920.2008.01831.x

Lawson EC, Wadham JL, Tranter M, Stibal M, Lis GP, Butler CEH, Laybourn-Parry J, Nienow P, Chandler D, Dewsbury P. 2014. Greenland Ice Sheet exports labile organic carbon to the Arctic oceans. *Biogeosciences* **11** : 4015–4028. DOI: 10.5194/bg-11-4015-2014

Laybourn-Parry J, Tranter M, Hodson AJ. 2011. *The Ecology of Snow and Ice Environments*. Oxford University Press: Oxford

Legrand M, Angelis M De. 1996. Light carboxylic acids in Greenland ice: A record of past forest fires and vegetation emissions from the boreal zone. *Journal of Geophysical Research* **101** : 4129–4145.

Legrand M, De Angelis M, Maupetit F. 1993. Field investigation of major and minor ions along Summit (Central Greenland) ice cores by ion chromatography. *Journal of Chromatography* **640** : 251–258. DOI: 10.1016/0021-9673(93)80188-E

Legrand M, Preunkert S, Jourdain B, Guilhermet J, Fain X, Alekhina I, Petit JR. 2013. Water-soluble organic carbon in snow and ice deposited at Alpine, Greenland, and Antarctic sites: a critical review of available data and their atmospheric relevance. *Climate of the Past Discussions* **9** : 2357–2399. DOI: 10.5194/cpd-9-2357-2013

Legrand M, Preunkert S, Schock M, Cerqueira M, Kasper-Giebl A, Afonso J, Pio C, Gelencsér A, Dombrowski-Etchevers I. 2007. Major 20th century changes of carbonaceous aerosol components (EC, WinOC, DOC, HULIS, carboxylic acids, and cellulose) derived from Alpine ice cores. *Journal of Geophysical Research* **112** : D23S11. DOI: 10.1029/2006JD008080

Legrand M, Preunkert S, Wagenbach D, Cachier H, Puxbaum H. 2003. A historical record of formate and acetate from a high-elevation Alpine glacier: Implications for their natural versus anthropogenic budgets at the European scale. *Journal of Geophysical Research: Atmospheres* **108** : 4788. DOI: 10.1029/2003JD003594

Legrand M, Saigne C. 1988. Formate, Acetate and Methanesulfonate in Antarctic ice: Some geochemical implications. *Atmospheric Environment* **22** : 1011–1017.

Li X, Qin D, Zhou H. 2001. Organic acids: Differences in ice core records between Glacier 1, Tianshan, China and the polar areas. *Chinese Science Bulletin* **46** : 80–83.

Li Z, Edwards R, Mosley-Thompson E, Wang F, Dong Z, You X, Li H, Li C, Zhu Y. 2006. Seasonal variability of ionic concentrations in surface snow and elution processes in snow–firn packs at the PGPI site on Úrúmqi glacier No. 1, eastern Tien Shan, China. *Annals of Glaciology* **43** : 250–256.

Liestøl O. 1974. Glaciological work in 1972. In *Årbok 1972* , . Norsk Polarinstitutt: Oslo; 125–135.

Lilbæk G, Pomeroy JW. 2008. Ion enrichment of snowmelt runoff water caused by basal ice formation. *Hydrological Processes* : 1–9. DOI: 10.1002/hyp

Liu G-X, Hu P, Zhang W, Wu X, Yang X, Chen T, Zhang M, Li S-W. 2012. Variations in soil culturable bacteria communities and biochemical characteristics in the Dongkemadi glacier forefield along a chronosequence. *Folia Microbiologica* DOI: 10.1007/s12223-012-0159-9

Luthcke SB, Arendt AA, Rowlands DD, Carthy JJMC, Larsen CF. 2008. Recent glacier mass changes in the Gulf of Alaska region from GRACE mascon solutions. *Journal of Glaciology* **54** : 767–777.

Lutz S, Anesio AM, Jorge Villar SE, Benning LG. 2014. Variations of algal communities cause darkening of a Greenland glacier. *FEMS Microbiology Ecology* **89** : 402–14. DOI: 10.1111/1574-6941.12351

Lysä A, Lønne I. 2001. Moraine development at a small High-Arctic valley glacier: Rieperbreen, Svalbard. *Journal of Quaternary Science* **16** : 519–529. DOI: 10.1002/jqs.613

Macheret YY, Zhuravlev AB. 1982. Radio Echo-sounding of Svalbard glaciers. *Journal of Glaciology* **28** : 295–314.

Machguth H, Paul F, Hoelzle M, Haeberli W. 2006. Distributed glacier mass-balance modelling as an important component of modern multi-level glacier monitoring. *Annals of Glaciology* **43** : 335–343. DOI: 10.3189/172756406781812285

Mader HM, Pettitt ME, Wadham JL, Wolff EW, Parkes RJ. 2006. Subsurface ice as a microbial habitat. *Geology* **34** : 169–172. DOI: 10.1130/G22096.1

Maire A le, Bourguet W, Balaguer P. 2010. A structural view of nuclear hormone receptor endocrine disruptor interactions. *Cellular and Molecular Life Sciences* DOI: 10.1007/s00018-009-0249-2

Margesin R, Neuner G, Storey KB. 2007. Cold-loving microbes, plants, and animals - fundamental and applied aspects. *Die Naturwissenschaften* **94** : 77–99. DOI: 10.1007/s00114-006-0162-6

Margesin R, Zacke G, Schinner F. 2002. Characterization of Heterotrophic Microorganisms in Alpine Glacier Cryoconite. *Arctic, Antarctic and Alpine Research* **34** : 88–93.

Masclat P, Hoyau V, Jaffrezo JL, Cachier H. 2000. Polycyclic aromatic hydrocarbon deposition on the ice sheet of Greenland . Part I : superficial snow. *Atmospheric Environment* **34** : 3195–3207.

Mattson LE. 2000. The influence of a debris cover on the mid-summer discharge of Dome Glacier, Canadian Rocky Mountains. 25–33 pp.

McNeill VF et al. 2012. Organics in environmental ices: sources, chemistry, and impacts. *Atmospheric Chemistry and Physics Discussions* **12** : 8857–8920. DOI: 10.5194/acpd-12-8857-2012

McSween HY, Richardson SM, Uhle ME. 2003. *Geochemistry. Pathways and Processes* . 2nd ed. Columbia University Press: New York

Meier MF, Dyurgerov MB, Rick UK, O’Neel S, Pfeffer WT, Anderson RS, Anderson SP, Glazovsky AF. 2007. Glaciers dominate eustatic sea-level rise in the 21st century. *Science* **317** : 1064–7. DOI: 10.1126/science.1143906

Meier MF, Tangborn W V. 1965. Net budget and flow of South Cascade Glacier, Washington. *Journal of Glaciology* **5** : 547–566.

Meyer T, Lei YD, Muradi I, Wania F. 2009a. Organic contaminant release from melting snow. 1. Influence of chemical partitioning. *Environmental science & technology* **43** : 657–62.

Meyer T, Lei YD, Muradi I, Wania F. 2009b. Organic contaminant release from melting snow. 2. Influence of snow pack and melt characteristics. *Environmental science & technology* **43** : 663–8.

Meyer T, Wania F. 2011. Modeling the elution of organic chemicals from a melting homogeneous snow pack. *Water research* **45** : 3627–37. DOI: 10.1016/j.watres.2011.04.011

Miller JN, Miller JC. 2005. *Statistics and chemometrics for analytical chemistry* . 5th ed. Pearson. Prentice Hall: Harlow

Mindl B, Anesio AM, Meirer K, Hodson AJ, Laybourn-Parry J, Sommaruga R, Sattler B. 2007. Factors influencing bacterial dynamics along a transect from supraglacial runoff to proglacial lakes of a high Arctic glacier [corrected]. *FEMS microbiology ecology* **59** : 307–17. DOI: 10.1111/j.1574-6941.2006.00262.x

Mnif W, Hassine AIH, Bouaziz A, Bartegi A, Thomas O, Roig B. 2011. Effect of endocrine disruptor pesticides: a review. *International Journal of Environmental Research and Public Health* **8** : 2265–303. DOI: 10.3390/ijerph8062265

Moholdt G, Hagen JO, Eiken T, Schuler T V. 2010a. Geometric changes and mass balance of the Austfonna ice cap, Svalbard. *The Cryosphere* **4** : 21–34.

Moholdt G, Nuth C, Hagen JO, Kohler J. 2010b. Recent elevation changes of Svalbard glaciers derived from ICESat laser altimetry. *Remote Sensing of Environment* **114** : 2756–2767. DOI: 10.1016/j.rse.2010.06.008

Moholdt G, Wouters B, Gardner AS. 2012. Recent mass changes of glaciers in the Russian High Arctic. *Geophysical Research Letters* **39** : L10502. DOI: 10.1029/2012GL051466

Møller AK, Sjøborg DA, Abu Al-Soud W, Sørensen SJ, Kroer N. 2013. Bacterial community structure in High-Arctic snow and freshwater as revealed by pyrosequencing of 16S rRNA genes and cultivation. *Polar Research* **32** : 17390. DOI: 10.3402/polar.v32i0.17390

Müller F. 1962. Zonation in the accumulation area of the glaciers of Axel Heiberg Island, N.W.T., Canada. *Journal of Glaciology* **4** : 302–311.

- Müller F, Keeler CM. 1969. Errors in short-term ablation measurements on melting ice surfaces. *Journal of Glaciology* **8** : 91–105.
- Müller T, Leya T, Fuhr G. 2001. Persistent Snow Algal Fields in Spitsbergen: Field Observations and a Hypothesis about the Annual Cell Circulation. *Arctic, Antarctic and Alpine Research* **33** : 42–51.
- Murray T, Gooch DL, Stuart GW. 1997. Structures within the surge front at Bakaninbreen, Svalbard, using ground-penetrating radar. *Annals of Glaciology* **24** : 122–129.
- Nakawo M, Rana B. 1999. Estimate of Ablation Rate of Glacier Ice under a Supraglacial Debris Layer. *Geografiska Annaler, Series A: Physical Geography* **81** : 695–701. DOI: 10.1111/1468-0459.00097
- Nelson DW, Sommers LE. 1996. Total Carbon, Organic Carbon, and Organic Matter. In *Methods of Soil Analysis. Part 3 - Chemical Methods.* , Sparks DL, Page AL, Helmke PA, Loeppert RH, Soltanpour PN, Tabatabai MA, Johnston CT, and Sumner ME (eds). Soil Science Society of America & American Society of Agronomy: Madison, Wisconsin, USA; 961–1010.
- Van Nevel S, Koetzsch S, Weilenmann H-U, Boon N, Hammes F. 2013. Routine bacterial analysis with automated flow cytometry. *Journal of Microbiological Methods* **94** : 73–76. DOI: 10.1016/j.mimet.2013.05.007
- Nicholls RJ, Cazenave A. 2010. Sea-level rise and its impact on coastal zones. *Science (New York, N.Y.)* **328** : 1517–20. DOI: 10.1126/science.1185782
- Niedźwiedz T. 2003. Contemporary variability of atmospheric circulation, temperature and precipitation in Spitsbergen. *Problemy Klimatologii Polarnej* **13** : 79–92.
- Nizetto L et al. 2010. Past, Present, and Future Controlson Levels of Persistent OrganicPollutants in the Global Environment. *Environmental Science & Technology* **44** : 6526–6531.
- Norwegian Meteorological Institute. 2013. eKlima: Free access to weather- and climate data from Norwegian Meteorological Institute, from historical data to real time observations [online] Available from: <http://sharki.oslo.dnmi.no>
- Nowak A, Hodson A. 2013. Hydrological response of a High-Arctic catchment to changing climate over the past 35 years a case study of Bayelva watershed, Svalbard. *Polar Research* **32** DOI: <http://dx.doi.org/10.3402/polar.v32i0.19691>
- Nuth C, Moholdt G, Kohler J, Hagen JO, Kääb A. 2010. Svalbard glacier elevation changes and contribution to sea level rise. *Journal of Geophysical Research* **115** : F01008. DOI: 10.1029/2008JF001223
- Nuttall A, Hagen JO, Dowdeswell J. 1997. Quiescent-phase changes in velocity and geometry of Finsterwalderbreen, a surge-type glacier in Svalbard. *Annals of Glaciology* **24** : 249–254.
- Olivier S et al. 2003. Glaciochemical investigation of an ice core from Belukha glacier, Siberian Altai. *Geophysical Research Letters* **30** : 2019. DOI: 10.1029/2003GL018290

Opsahl S, Benner R, Amon RMW. 1999. Major flux of terrigenous dissolved organic matter through the Arctic Ocean. *Limnology and Oceanography* **44** : 2017–2023.

Painter TH, Flanner MG, Kaser G, Marzeion B, Vancuren RA, Abdalati W. 2013. End of the Little Ice Age in the Alps forced by industrial black carbon. DOI: 10.1073/pnas.1302570110/-/DCSupplemental.www.pnas.org/cgi/doi/10.1073/pnas.1302570110

Pälli A, Moore JC, Rolstad C. 2003. Firn-ice transition-zone features of four polythermal glaciers in Svalbard seen by ground-penetrating radar. *Annals of Glaciology* **37** : 298–304.

Paterson WSB. 1994. The physics of glaciers . 3rd ed. Pergamon Press: Oxford

Paul F, Huggel C, Kääb A. 2004. Combining satellite multispectral image data and a digital elevation model for mapping debris-covered glaciers. *Remote Sensing of Environment* **89** : 510–518. DOI: 10.1016/j.rse.2003.11.007

Paul F, Machguth H, Kääb A. 2005. On the impact of glacier albedo under conditions of extreme glacier melt: the summer of 2003 in the Alps. *EARSeL eProceedings* **4** : 139–149.

Pautler BG, Simpson AJ, Simpson MJ, Tseng L-H, Spraul M, Dubnick A, Sharp MJ, Fitzsimons SJ. 2011. Detection and structural identification of dissolved organic matter in Antarctic glacial ice at natural abundance by SPR-W5-WATERGATE 1H NMR spectroscopy. *Environmental science & technology* **45** : 4710–7. DOI: 10.1021/es200697c

Pautler BG, Woods GC, Dubnick A, Simpson AJ, Sharp MJ, Fitzsimons SJ, Simpson MJ. 2012. Molecular characterization of dissolved organic matter in glacial ice: coupling natural abundance 1H NMR and fluorescence spectroscopy. *Environmental Science & Technology* **46** : 3753–61. DOI: dx.doi.org/10.1021/es203942y

Pellicciotti F, Brock B, Strasser U, Burlando P, Funk M, Corripio J. 2005. An enhanced temperature-index glacier melt model including the shortwave radiation balance: development and testing for Haut Glacier d’Arolla, Switzerland. *Journal of Glaciology* **51** : 573–587.

Pellicciotti F, Carenzo M, Helbing J, Rimkus S, Burlando P. 2009. On the role of subsurface heat conduction in glacier energy-balance modelling. *Annals of Glaciology* **50** : 16–24.

Petit JR et al. 1999. Climate and atmospheric history of the past 420 000 years from the Vostok ice core, Antarctica. *Nature* **399** : 429–436.

Plaschke M, Römer J, Klenze R, Kim J. 1999. In situ AFM study of sorbed humic acid colloids at different pH. *Colloids and Surfaces A: Physicochemical and Engineering Aspects* **160** : 269–279. DOI: 10.1016/S0927-7757(99)00191-0

Pope A, Murray T, Luckman A. 2007. DEM quality assessment for quantification of glacier surface change. *Annals of Glaciology* **46** : 189–194. DOI: http://dx.doi.org/10.3189/172756407782871792

Price PB. 2000. A habitat for psychrophiles in deep Antarctic ice. *Proceedings of the National Academy of Sciences of the United States of America* **97** : 1247–51.

Price PB. 2007. Microbial life in glacial ice and implications for a cold origin of life. *FEMS Microbiology Ecology* **59** : 217–231. DOI: 10.1111/j.1574-6941.2006.00234.x

Price PB, Bay RC. 2012. Marine bacteria in deep Arctic and Antarctic ice cores: a proxy for evolution in oceans over 300 million generations. *Biogeosciences* **9** : 3799–3815. DOI: 10.5194/bg-9-3799-2012

Price PB, Sowers T. 2004. Temperature dependence of metabolic rates for microbial growth, maintenance, and survival. *Proceedings of the National Academy of Sciences of the United States of America* **101** : 4631–6. DOI: 10.1073/pnas.0400522101

Priscu JC, Tulaczyk S, Studinger M, Kennicutt MC, Christner BC, Foreman CM. 2008. Antarctic Subglacial Water: origin, evolution and ecology. In *Polar Lakes and Rivers: Limnology of Arctic and Antarctic Aquatic Ecosystems*, Laybourn-Parry J and Vincent WF (eds). Oxford University Press; 119–135.

Quinn GP, Keough MJ. 2007. *Experimental Design and Data Analysis for Biologists*. 1st ed. Cambridge University Press: New York

R Core Team. 2012. R: A language and environment for statistical computing.

Radić V, Bliss A, Beedlow a. C, Hock R, Miles E, Cogley JG. 2014. Regional and global projections of twenty-first century glacier mass changes in response to climate scenarios from global climate models. *Climate Dynamics* **42** : 37–58. DOI: 10.1007/s00382-013-1719-7

Radić V, Hock R. 2011. Regionally differentiated contribution of mountain glaciers and ice caps to future sea-level rise. *Nature Geoscience* **4** : 91–94. DOI: 10.1038/ngeo1052

Raper SCB, Braithwaite RJ. 2006. Low sea level rise projections from mountain glaciers and icecaps under global warming. *Nature* **439** : 311–3. DOI: 10.1038/nature04448

Remias D, Lütz-Meindl U, Lütz C. 2005. Photosynthesis, pigments and ultrastructure of the alpine snow alga *Chlamydomonas nivalis*. *European Journal of Phycology* **40** : 259–268. DOI: 10.1080/09670260500202148

Reznichenko N, Davies T, Shulmeister J, McSaveney M. 2010. Effects of debris on ice-surface melting rates: an experimental study. *Journal of Glaciology* **56** : 384–394. DOI: <http://dx.doi.org/10.3189/002214310792447725>

Rignot E, Velicogna I, van den Broeke MR, Monaghan a., Lenaerts JTM. 2011. Acceleration of the contribution of the Greenland and Antarctic ice sheets to sea level rise. *Geophysical Research Letters* **38** : L05503. DOI: 10.1029/2011GL046583

Robin G de Q. 1975. Velocity of radio waves in ice by means of a bore-hole interferometric technique. *Journal of Glaciology* **15** : 151–159.

Rogerson PA. 2010. *Statistical Methods for Geography. A Student's Guide*. 3rd ed. SAGE Publications Inc.: Los Angeles - London - New Delhi - Singapore - Washington DC

Rohde R a, Price PB, Bay RC, Bramall NE. 2008. In situ microbial metabolism as a cause of gas anomalies in ice. *Proceedings of the National Academy of Sciences of the United States of America* **105** : 8667–72. DOI: 10.1073/pnas.0803763105

Rutter N, Hodson A, Irvine-Fynn T, Solås MK. 2011. Hydrology and hydrochemistry of a deglaciating high-Arctic catchment, Svalbard. *Journal of Hydrology* **410** : 39–50. DOI: 10.1016/j.jhydrol.2011.09.001

Šabacká M, Priscu JC, Basagic HJ, Fountain AG, Wall DH, Virginia RA, Greenwood MC. 2012. Aeolian flux of biotic and abiotic material in Taylor Valley, Antarctica. *Geomorphology* **155-156** : 102–111. DOI: 10.1016/j.geomorph.2011.12.009

Sattler B, Puxbaum H, Psenner R. 2001. Bacterial growth in supercooled cloud droplets. *Geophysical Research Letters* **28** : 239–242.

Sauter T, Möller M, Finkelnburg R, Grabiec M, Scherer D, Schneider C. 2013. Snowdrift modelling for the Vestfonna ice cap, north-eastern Svalbard. *The Cryosphere* **7** : 1287–1301. DOI: 10.5194/tc-7-1287-2013

Sävström C, Mumford P, Marshall W, Hodson AJ, Laybourn-Parry J. 2002. The microbial communities and primary productivity of cryoconite holes in an Arctic glacier (Svalbard 79°N). *Polar Biology* **25** : 591–596. DOI: 10.1007/s00300-002-0388-5

Schlesinger WH, Bernhardt ES. 2013. Biogeochemistry: an analysis of global change . 3rd ed. Academic Press, Elsevier: Oxford

Schmid P, Bogdal C, Blüthgen N, Anselmetti FS, Zwysig A, Hungerbühler K. 2011. The missing piece: sediment records in remote mountain lakes confirm glaciers being secondary sources of persistent organic pollutants. *Environmental science & technology* **45** : 203–8. DOI: 10.1021/es1028052

Schohl G a, Ettema R. 1986. Theory and Laboratory Observations of Naled Ice Growth. *Journal of Glaciology* **32** : 168–177.

Schütte UME, Abdo Z, Foster J, Ravel J, Bunge J, Solheim B, Forney LJ. 2010. Bacterial diversity in a glacier foreland of the high Arctic. *Molecular Ecology* **19** : 54–66. DOI: 10.1111/j.1365-294X.2009.04479.x

Sharp RP. 1951. Features of the Firn on Upper Seward Glacier St . Elias Mountains, Canada. *The Journal of Geology* **59** : 599–621.

Sicart JE, Hock R, Six D. 2008. Glacier melt, air temperature, and energy balance in different climates: The Bolivian Tropics, the French Alps, and northern Sweden. *Journal of Geophysical Research* **113** : D24113. DOI: 10.1029/2008JD010406

Sicart JE, Ribstein P, Francou B, Pouyaud B, Condom T. 2007. Glacier mass balance of tropical Zongo glacier, Bolivia, comparing hydrological and glaciological methods. *Global and Planetary Change* **59** : 27–36. DOI: 10.1016/j.gloplacha.2006.11.024

Sigl M et al. 2009. Instruments and Methods: Towards radiocarbon dating of ice cores. *Journal of Glaciology* **55** : 985–996.

Sigler W V, Crivii S, Zeyer J. 2002. Bacterial succession in glacial forefield soils characterized by community structure, activity and opportunistic growth dynamics. *Microbial ecology* **44** : 306–16. DOI: 10.1007/s00248-002-2025-9

Singer GA, Fasching C, Wilhelm L, Niggemann J, Steier P, Dittmar T, Battin TJ. 2012. Biogeochemically diverse organic matter in Alpine glaciers and its downstream fate. *Nature Geoscience* **5** : 710–714. DOI: 10.1038/ngeo1581

- Skidmore ML, Foght JM, Sharp MJ. 2000. Microbial life beneath a high arctic glacier. *Applied and environmental microbiology* **66** : 3214–20.
- Slangen ABA, Carson M, Katsman CA, van de Wal RSW, Köhl A, Vermeersen LLA, Stammer D. 2014. Projecting twenty-first century regional sea-level changes. *Climatic Change* **124** : 317–332. DOI: 10.1007/s10584-014-1080-9
- Sow M, Goossens D, Rajot JL. 2006. Calibration of the MDCO dust collector and of four versions of the inverted frisbee dust deposition sampler. *Geomorphology* **82** : 360–375. DOI: 10.1016/j.geomorph.2006.05.013
- Statsoft. 2013. Electronic Statistics Textbook [online] Available from: <http://www.statsoft.com/textbook>
- Stibal M et al. 2012a. Methanogenic potential of Arctic and Antarctic subglacial environments with contrasting organic carbon sources. *Global Change Biology* **18** : 3332–3345. DOI: 10.1111/j.1365-2486.2012.02763.x
- Stibal M, Lawson EC, Lis GP, Mak KM, Wadham JL, Anesio AM. 2010. Organic matter content and quality in supraglacial debris across the ablation zone of the Greenland ice sheet. *Annals of Glaciology* **51** : 1–8. DOI: 10.3189/172756411795931958
- Stibal M, Sabacká M, Kastovská K. 2006. Microbial communities on glacier surfaces in Svalbard: impact of physical and chemical properties on abundance and structure of cyanobacteria and algae. *Microbial ecology* **52** : 644–54. DOI: 10.1007/s00248-006-9083-3
- Stibal M, Telling J, Cook J, Mak KM, Hodson AJ, Anesio AM. 2012b. Environmental controls on microbial abundance and activity on the greenland ice sheet: a multivariate analysis approach. *Microbial ecology* **63** : 74–84. DOI: 10.1007/s00248-011-9935-3
- Stibal M, Tranter M. 2007. Laboratory investigation of inorganic carbon uptake by cryoconite debris from Werenskioldbreen, Svalbard. *Journal of Geophysical Research* **112** : G04S33. DOI: 10.1029/2007JG000429
- Stibal M, Tranter M, Benning LG, Řehák J. 2008a. Microbial primary production on an Arctic glacier is insignificant in comparison with allochthonous organic carbon input. *Environmental Microbiology* **10** : 2172–8. DOI: 10.1111/j.1462-2920.2008.01620.x
- Stibal M, Tranter M, Telling J, Benning LG. 2008b. Speciation, phase association and potential bioavailability of phosphorus on a Svalbard glacier. *Biogeochemistry* **90** : 1–13. DOI: 10.1007/s10533-008-9226-3
- Stubbins A et al. 2012. Anthropogenic aerosols as a source of ancient dissolved organic matter in glaciers. *Nature Geoscience* **5** : 198–201. DOI: 10.1038/ngeo1403
- Sturm M, Holmgren J, König M, Morris K. 1997. The thermal conductivity of seasonal snow. *Journal of Glaciology* **43** : 26–41.
- Takeuchi N. 2001. The altitudinal distribution of snow algae on an Alaska glacier (Gulkana Glacier in the Alaska Range). *Hydrological Processes* **15** : 3447–3459. DOI: 10.1002/hyp.1040

Takeuchi N. 2002a. Optical characteristics of cryoconite (surface dust) on glaciers: the relationship between light absorbency and the property of organic matter contained in the cryoconite. *Annals of Glaciology* **34** : 409–414.

Takeuchi N. 2002b. Surface albedo and characteristics of cryoconite (biogenic surface dust) on an Alaska glacier, Gulkana Glacier in the Alaska Range. *Bulletin of Glaciological Research* **19** : 63–70.

Takeuchi N. 2004. A Snow Algal Community on Tyndall Glacier in the Southern Patagonia Icefield, Chile. *Arctic, Antarctic and Alpine Research* **36** : 92–99.

Takeuchi N. 2009. Temporal and spatial variations in spectral reflectance and characteristics of surface dust on Gulkana Glacier, Alaska Range. *Journal of Glaciology* **55** : 701–709. DOI: 10.3189/002214309789470914

Takeuchi N, Kohshima S, Goto-Azuma K, Koerner RM. 2001a. Biological characteristics of dark colored material (cryoconite) on Canadian Arctic glaciers (Devon and Penny ice caps). *Mem. Natl. Inst. Polar Res.* : 495–505.

Takeuchi N, Kohshima S, Seko K. 2001b. Structure, Formation, and Darkening Process of Albedo-Reducing Material (Cryoconite) on a Himalayan Glacier: A Granular Algal Mat Growing on the Glacier. *Arctic, Antarctic, and Alpine Research* **33** : 115–122.

Takeuchi N, Nishiyama H, Li Z. 2010. Structure and formation process of cryoconite granules on Urúmqi glacier No. 1, Tien Shan, China. *Annals of Glaciology* **51** : 9–14.

Takeuchi N, Uetake J, Fujita K, Aizen VB, Nikitin SD. 2006. A snow algal community on Akkem glacier in the Russian Altai mountains. *Annals of Glaciology* **43** : 378–384. DOI: 10.3189/172756406781812113

Tedesco L, Vichi M, Haapala J, Stipa T. 2008. An enhanced sea-ice thermodynamic model applied to the Baltic sea. *Boreal Environmental Research* : 1–26.

Telling J, Anesio AM, Hawkings J, Tranter M, Wadham JL, Hodson AJ, Yallop ML. 2010. Measuring rates of gross photosynthesis and net community production in cryoconite holes: a comparison of field methods. *Annals of Glaciology* **51** : 153–162.

Telling J, Anesio AM, Tranter M, Stibal M, Hawkings J, Irvine-Fynn T, Hodson A, Butler C, Yallop M, Wadham J. 2012. Controls on the autochthonous production and respiration of organic matter in cryoconite holes on high Arctic glaciers. *Journal of Geophysical Research* **117** : G01017. DOI: 10.1029/2011JG001828

Thomson GWM. 1946. The Antoine equation for vapor-pressure data. *Chemical Reviews* **38** : 1–39.

Tranter M. 2003. Geochemical Weathering in Glacial and Proglacial Environments. In *Treatise on Geochemistry, Volume 5: Surface and Ground Water, Weathering, and Soils* , Drever JI (ed). Elsevier; 189–205.

Tranter M, Brimblecombe P, Davies TD, Vincent CE, Abrahams PW, Blackwood I. 1986. The composition of snowfall, snowpack and meltwater in the Scottish Highlands - evidence for preferential elution. *Atmospheric Environment* **20** : 517–525.

Tranter M, Brown GH, Hodson AJ, Gurnell AM. 1996. Hydrochemistry as an indicator of subglacial drainage system structure: a comparison of alpine and sub-polar environments. *Hydrological Processes* **10** : 541–556.

Tung HC, Bramall NE, Price PB. 2005. Microbial origin of excess methane in glacial ice and implications for life on Mars. *Proceedings of the National Academy of Sciences of the United States of America* **102** : 18292–6. DOI: 10.1073/pnas.0507601102

Uetake J, Kohshima S, Nakazawa F, Suzuki K, Kohno M, Kameda T, Arkhipov S, Fujii Y. 2006. Biological ice-core analysis of Sofiyskiy glacier in the Russian Altai. *Annals of Glaciology* **43** : 70–78.

Vézina S, Vincent WF. 1997. Arctic cyanobacteria and limnological properties of their environment: Bylot Island, Northwest Territories, Canada (73°N, 80°W). *Polar Biology* **17** : 523–534. DOI: 10.1007/s003000050151

Villa S, Vighi M, Maggi V, Finizio A, Bolzacchini E. 2003. Historical Trends of Organochlorine Pesticides in an Alpine Glacier. *Journal of Atmospheric Chemistry* **46** : 295–311.

Voisin D et al. 2012. Carbonaceous species and humic like substances (HULIS) in Arctic snowpack during OASIS field campaign in Barrow. *Journal of Geophysical Research* **117** : D00R19. DOI: 10.1029/2011JD016612

Voisin D, Jaffrezo JL, Houdier S, Barret M. 2009. Carbonaceous species and HUmic Like Substances in Arctic Snow: contribution to the speciation of total carbon and optical properties during OASIS – Barrow 2009 campaign . Why would we look at the carbon content in arctic snowpacks ?

Wadham JL, De'ath R, Monteiro FM, Tranter M, Ridgwell a., Raiswell R, Tulaczyk S. 2013. The potential role of the Antarctic Ice Sheet in global biogeochemical cycles. *Earth and Environmental Science Transactions of the Royal Society of Edinburgh* **104** : 55–67. DOI: 10.1017/S1755691013000108

Wadham JL, Nuttall A-M. 2002. Multiphase formation of superimposed ice during a mass-balance year at a maritime high-Arctic glacier. *Journal of Glaciology* **48** : 545–551.

Wadham JL, Tranter M, Skidmore M, Hodson AJ, Prisco J, Lyons WB, Sharp M, Wynn P, Jackson M. 2010. Biogeochemical weathering under ice: Size matters. *Global Biogeochemical Cycles* **24** : 1–11. DOI: 10.1029/2009GB003688

Waller RI. 2001. The influence of basal processes on the dynamic behaviour of cold-based glaciers. *Quaternary International* **86** : 117–128.

Wang J, Yao T, Xu B, Wu G, Xiang S. 2004. Formate and acetate records in the Muztagata ice core, Northwest Tibetan Plateau. *Chinese Science Bulletin* **49** : 1620–1624. DOI: 10.1007/BF03184132

Wang X, Yao T, Wang P, Wei-Yang, Tian L. 2008a. The recent deposition of persistent organic pollutants and mercury to the Dasuopu glacier, Mt. Xixiabangma, central Himalayas. *The Science of the Total Environment* **394** : 134–43. DOI: 10.1016/j.scitotenv.2008.01.016

Wang XP, Xu BQ, Kang SC, Cong ZY, Yao TD. 2008b. The historical residue trends of DDT, hexachlorocyclohexanes and polycyclic aromatic hydrocarbons in an ice core from Mt. Everest,

central Himalayas, China. *Atmospheric Environment* **42** : 6699–6709. DOI: 10.1016/j.atmosenv.2008.04.035

Warren SG, Wiscombe WJ. 1980. A model for the spectral albedo of snow. II: Snow containing atmospheric aerosols. *Journal of the Atmospheric Sciences* **37** : 2734–2745.

Williams MW, Knauf M, Cory R, Caine N, Liu F. 2006. Nitrate content and potential microbial signature of rock glacier outflow, Colorado Front Range. *Earth Surface Processes and Landforms* **10** DOI: 10.1002/esp

Williams MW, Melack JM. 1991. Solute chemistry of snowmelt and runoff in an alpine basin, Sierra Nevada. *Water Resources Research* **27** : 1575–1588.

Woodward J, Murray T, Clark RA, Stuart GW. 2003. Glacier surge mechanisms inferred from ground-penetrating radar: Kongsvegen, Svalbard. *Journal of Glaciology* **49** : 473–480.

Woodward J, Sharp M, Arendt A. 1997. The influence of superimposed-ice formation on the sensitivity of glacier mass balance to climate change. *Annals of Glaciology* **24** : 186–190.

Wynn PM, Hodson AJ, Heaton THE, Chenery SR. 2007. Nitrate production beneath a High Arctic glacier, Svalbard. *Chemical Geology* **244** : 88–102. DOI: 10.1016/j.chemgeo.2007.06.008

Xu B, Wang M, Joswiak DR, Cao J-J, Yao T-D, Wu G-J, Yang W, Zhao H-B. 2009. Deposition of anthropogenic aerosols in a southeastern Tibetan glacier. *Journal of Geophysical Research* **114** : D17209. DOI: 10.1029/2008JD011510

Xu B, Yao T, Liu X, Wang N. 2006. Elemental and organic carbon measurements with a two-step heating–gas chromatography system in snow samples from the Tibetan Plateau. *Annals of Glaciology* **43** : 257–262. DOI: 10.3189/172756406781812122

Xu J, Zhang Q, Li X, Ge X, Xiao C, Ren J, Qin D. 2013. Dissolved organic matter and inorganic ions in a central Himalayan glacier—insights into chemical composition and atmospheric sources. *Environmental Science & Technology* **47** : 6181–8. DOI: 10.1021/es4009882

Xu Y, Simpson AJ, Eyles N, Simpson MJ. 2010. Sources and molecular composition of cryoconite organic matter from the Athabasca Glacier, Canadian Rocky Mountains. *Organic Geochemistry* **41** : 177–186. DOI: 10.1016/j.orggeochem.2009.10.010

Yallop ML et al. 2012. Photophysiology and albedo-changing potential of the ice algal community on the surface of the Greenland ice sheet. *The ISME Journal (Multidisciplinary Journal of Microbial Ecology)* **6** : 2302–13. DOI: 10.1038/ismej.2012.107

Yang M, Howell SG, Zhuang J, Huebert BJ. 2009. Attribution of aerosol light absorption to black carbon, brown carbon, and dust in China – interpretations of atmospheric measurements during EAST-AIRE. *Atmospheric Chemistry and Physics* **9** : 2035–2050.

Yasunari TJ, Bonasoni P, Laj P, Fujita K, Vuillermoz E, Marinoni a., Cristofanelli P, Duchi R, Tartari G, Lau K-M. 2010. Estimated impact of black carbon deposition during pre-monsoon season from Nepal Climate Observatory – Pyramid data and snow albedo changes over Himalayan glaciers. *Atmospheric Chemistry and Physics* **10** : 6603–6615. DOI: 10.5194/acp-10-6603-2010

Yoshimura Y, Kohshima S, Takeuchi N, Seko K, Fujita K. 2006. Snow algae in a Himalayan ice core: new environmental markers for ice-core analyses and their correlation with summer mass balance. *Annals of Glaciology* **43** : 148–153. DOI: 10.3189/172756406781812276

Zemp M, Jansson P, Holmlund P, Gärtner-Roer I, Koblet T, Thee P, Haeberli W. 2010. Reanalysis of multi-temporal aerial images of Storglaciären, Sweden (1959–99) – Part 2: Comparison of glaciological and volumetric mass balances. *The Cryosphere* **4** : 345–357. DOI: 10.5194/tc-4-345-2010

Zhang SH, Hou SG, Yang GL, Wang JH. 2010. Bacterial community in the East Rongbuk Glacier, Mt. Qomolangma (Everest) by culture and culture-independent methods. *Microbiological Research* **165** : 336–45. DOI: 10.1016/j.micres.2009.08.002

Zhao Z, Li Z, Edwards R, Wang F, Li H, Zhu Y. 2006. Atmosphere-to-snow-to-firn transfer of NO₃⁻ on Ürümqi glacier No. 1, eastern Tien Shan, China. *Annals of Glaciology* **43** : 239–244. DOI: <http://dx.doi.org/10.3189/172756406781812410>

Appendix 1. Thermistor data correction

The temperature data from thermistor strings were error-corrected using a Matlab-based code (authorship of the code and processing by Nick Rutter, University of Northumbria). Upper temperature limits were set to remove artefacts in the temperature series: 0°C on two lowermost thermistors (which remained deep in the ice for the full study period), 2°C and 5°C for 6th and 7th thermistor from the bottom of the string, and 20°C for the second highest thermistor, which was quickly exposed to atmospheric influence. Above these thresholds all data were replaced with interpolated temperatures ('naninterp' Matlab function). Some of the thermistor datasets showed high variability in short timesteps, which cannot be attributed to ambient temperature change deep in the ice or snow. Therefore, a maximum temperature gradient of 0.1°C between consecutive measurements and a maximum standard deviation of 0.1°C over 7 hour were imposed, such that any signal exceeding these criteria were treated as noise and removed. The 7th thermistor (from the base of the string) showed unrealistic fluctuations reaching far above 0°C within the snowpack, therefore this data series was smoothed manually by interpolating between valleys around each unrealistic peak. The 5th thermistor from the base of the string has been excluded from the temperature profile since its isothermal temperature reached 2°C instead of 0°C, while the temperature record before then was unrealistically low if a constant correction of -2°C was applied.